Quaternary tectonics and seismic stratigraphy
of the western Black Sea shelf

Dissertation

zur Erlangung des Doktorgrades der Naturwissenschaften

im Department Geowissenschaften

der Universität Hamburg

vorgelegt von

Philipp Konerding

aus Kiel

Hamburg 2008

Als Dissertation angenommen vom Department Geowissenschaften der Universität Hamburg

Auf Grund der Gutachten von **Prof. Dr. How Kin Wong**

und **Dr. Thomas Lüdmann**

Hamburg, den _____16.01.2009_____ _____

Prof. Dr. Kay-Christian Emeis

Leiter des Department Geowissenschaften

Table of Contents

Abstract

Interpretation of high and very high resolution reflection seismic data from the western Black Sea shelf yielded a seismic stratigraphic model of the Late Quaternary deposits on the southwestern Black Sea shelf. This model was combined with borehole information to carry out a regional subsidence analysis, so that the influence of tectonics and sediment compaction could be ruled out in the estimation of sea-level changes in the Black Sea.

Mio-Pliocene sediments form the baseline of the interpretation. On top of it four Quaternary seismic stratigraphic units were identified on the western Black Sea shelf; they are named in chronological order Unit 4 to Unit 1 (U4 – U1). Pliocene deposits are built up by gently basinward dipping layers of relatively high and approximately uniform thickness. Buried graben structures attest to the influence of extensional tectonics until the Upper Pliocene. Later, strong erosion left a rugged surface on the inner and middle shelf that was later overlain by a thin layer of Quaternary to Holocene sediments. The Pliocene is followed by the oldest observed Quaternary seismic sequence (Unit 4, U4); it comprises layers of Lower Quaternary age that dip towards the basin at a steeper angle than those of the Pliocene. Within U4 the oldest of three Quaternary shelfedge delta systems in the study area was found, that supposedly marks an Early Quaternary sea-level lowstand. A well-developed angular unconformity marks the transition to the overlying Unit 3 (U3). In the lower part of U3, interpreted coastal onlaps constrain a sea-level lowstand at this time. Prograding layers deposited during the succeeding transgression and highstand build up the upper part of the unit. A subsequent falling sea-level led to the development of another major unconformity; followed by the deposition of a succession of deltaic lobes on the outer shelf (Unit 2, U2) during the lowstand. The units U4, U3, and U2 are erosionally truncated by a shelf-wide regional unconformity and are overlain by sediments of the youngest Unit 1 (U1). This unit was formed during and since the last glacial lowstand.

Minor internal unconformities attest to high-order sea-level fluctuations within U1 that overprint the general transgressive trend since the last glacial maximum (LGM). These unconformities divide U1 into three subunits (U1-A to U1-C in chronological order). U1-A comprises a prograding shelf-edge delta system partially overlain by shore-parallel dunes deposited during low sea-levels at the last glacial maximum. The younger subdivisions U1-B and U1-C were deposited during the postglacial sea-level rise and the recent highstand. Sediments of subunit U1-B fill small topographic lows on the rugged erosional top surface of the units U3 and U2, while U1-C forms a landward-thickening package of retrogradational

wedges that cover large areas of the present-day shelf. In some areas, dune-like features occur in subunit U1-C that resemble in shape and size the dunes observed in U1-A. It can be speculated that these dunes mark two phases of sea-level lowstand: the first during and shortly after the last glacial maximum, and the second during the post-Early Holocene after the sedimentation of subunit U1-B.

Lowstand seismic indicators such as topset-to-foreset transitions of shelf-edge deltas or coastal onlaps within the mapped seismic units are used to reconstruct the uppermost Quaternary sea-level fluctuations in the Black Sea. To deduce past sea-levels from these lowstand indicators, the influence of tectonic and sedimentary subsidence must be removed. To quantify tectonic subsidence and to assess its regional trend, a subsidence analysis was carried out along two idealized profiles, one crossing the southwestern shelf from the northern Turkish sector to the southern Romanian sector and a second crossing the northwestern shelf from the southern Romanian Sector to the Ukrainian sector offshore Crimea.

The first profile shows that tectonic subsidence in the Bulgarian sector during the Quaternary increased in general linearly from NNE to SSW. Tectonic activities on the shelf off central Bulgaria increased during the deposition of unit U1. Along the second profile, subsidence during the Quaternary was analysed at different water depth levels. The results show an increasing trend of subsidence towards the deep basin in accordance with the model of an Atlantic-type margin subsiding at a constant rate about a fixed hinge line. Regional tectonic features such as the Peceneaga Camena and Sulina Tarkinkut faults divide the Quaternary sedimentary cover of the northwestern Black Sea shelf into blocks with significantly different subsidence rates; the highest values are found in the vicinity of the Viteaz Canyon. The southwestern and northeastern parts of the profile have been less affected by subsidence, with the least influence observed in the northeast.

The reconstruction of sea-level lowstands led to the following Quaternary seismic stratigraphic model for the western Black Sea shelf: The oldest seismic stratigraphic unit U4 is of Early Quaternary age and contains a shelfedge delta system indicative of a sea-level lowstand. This system corresponds most probably to the Günz Glacial (~900 ka). Results of subsidence analysis extrapolated to account for the relatively landward position of the lowstand indicator suggest that sea-level was at a position approximately comparable to that of the present-day. Coastal onlaps mark a sea-level lowstand during the deposition of the succeeding unit U3, which was very likely developed during the Mindel Glacial (~500 ka); the

sea-level at this time was −140 m. The deltaic sequence found in unit U2 is assigned to the sea-level lowstand during the Riss Glacial (~150 ka) that reached a minimum sea-level of about -125 m. Another lowstand was reached around the LGM at 20 ka; here levels as low as -116 m can be assumed. This lowstand led to the deposition of the shelfedge delta system within subunit U1-A.

The level of the Black Sea – at this time a freshwater lake disconnected from the global ocean - rose during the global warming in late glacial and Holocene times. Subunit U1-B found at depths < -85 m is interpreted to have formed during a minor phase of sea-level stillstand. Its deposition is possibly related to meltwater pulses between 18 and 15.5 ka and stopped after the sea-level fell below -90 m. During this post-glacial lowstand, coastal sedimentary features formed on the outer shelf. The rising global sea-level breached the Bosphorus sill around 8.4 ka when marine water entered the Black Sea. The subsequent transgression must have been rapid enough to preserve the lowstand coastal sedimentary structures. The retrogradationally stacked packages of the youngest subunit U1-C formed during the Holocene transgression, indicating at least slower phases of sea-level rise on the way to the present conditions.

Zusammenfassung

Hoch und sehr hoch auflösende reflexionsseismische Messdaten aus dem westlichen Schwarzen Meer wurden wurden interpretiert, um ein seismo-stratigraphisches Modell für die quartäre Sediemtationsgeschichte des südwestlichen Schelfs des Schwarzen Meers erstellen zu können. Durch eine Kombination der Ergebnisse dieser Interpretation mit Bohrungsbefunden konnte eine qualitative und quantitative Analyse der regionalen Subsidenzgeschichte durchgeführt werden. Diese Analyse ermöglichte eine um die Einflüsse der Effekte von tektonischer Aktivität und Sedimentkompaktion bereinigte Quantifizierung von Meeresspiegelschwankungen im Schwarzen Meer während des Quartärs.

Ablagerungen des Mio-Pliozän bilden die stratigraphische Basis der Interpretation der reflexionsseismischen Messdaten. Oberhalb dieser Basis konnten vier seismo-stratigraphische Einheiten des Quartärs auf dem westlichen Schelf des schwarzen Meeres identifiziert werden. Diese Einheiten wurden in chronologischer Reihenfolge als Unit 4 – 1 bezeichnet (U4 – U1). Ablagerungen des Pliozän bilden sanft beckenwärts einfallende Schichten von relativ hoher und praktisch konstanter Mächtigkeit. Verschüttete Grabenstrukturen bezeugen den Einfluss extensionaler tektonischer Prozesse bis in das obere Pliozän. Starke Erosion auf dem inneren und mittleren Schelf kennzeichnet den Übergang zum Quartär und hinterliess eine ausgeprägt unebene Oberfläche der Pliozänen Ablagerungen. Auf dieser lagern heute eine dünne Schicht Sedimente des Quartärs und Holozäns. Dem Pliozän folgt Unit 4 (U4), diese umfasst Sedimente des ältesten Quartärs. Sie fallen steiler in Richtung Becken ein als die Schichten des Pliozäns und ihre Durchschnittsmächtigkeit ist geringer. Innerhalb von U4 konnte das älteste von insgesamt drei *Shelfedge*-Deltasystemen im Quartär beobachtet werden, das einen frühquartären Meeresspiegeltiefstand anzeigt. Eine deutlich ausgeprägte Winkeldiskontinuität markiert den Übergang zur nächstjüngeren Einheit Unit 3 (U3). Im älteren Teil von U3 konnten *coastal onlaps* beobachtet werden, die eine Periode mit niedrigem Meeresspiegel kennzeichnen. Progradierende Ablagerungen der nachfolgenden Transgression und Meerespiegel-Hochstand machen danach den jüngeren Teil von U3 aus. Ein erneut fallender Meeresspiegel führte dann zur Ausbildung einer weiteren regionalen Diskontinuität und im folgenden zur Ablagerung von Unit 2 (U2). In dieser Einheit befindet sich eine weitere Abfolge von deltaischen Sedimentschüttungen, die sich abgelagert haben, während sich der Meeresspiegel in der Nähe des zyklischen Tiefstands befand. Teile der älteren Sequenzen U4, U3 und U2 wurden später durch Erosion beseitigt und auf der dabei entstandenen, den gesamten Schelf betreffenden Diskontinuität konnte sich die jüngste

untersuchte Einheit Unit 1 (U1) ablagern. U1 kann zeitlich dem letzten eiszeitlichen Maximum sowie der Periode im unmittelbaren Anschluss zugeordnet werden.

Untergeordnete interne Diskontinuitäten innerhalb von U1 sind das Ergebnis von Meeresspiegelschwankungen höherer Ordnung, die den generellen transgressiven Trend seit der letzten globalen Vereisungsperiode überdecken. Diese Diskontinuitäten unterteilen U1 in drei Untereinheiten (U1-A – U1-C) in chronologischer Reihenfolge. Die älteste Untereinheit U1-A besteht aus einem progradierenden *Shelfedge*-Deltasystem, entstanden während des letzten eiszeitlichen Maximums. Dieses Deltasystem wird in Teilen von küstenparallelen Dünen überlagert, die ebenfalls U1-A zugeordnet werden. Die beiden jüngeren Untereinheiten U1-B und U1-C wurden während des nacheiszeitlichen Meeresspiegelanstiegs und des bis in die heutige Zeit andauernden Hochstands abgelagert. Die Sedimente der Untereinheit U1-B füllen dabei kleinräumige topographische Senken in der unebenen, erodierten Oberfläche der älteren Einheiten U3 und U2, während U1-C von einem Paket sich landwärts verdickenden, retrogradierenden, keilförmigen Körpern aufgebaut ist, die weite Teile des heutigen Schelfgebietes im westlichen Schwarzen Meer bedecken. In manchen Gebieten konnten wiederum konservierte Dünenzüge beobachtet werden, die nach Größe und äußerer Form denen in U1-A beschriebenen ähneln. Es kann spekuliert werden, dass diese Dünensysteme zwei getrennte Phasen mit niedrigen Meeresspiegelständen widerspiegeln: eine erste noch während oder kurz nach dem letzten eiszeitlichen Maximum und eine zweite nach dem ältesten Holozän und Ablagerung von U1-B.

Indikatoren für Meeresspiegeltiefstände so wie *topset-to-foreset* Übergänge in *Shelfedge*-Deltasysytemen oder coastal onlaps innerhalb der kartierten seismo-stratigraphischen Einheiten wurden als Kalibrierungspunkte für die Rekonstruktion quartärer Meeresspiegelschwankungen herangezogen. Um vergangene Meersspiegelstände anhand von Tiefstandindikatoren festlegen zu können, muss der potentielle Einfluss tektonischer Prozesse und sedimentärer Subsidenz bestimmt und herausgerechnet werden. Um den Anteil tektonisch bedingter Subsidenz zu quantifizieren und einen regionalen Trend zu bestimmen, wurde eine Subsidenzanalyse entlang zweier idealisierter Profile durchgeführt. Das erste liegt auf dem südwestlichen Schelf und verbindet den nördlichen Türkischen Sektor des Schwarzen Meer mit dem südlichen Rumänischen Sektor und das zweite Profil durch den nordwestlichen Schelf vom südlichen Rumänischen Sektor in den Ukrainischen Sektor westlich der Krimhalbinsel.

Eine Analyse des ersten Profils zeigt, dass die tektonisch bedingte Subsidenz im Bulgarischen Sektor während des Quartärs mehr oder minder linear von NNE to SSW ansteigt; besonders starke tektonische Aktivität ist indiziert während der Ablagerung von U1. Entlang des zweiten Profils wurde die quartäre Subsidenz in verschiedenen Wassertiefen bestimmt. Die Ergebnisse zeigen zunehmende Subsidenzbeträge mit ansteigender Wassertiefe, entsprechend der Modellvorstellung für *Atlantic-type* Kontinentalränder an denen Subsidenz mit konstanten Raten um eine räumlich fixierte *hinge line* auftritt. Grosse, regionale Strukturen, wie die Peceneaga Camena und Sulina Tarkankut Störungssysteme zerteilen die quartäre Abfolge auf dem nordwestlichen Schelf in ausgedehnte Blöcke mit signifikanten Unterschieden in den beobachteten Subsidenzraten; die höchsten Werte können für die Umgebung des Viteaz Canyons angenommen werden, während die südwestlichen und nordöstlichen Teile des Profils auf eine geringere Beeinflussung durch Subsidenz hindeuten. Die geringsten Subsidenzbeträge wurden im Nordosten beobachtet.

Die Rekonstruktion von Meeresspiegeltiefständen führte zum im Folgenden beschriebenen quartären seismo-stratigraphischen Modell für den westlichen Schelf im Schwarzen Meer: Die älteste seismo-stratigraphische Einheit U4 enstand während des frühen Quartärs und enthält ein *Shelfedge*-Deltasystem, das einen Meeresspiegeltiefstand zur Zeit seiner Bildung anzeigt. Dieses System korreliert vermutlich mit der Günz-Kaltzeit (~900 ka). Extrapolation (auf Grund der relativ weit auf dem inneren Schelf gelegen Position des Deltasystems) von Ergebnissen der Subsidenzanalyse legt einen Paläomeeresspiegel nahe, der ungefähr dem heutigen entspricht. Coastal onlap Reflektorkonfigurationen markieren einen Meeresspiegeltiefstand während der Sedimentation der nachfolgenden Einheit U3; entsprechend der Zuordnung von U4 kann U3 also der Mindel-Kaltzeit (~500 ka) zugeordnet werden, mit einem Meerespiegel zur Zeit der Bildung von U3 von −140 m. Das nächstjüngere Deltasystem in U2 kann der Riss-Kaltzeit (~150 ka) zugeordnet werden; für diese Periode wird ein Meeresspiegeltiefstand von ca. -125 m angenommen. Ein weiterer Meeresspiegeltiefstand wurde schliesslich zur Zeit des letzten eiszeitlichen Maximums mit -116 m erreicht. Die Entstehung des *Shelfedge*-Deltasystems in U1-A kann hiermit in Verbindung gebracht werden.

Der Meeresspiegel des Schwarzen Meeres – zu dieser Zeit ein Süsswassersee ohne Verbindung zu anderen Meeresgebieten – stieg im Zuge der globalen Klimaerwärmung während der Endphase der letzten Eiszeit und während des Holozäns. Die Untereinheit U1-B ist auf Tiefen grösser als -85 m beschränkt und kann mit untergeordneten Phasen von Meeresspiegelstillstand in Verbindung gebracht werden. Die Ablagerung dieser Einheit ist

vermutlich das Produkt von pulsartig eingetragenem Schmelzwasser in das Schwarze Meer zwischen 18 und 15 ka und endete, als der Meerespiegel unter -90 m gefallen war. Während dieses nacheiszeitlichen Meeresspiegeltiefstands entstanden für Küstengebiete typische Sedimentkörper wie z.B. Dünen auf dem äusseren Schelf. Der weiterhin ansteigende globale Meeresspiegel erreichte schliesslich um 8.4 ka die für eine Verbindung zum Ozean nötige Höhe und Meerwasser konnte in das bis dahin mit Süsswasser gefüllte Schwarze Meer eindringen. Die nun folgende Transgression muss schnell genug stattgefunden haben um zumindest einen Teil der in sub-aerischen Küstengebieten entstandenen Strukturen zu erhalten. Die retrograd abgelagerten Sedimentpakete der jüngsten Untereinheit U1-C entstanden im weiteren Verlauf der Holozänen Transgression und indizieren zumindest mehrere deutlich verlangsamte Phasen des Meeresspiegelanstieges auf dem Weg zu den heute vorliegenden Verhältnissen.

Rezumat

Interpretarea de date seismice de mare și foarte mare rezoluție de pe șelful vestic al Mării Negre a evidențiat un model seismico-stratigrafic de depozite ale Cuaternarului Trâziu pe șelful sud-vestic al Mării Negre. Acest model a fost utilizat împreună cu date de sondă pentru o analiză de subsidență regională, astfel încât influența proceselor tectonice și a compactării cu sedimente putând fi excluse în estimarea fluctuațiilor nivelului mării.

Având ca bază formațiunea Mio-Pliocenă, patru unități seismico-stratigrafice au fost identificate în cadrul Cuaternarului de pe șelful vestic al Mării Negre; în ordine cronologică, acestea au fost denumite Unit 4 (U4) – Unit 1 (U1). Depozitele pliocene sunt formate de strate ușor înclinate în direcția bazinului, cu grosimi mari și relativ uniforme. Prezența structurilor de graben îngropat atestează influența proceselor tectonice până în Pliocenul Târziu. Ulterior, eroziunea puternică a dus la formarea unei suprafețe inegale pe șelful mediu și extern, care mai târziu a fost suprapusă de un strat subțire de depozite cuaternar-holocene. Pliocenul a fost urmat de prima secvență seismică cuaternară observată. (Unit 4, U4); aceasta conține strate de vârstă Cuaternar Inferior, care sunt înclinate în direcția bazinului la un unghi mai mare decât al depozitelor pliocene. În cadrul unității U4 a fost observat cel mai vechi dintre cele 3 sisteme deltaice de margine de șelf din area de studiu, care probabil marchează un lowstand al Cuaternarului Inferior. Tranziția către unitatea U3 este marcată de o discontinuitate unghiulară bine dezvoltată. La partea bazală a unității U3 au fost identificate onlap-uri costale, confirmând existența unei perioade de lowstand, în timp ce strate progradante, depuse în timpul perioadelor ulterioare de transgresiune și highstand, caracterizează partea superioară a unității. Coborârea ulterioară a nivelului mării a condus la formarea următoarei discontinuități majore; în timpul lowstand-ului corespunzător a început depunerea unității U2, caracterizată de o succesiune de lobi deltaici pe șelful extern. Unitățile U4, U3 și U2 sunt marcate de o discontinuitate regională de trunchiere erozională prezentă pe întreg șelful. Aceste unități sunt suprapuse de sedimente ale celei mai tinere unități, U1. Unitatea U1 a fost formată în timpul ultimului lowstand glaciar.

În cadrul unității U1 pot fi observate discontinuități interne minore, care evidențiază tendința generală de transgresiune începand cu maximul ultimului glaciar. U1 a fost ulterior divizată în 3 subunități (în ordine cronologică, de la U1-A până la U1-C). Subunitatea U1-A este formată din sisteme deltaice progradante de margine de șelf, parțial suprapuse de dune paralele cu plaja. U1-B și U1-C au fost depuse în timpul ridicării postglaciare a nivelului mării și a highstand-ului recent. Sedimente ale subunității U1-B au fost depuse sub formă de mici

depresiuni topografice la partea superioară a suprafeței erozionale a unităților U3 și U2, în timp ce U1-C formează un pachet de pene retrogradaționale îngroșate în direcția uscatului, care acoperă arii extinse ale șelfului actual. În anumite zone, formațiuni în formă de dune au fost observate în cadrul subunității U1-C, care se identifică în formă și mărime cu dunele descrise mai sus. Presupunem că aceste dune marchează două faze ale lowstand-ului nivelului mării: prima în timpul și imediat după maximul ultimului glaciar, iar cea de-a doua în timpul perioadei care a urmat Holocenului Timpuriu, după sedimentarea subunității U1-B.

Indicatori seismici ai perioadei de lowstand, cum ar fi tranziții de la topset la foreset ale sistemelor deltaice de margine de șelf sau onlap-uri costale identificate în unitățile seismice, au fost interpretate pentru reconstituirea fluctuațiilor nivelului mării din timpul Cuaternarului Trâziu în Marea Neagră. Pentru a deduce paleo-nivelul mării din acești indicatori de lowstand, s-a luat în considerare influența proceselor tectonice și a subsidenței sedimentare; pentru a cuantifica subsidența tectonică și a-i evalua tendința regională, s-a realizat o analiză de subsidență de-a lungul a două profile, unul traversând șelful sud-vestic, de la sectorul nord turc până la sectorul sud românesc, iar celălalt traversând șelful nord-vestic, de la sectorul sud românesc până la sectorul ucrainean din Peninsula Crimeea.

Primul profil arată că subsidența tectonică în sectorul bulgar a avut o evoluție liniară în timpul Cuaternarului, crescând, în general, de la NNE la SSW. Se presupune o activitate tectonică intensă pe șelful central bulgar în timpul depunerii unității U1. De-a lungul celui de-al doilea profil, analiza de subsidență a fost realizată pentru toată perioada cuaternară la diverse adâncimi ale apei. Se observă o creștere a subsidenței în direcția bazinului, ceea ce este în concordanță cu modelul unei margini de subsidare de tip Atlantic. Formațiuni tectonice regionale, cum ar fi faliile Peceneaga-Camena și Sulina-Tarkinkut, împart secțiunea cuaternară de nord-vest în blocuri cu diferențe semnificative ale ratelor de subsidență; valori maxime ale ratei de subsidență au fost identificate în apropierea Canionului Viteaz. Părțile de sud-vest și nord-est au fost mai puțin afectate de subsidență, cea mai scăzută influență fiind sesizată în nord-est.

Reconstituirea lowstand-urilor nivelului mării a condus la următoarea clasificare a unităților seismico-stratigrafice în Cuaternarul de pe șelful vestic al Mării Negre. Cea mai veche unitate seismico-stratigrafică, U4, este de vârstă cuaternar-timpurie și conține un sistem deltaic de margine de șelf, indicând un lowstand al nivelului mării. Acest sistem a fost atribuit perioadei glaciarului Günz (~900 MA). Rezultatele analizei de subsidență au fost extrapolate pentru a lua în considerare poziția relativ apropiată de țărm a indicatorului de lowstand, iar nivelul corespunzător al mării a fost estimat a fi aproximativ comparabil cu

nivelul actual al mării. Onlap-urile costale marchează un lowstand în perioada depunerii unității U3, acumulată probabil în timpul glaciarului Mindel (~500 MA); nivelul mării a fost la acea perioadă de -140 m. Secvența deltaică găsită în unitatea U2 a fost atribuită lowstand-ului nivelului mării din timpul glaciarului Riss (~150 MA), corespunzător unei adâncimi a apei de 125 m. Un alt lowstand a avut loc în jurul LGM, la 20 MA, care a atins 116 m în adâncime și care a dus la depunerea lui ·A (subunitatea U1-A).

În timpul încălzirii globale de la sfârșitul glaciarului și Holocenului, nivelul Mării Negre a crescut ca urmare a condițiilor climatice. Subunitatea U1-B a fost interpretată ca fiind formată în timpul unor faze minore de stillstand ale nivelului mării și a fost găsită la o adâncime de peste 85 m. Depunerea subunității U1-B este probabil legată de etapele de topire a apei dintre 18 și 15.5 MA și s-a oprit după ce nivelul mării a scăzut din nou sub 90 m. În timpul acestui lowstand post-glaciar, pe șelful extern s-au depus formațiuni sedimentare de coastă. Creșterea globală a nivelului mării a atins Strâmtoarea Bosfor la aproximativ 8.4 MA, când apa marină a pătruns în Marea Neagră; transgresiunea care a urmat trebuie să fii fost suficient de rapidă pentru a fi păstrat formațiunile de coastă formate în timpul lowstand-ului precedent. Pachetele retrogradaționale ale subunității U1-C s-au format în timpul transgresiunii holocene, indicând faze ușoare de ridicare a nivelului mării care au condus la condițiile actuale.

1. Introduction

Among the marginal seas of the world, the Black Sea takes up a special position with a unique, almost isolated geographical position: It covers an area of more than 400,000 km² and is connected to the global oceans only through a chain of narrow and shallow sea straits via the Marmara Sea and the Mediterranean Sea.

The Black Sea has been the subject of numerous scientific investigations since the first bathymetric and sedimentological studies carried out by Andrusov in 1890 (Andrusov, 1890). Examples of important early research efforts are the expeditions of the American R/V Atlantis II in 1969 (Degens & Ross, 1970, 1974) and R/V Knorr in 1988 (Murray, 1991). In 1995, the Black Sea was the target of the Deep Sea Drilling Project (DSDP Leg 42B) and several deep holes were drilled in the Black Sea Basin for scientific purposes (Ross et al., 1978).

These groundbreaking research programs focused mainly on the youngest sedimentary history, geochemistry, development and structure or the hydrographical regime of the Black Sea. They demonstrated that the Black Sea is one of the most interesting areas for paleoenvironmental research: Because of its geographical isolation, any change in the basin itself as well as in the adjacent land areas evokes a particularly sensitive reaction. This leads in turn to paleoenvironmental records of unprecedented detail.

One project that takes advantage of this high-resolution opportunity is the ASSEMBLAGE project (ASSEssMent of the BLAck Sea sedimentary system since the last Glacial Extreme; Section 1.1). It provides the framework for the present dissertation. The ASSEMBLAGE project benefited from results from three German-Romanian-Russian research cruises carried out in the western Black Sea off Romania in 1992, 1993 and 1994 (e.g., Wong et al., 1994), from the German-Russian project GHOSTDABS (Gas Hydrates: Occurrence, Stability, Transformation, Dynamics and Biology in the Black Sea) west of the Crimean Peninsula, the Ukraine, as well as from the French-Romanian projects BLASON 1 and 2 (BLAck Sea Over the Neoeuxinian) carried out between 1996 and 2001.

1.1 The ASSEMBLAGE project

ASSEMBLAGE (Fig. 1.1) is a multi-national, multi-disciplinary research project organized as a cooperation of 14 European universities and research institutions from France, Germany, Romania, Spain, Italy and Bulgaria. The project was funded by the European

Union within the Fifth Research and Development Framework Program (1998 to 2002) under the key action 'Sustainable Marine Ecosystems' in the larger thematic group 'Energy, Environment and Sustainable Development'; one of four in the framework program.

Fig. **1.1**: ASSEMBLAGE project logo

The four central scientific questions tackled by the project are:

1. What are the history of and the factors controlling the connection between the Mediterranean and the Black Sea?

2. What do we know about the architecture and growth pattern of the sedimentary systems in the northwestern Black Sea, including the Danube prodelta and the Danube-Dniestr and Dniepr deep-sea fans?

3. What can be derived from the sedimentary record on past global changes regarding the climate, the structure and functioning of different ecosystems, and sea-level variation?

4. How are gas hydrate occurrences distributed and is a preliminary economic evaluation possible?

The project was organized into 10 work packages. They cover a broad spectrum of research topics from geomorphology, geochemistry, stratigraphy and geophysics through gas hydrate research to hydrographical and sedimentary modeling.

This study is a part of the work package "Seismic and Sequence Stratigraphy", in which a sequence stratigraphic model of the southwestern Black Sea since the last glacial maximum was established through the combination of geophysical measurements and geological observations.

1.2 The aim of this study in the context of recent Black Sea research

The response of the Black Sea to environmental changes that occurred after the last glacial maximum is the subject of a lively scientific debate during the past 20 years. An issue of particular interest is sea-level changes associated with global warming in post-glacial times. Figure 1.2 shows a graphical comparison of the Black Sea region during the last glacial and the present situation, illustrating the dramatic loss of dry land due to rising sea-levels.

The development of the Black Sea region moved into the center of attention of not only the scientific community but also of the general public after Ryan et al. (1997) published a study on the northern Black Sea and suggested a 'catastrophic' event in the Black Sea region: The rising post-glacial sea-level breached the Strait of Bosphorus and inflowing marine waters re-filled the Black Sea Basin in a catastrophically short time, transforming the giant freshwater lake with a water level of around -150 m into the modern Black Sea.

This event is supposed to have contributed to the myth of 'Noah's flood' (Mestel, 1997), because the catastrophic flood that occurred around 7100 years before present inundated the living space of early human settlers on the Black Sea shelves. Their memory of this event found its way into the myths of the ancient population along the Black Sea coast and finally into the biblical story of Noah.

The hypothesis quickly found its supporters and dissenters, and the controversy is still not resolved today. The significant rise of the water level in the Black Sea after the last glacial is in itself undisputed, but the timing and characteristics remain controversial. Several studies support the flood hypothesis (e.g., Lericolais et al., 2006; Ryan et al., 2003; Algan et al., 2002; Uchupi & Ross, 2000; Ballard et al., 2000; Ryan & Pitman, 1999; Brown, 1999; McInnis, 1998). Others disagree, however, some even arguing that it was in fact the Black Sea that breached the Bosphorus and waters have been flowing into the Marmara Sea during the early Holocene (e.g., Hiscott et al., 2007; Konikov et al., 2007; Yanko-Hambach, 2006, 2004; Konikov, 2005, 2004; Lavchenkov & Kadurin, 2005; Kerey et al., 2004; Chepalyga et

al., 2002; Kaminski et al., 2002; Aksu et al., 2002a; Hiscott & Aksu, 2002; Aksu et al., 1999, Aksu et al., 1995a, b).
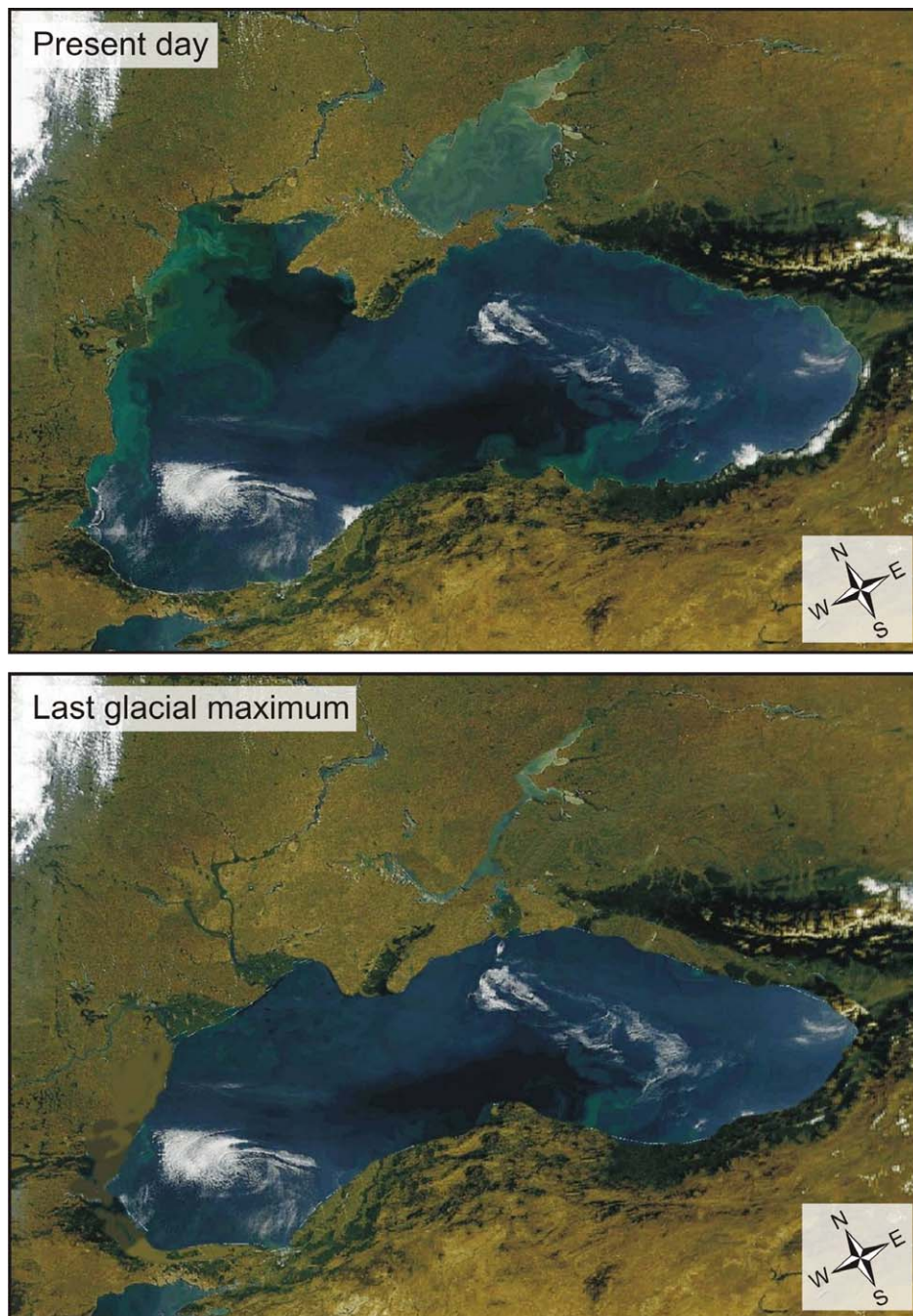
Fig. **1.2**: Graphical reconstruction of environmental changes in the Black Sea region since the last glacial maximum. The upper panel shows a recent satellite image of the Black Sea and its surroundings. The lower panel reconstructs the region at the time of the last glacial maximum, showing the vast dry shelf areas of the northwestern and western Black Sea. Depending on the much disputed timing of the sea-level change that lead to the present picture, the circumstances shown in the lower panel might have lasted much longer than the last glacial and the transition might have taken place in a 'catastrophic' flooding event. Source for satellite imagery and paleogeographic reconstruction: http://daac.gsfc.nasa.gov.

The work presented here aims at adding further pieces to the puzzle of the youngest geological history of the Black Sea, so that the existing models of sea-level development can be better verified or refuted. By establishing a link to the underlying geology as well as to environmental changes that occurred in the Black Sea and its surrounding areas, it is hoped that our results may be considered less controversial.

2. The Black Sea region

2.1 Geography, climatology

The Black Sea covers an area of approximately 423,000 km^2 between the southeastern European and northwestern Asian mainlands. Its extents are about 1,000 km in the east-west direction and about 600 km from north to south.

Six states border the Black Sea: Ukraine and Russia to the north, Georgia to the east, Turkey to the south and Romania and Bulgaria to the west. Their political boundaries and the some important geographical features of the region such as the main rivers or mountain ranges are shown in Fig. 2.1.
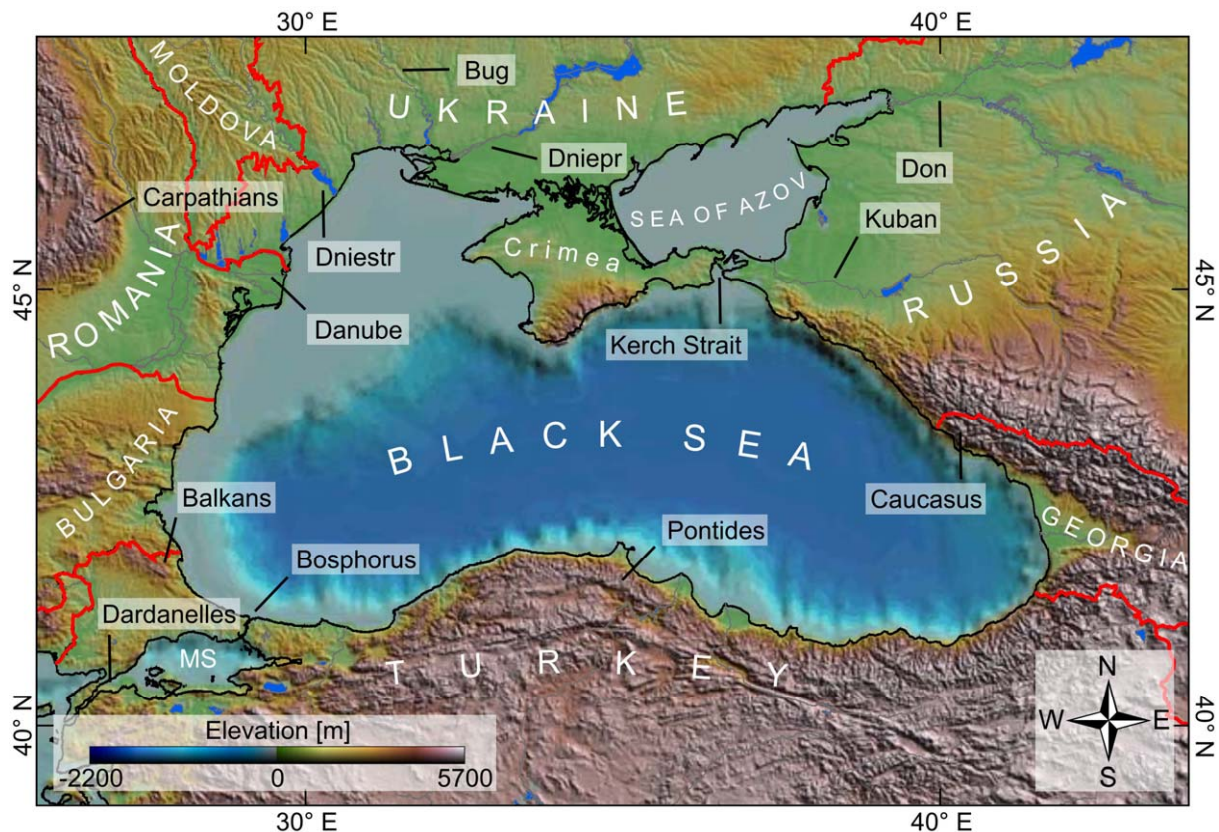
Fig. 2.1: Topographic map of the Black Sea and the surrounding countries with their main geographical features: Mountain ranges, rivers, sea straits. Political boundaries are drawn in red. Abbreviation: MS – Marmara Sea.

A number of Alpine mountain chains surround the Black Sea, namely the Caucasian and Crimean mountains in the north, the Pontides in the south and the Balkans in the west. Narrow and shallow straits connect the Black Sea to the Mediterranean: The Bosphorus strait

connects the Black Sea and the Marmara Sea, and the Dardanelles connect the Marmara and Mediterranean Seas. The Kerch Strait in the north is the connection to the Sea of Azov, an extremely shallow sea area (average depth 13 m) between Russia and the Ukraine.

The western Black Sea lies in the transition area between three climatic zones: (1) a temperate continental climatic zone that dominates the northern Black Sea and the eastern Danube lowlands with savannah grasslands and <600 mm yr^{-1} precipitation, (2) a humid climatic regime of the mid-latitudes in southeastern Europe with temperate mixed forests and a precipitation of >1000 mm yr^{-1} typical of the western Black Sea, and (3) Mediterranean climate which prevails in the southwestern Black Sea towards the Sea of Marmara (Mudie et al., 2002).

2.2 Hydrology, physical oceanography

The volume of the Black Sea is about 534,000 km^3. Several major European rivers drain into the northwestern Black Sea, namely the Danube in Romania and Dniepr, Dnjestr and Bug in the Ukraine. The Danube is Europe's second largest river and is by far the largest source of freshwater input into the Black Sea. The mean annual freshwater discharge of the Danube was about 190.7 km^3 yr^{-1} before damming in 1972 (Iron Gates 1) and 1984 (Iron Gates 2; Panin & Jipa, 2002, 1998; Bondar et al., 1991). In total, the freshwater input via rivers amounts to ~370 km^3 yr^{-1} (Tab. 2.1). This inflow shows clear seasonal variations with peak levels in April and May.

	Length [km]	Drainage basin area [km²]	Water flux [km³/yr]	Bedload transport [10⁶ t/yr]
1. Northwestern Black Sea				
Danube	2860	817000	190.70	51.70
Dniestr	1360	72100	9.80	2.50
Dniepr	2285	503000	52.60	2.12
Southern Bug	806	63700	2.60	0.53
	Sub-total 1:	1455800	255.70	56.85
2. Sea of Azov				
Don	1870	442500	29.50	6.40
Kuban	870	57900	13.40	8.40
	Sub-total 2:	500400	42.90	14.80
3. Others				
Caucasian coastal rivers			41.00	29.00
Anatolian coastal rivers			29.70	51.00
Bulgarian coastal rivers			3.00	0.50
	Total:	1956200	372.30	152.15

Tab. 2.1: Length, drainage basin size, freshwater input and sediment load of river systems draining into the Black Sea, from Panin & Jipa (1998).

The drainage basin of the Danube covers an area of more than 817.000 km^2. Together with large areas of eastern Europe that are drained by the Dniepr and the Don, and parts of northern Turkey and Georgia drained by numerous smaller rivers, the complete drainage basin has an area of 2,300,000 km^2 (Degens et al., 1978). It covers in total about 20% of central and eastern Europe (Fig. 2.2; UNESCO 1993, 1969).

Today there is a yearly net export of ~300 km^3 yr^{-1} water from the Black Sea to the Mediterranean across the Bosphorus Strait and the Dardanelles, because precipitation over the Black Sea (~300 km^3 yr^{-1}) and freshwater input via rivers (~350 km^3 yr^{-1}) exceed the regional evaporation of ~350 km^3 yr^{-1} (Özsoy et al., 1995).
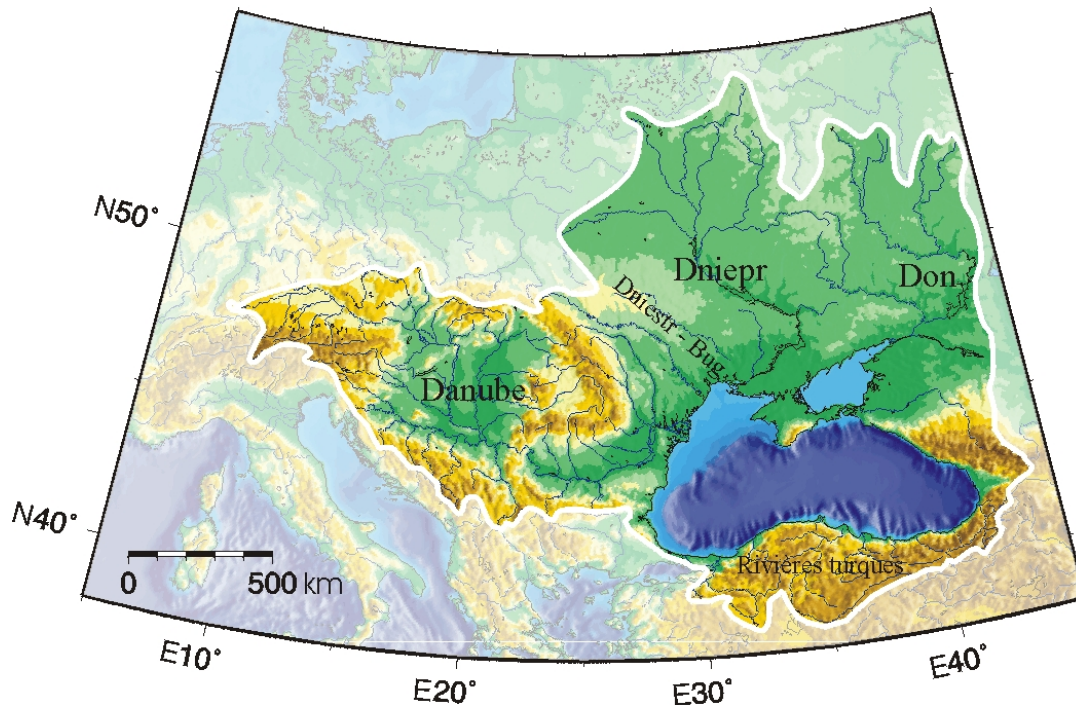
Fig. **2.2**: Drainage basin of the Black Sea; from Gillet (2004). The large river systems Danube, Dniestr-Bug, Dniepr and Don situated to the north and northwest of the Black Sea drain about 20% of central and eastern Europe. A number of rivers in northern Turkey and Georgia contribute to a much smaller extent (compare Tab. 2.1).

Because of the narrow outlet through the Bosphorus Strait, the Black Sea level follows the inter-annual variations of the freshwater input to ~50 cm (Özsoy et al., 1995, 1996). Smaller-scale sea-level oscillations occur in response to variations in barometric pressure (Özsoy et al., 1996). The Black Sea-level lies on average 30 cm (±10 cm) above the level of the Sea of Marmara (Beşiktepe et al., 1994) and the Marmara Sea-level is approximately 5-27 cm above the level of the northern Aegean Sea (Bogdanova, 1969).
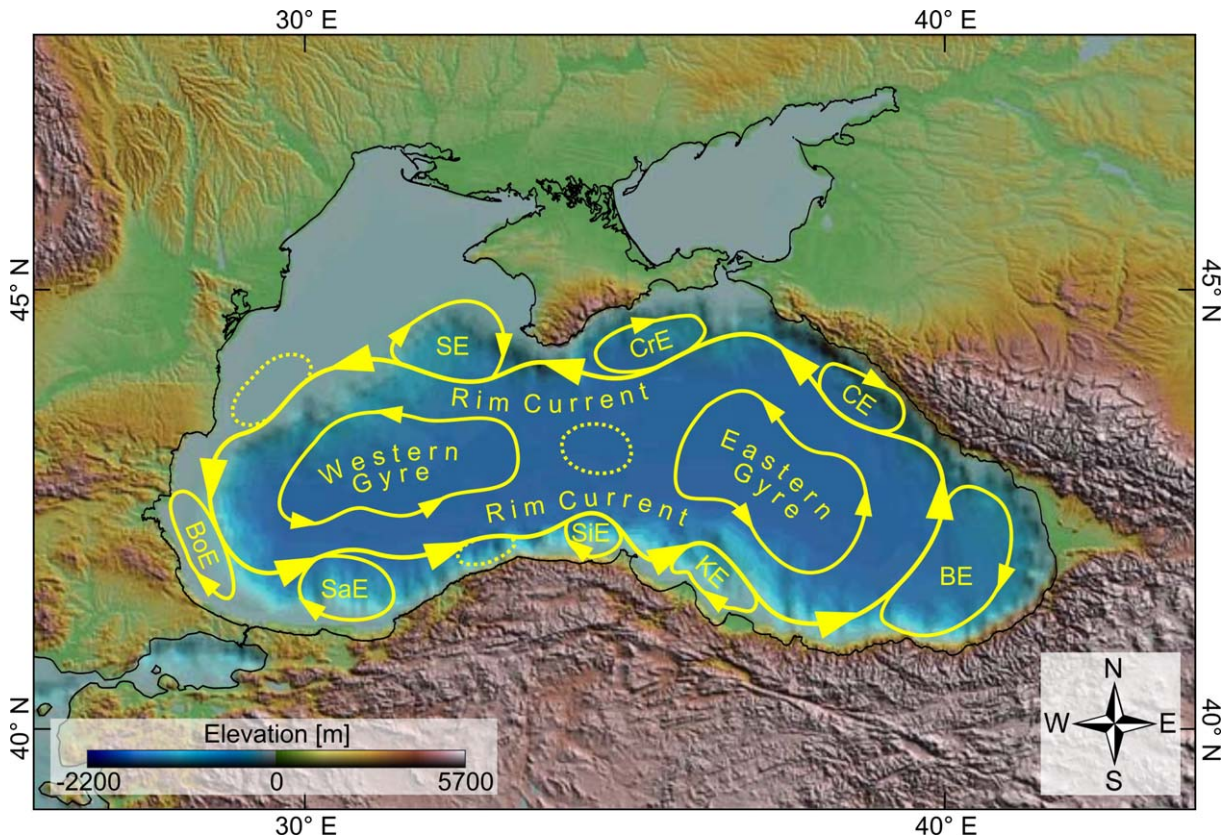
Fig. **2.3**: Schematic surface-water circulation in the Black Sea (from Oğuz et al., 1993). Abbreviations: SE – Sevastopol Eddy, CrE – Crimea Eddy, CE – Caucasus Eddy, BE – Batumi Eddy, KE – Kizihrmak Eddy, SiE – Sinop Eddy, SaE – Sakarya Eddy, BoE – Bosphorus Eddy.

2.3 Physiography

There are four main physiographic provinces in the Black Sea Basin: The continental shelf, the slope, the basin apron and the abyssal plain (Mamaev & Musin, 1997). Fig. 2.4 shows the principal bathymetry of the Black Sea Basin, the spatial distribution of the four physiographical provinces is shown in Fig. 2.5.

The **continental shelf** in the Black Sea is in most areas delineated by the 100 m isobath (Degens & Ross, 1974). In front of the Danube mouth it reaches a depth of 120, on the northern shelf offshore of the Crimea Peninsula and at the outlet of the Sea of Azov, it extends to a depth of 130 m. Locally around the Viteaz Canyon (Fig. 2.4) even 140 m (south of the Canyon) or 170 m (north of the Canyon) are reached; most likely because of recent tectonic movements. The western and the northwestern shelves are wide, reaching 140 km off the Danube mouth and a maximum width of 190 km off western Crimea. Near the Kerch Strait (Fig. 2.1) the shelf is about 40 km wide. The southern and eastern shelves are much narrower: From 20 km to almost 0 km in the southeastern corner of the Black Sea.
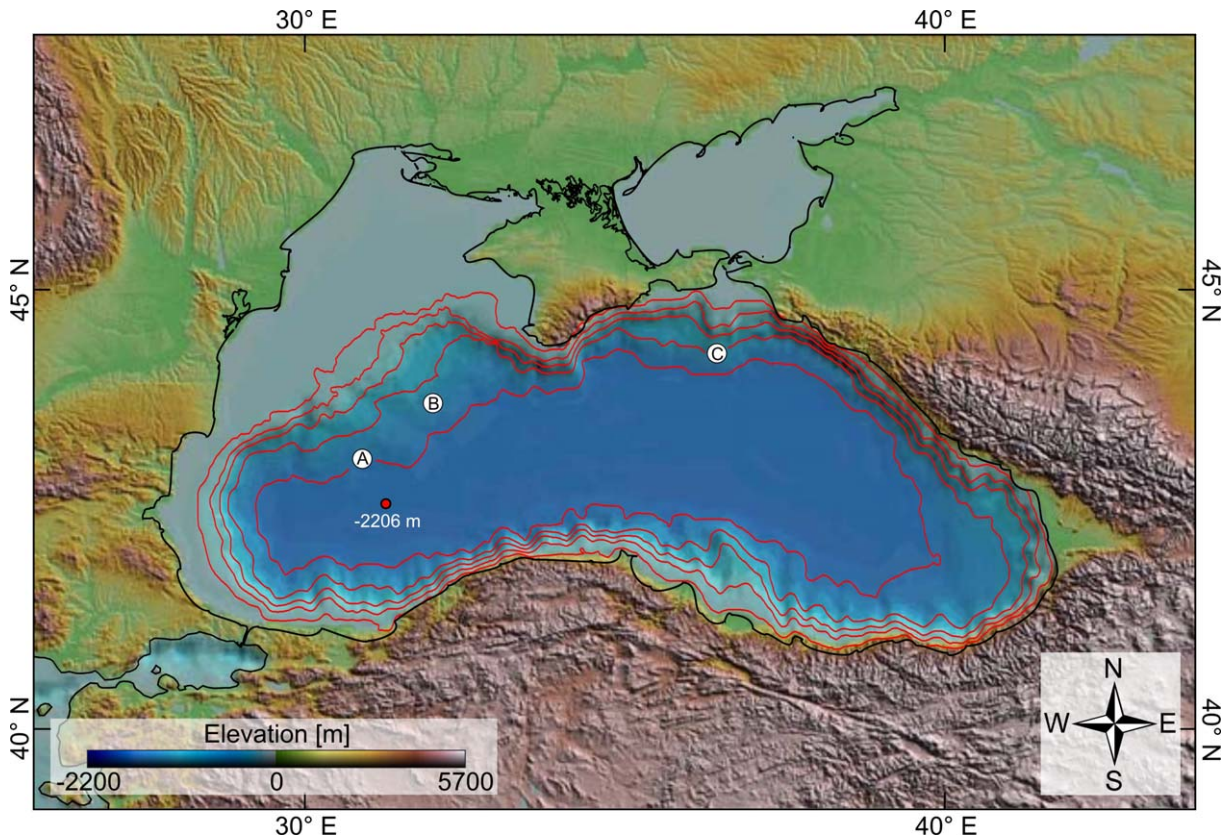
Fig. **2.4**: Simplified bathymetry of the Black Sea basin. The red lines give the 100, 500, 1500 and 2000 m isobaths; the red dot marks the deepest point within the present-day Black Sea basin at a water depth of 2,206 m. A and B mark the position of the Danube and Dniepr/Dniestr deep sea fans in the northwestern Black Sea, C marks the Don/Kuban fan in the northeastern Black Sea.

The **continental slope** is usually steep (~2.5%; Ross et al., 1974) and highly dissected by canyons, especially in the areas with narrow shelves in the eastern and southern Black Sea. The slopes of the northwestern and northern Black Sea are less steep, high fluvial sediment input leads instead to the deposition of sedimentary fans: The Danube and the Dniepr/Dniestr fan systems are situated on the northwestern slope, the Don/Kuban fan lies off the Kerch Strait that connects the Black Sea and the Sea of Azov.

Terrestrial sediments are deposited on the **basin apron**. It is less steep than the slope, gradients range from 0.1% to 2.5% and its width is a function of sediment input, with maximum values reached in the sedimentary fans of the northwestern Black Sea.

The central Black Sea Basin is characterized by the flat **abyssal plain** with slope gradients of less than 0.1%. The deepest point of the Black Sea lies in the western part of the abyssal plain; it has a water depth of 2,206 m.
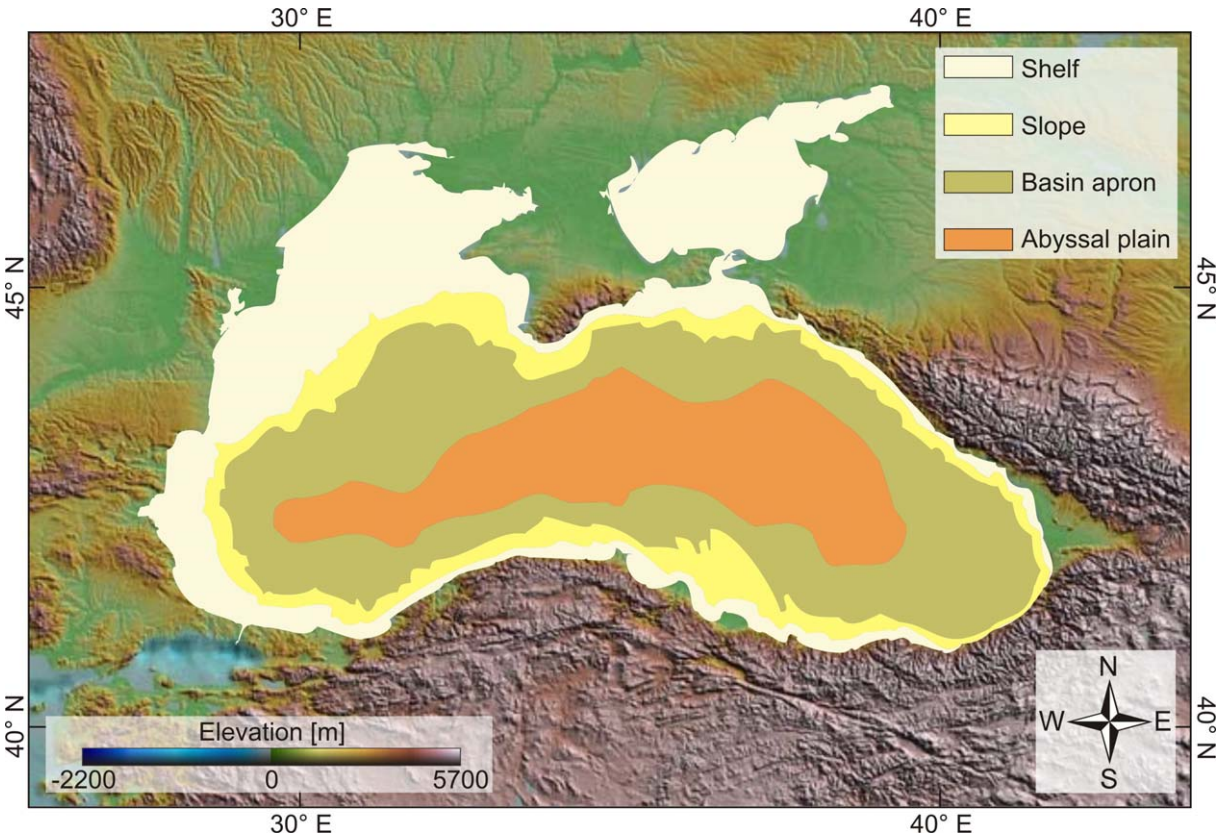
Fig. **2.5**: Distribution of the four physiographical provinces continental shelf, slope, basin apron and abyssal plain in the Black Sea. After Mamaev & Musin (1997).

3. Regional Geology

3.1 Introduction

For an overview of the tectonics and sedimentary geology in the Black Sea region, a stratigraphic classification that differs from the Mediterranean standard during Oligo-Pliocene times is used. The nomenclature is shown in Tab. 3.1.

Era	System	Series	Epoch	Stages	Regional stages	Age [ma]
Cenozoic				Quaternary		1.75
	Neogene	Pliocene		Gelasian	Romanian	
				Placenzian		4.5
				Zanclean	Dacian	5.3
		Miocene	Late	Messinian	Pontian	
				Tortonian	Meotian	
					Sarmatian	11
			Middle	Serravalian	Badenian	
				Langhian		
			Early	Burdigalian		15.8
				Aquitanian	Maykopian	20.3
	Paleogene	Oligocene	Late	Chattian		23.5
			Early	Rupelian		28
		Eocene	Late	Priabonian		33.7
				Bartonian		37
			Middle	Lutetian		40
			Early	Ypresian		46
		Paleocene	Late	Thanetian		53
				Selandian		
			Early	Danian		65

Tab. 3.1: Geological timescale of the Cenozoic era. Fields underlain in yellow give the stage classification used in this study. For the western Black Sea, regional stages that differ from the Mediterranean nomenclature are used for the Oligo-Pliocene. After Gillet et al. (2003).

3.2 Regional tectonic framework

The Black Sea Basin was formed by back-arc extension when oceanic crust of the Tethys Ocean was subducted along its northern margin during Triassic to Miocene times (Okay et al., 1994; Görür, 1988; Zonenshain & Le Pichon, 1986; Degens et al., 1986; Dercourt et al., 1986; Letouzey et al., 1977; Boccaletti et al., 1974; Adamia et al., 1974).
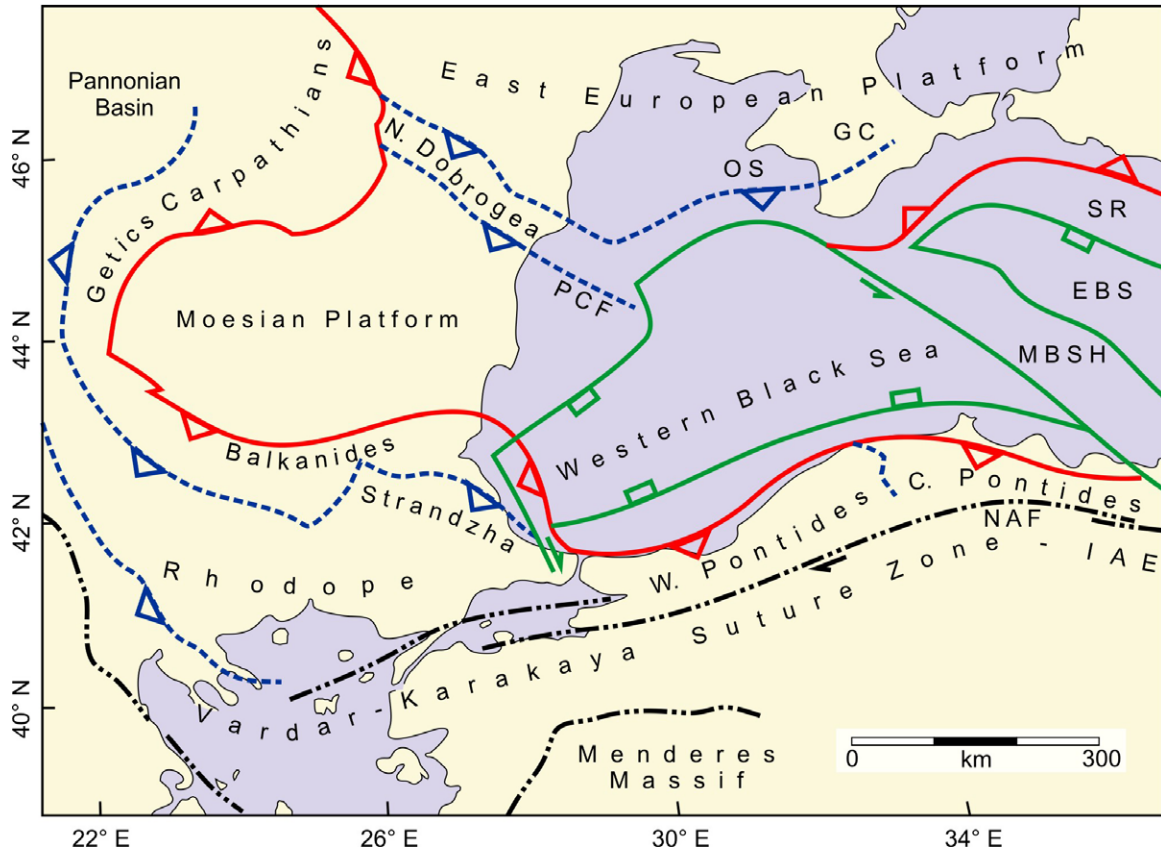
Fig. 3.1: Recent large-scale tectonic regime of the Black Sea region; from Banks & Robinson (1997). Red lines with thrust marks give Alpine (Tertiary) compressive fronts, blue dashed lines give Cimmeride (Jurassic) thrusts. Green lines with downthrown marks give the extensional and strike-slip boundaries of the Western and Eastern (EBS) Black Sea Basins. Black lines with a dash-double-dot signature mark the superimposed Cimmeride (Vardar-Karakaya) and Alpine (Izmir-Ankara-Erzincan, IAE) suture zones and the North Anatolian Fault System (NAF). Abbreviations: GC – Gorniy Crimea; MBSH – Mid-Black Sea High; OS – Odessa Shelf; PCF – Peceneaga Camena Fault; SR – Shatsky Ridge.

The Black Sea basin is separated structurally in two sub-basins with different timing and orientation of extension: The western and eastern Black Sea basins (Fig. 3.1; Okay et al., 1994; Finetti et al., 1988; Ross et al., 1974). The western Black Sea basin has an oceanic basement and a sedimentary cover of up to 19 km thickness whereas the basement of the eastern Black Sea basin is formed by continental crust and 10-12 km thick sediments. These

two parts are separated by a strike-slip system along the Mid Black Sea Ridge and Andrusov Ridge which are made of continental crust and a 5-6 km thick sedimentary cover.

The plate tectonic development of the Black Sea region is decisively influenced by the stepwise closure of the Tethys Ocean and the subsequent collision between the African and Eurasian plates. Snapshots of the plate tectonic history since the Triassic are shown in Fig. 3.2.

A - Late Triassic (210 ma)
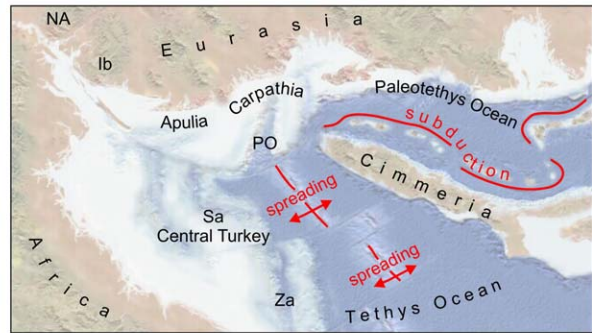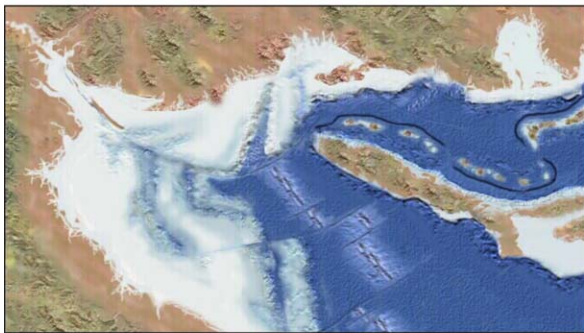
B - Middle Cretaceous (100 ma)
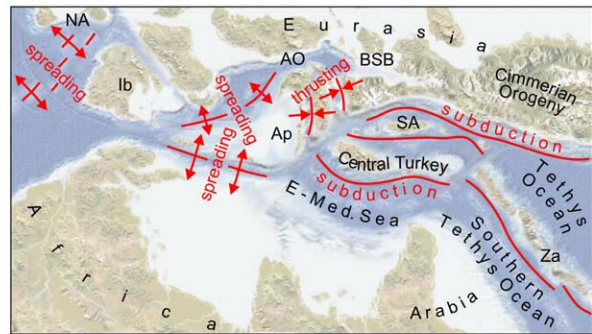
C - Late Miocene (6 ma)
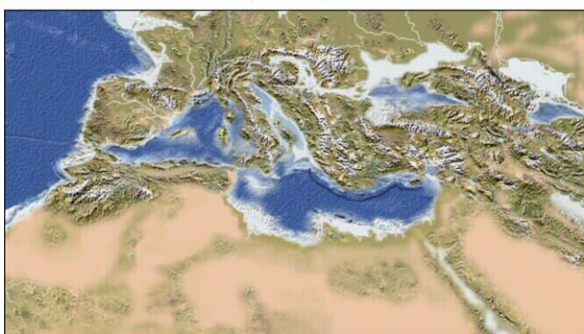
Fig. 3.2: The three panels A-C show the plate tectonic development of the Mediterranean and Black Sea regions since the Late Triassic (210 ma, panel A) through the Middle Cretaceous (100 ma, panel B) to the Late Miocene (6 ma, panel C). Abbreviations: AO – Alpine Ocean, Ap – Apulia, BSB – Black Sea Basin, CB – Caspian Basin, CO – Carpathian Orogeny, Ib – Iberia, MP – Moesian Platform, NA – North America, Py – Pyrenees, PO – Pindos Ocean, Sa – Sakarya, Za – Zargos. Picture reference: http://jan.ucc.nau.edu/~rcb7/paleogeographic_alps.html.

3.3 Development of the Black Sea Basin

3.3.1 Pre-rift development

The Pre-Triassic units of the Black Sea region comprise a metamorphic basement of former Proterozoic-Early Paleozoic sediments and granitoids (Robinson et al., 1996). These are overlain by Paleozoic sedimentary rocks, mainly Silurian to Lower Devonian shales, Devonian to Carboniferous carbonates and coal-bearing clastic sediments of Upper Carboniferous age. Heterogeneous Permian deposits such as continental clastics, limestones, evaporites and volcanics exist on the Moesian Platform; in other areas the Permian is represented by a major unconformity (Robinson et al., 1996).

Red continental clastics of the Triassic follow the Permian hiatus, sometimes with intercalated limestones of Middle Triassic age. Late Triassic flysch sedimentation and ophiolitic volcanics indicate opening of an oceanic back-arc basin as the Neotethys subducted northward. This basin still existed during the Early Jurassic and is characterized by continued flysch deposition in widespread areas in the Pontides, Bulgaria, Romania and Crimea. The Middle-Upper Jurassic Cimmeride Orogeny that took place when the Cimmeride continent and Gondwana split up led to another regional unconformity (Robinson et al., 1996).

Subsequent closure of the back-arc basin was completed by the Early Cretaceous and microplate collision led to a compressive, magmatic event (Robinson et al., 1996; Ustaömer & Robertson, 1994) that can be clearly recognized in the Strandzha Range of Bulgaria (Chatalov, 1990), in Northern Dobrogea (Visarion et al., 1990) and on the Crimean Peninsula (Karantsev, 1982). In the Neocomian, uniform carbonate sedimentation started throughout the entire Black Sea region. It was only interrupted locally by evaporite deposition off the Bulgarian and Romanian coasts (Robinson et al., 1996).

3.3.2 Timing and mechanism of the Black Sea basin opening

A number of models for the development of the Black Sea Basin exist in the literature. Figure 3.3 shows exemplarily the tectonic reconstruction of the development of the western Black Sea basin by Banks & Robinson (1997). It is compared to others in the text below.

The opening of the present-day Black Sea basin started during the Upper Cretaceous when rifting occurred on the northern side of an island arc that was formed during the

northward subduction of the Neotethys. The western Black Sea basin is considered to be older than its eastern counterpart (Banks & Robinson, 1997; Fig. 3.3). It started to rift during Late Barremian and continued until Albian or Cenomanian (Görür, 1988).
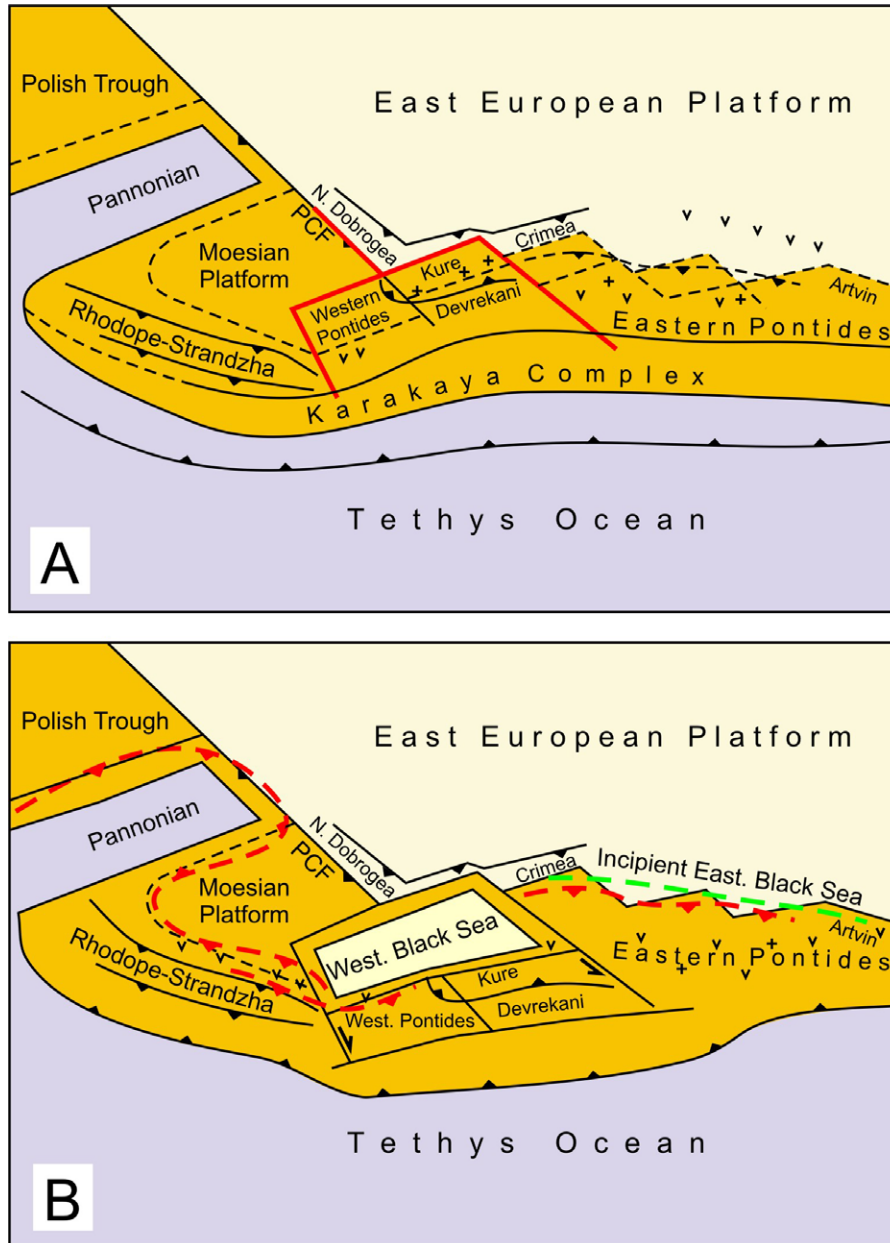
Fig. 3.3: Regional tectonic reconstructions of the development of the western Black Sea basin by Banks & Robinson (1997). PCF: Peceneaga Camena Fault, v and + are volcanics and intrusives. The upper panel (A) restores the western Black Sea region during the Late Jurassic following the Cimmeride compression after the closure of Triassic back-arc basins such as the Kure and Artvin basins. The incipient positions of the western Black Sea boundary faults are marked in red. Panel B shows the reconstruction for the Late Cretaceous after the western Black Sea basin opened but prior to the onset of Alpine compression (dashed red lines with thrust marks). The eastern Black Sea basin (incipient position marked with a dashed green line) is thought to have opened later during the Paleocene-Eocene.

The timing of the opening of the eastern Black Sea basin is less certain, rifting probably started during the Middle Paleocene; both parts became connected in their post-rift phase during the Pliocene (Banks & Robinson, 1997). A second model (Nikishin et al., 2003) differs slightly from this scenario. It suggests an opening period of about ten million years between the Cenomanian and the Coniacian for both the western and eastern Black Sea basins.

The western Pontides south of the western Black Sea basin have a stratigraphy similar to the Moesian Platform on the Romanian and Bulgarian shelves (Banks & Robinson, 1997; Săndulescu, 1978) and are thus considered to be a part of the Moesian and Scythian platforms that rifted across the western Black Sea to its present-day position (Banks & Robinson, 1997; Okay et al., 1994).

During the Late Eocene-Oligocene, the western Pontides became affected by compressional tectonics, implying the presence of two strike-slip transfer margins on the eastern and western sides of the western Black Sea (Banks & Robinson, 1997, Fig. 3.3; Okay et al., 1994; Görür, 1988). The exact location of these transfer margins is a subject of debate. According to Banks & Robinson (1997, Fig. 3.3) the western transfer margin is located across Thrace between Strandzha and the western Pontides, although the exact position cannot be distinguished because of an Eocene sedimentary cover. Its offshore prolongation also cannot be followed clearly because of the obfuscating influence of the Tertiary compressive deformation fronts of Strandzha and the Balkanides (Banks & Robinson, 1997; Dachev et al., 1988).

In the eastern part of the western Black Sea Basin, Okay et al. (1994) suggested a transfer margin that continues from the North Kilia Depression southward to the present-day depocenter of the western Black Sea basin. Banks & Robinson (1997) however did not find a corresponding fault on seismic lines along the proposed track and assumed a more easterly position close to the southwestern edge of the Andrusov Ridge.

3.3.3 Post-rift development

A post-rift sedimentary fill of more than 10 km fills the Black Sea basin today. Because the western Black Sea Basin is considerably older than its eastern counterpart, the largest thickness values are reached here (Robinson et al., 1996). A compiled depth map of the break-up unconformity in the Black Sea Basin giving the thickness distribution of the post-rift sedimentary fill is shown in Fig. 3.4.

When subduction of the Neotethys came to a halt during the Early Tertiary, a tectonically quiet phase observable in the sedimentary record of both sub-basins set in. From the Late Paleocene to Middle Eocene, carbonate sedimentation occurred in the shelf areas, whereas clastic turbidites deposited in the deeper basins. Throughout this time, both the Pontides and the Caucasus region were dominated by extensional tectonics (Nikishin et al., 2003, 2001; Yilmaz et al., 1997).
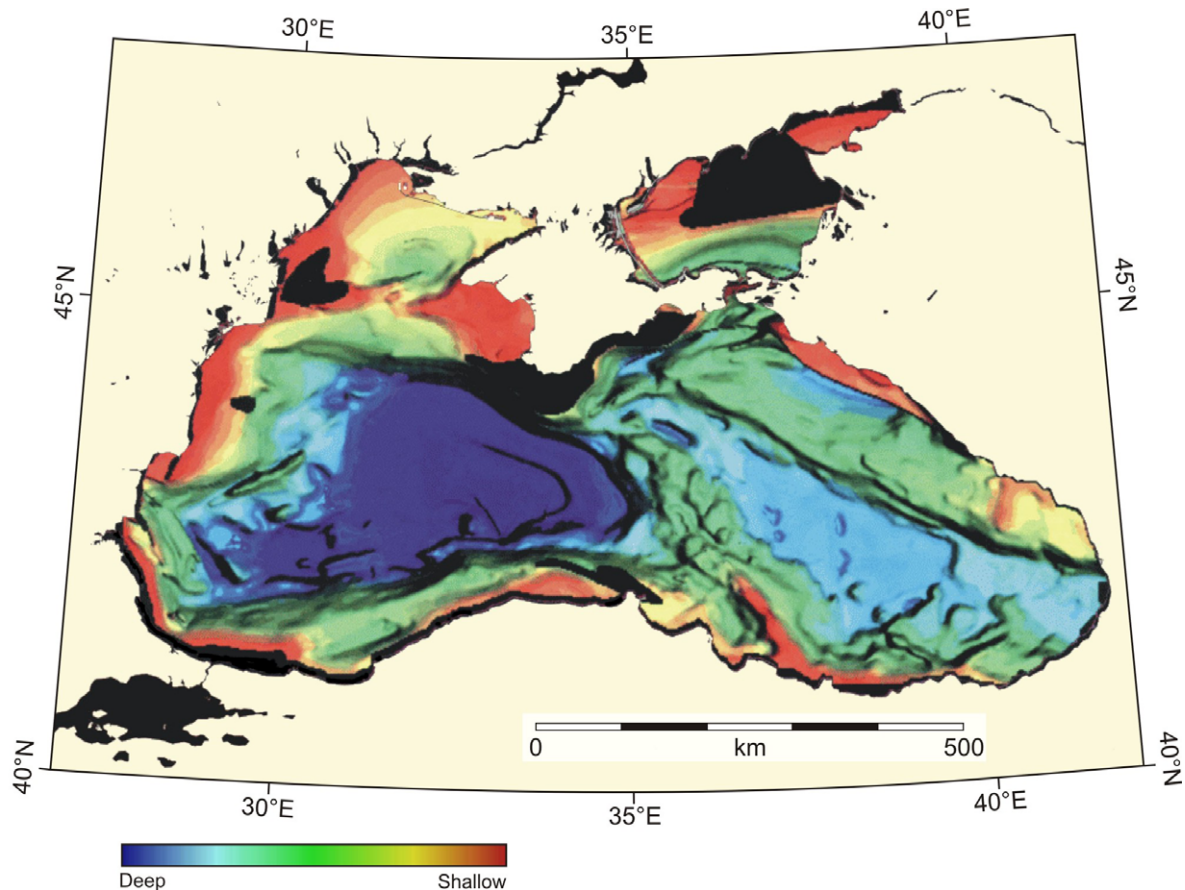
Fig. **3.4**: Depth map to the break-up unconformity of the western and eastern Black Sea basins based on the interpretation of >50,000 km of reflection seismic profiles (modified after Robinson et al., 1996). The resulting surface is strongly diachronous as the two sub-basins are not of the same age: It is probably Late Cretaceous in the west and Uppermost Eocene in the east (Robinson et al., 1996).

The tectonic regime turned from extension to compression in the southern Pontides during Late Cretaceous and in areas of the Greater Caucasus since the Paleocene. By the Late Eocene, the entire Black Sea region became affected by compressive tectonics. This development is manifested in folding of the Balkanides, inverted half-graben structures of the Pontides, as well as minor inverted features on the Romanian shelf and in the Gulf of Odessa (Robinson et al., 1996).

31

Widespread basaltic, alkali-basaltic and andesitic volcanism and volcaniclastic flysch sedimentation mark a phase of strong subsidence in the deep basin during the Eocene (Nikishin et al., 2003).

Since the Oligocene, several compressive phases have been recorded in the Caucasus-Black Sea-Pontides region; these are associated with the collision between the European and Arabic plates (Nikishin et al., 2003; Dercourt et al., 1993). Uplift in the Carpathians during the Upper Miocene led to shoaling of the Black Sea Basin with a maximum water depth of only several hundred meters (Robinson et al., 1996; Ross, 1978).
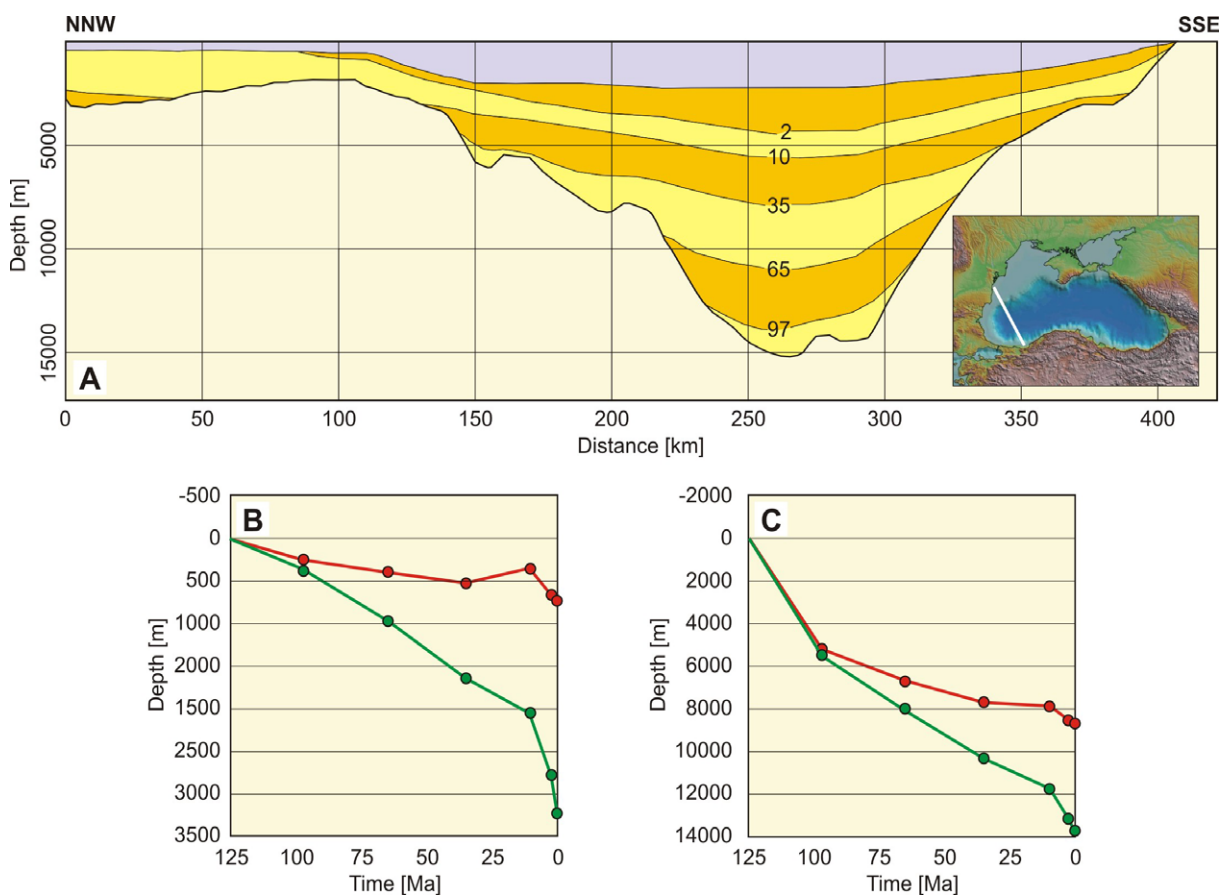
Fig. **3.5**: Panel A: Modeled thickness distribution of post-rift sediments along a NNW-SSE tending profile through the western Black Sea basin modified after Robinson et al. (1995). The white line on the inset gives the profile location; numbers give the ages of simulated stratigraphic markers in Ma: Top-Albian (97), Top-Cretaceous (65), Top-Eocene (35), Intra-Sarmatian (10) and End-Pliocene (2). The lower panels give the basement subsidence (green curves) and water-loaded tectonic subsidence (red curves) for the basin margin (panel B) and basin center (panel C). After Robinson et al. (1995).

To verify the geological interpretations described above, the syn-rift and post-rift sedimentation and subsidence histories of the western Black Sea basin was modeled

(Robinson et al., 1995). The resulting stratigraphic distribution in the western Black Sea basin is shown in Fig. 3.5 along with subsidence curves for the time interval since the Middle Cretaceous.

The model predicts a rapid syn-rift basement subsidence in the central part of the basin, leading to only poorly developed syn-rift sediments and a paleo-water depth of about 5,000 m at the end of the rifting. The early post-rift phase was characterized by sediment by-pass at the basin margins and subsequent high sedimentation rates in the basin center. The high sediment supply at the basin center could compensate for the post-rift thermal subsidence and the sediments started to fill up the basin towards the sea-level. This trend continued until the Upper Miocene. The rising sediment load in the basin had the effect of an increasing tectonic subsidence and thus basement subsidence, leading to a rapid deepening of the western Black Sea up to around 2,800 m until the Pliocene.

The effects of water replacement by sediments on subsidence ceased during the Upper Pliocene, nevertheless further basement subsidence was required to create accommodation space for the thick Quaternary sedimentary succession in the western Black Sea. The increase in sediment supply and associated loading might be related to glaciation of most of the catchment area in northern Europe or the beginning of the contribution of the Danube to the Black Sea basin fill.

3.4 Structural units surrounding the western Black Sea Basin

Figure 3.6 shows the regional structural units that surround the Black Sea basin area today. These are separated by major strike-slip fault systems in the northern part of the Black Sea and by the thrust fronts of the Balkans and the Pontides in the western and southern Black Sea respectively. A short summary according to Dinu et al. (2002) is given below; the order of description of the units is counterclockwise from north to south.

3.4.1 East European Platform

The Black Sea basin is located at the southern rim of the East European Platform (Fig. 3.6). Extending from the Ukrainian mainland onto the northwestern shelf, the East European Platform consists of an 8-10 km thick sediment cover over a pre-Riphean (Late Proterozoic) basement of gneiss, granite-gneiss and granitoids (Dinu et al., 2002). This cover was developed in three major cycles separated by tectonic uplift and subsequent erosion

(Seghedi et al., 2004; Paraschiv, 1985; Pătruliuş & Iordan, 1974; Iliescu, 1974; Macarovici, 1971; Barbu et al., 1969).

The oldest cycle is of Paleozoic age and was deposited between the Late Vendian and the Devonian. It consists of Late Vendian to Ordovician coarse siliciclastics, Silurian graptolite shales and Early Devonian black limestones that are succeeded by quartz sandstones. The second cycle comprises Cretaceous to Mid-Eocene sediments: shallow marine clastics, evaporates and limestones of the Lower Cretaceous, and Upper Cretaceous terrigenous clastics and limestones. The deposition of the second sedimentary cycle shows frequent, short interruptions. The third and youngest cycle was deposited during the Tertiary after the Kossovian marine transgression. Clastic sediments and carbonates interbed with air-fall tuffs and evaporites (Seghedi et al., 2004).
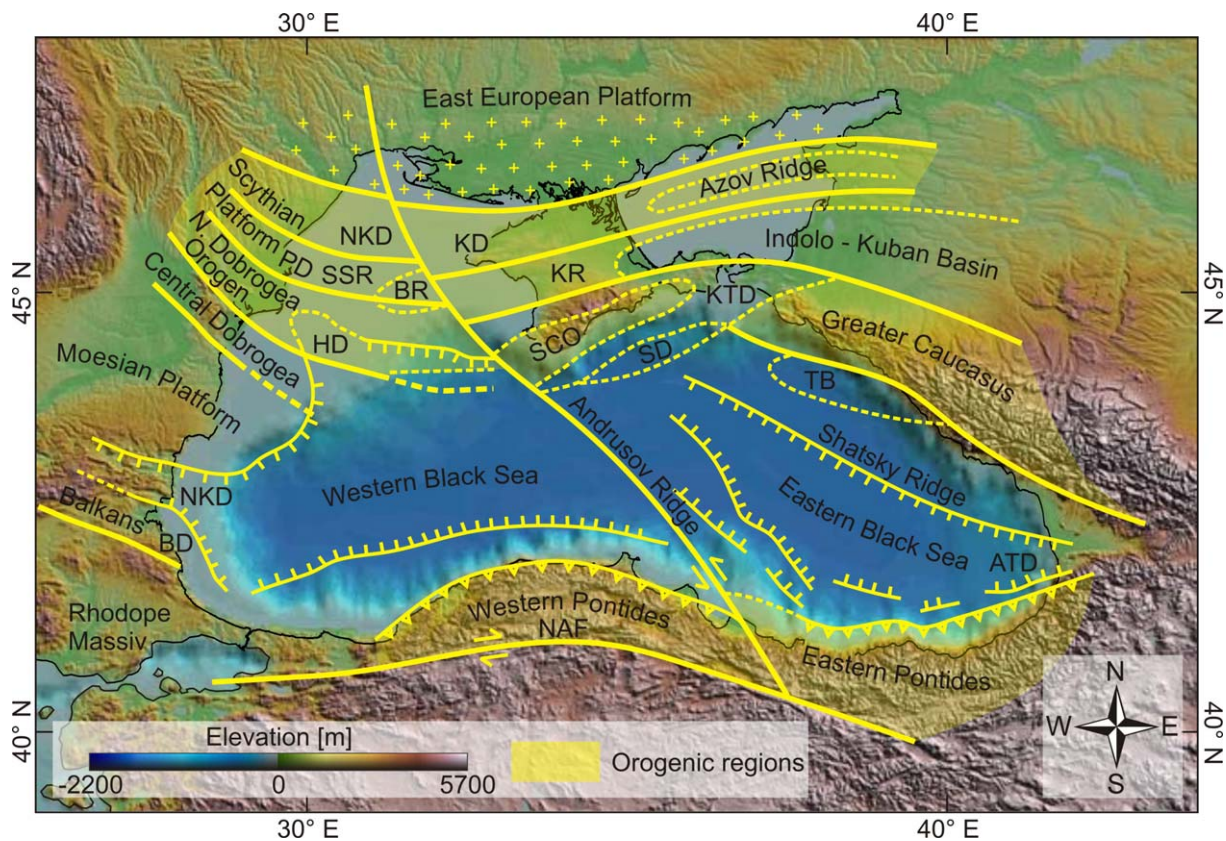
Fig. **3.6**: Main tectonic units surrounding the Black Sea modified after Dinu et al. (2002). Abbreviations: PDD – Pre-Dobrogean Depression; NKD – North Kilia Depression; SSR – Suvorov-Snake Island Depression; BR – Bubkin Ridge; HD – Histria Depression; BD – Burgas Depression; KD – Karkinit Depression; KR – Kramsky Ridge; SCO – South Crimea Orogen; KTD – Kerci-Taman Depression; SD – Sorokin Depression; TB – Tuapse Basin; ATD – Achara-Trialet Depression; NAF – North Anatolian Fault.

3.4.2 Scythian Platform

The Scythian Platform is located in the northeastern Black Sea south of the East European Platform (Fig. 3.6). Several sedimentary cycles of several hundred to 5,000 m thickness occurred on the Scythian Platform between Lower Jurassic and Neogene times. Sandstones and limestones intercalate, sometimes intrusive and effusive rocks occur as well (Dinu et al., 2002). The sedimentary cover of the Scythian Platform overlies a Proterozoic to Paleozoic basement that underwent tectonic deformation around the Triassic-Jurassic boundary (Dinu et al., 2002; Nishikin et al., 2001, 2003; Milanovsky, 1991; Muratov, 1969).

3.4.3 North Dobrogea Orogen

Between the Scythian Platform in the north and the Moesian Platform (described below) in the south is the North Dobrogea Orogen (Fig. 3.6). The structural base of this unit is a Permo-Triassic rift basin with a continental siliciclatic depositional environment that changed to carbonate-dominated sedimentation during the Lower Scythian (Seghedi at al. 2004). Upper Triassic inversion tectonics led to the deposition of terrigenous turbidites when the Hercynian basement in the western part of the North Dobrogea Orogen was uplifted along the inverted syn-rift extensional faults (Seghedi et al., 2004). After a tectonically quiescent period, inversion movements continued from Early Cretaceous to Albian times. During the Upper Cretaceous, shallow marine sediments were deposited throughout the North Dobrogea Orogen (Seghedi et al., 2004).

3.4.4 Moesian Platform

Most of the Romanian and parts of the Bulgarian shelves are the offshore continuation of the Moesian Platform (Fig. 3.6); its two main structural units are Central Dobrogea in the north and the Southern Dobrogea in the south. Both were deformed by Late Variscan tectonic movements (Nikishin at al., 2003; Banks, 1997; Okay et al.; 1994). The basement of the Moesian Platform consists of Archean to Paleoproterozoic metamorphic complexes; a Late Proterozoic volcano-sedimentary sequence occurred also in Southern Dobrogea.

A Paleozoic to Cenozoic suite of sedimentary rocks developed on the northern Moesian Platform: Upper Cambrian to Middle Devonian marine clastics, Middle Devonian to Lower Carboniferous carbonates and a Carboniferous paralic coal-bearing clastic series. Permo-Triassic rocks are of the Germanic facies: A lower and an upper clastic sequence are

separated by carbonates. The Middle Jurassic is represented by detrital sediments. These are followed by calcareous deposits of Upper Jurassic to Barremian age. During the Late Cretaceous, marly limestones developed. The Tertiary reflects a shallow marine to terrestrial evolution of the basin: Limestones of the Eocene are followed by progressively more detrital rocks of the Badenian to the Pleistocene. A Quaternary loess layer overlies discontinuously the older units (Seghedi et al., 2004).

The composition of the southern part of the Moesian Platform is somewhat different: a folded Paleozoic basement is overlain by up to 5 km of Mesozoic to Quaternary, dominantly shallow marine sediments (Dabovski et al., 2004). The Paleozoic deposits comprise Late Ordovician to Devonian shales and carbonates and a locally developed cover of coal-bearing Carboniferous formations and red Permian sandstones (Dabovski et al., 2004; Haydoutov & Yanev, 1997). The oldest Mesozoic sediments are Lower to Middle Triassic carbonates followed by terrigenous or calcareous sediments of Jurassic to Cretaceous age. The Lower Tertiary (Paleogene) is, depending on location, continental or marine; the Upper Tertiary (Badenian to Pontian) is only locally present as marine sediments of a transitional zone between the Central and Eastern Parathethys (Dabovski et al., 2004).

3.4.5 Balkans

The Balkans was formed by Alpine folding and thrusting due to the collision between the Moesian Platform in the north and the Rhodope Massif to the south (Fig. 3.6). Three north-vergent thrust units were formed: Fore-Balkan, Stara Planina and Srednogorie (Dinu et al., 2002; Banks, 1997).

3.4.6 Rhodope Massif

The southern continuation of the Balkans is the Rhodope Massif (Fig. 3.6) which is mostly made up of Precambrian to Paleozoic units that have been deformed first by Variscan and later by Mesozoic (pre-Maastrichtian) movements (Nikishin et al., 2003; Banks, 1997; Burg et al., 1996).

3.4.7 Western Pontides

The Western Pontides are situated on the Asian side of the Bosphorus bordering the southwestern and southern Black Sea (Fig. 3.6). They are formed by a crystalline Late

Proterozoic basement with granitoids that have been dated to an age of 590 to 560 Ma (Stephenson et al., 2004; Chen et al., 2002; Ustaömer & Rodgers, 1999). Early Ordovician to Late Carboniferous sedimentary rocks overlie the basement.

Central Alpine Europe		Black Sea	Age [ka]
		New Black Sea	7-10
		Old Black Sea	
Würm	II	New Euxinian	25
Würm	I-II	Surozhian	50
Würm	I	Post-Karangatian	75
Riss-Würm		Karangatian	110-125
Riss		Post-Uzunlarian	
Riss		Uzunlarian	
Riss		Late Drevne-Euxinian	
Riss		(Regression)	230
Mindel-Riss		Paleouzunlarian	
Mindel-Riss		Early Drevne-Euxinian	300-370
Mindel		Old Euxinian	500
Günz-Mindel		Post-Chaudian	700
Günz		Chaudian	
Danube-Günz		Chaudian	

Tab. **3.2**: Middle-Late Quaternary stratigraphic stages in the Black Sea region and their correlation to Alpine stages of central Europe; compiled by Winguth (1998) after Romanescu (1996), Koreneva & Kartashova (1978), Ross (1978) and Degens & Ross (1972).

In the eastern part of the Western Pontides, the Carboniferous series comprises coal deposits of economic importance (Stephenson et al., 2004; Dean et al., 2000; Görür et al., 1997). The oldest Mesozoic sediments are thick terrigenous sandstones and Triassic conglomerates. They are unconformably overlain by Jurassic sandstones and limestones followed by a thick series of Lower Cretaceous turbidites, of which the latter are possibly related to the opening of the Western Black Sea Basin (Stephenson et al., 2004; Sunal & Tüysüz, 2002; Tüysüz, 1999; Görür, 1988). Late Mesozoic to Tertiary sedimentation can be

traced until the Eocene; chalks were deposited during the Maastrichtian and the Paleocene, while thick turbidites followed in the Eocene (Stephenson et al., 2004).

3.5 Quaternary geology of the western Black Sea

As in the case of the Tertiary (Tab. 3.1), regional stage names are used in the Quaternary stratigraphy of the Black Sea. The regional stratigraphic chart for the Quaternary and the correlation to Alpine stages of central Europe are shown in Tab. 3.2.

The base of the Quaternary in the Black Sea Basin was drilled at two DSDP sites (380 and 381; Schrader, 1978; Ross, 1978). Correlation of seismic data with these DSDP holes and with petroleum exploration wells indicates a maximum Quaternary thickness of 2,000 m (Finetti et al., 1988) to 2,500 m (Robinson et al., 1995) in the central basin. Wong et al. (1994) also found more than 2,000 m of Late Pleistocene to Recent sediments in the Danube and Dniepr fan complexes.

Below, the Quaternary geology of the Danube Delta/northwestern shelf, southwestern shelf and slope/deep basin is described separately, while the geological history since the last glacial maximum is described in Chapter 3.6.

3.5.1 Danube Delta and northwestern shelf

The most important source of freshwater and sediments in the Black Sea Basin is the Danube river system which discharges to the northwestern shelf (Tab. 2.1). The course of the Danube follows roughly the chain of former Paratethys basins: from the Vienna Basin through the Pannonian and Dacic basins to the Euxinian Basin/Black Sea. The present-day Danube is the result of the joining of several paleo-river systems with differing flow directions (e.g., from the Carpathians westwards into the Pannonian Basin and eastwards into the Dacic Basin). They are thought to form a single, eastward flowing river that drains into the Black Sea since the Late Pliocene – Early Quaternary (Marović et al., 1997; Banu, 1967; Posea, 1964; Ianovici et al., 1960). Since that time, the Danube has been building Europe's second largest delta (after the Volga Delta in the Caspian Sea) in northeastern Romania and southwestern Ukraine. Geologically it is situated in the southern part of the Predobrogean Depression, which has been repeatedly affected by strong subsidence and sediment accumulation since the Paleozoic (Pătruţ et al., 1983; Fig. 3.7). The Predobrogean Depression is separated from the North-Dobrogea Orogen in the south by the St. George

Fault Zone that strongly influences the course of the Danube in the southern part of the delta (Panin & Jipa, 2002).
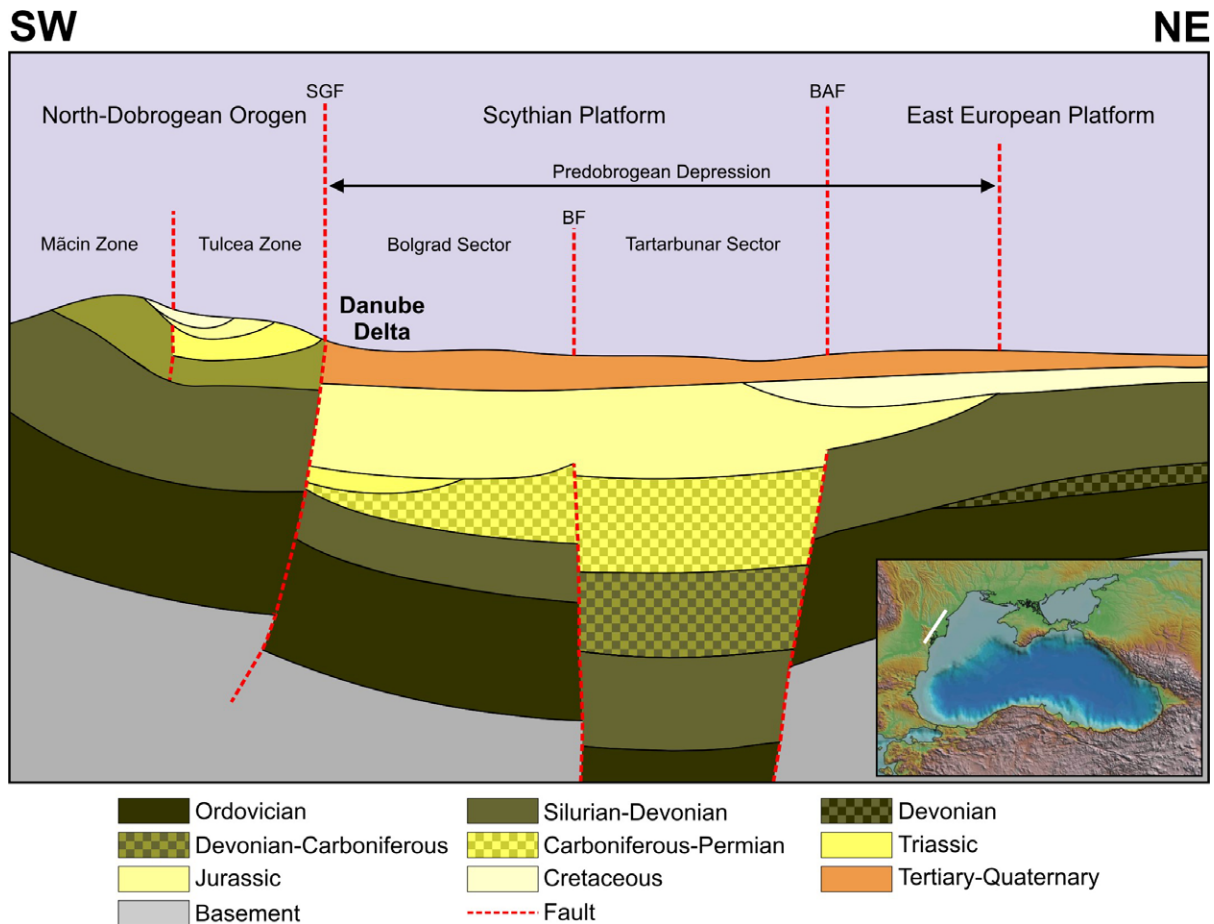
Fig. **3.7**: Geological cross-section through the Danube Delta region according to Pâtrut et al. (1983). White line in the inset gives the approximate profile location. Abbreviations: SGF – St. George Fault, BF – Bolgrad Fault, BAF – Baimaclia-Artiz Fault.

Sediment deposition and with it delta building occurs only during sea-level highstands when just a fraction of the sediments delivered reaches the open Black Sea. Subsequent lowstands, however, lead to a seaward shift of the depocenter and sediments are transported through the Viteaz Canyon into the sedimentary fans on the northwestern Black Sea slope and beyond (Chapter 3.5.2). Most of the sediments accumulated during the previous delta-building phase are eroded during sea-level lowstands, so that the present-day Danube Delta surface is largely a product of the Holocene highstand (Chapter 3.6.3.2). High-resolution seismic data show that the thickness of the delta sediments ranges between 10 and 350 m (Panin & Jipa, 2002; Spânoche & Panin, 1997).

Sediments that actually reach the northwestern Black Sea during periods of high sea-level is transported southward sub-parallel to the coast; these sediments are mostly deposited on the western shelf as well (compare the water circulation model in Fig. 2.3; Panin, 1989; Shimkus & Trimonis, 1974; Zenkovitch, 1960).

Quaternary sedimentation on the northwestern Black Sea shelf was quiet and has only to a minor extent been affected by syn-sedimentary tectonics. The transitions to the underlying Romanian and Dacian (Tab. 3.1) deposits are conformable (C. Konerding, 2006). The thickness distribution of the combined Romanian/Quaternary section on the northwestern shelf based on the interpretation of industrial reflection seismic data and wells is shown in Fig. 3.8. It increases slowly basinward from 0 m in coastal areas south of the Danube Delta to about 600 m on the upper continental slope (C. Konerding, 2006). Compared to the older formations, only a few northeast-southwest trending fault systems (mostly Oligocene or older in age and later reactivated during the Pontian) have been active in the Quaternary. They produced offsets on the order of a few meters to tens of meters and are separated by northwest-southeast trending transfer faults (Fig. 3.8; C. Konerding, 2006).
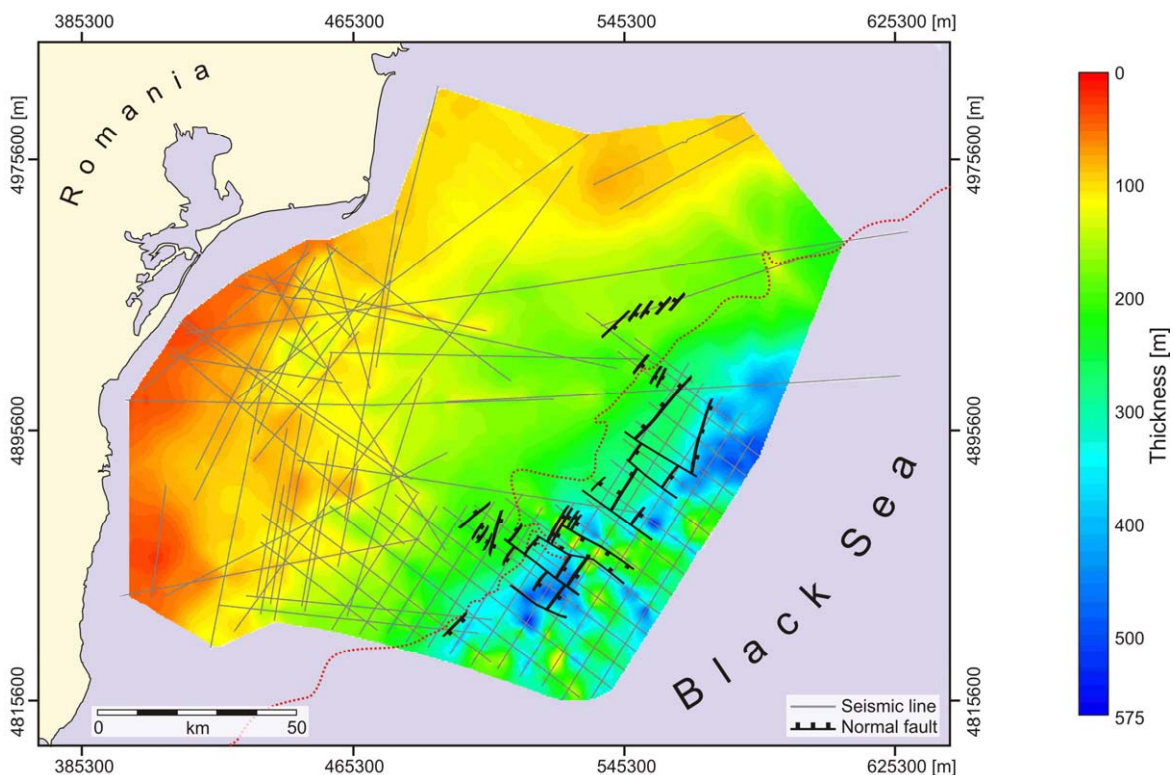

Fig. 3.8: Thickness distribution and tectonics of the combined Romanian-Quaternary section on the northwestern Black Sea shelf off Romania. From C. Konerding (2006). The interpretation is based on industrial seismic lines (drawn in grey). The red dotted line gives the approximate position of the present-day shelf edge along the 100 m isobath for orientation.

The combination of the Romanian and Quaternary into one single unit is a common practice for the Romanian sector of the Black Sea, especially in industrial borehole descriptions or seismic interpretations. A subdivision is difficult because the sedimentological and depositional characteristics of the Romanian and Quaternary units are highly similar. In contrast, in the Bulgarian and Ukrainian sectors, the Quaternary and Pleistocene units are generally separated and a unit of Romanian age is normally not distinguished.

3.5.2 Slope and deep basin

The deep-sea fans built up by the rivers Danube, Dniestr, Bug and Dniepr (Figs. 3.9 and 2.4) are the largest Quaternary geological features of the western Black Sea. According to Paluska & Degens (1979) these rivers started to drain into the Black Sea during the Chaudian (Günz glaciation), thus providing an upper limit for the age of the fan system. The deep-sea fans have been divided in two individual systems: the Danube fan and a fan system fed by Dniestr, Bug and Dniepr (named Dniepr Fan hereafter). These two fans slightly interfinger (Winguth et al., 2000); approximate boundaries have been mapped by Wong et al. (1994) and Popescu et al. (2001) and are shown in Fig. 3.9.

Deep sea fan development is controlled mainly by sea-level change, and the cyclicity of falling and rising water levels is responsible for the development of the typical deep sea fan sequences (Weimer, 1990): During highstands, when the coastline is located far landward of the shelfedge, delta systems at the river mouths serve as the depocenter of fluvial sediments, leaving the slope and basin sediment-starved. When the sea-level starts to fall, the depocenter moves seaward towards the shelfedge. Rapid deltaic sedimentation at the shelfedge results in overpressuring of the prodelta and slope sediments. Sediment failure and the subsequent mass transport processes characterize this early stage of sequence development and lead to important deposits on the slope.

When the retrograding canyons at the shelfedge become connected to the incised fluvial valleys on the shelf, channelized turbidity flow starts to form channel-levee systems on the slope. In this way, the deepsea fan becomes the main depositional system during sea-level lowstands: Coarse sediments remain in the channels or forms lobes at the channel mouths, finer sediments build up the levees and overbank deposits. At times of rising sea-level and a landward migrating depocenter, the incised channels are filled with finer sediments, whereas the slope and the deep basin are dominated by hemipelagic sedimentation.
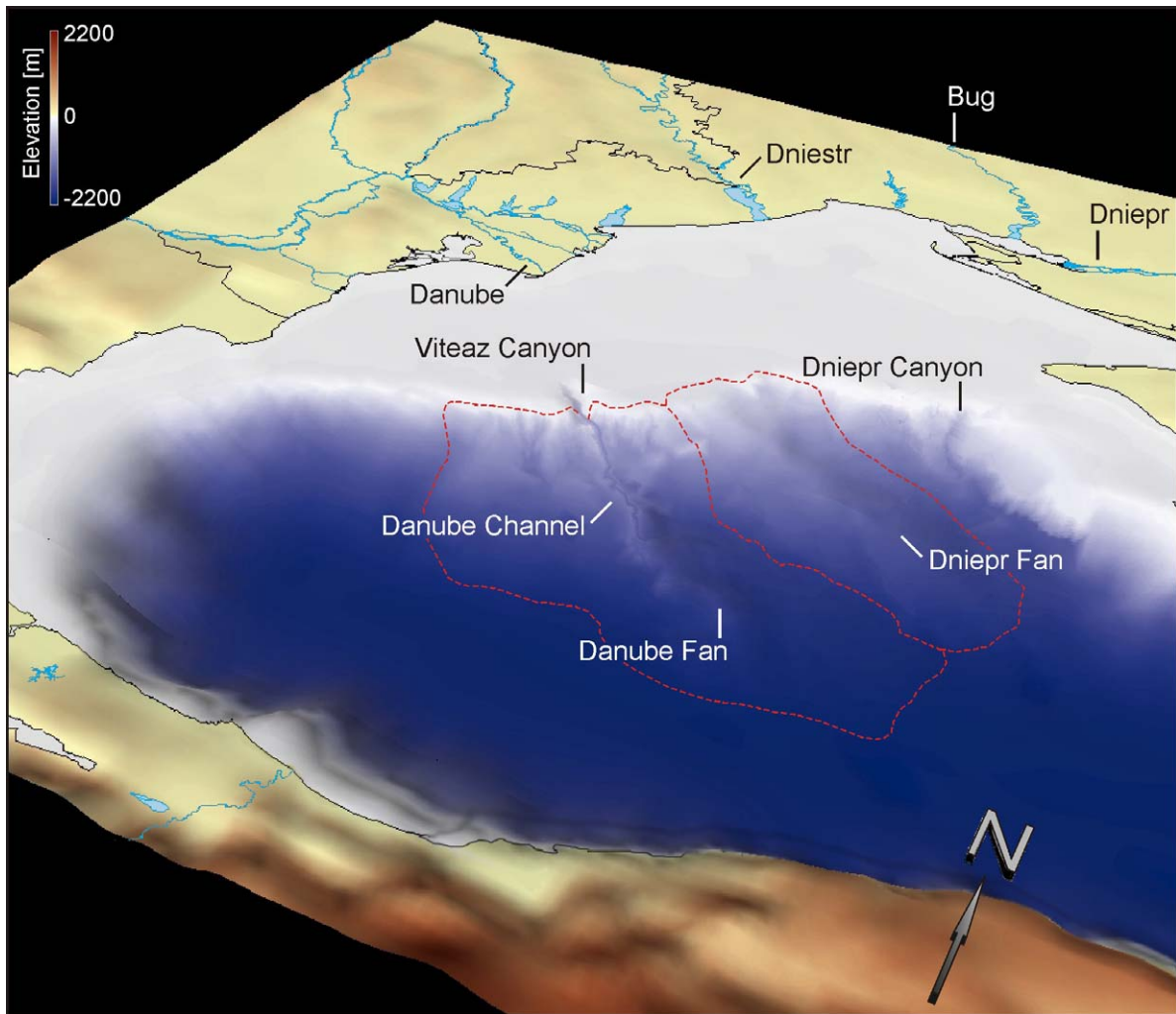
Fig. **3.9**: 3D view of a digital elevation model (for a description of the database see Section 4.1.3) of the western Black Sea and surrounding land areas with major rivers that drain into the northwestern Black Sea. Sediments are transported through canyons and channel systems into the sedimentary fans. Red dashed lines give the approximate boundaries of the Danube and Dniepr fans on the seafloor as mapped by Popescu et al. (2001).

Based on seismic stratigraphic interpretation of profiles crossing the Danube and Dniepr fans, Winguth et al. (2000) established a regional sea-level curve for the northwestern Black Sea (Fig. 3.10) and deduced a sedimentary and stratigraphic model for it. According to this model, the Danube fan is built up by six seismic sequences that have been dated by correlation with the global SPECMAP δ^{18}O curve of Imbrie et al. (1984, Fig. 3.10). This correlation yielded an age of approximately 900 ka for the oldest fan sediments in the Danube fan, whereas sedimentation in the Dnieper fan started about 100 ka later. The duration of the Quaternary water level cycles in the northwestern Black Sea found by Winguth et al. (2000) varies between 50 and 130 ka, thus they were interpreted to be 5th and 6th order cycles in the sense of Fulthorpe (1991) and Carter et al. (1991).
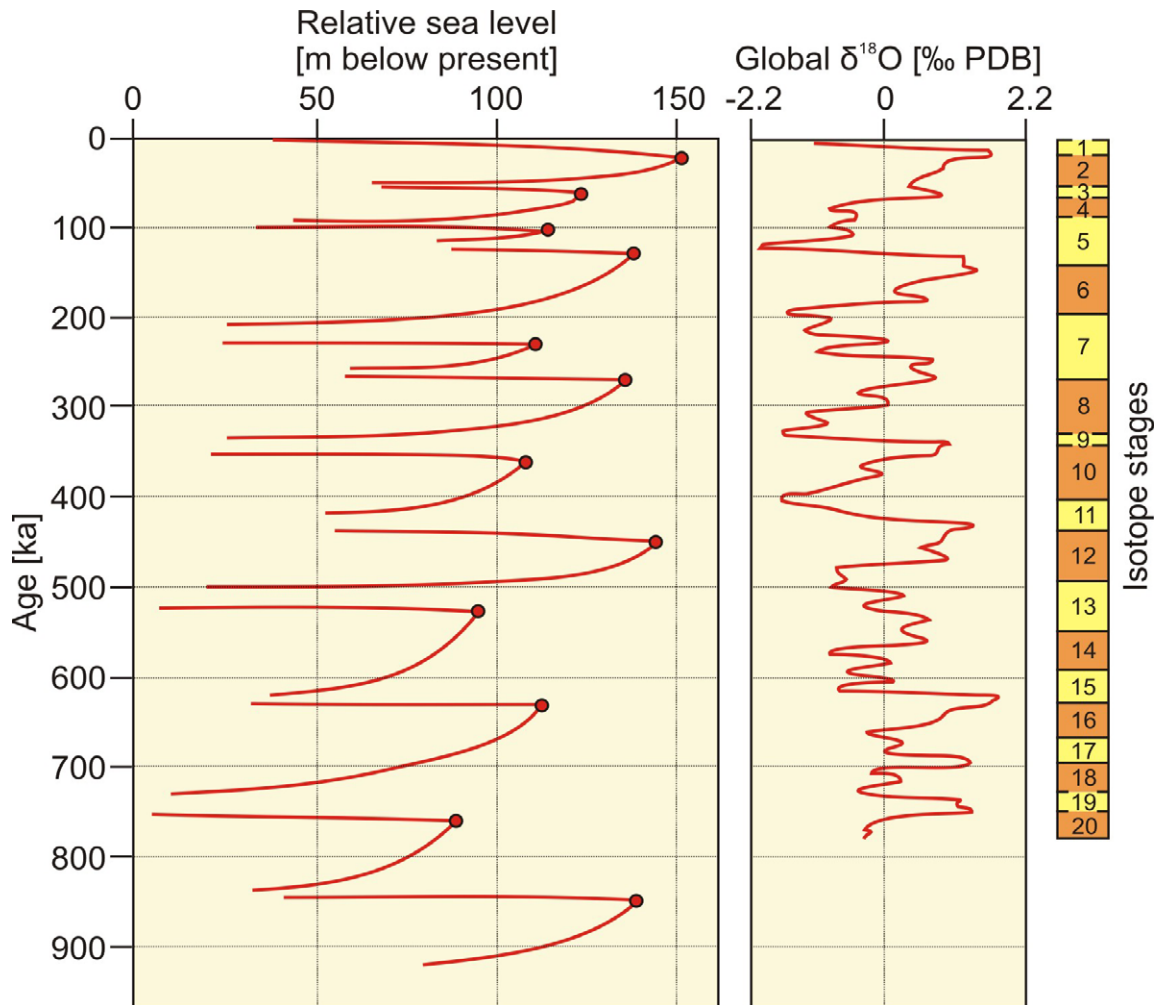
Fig. **3.10**: The left panel shows the regional sea-level curve of Winguth et al. (2000) for the last ~900 kyr in the northwestern Black Sea; the middle and right panels give the SPECMAP $\delta^{18}O$ curve (Imbrie et al., 1984) and isotope stages for comparison.

The youngest of the channel-levee systems that together built up the younger portion of the Danube fan is the most outstanding bathymetric feature on the recent western slope of the Black Sea (Danube channel in Fig. 3.9). It is directly connected to the Viteaz Canyon and developed below a water depth of 800 m during the Neoeuxinian (marine isotope stage 2, Fig. 3.10), the last sea-level lowstand in the Black Sea.

This youngest channel-levee system was internally subdivided into four sedimentary cycles, each of which starts with channel bifurcation, followed by deposition of HARP units (High Amplitude Reflection Packets as described by Flood et al. (1991) in the Amazon Fan) and subsequent development of a new channel path (Popescu et al., 2001). Channel avulsion and bifurcation need not be directly linked to water level fluctuations, since according to this model more than one channel formed during a single phase of low sea-

levels. The northward migration pattern from one cycle to the next implies that the process is most likely a result of the Coriolis effect (Popescu et al., 2001).

3.5.3 Southwestern Shelf

Seismic stratigraphic studies carried out on the southwestern Black Sea shelf showed that five distinct seismic sequences (named Unit 5 to 1 in chronological order; Fig. 3.11) separated by four unconformities make up the sedimentary record since the Middle Eocene (Aksu et al., 2002).

The four older seismic stratigraphic units 5-2 offlap towards the preset-day shelfedge so that older units occur landward of their respective younger successor. These units are truncated by the youngest regional unconformity and are overlain by Unit 1 (Aksu et al., 2002).
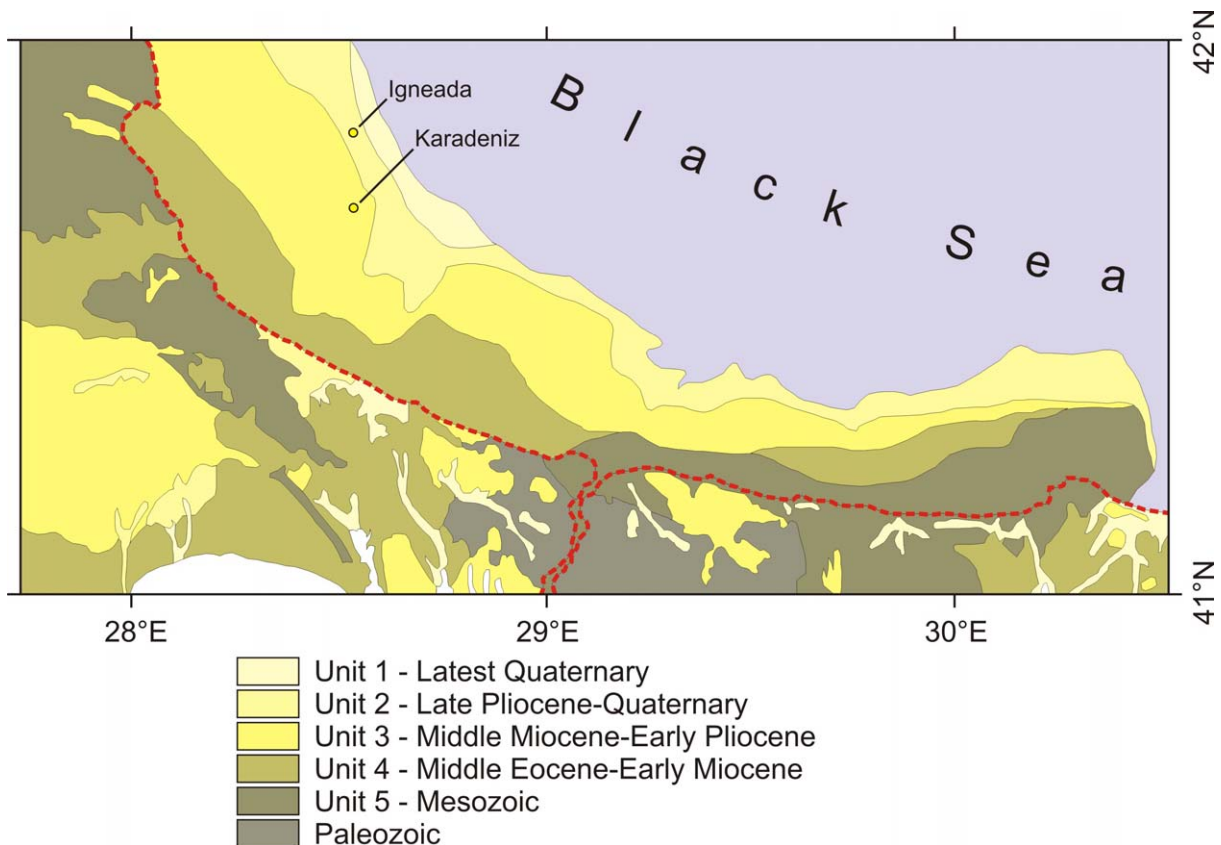
Fig. 3.11: Geological map of the southwestern Black Sea and northwestern Turkey, assembled by Aksu et al. (2002); the red dashed lines give the present-day shoreline. The onshore area is compiled from map sheets by Sakinç et al. (1999), Ternek (1964) and Tokay (1964). The offshore units have been mapped by Aksu et al. (2002) using seismic stratigraphic methods. Yellow dots give the position of the two exploration wells Igneada and Karadeniz on the Turkish shelf.

A generalized depositional pattern of the seismic stratigraphic units found on the southwestern shelf is shown in Fig. 3.12. According to Aksu et al. (2002), the stratigraphic and sedimentary classification of the seismic units is as follows: The oldest sequence (Unit 5) is spatially restricted to the inner and middle shelf, to a water depth less than 75 m. It consists of slightly to moderately folded and faulted Mesozoic volcano-sedimentary deposits. The overlying unconformable Unit 4 is made up of Eocene to Miocene sediments that are less affected by tectonics. Units 3 and 2 consist of relatively undeformed north-dipping clinoforms; they occur between 75 and 90 m water depth on the present-day outer shelf. Unit 3 is supposed to be of Miocene to Pliocene age, Unit 2 contains uppermost Pliocene to Quaternary sediments with a conformable transition from Pliocene to Quaternary. The youngest Unit 1 differs from the older sequences in its depositional characteristics. It was divided into four subunits: The stratigraphically lowest parts of Unit 1 (Subunit 1A) are restricted to an area close to the present-day shelfedge. They are made up of stacked, oblique-prograding packages deposited conformably on top of Unit 2. In contrast, the subunits 1B to 1D form a thin veneer of sediments unconformably overlying the older units on most of the southwestern shelf.
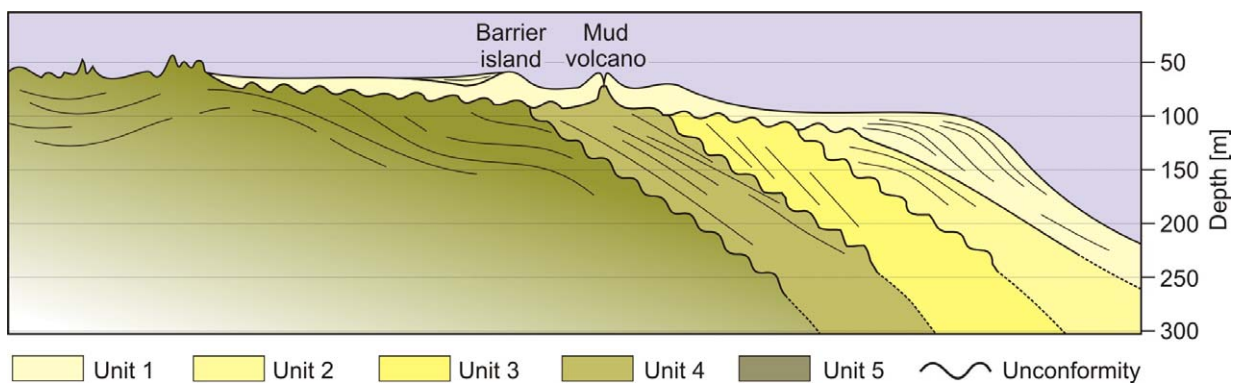
Fig. 3.12: Generalized stratigraphic and depositional pattern on the southwestern Black Sea shelf. Five distinct seismic stratigraphic units (units 5-1; for a stratigraphic classification see Fig. 3.11) separated by four regional seismic unconformities have been identified. From Aksu et al. (2002).

The seismic architecture of Subunit 1A was interpreted to resemble lowstand shelfedge delta lobes, as they have been found in many other parts of the world (e.g., Hiscott, 2001; Aksu et al., 1999; Chiocci et al., 1997; Anderson et al., 1996). Four distinct delta lobes have been identified and attributed to times of glacially lowered sea-levels during the Quaternary. The youngest delta lobe has thus been deposited during the last glacial maximum, at a sea-level of about -110 m (constrained by the topset-foreset transition of the deltaic sediments;

Aksu et al., 2002). The younger subunits 1B-1D overlie the youngest regional unconformity, their characteristics are described in detail in section 3.6.3.4.

3.6 Late-glacial to Holocene development of the Black Sea

3.6.1 Paleoceanography

During the last glacial (Surozhian / Middle Würm, 50-40 ka; Tab. 3.2) marine conditions characterized the Black Sea as the sea-level stood close to the present level (-10 to 0 m; Popov, 1975). The salinity was also comparable to present-day values (Ostrovskiy et al., 1977), and it is likely that the deep waters in the Black Sea contained a high content of hydrogen sulfide leading to formation of sapropel and pyrite (Neprochnov, 1980).

The Surozhian transgression can be divided into two phases, a first phase that reached approximately -10 m and a later phase that might have reached values slightly above the present level (Ostrovskiy et al., 1977). Deposits bearing Surozhian fauna have been found in marine terraces at a height of 15 – 20 m along the Caucasian coast. In other areas around the Black Sea, they occur at lower elevations (e.g., in the Kerch Strait, Karkinit Bay and Peninsula, Gallitzin Rise, Shagan Lagoon; Trashchuk & Bolivets, 1978; Shnyukov & Trashchuk, 1976; in the Danube Delta; Panin, 1983).

The Neoeuxinian period follows the Surozhian at around 25 ka (Tab. 3.2). It is characterized by a strong regression leading to an isolation of the Black Sea and increasingly fresher waters in the basin; the depositional transition from the so-called 'Tarkankut Layers' which still contain marine fauna to the 'Karkinit Horizon' that contains brackish fauna and only a few marine remnants marks this development (Ostrovskiy et al., 1977). During the last glacial maximium (~19 – 15 ka) the Black Sea had turned into a freshwater lake with a salinity of 3-7 ‰ and well-oxygenated, H_2S-free waters (Nevesskaya, 1965).

Many researchers suggest a drastic sea-level drop during the Neoeuxinian to values between -90 m to -150 m, a detailed overview is given in the following section. This was accompanied by a distinct basinward advance of the shoreline in the Black Sea region and widely exposed shelf areas. During this time, tributary rivers such as the Danube and the Dniepr cut deep valleys (to a depth of -90 m) into the outer shelf (Popescu et al., 2004; Ryan et al., 2003).

Tab. 3.3: Synthesis of research results on the stratigraphy and paleoenvironment in the Black Sea region after the last glacial maximum. The stratigraphic framework is provided by Sherbakov & Babak (1979) and Fedorov (1978), it was extended with information on archaeology (Todorova, 1989), sea level history (Fedorov, 1988), stratigraphy (Shopov et al., 1992) as well as palynology and microfaunas (Filipova-Marinova, 2004).

Age [ka]	Section	Alpine stratigraphic scale	Archaeological chronology (Todorova, 1989)	Transgressions and hydrological regime (Fedorov, 1988)	Regional stages	Sublayers	Molluscan fauna	Pollen assemblages	Costal vegetation	Dinocyst assemblages	Palaeoecological reconstruction
3	Holocene	Subatlantic	Iron Age	Nymphean Transgression / Fanagorian Regression	Black Sea / Neoeuxinian	New Black Sea	*Modiolus phaseolinus, Spirula subtruncata triangula*	*Quercus, Ulmus, Carpinus, Fagus, Alnus, Salix*	Mixed Oak forests and formations of flooded forests along the river valleys	*Lingulodinium machaerophorum, Spiniferites ramosus, Peridinium sp.*	Increase of humidity and decrease of temperature; salinity similar to present-day conditions
5		Subboreal	Bronze Age	New Black Sea Transgression		Old Black Sea	*Mytilus galloprovincialis, Cardium papillosum, Cardium exigum, Cardium edule, Hydrobia ventrosa, Monodacna caspia caspia*	*Quercus, Carpinus betulus, Corylus, Ulmus*	Mixed Oak forests; increase of *Carpinus betulus*	Maximum of *Lingulodinium machaerophorum, Cymatiosphaera globulosa*	Slightly drier climate
		Atlantic	Transitional period / Eneolithic	Increase of salinity				Maximum of *Quercus, Carpinus betulus, Corylus, Ulmus, Tilia*	Balanced mixed Oak forests		Climatic optimum: Maximum of temperature and humidity; increased salinity
8			Neolithic	First invasion of Mediterranean waters				*Quercus, Ulmus, Corylus*	Open Oak forests		Amelioration of the climate
9		Boreal						*Quercus, Betula, Corylus, Artemisia, Chenopodiaceae*	Xerophytic herb communities; tree stands		
		Preboreal		Regression							
11	Upper Pleistocene (Würm) / Late Glacial	Younger Dryas				Upper	*Monodacna caspia caspia, Dreissena rostriformis distincta, Dreissena polymorpha regularis, Clessiniola variabilis*	*Artemisia, Chenopodiaceae*	Steppe	*Tectatodinium psilatum, Spiniferites cruciformis*	Cold and dry climate; slight freshening
12		Alleröd		Neoeuxinian Transgression, outflow to the Mediterranean				*Pinus, Artemisia, Chenopodiaceae*	Pine forests and steppe		Cool climate; fresh to brackish water
		Older Dryas						*Artemisia, Chenopodiaceae, Poaceae*	Steppe		Cool climate; fresh to brackish water
13		Bölling						*Pinus diploxylon, Artemisia*	Pine forests and steppe		Cool climate; fresh to brackish water
	Pleniglacial					Lower	Continental sediments	*Artemisia, Chenopodiaceae*	Steppe		Cold and dry climate; fresh to brackish water

After the last glacial maximum, a period of warming began that lasts until today. With the glacial ice caps in Scandinavia and the Alps beginning to shrink, melt water input led to a rapidly increasing water level in the Black Sea. The general trend towards a warmer climate was not linear, phases of relatively warm climate such as the Bølling/Allerød (13-11 ka) or the early Holocene around 9 ka alternate with colder periods during the Younger Dryas (11-10 ka) or around 8.2 ka (the so-called '8.2 ka Event'). This climatic variability finds its expression in paleoenvironmental proxies such as pollen assemblages or fauna communities. Table 3.3 shows a synthesis of the principal stratigraphic scheme derived from research along the Black Sea coasts and on the shelf (Fedorov, 1978) as well as on the slope and deep basin (Sherbakov & Babak, 1979) with additional stratigraphic and paleoenvironmental information from Filipova-Marinova (2004), Shopov et al. (1992), Todorova (1989) and Fedorov (1988).

The most severe changes in the Black Sea occurred however after the re-connection between the Black Sea and the Mediterranean was established. Around 9-7.5 ka a two-way water exchange developed and inflowing Mediterranean waters started to transform the Neoeuxinian Lake into an anoxic brackish basin (Panin & Popescu, 2007). The timing and characteristics of the Early Holocene connection between the Mediterranean and the Black Sea are discussed in detail in the following section.

3.6.2 Connections to adjacent sea areas

It is crucial for an understanding of the youngest geological development of the Black Sea to establish a model that explains the timing and the mechanisms of the connection between the Black Sea and the adjacent seas: with the Mediterranean Sea via the Sea of Marmara in the west and with the Caspian Sea in the east.

3.6.2.1 Mediterranean Sea and Marmara Sea

Several different scenarios have been proposed in the past for the reconnection of the Black Sea with the Mediterranean Sea. These include a continuous outflow of Black Sea waters into the Sea of Marmara during glacial and Holocene times (Degens & Ross, 1974; Lane-Serff et al., 1997), as well as an evaporative sea-level drawdown of the Black Sea during glacial times, leading to a decoupling from the Mediterranean at a level of -90 m to -110 m (Chepalyga, 1984), or -100 m to -110 m (Görür et al., 2001; Demirbag et al., 1999),

or -110 m (Aksu et al., 2002), or -140 m (Ryan et al., 1997) or as much as -150 m (Winguth et al., 2000).

Until the beginning of the 1990's, the rate of rise in the level of the Black Sea after the last glacial lowstand was considered to be slow and analogous to that postulated for the Mediterranean Sea. A connection between them was established between 9 and 7.5 ka, and the Mediterranean and the Black Sea reached the same level soon thereafter. Joint Russian-American research carried out in 1993 led to the so-called "Noah's flood hypothesis", with very rapid ("catastrophic") flooding of the Black Sea with Mediterranean waters at about 7.5 ka (Ryan et al., 1997). Memories of this event are thought to form the basis of the biblical story of Noah, since the living space of early settlers along the Black Sea coast was supposedly inundated during the flooding.

In the catastrophic flood hypothesis, the Black Sea level was because of meltwater input high enough in early post-glacial times to allow outflow via the Sea of Marmara into the Aegean Sea. Before around 12 ka, the retreat of the Scandinavian ice sheets led to a redirection of meltwaters into the North Sea. Without meltwater input and under an increasingly cold and dry climate in the Black Sea region during the Younger Dryas (11-10 ka), the Black Sea level fell again to a lowstand. The Mediterranean sea-level, however, was rising at the same time, reaching the Bosphorus sill depth around 7.5 ka. The sill depth assumed in this model is with -35 m relatively close to its present-day depth of -32 m. This assumption, however, is by no means undisputed (see below for a comparison of different models).

Ryan et al. (1997) postulated a massive intrusion of Mediterranean waters into the Black Sea at about 7.5 ka, with input rates several hundred times higher than the largest known waterfalls. The idea of a flooding event in the Black Sea is mainly based on three facts: Firstly, cores reveal a buried erosional surface on the broad northern continental margin reaching below the shelf break (Evsylekov & Shimkus, 1995; Major, 1994). Secondly, indicators of sub-aerial exposure were found to a depth of 123 m, giving evidence to a Black Sea level well below the Bosphorus bedrock sill at -70 m (Algan et al., 2001; Gökasan et al., 1997). Thirdly, a uniform marine mud drape was deposited onto the subaerial surface. This drape shows no thickness variations in depressions or on the crest of dunes and no signs of landward-directed onlap (Ryan, 2004). Therefore, the transgression must have been rapid enough to preserve the former land surface from intense erosion and to keep the time for syn-transgressive sedimentation too short for the development of retrogradational

depositional features. Findings supporting at least a rapid and abrupt reconnection between the Marmara Sea and the Black Sea have also been published by Major et al. (2006, 2002), Giosan et al. (2005), Sidall et al. (2004), and Myers et al. (2003). In Contrast, Hiscott et al. (2006, 2002) and Aksu et al. (2002a) contradicted the rapid reconnection model and proposed a non-catastrophic, gradual process.
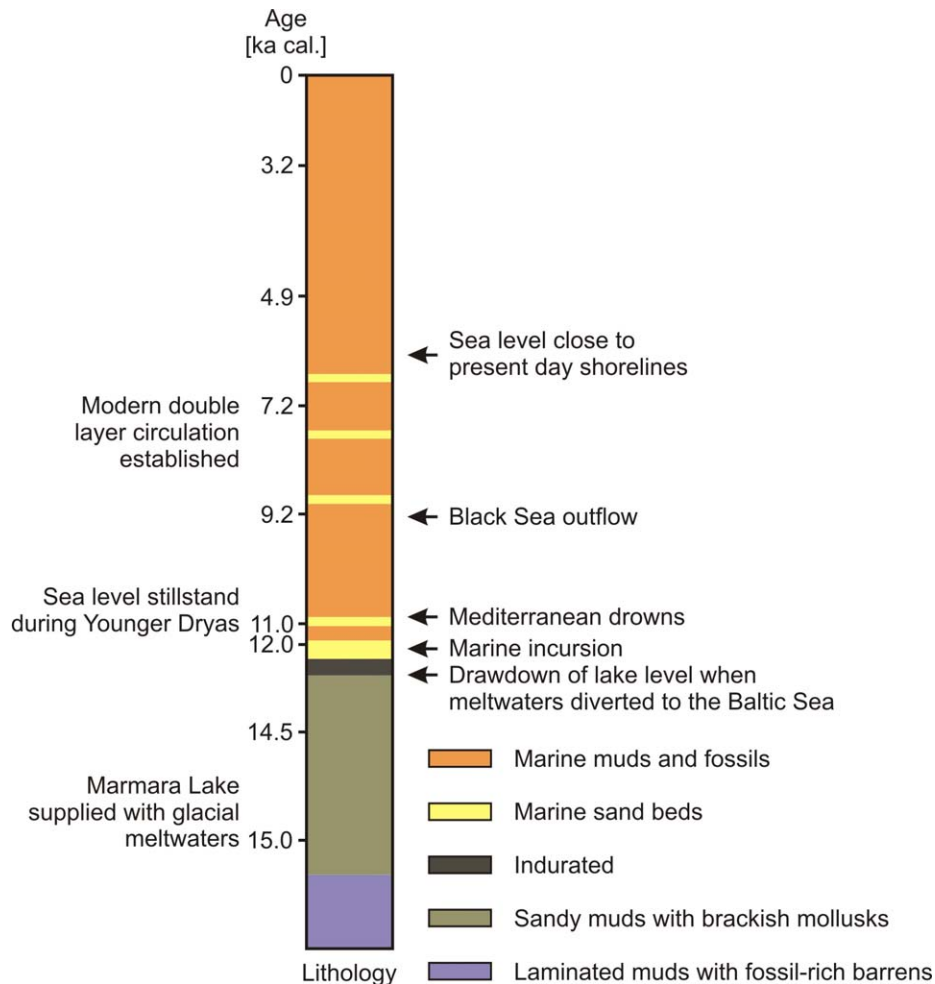
Fig. **3.13**: Summary of lithologies and fossil record found in sediments of the last 15,000 years in the Marmara Sea correlated to calibrated radiocarbon dating; from McHugh et al. (2008). The main paleoceanographic characteristics of the Marmara Sea are described on the left, black arrows on the right mark the main events in the oceanographic development.

To understand the timing of the connection between the Marmara and Black seas and to verify the possibility of a rapid flooding in the Black Sea, the sill depth of the Bosphorus Strait at the time of connection must be known (Myers et al., 2003; Sperling et al., 2003; Major et al., 2002). The present-day depth of the Bosphorus sill is -32 m, but other values for the past sill depth have also been suggested. A deep Bosphorus sill of -80 m, for example, would allow a connection of the Black and Marmara Seas as early as 14 ka (Major

et al., 2002) and a shallow sill of -35 m would be required to create the 'Noah's flood' scenario around 8.4 ka (Ryan et al., 2003). Sperling et al. (2003) suggested a sill depth 7 m higher than today, as it would fit best to the salinity evolution of the Marmara and Aegean Seas at around 8.7 ka. Yaltirak et al. (2002) showed that for the reconnection of the Marmara Sea and the Mediterranean through the Dardanelles Strait, the timing cannot be addressed as a function of sea-level change alone. Tectonic uplift induced by local compression associated with a restraining bend in the western segment of the North Anatolian Fault has most likely played an important role as well (Fig. 3.6). A similar influence should not be ruled out for the Bosphorus Strait (Yaltirak et al., 2002).

Findings in the Marmara Sea do mostly not add much support for between the Back Sea and the Marmara Sea, as A more-or-less constant outflow of Black Sea waters into the Marmara Sea rather than a 'catastrophic' mode of reconnection is concluded in many studies in the Sea of Marmara (McHugh et al., 2008; Hiscott et al., 2007, 2002; Kerey et al., 2004; Kaminski et al., 2002; Aksu et al., 2002a, 2002 b). Figure 3.13 shows a compiled lithological column for Marmara Sea sediments younger than 15-16 ka together with a reconstruction of the major events during the development of the Black Sea – Marmara Sea – Mediterranean corridor as proposed by McHugh et al. (2008). This reconstruction allows for a lake stage in the Marmara Sea during glacial times with a Marmara Lake that was supplied by glacial melt-waters from the Black Sea between ~15.5 and 14.5 ka. During the Bølling/Allerød (14.5–13.0 ka), warmer conditions were assumed that probably prevailed until marine waters incurred around 12 ka. At this time, the Black Sea was supposedly either isolated or spilling into the Marmara Sea at a low rate. The Younger Dryas (11.5–10.5 ka) is marked by a time of sea-level stillstand that ended once strong outflow from the Black Sea was established at ~9.2 ka, leading to the development of a two-layer circulation between the Marmara Sea and the Black Sea (Major et al., 2006; Murray, 2006; Fontanier et al., 2003, 2002; Evans et al., 2002; Schonfeld, 2001, 1997; Kaminski et al., 2001; den Dulk et al., 2000). This modern mode of connection was well-established around 6 ka when the Marmara Sea level had reached approximately the present-day shoreline (McHugh et al., 2008).

Most of the models described above consider inflow into the Black Sea basin after the connection to the Mediterranean was established. An opposing scenario has also been suggested: Aksu et al. (2002a) assumed that a positive water balance drove the Black Sea level above the Bosporus sill depth at around 11.4 to 12.8 ka and Black Sea waters flowed into the Sea of Marmara. Evidence for this scenario comes from westward directed cross-stratification of deposits in the western Marmara Sea (Aksu et al., 1999), and the existence

of a subaqueous delta system south of the Bosphorus Strait in the Marmara Sea (Hiscott et al., 2007, 2002; Aksu et al., 2002a, 2002b). Eriş et al. (2007) doubted the significance of the latter features for the reconstruction of outflow from the Black Sea or sea-level changes and attributed the deposition of the delta system to increasing sediment supply from local river systems during a time when the Holocene sea had almost reached its current level.

3.6.2.2 Caspian Sea

Another important factor that controls the water balance in the Black Sea Basin is the connection to the Caspian Sea in the east (Grosswald & Hughes, 2002; Kroonenberg et al., 1997). This connection is established through the Manych Depression that is situated today at a height of 25 m above sea-level (Mangerud et al., 2001; Popov, 1983). Former beach terraces indicate that the highest lake level in the Caspian Sea during deglaciation was at +50 m and would therefore allow for flooding of the Manych Depression (Kroonenberg et al., 1997). During the last glacial, huge ice masses blocked rivers from flowing into the Arctic Ocean and meltwater was directed instead southward through the Baltic Basin and via the Volga river system into the Caspian Sea (Mangerud et al., 2004).

3.6.3 Late glacial and Holocene geology

3.6.3.1 Stratigraphy

A unified regional stratigraphic chart for late glacial and the transition to the Holocene for the Black Sea is still lacking. Various stratigraphic models based on bio- and lithostratigraphy have been proposed; a compilation by Ryan et al. (2003) is shown in Fig. 3.14.

A common feature to all the stratigraphic schemes is the separation of an older freshwater stage in the Black Sea from a younger marine stage that began around 7 ka and lasts until today. The base of the marine stage is defined by the first appearance of Mediterranean species in Black Sea sediments and this level is also used most often to define the beginning of the Holocene – an age assignment several thousand years younger than the conventional Pleistocene/Holocene boundary of around 10.5 ka.

Shimkus et al. (1978; Fig. 3.14, Panel 7) resolved this problem by introducing a freshwater early Holocene unit (HL_I) that began synchronously with the global standard and is separated at 7.2 ka from the marine Middle and Late Holocene units (HL_{II}, HL_{III}). The

stage HL_I corresponds to the Upper Neoeuxine in other stratigraphic schemes and the first appearance of molluscs such as *Dreissena rostriformis bugensis*, *Monodacna caspia* or *Dreissena polymorpha regularis* within it marks the onset of salinization (Sherbakov & Babak, 1979). Research on deep basin cores showed that the first sign of an increasing content of the heavier oxygen isotope ^{18}O appeared at a similar level; it was dated to ~8.5 ka by interpolation (Fig. 3.14, Panel 5; Degens & Ross, 1974; Deuser, 1972).
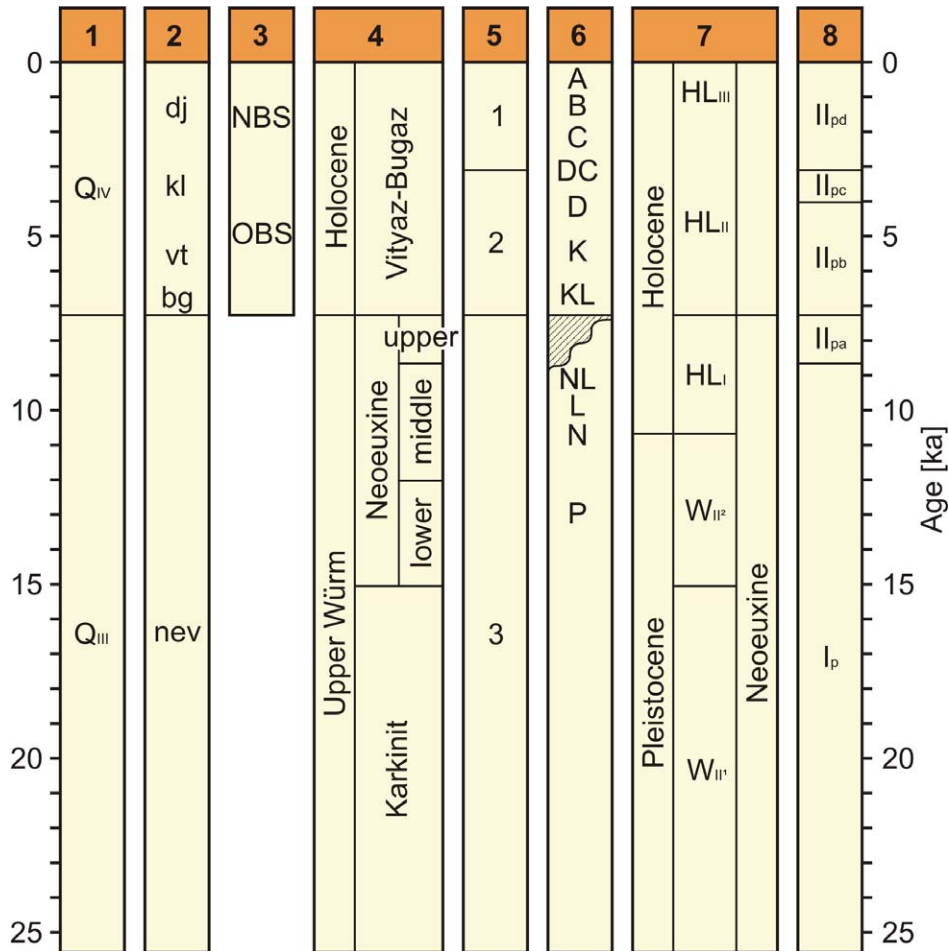
Fig. 3.14: Regional stratigraphic models for the past 25 ka compiled by Ryan et al. (2003). **Panel 1**: Stages commonly used for continental and marine stratigraphic correlation (Skiba et al., 1976; Kuprin et al., 1974; Popov, 1973; Popp, 1969). **Panel 2**: Stratigraphy based on distinct strata observed in outcrops and cores (Dimitrov, 1982; Nevesskaya, 1965); nev – Neoeuxine, bg – Bugaz bed, vt – Vityazevskian beds, kl – Kalamitian beds, dj – Djemenitian beds. **Panel 3**: OBS – Old Black Sea Beds, NBS – New Black Sea Beds (Markov et al., 1965; Nevesskaya, 1965). **Panel 4**: Stratigraphy of the Neoeuxinian deposits (Sherbakov & Babak, 1979). **Panel 5**: Lithostratigraphy of basin floor cores (Degens & Ross, 1974). **Panel 6**: Lithostratigraphy of cores from northern and western Black Sea shelf (Shopov et al., 1986). **Panel 7**: Stratigraphy derived from diatoms and pollen in deep basin sediments (Shimkus et al., 1978). **Panel 8**: Pollen assemblage zones in deep water cores from the western Black Sea (Atanassova, 1995); I_P – Dominance of herbs and grasses (dry, cold climate), II_{PA} – Enlargement of oak forests, II_{PB} – Oak forest maximum, II_{PC} – Enlargement of herb communities, II_{PD} – Formation of 'Longoz Forests' along river valleys.

3.6.3.2 Development of the Danube Delta

The present-day Danube Delta was formed during the Late-Pleistocene sea-level highstands (Karangatian, Surozhian; Tab. 3.2) and during the Holocene; possible earlier stages of delta evolution in the Lower Quaternary are missing due to erosion during phases of sea-level lowstands. The geomorphology of the Danube Delta is controlled by the interaction of influence of the Danube river system (sediment and water discharge, flow energy) and the Black Sea (wave energy, currents, sea-level changes).
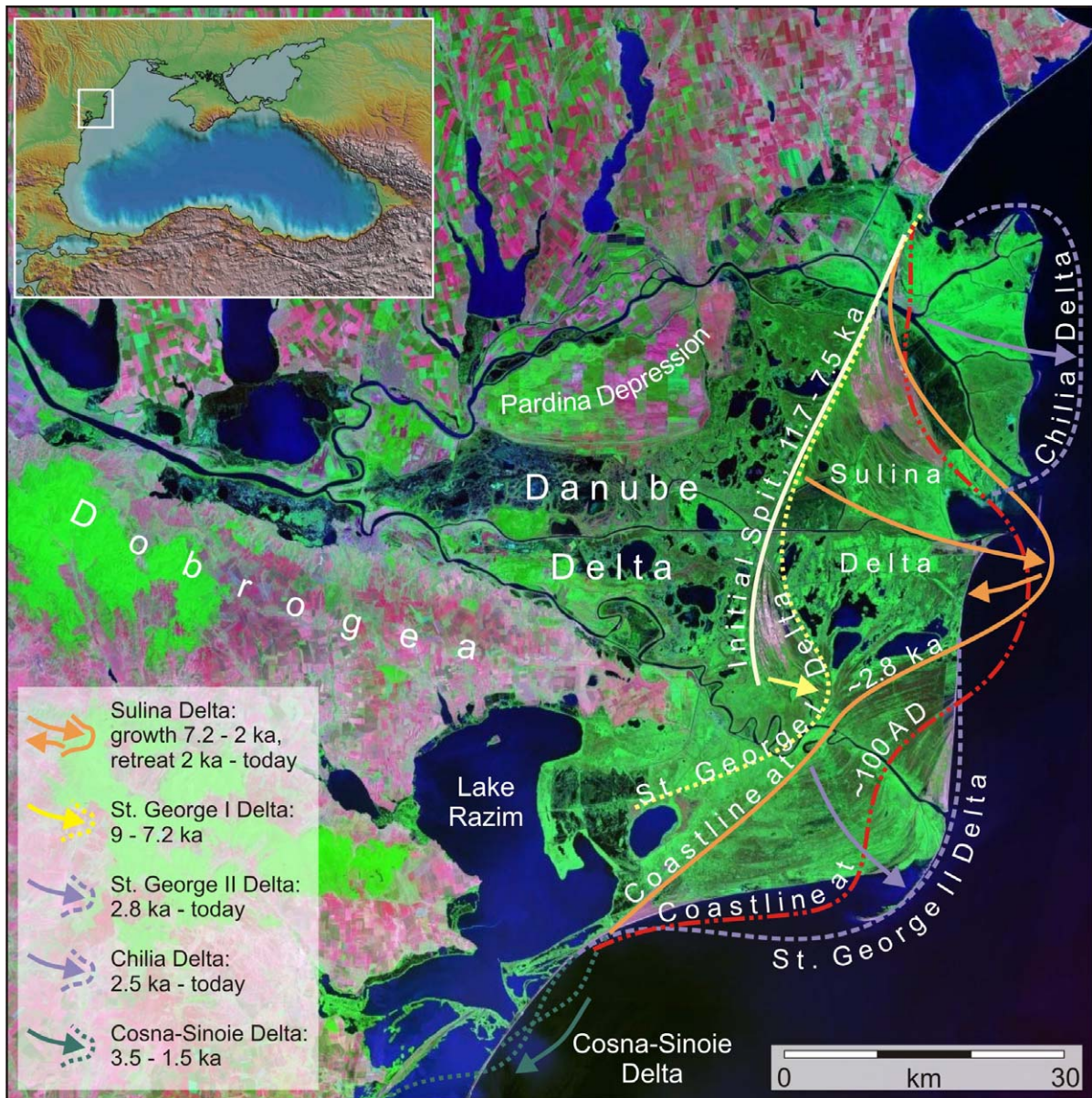

Fig. 3.15: Post-glacial development of the Danube Delta and coastline migration after Panin (1997). Arrows give the progradation or retreat directions for the different delta lobes. The white-framed inset gives the map location. Reference for underlying Landsat imagery: http://upload.wikimedia.org/ wikipedia/commons/d/d0/Danube_delta_Landsat_2000.jpeg

A continuous succession of prograding delta lobes was formed in the Danube Delta (Panin & Popescu, 2007; Noakes & Herz, 1983; Panin et al., 1983; Panin & Panin, 1967) with the beginning of the process dating possibly as far back as 12,000 years (Panin et al., 1983). A more recent study suggests, however, a much younger origin (less than 6,000 years according to Giosan et al., 2006). Based on geomorphologic, structural, textural, geochemical, mineralogical and faunal analyses and in particular extensive ^{14}C dating of Danube Delta sediments, the main developmental stages of the delta can be established and combined into chronological models of the delta development (Fig. 3.15, 3.16; Giosan et al., 2006; Panin, 1997; Panin, 1989; Noakes & Herz, 1983; Panin et al., 1983; Panin; 1974). Two different models are described below: The 'older' scenario after Panin et al. (1983) and the 'younger' based on Giosan et al. (2006).

The delta history proposed by Panin et al. (1983) comprises the following stages: Starting with the Leţea-Caraorman initial spit that was active between 11.7 and 7.5 ka, the St. George I Delta developed between 9 and 7.2 ka (progradation rate 3-5 m/yr). The Sulina Delta developed later between 7.2 and 2 ka (progradation rate 6-9 m/yr), since then the coastline in the Sulina Delta area retreats at a rate of 5-6 m/yr to its present-day position. Sediment deposition moved to the St. George II Delta and to the Chilia Delta; the former started to develop around 2.8 ka and the latter about 2.5 ka. The St. George II Delta progrades at a rate of 8-9 m/yr, and the Chilia Delta at 8-10 m/yr. The southernmost delta lobes are those of the Cosna-Sinoie Delta, they developed between 3.5 and 1.5 ka.

These observations have been interpreted as evidence against a sea-level lowstand during the Younger Dryas and a subsequent flooding of the Black Sea in the sense of Ryan et al. (1997, 2003). They point instead to a sea-level highstand close to the present level at around 11.7 ka with no signs of 'catastrophic' events afterwards, mostly because such events would have left gaps in the progradation of the delta lobes that have not yet been found (Panin & Popescu, 2007).

The chronological model described above, however, is questioned by a recent reassessment of the history of the Danube Delta carried out by Giosan et al. (2006). Through more refined dating methods and careful sample selection in coastal deposits of the deltaic region, ages for the different delta lobes and barriers have been obtained that are several thousand years younger than previously reported.

Giosan et al. (2006) link the inception of the open-coast Danube Delta to the deposition of the most landward beach ridges in the St. George I delta lobe and date these features to 5.21 ka ± 210 yr. The end of the development of the St. George I lobe and the transition to the Sulina lobe is dated to 3.64 ka ± 140 yr. The Sulina delta lobe underwent a phase of rapid growth until approximately 2 ka that might be related to humid climate conditions in the Danube drainage basin and thus increased river discharge (Barber et al., 2004).Growth of the Sulina Delta came to an end at approximately 1.7-2 ka when the buildup of the St. George II delta began. The youngest delta lobe in the Danube Delta system is the Chilia lobe that did not become active before 1.2 ka (Giosan et al., 2006).
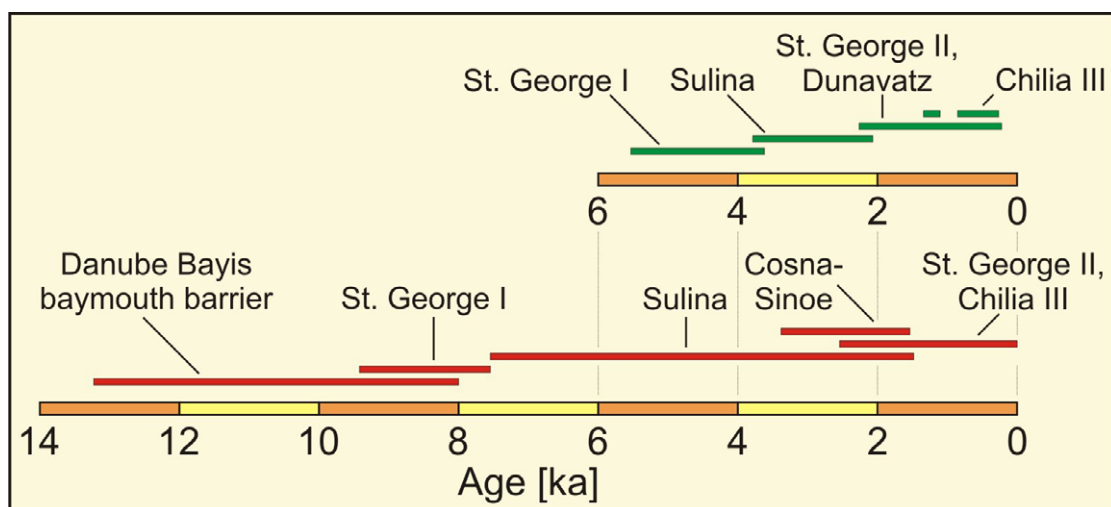
Fig. **3.16**: Comparison of two chronological models for the development of the different lobes and/or barriers in the Danube Delta (after Giosan et al., 2006). The lower model (red bars) was proposed by Panin et al. (1983) and dates the earliest features (Danube Bayis baymouth barrier) back to more than 12,000 years. The upper model (green bars) in contrast was based on the findings by Giosan et al. (2006). Here, the development of the Danube Delta started much later (less than 6,000 years before present) with the St. George I Delta.

Because of the much younger age assignments compared to the model of Panin (1997), the development of the Danube Delta as proposed by Giosan et al. (2006) is does not have any direct implications on the catastrophic Black Sea flood hypothesis. However, it gives insight into the Late Holocene relative sea-level history in the Danube Delta. The sea-level was modeled to be relatively stable within an interval of +1.5 m to -2 m during the past ~5000 years without any signs of large-amplitude short-term variations. This apparently contradicts older basin-wide sea-level reconstructions that feature an Old Black Sea highstand (~4.5 ka) and a younger, Phanagorian lowstand (~2.5 ka; e.g. Chepalyga, 1984), as well as archeological findings from around the Black Sea where submerged settlements imply rising sea-levels. To make all sea-level reconstructions comparable and to allow

compiling a basin-wide sea-level history for the Black Sea, the influence of local factors such as differences in the regional tectonic development needs to be taken into account (Giosan et al., 2006).

3.6.3.3 Sedimentary record in the Black Sea basin

The sedimentation in the Black Sea basin is significantly influenced by input from the Danube (Section 2.2). Other large rivers of the region such as Dniepr, Dniestr or Don play today only a minor role in sediment delivery to the Black Sea, their importance, however, might have been higher during the last deglacial (Bahr et al., 2005). Measurements on sediment cores from deeper parts of the Black Sea slope or basin provide uninterrupted records of the sedimentary history. Based on stable isotope and grain size measurements as well as XRF-scans (measurement of bulk intensities of major chemical elements; Fig. 3.17) on gravity cores from a transect crossing the lower shelf to the middle slope, Bahr et al. (2005) could create such a continuous record of the main sedimentary characteristics in the northwestern Black Sea for the past 30,000 years.

The sediments on the upper Black Sea slope can be subdivided into three typical units (Panel 5, Fig. 3.14; Degens & Ross, 1974). These are, in chronological order: The lacustrine Unit III of homogenous to centimeter-scale laminated muddy clay, and the marine units II and I, both of Holocene age. Unit II is made of sapropelic sediments and the youngest Unit I consists of finely laminated coccolith ooze. The two younger units together have a more-or-less constant thickness of 45 cm. On the lower slope, the Holocene units are largely missing. The sedimentary record found in cores on the Black Sea slope reflects the hydrological and paleoenvironmental variations in the region since the last glaciation and is summarized below.

Stable climatic conditions characterize the last glaciation (28.5-18 ka). The low sea-level at that time led to a progradation of the Danube Delta towards the deeper basin. Subsequently, sediments on the western Black Sea slope have a relatively high sand content.

Between 18 and 15.5 ka, a characteristic series of four reddish clay layers was deposited on the slope. These have been linked to pulses of meltwater from the Scandinavian ice sheet that seemed to have reacted very sensitively to high-latitude climate variations. The Scandinavian meltwater is thought to have entered the Black Sea through the Caspian Sea, where brownish 'chocolate clays' have been described (e.g., Kroonenberg et al., 2001) and

interpreted to be the sedimentary equivalent of the red clay layers of the Black Sea (Bahr et al., 2005; Ryan et al., 2003). The red layers correlate to time intervals of slightly increased $\delta^{18}O$ (measured in the GRIP ice core; Fig. 3.17) and thus warmer climatic conditions. Geochemical characteristics of the red layers such as a reduced Mn content support stronger freshwater input, an increased Ti/Ca ratio within the red layers shows an associated increase in terrigenous sediment input (Fig. 3.17).
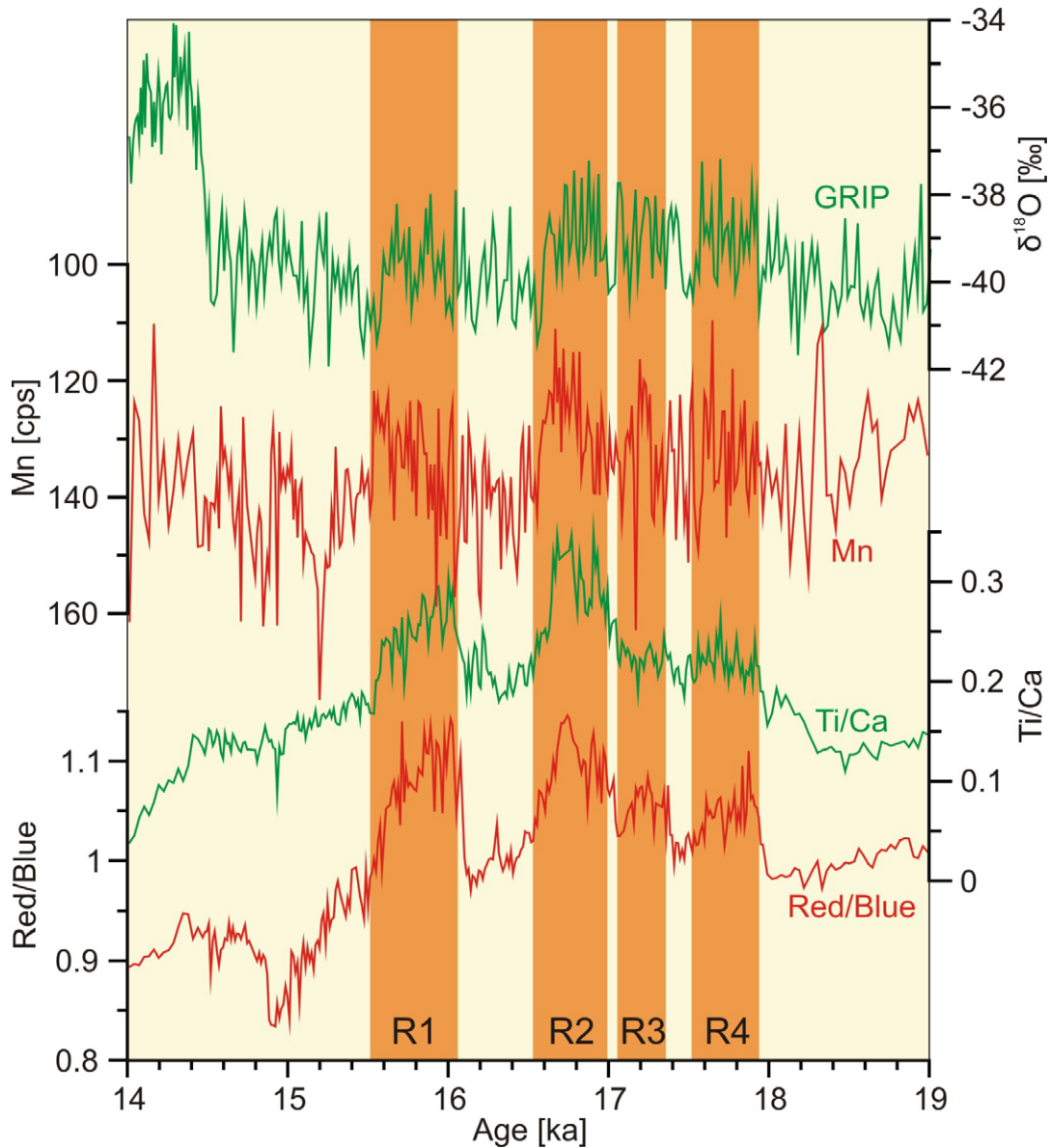
Fig. 3.17: Correlation of red clay layers (R4-R1 in chronological order) in the Black Sea to the oxygen isotope record of the GRIP ice core, indicating their deposition in times of relatively warm climate. Also plotted are Mn-intensity, Ti/Ca ratio and the spectral red/blue ratio. From Bahr et al. (2005).

After the deposition of the red clays, sedimentation in the Black Sea developed mainly in response to climate variations. Authigenic calcite precipitation through enhanced

phytoplankton activity characterizes the sedimentation in lakes under warmer climatic conditions (Bahr et al., 2005; Leng & Marshall, 2004). Such conditions prevailed during the Bølling/Allerød (Tab. 3.3) and later during the Early Holocene; high calcite contents characterize sedimentation during these periods. Colder conditions in contrast led to reduced calcite contents and relatively high amounts of terrigenous material in the sediments. Two phases of cool climate interrupt the warming trend, first the Younger Dryas (Tab. 3.3) and later the '8.2 ka Event' (section 3.6.1). Sedimentation during these intervals is predominantly clastic.

3.6.3.4 Depositional systems on the shelf and upper slope

The depositional pattern of late glacial to Holocene sediments in the Black Sea primarily reflects the water-level changes that occurred during that period. Several models derived from the analysis of very high-resolution seismic reflection profiles and dated sediment cores have been proposed and are described below.

The depositional model of Aksu et al. (2002) for the Lower Quaternary of the southwestern Black Sea is presented in section 3.5.3. According to the nomenclature established there, the uppermost Quaternary is represented by the seismic stratigraphic unit 1 (Figs. 3.11 and 3.12); the oldest of its subunits (1A) is interpreted to be made up of four lowstand systems tracts deposited during times of low sea-levels towards and at the last glacial maximum (section 3.5.3). The post-glacial to Holocene sea-level rise is manifested in the transgressive subunits 1B and 1C, and the youngest subunit 1D is formed by a Holocene highstand systems tract (Aksu et al., 2002). The transgressive systems tracts that follow glacial sedimentation consist of back-stepping, internally seaward-prograding parasequences. The deposits of subunit 1B have been interpreted to be barrier islands (Fig. 3.12) or beaches based on their geometry and seismic facies as well as similarity to deposits described previously (e.g., Aksu et al., 1999; Kraft et al., 1987).

Subunit 1C is characterized by mound shaped sediment ridges, sediment waves or current-generated marine bars; some sediment bodies within subunit 1C have also been interpreted as mud volcanoes. These deposits are spatially arranged in clusters of parallel ridges at progressively shallower water depths, resembling sedimentation during rising sea-levels. The shorelines were stable when sediment supply and sea-level rise kept pace with each other and jumped landward when the rate of sea-level rise exceeded the rate of sediment supply (Aksu et al., 2002).

Subunit 1D comprises the youngest sediments on the Black Sea shelf. It forms a thin veneer of sediments that unconformably overlies the older morphology. The onset of the deposition of this subunit is interpreted as the maximum flooding surface towards the present sea-level highstand (Aksu et al., 2002).

The model of Aksu et al. (2002) does not favor the idea of a catastrophic flooding of the Black Sea shelf (section 3.6.2). The original concept of Ryan et al. (1997) that includes a catastrophic flood is the basis for a competing depositional model described below. Major (2002) created a set of graphical snapshots that summarize the depositional development in agreement with this model. They are shown in Fig. 3.18 for comparison.

After the last glacial maximum around 15 ka (Panel A, Fig. 3.18), meltwater from the Eurasian ice sheet and the Alpine ice dome led to rising sea-levels and finally to an overflow from the Caspian Sea into the Black Sea and from the Black Sea into the Mediterranean. Between 13.4 and 11 ka (Panel B, Fig. 3.18) the sea-level decreased during times of climatic aridity leading to forced-regression type sedimentation on the slope. The lowest sea-level thought to be reached during this regression was -105 m. Erosion through wave action and sub-aerial exposure led synchronously to the formation of a sedimentary unconformity on the upper slope and shelf (Panel C, Fig. 3.18).

The water balance in both Black Sea and Caspian Sea basins switched from evaporation to precipitation during the colder climate of the Younger Dryas (11 ka – 10 ka; Panel D, Fig. 3.18). The water level of the Caspian Sea was driven above the sill of the Manych Depression and Caspian waters spilled into the Black Sea. In the Black Sea itself, a freshwater layer with *Dreissena* coquina was deposited up to a level of 30 m below the present-day sea-level. The global sea-level was at this time more than 20 m below the Black Sea. Transgressive systems tracts were deposited during this interval leading to coastal onlap over the unconformity that formed before (Panel D, Fig. 3.18).

Panel E (Fig. 3.18) shows the situation at 8.5 ka after the climate warmed during the Early Holocene. This new phase of aridity and evaporation in the Black Sea region drove the sea-level down to values around or even below the present-day shelfedge. The *Dreissena* coquina that developed with inflow of Caspian freshwater during the colder Younger Dryas was eroded and shell fragments together with calcareous beach sands and quartz sand from dried riverbeds on the shelf formed aeolian coastal dunes.

Offshore   **Onshore**

A   ~15 ka

B   13.4-11 ka

C   11 ka

D   11-10 ka

E   8.5 ka

F   Present day

Lowstand/regression   Mud drape
Highstand/transgression   Unconformity
Coastal dunes   Erosion
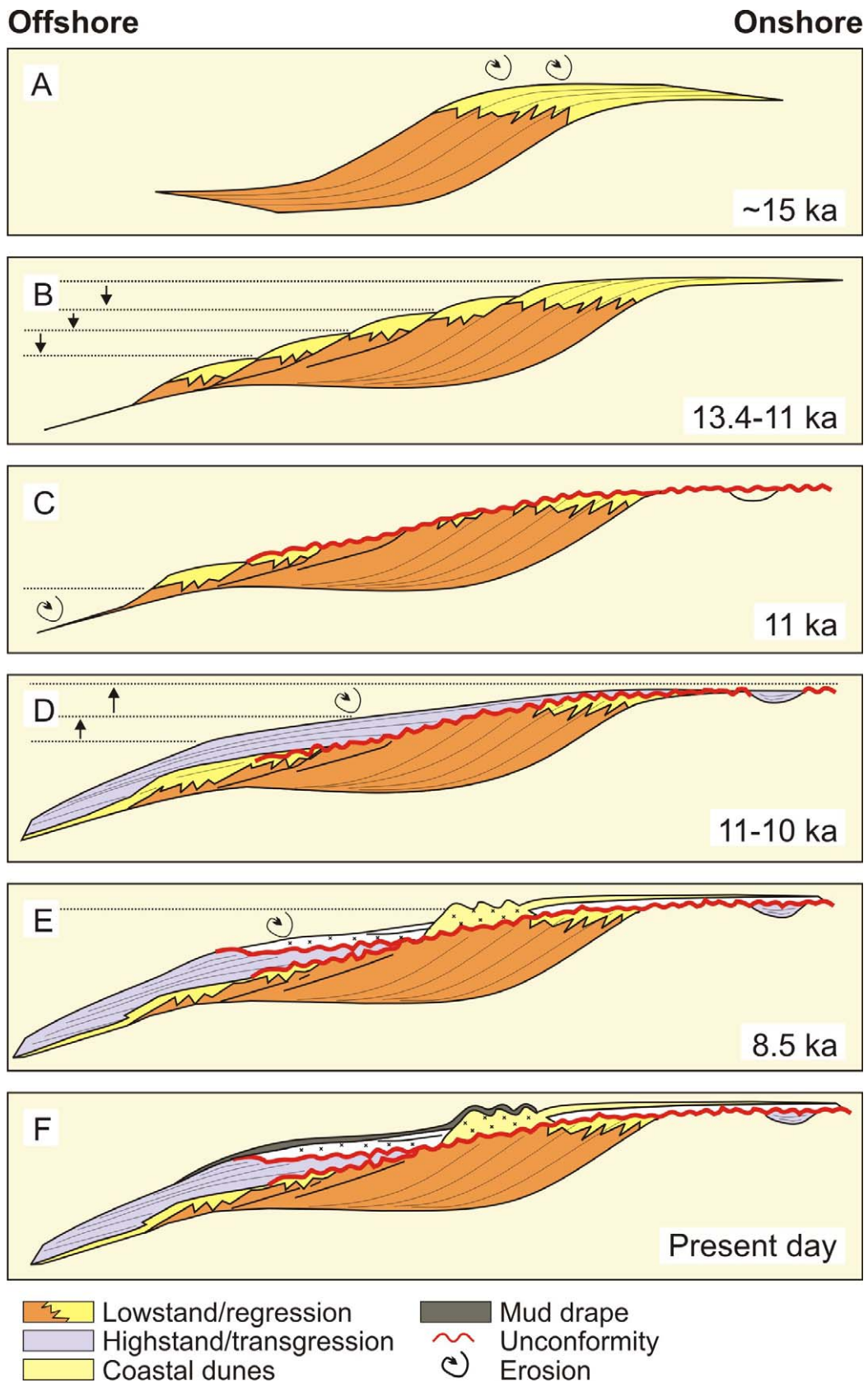
Fig. **3.18**: Post-glacial development of the Black Sea shelf in six idealized panels (A-F, in chronological order). Dotted lines and arrows give the development of the sea-level at the time the 'snapshot' was taken. The cross-sections are based on interpretation of seismic reflection profiles and sediment cores from the outer Ukrainian shelf. From Major (2002).

According to Ryan et al. (2003), the last transgression in the Black Sea started at 8.4 ka after the rising global sea-level led to a connection between the Mediterranean and the Black Sea. The result is shown in the present-day snapshot of Panel F (Fig. 3.18). The transition from brackish to marine waters in the Black Sea can be followed in the sedimentary record between 8.4 and 7.1 ka: a thin drape sheet of muddy sediments that lacks signs of coastal onlap and is uniformly distributed over the conserved coastal landscape of the Early Holocene developed till today (Panel E, Fig. 3.18). These characteristics of the Holocene sedimentation after the last transgression gave rise to the idea of a particularly rapid, possibly 'catastrophic', flooding event in the Black Sea.

4. Data and Methods

4.1 Data

This study is based primarily on the interpretation of reflection seismic data and borehole/gravity core information. The data used are discussed below.

4.1.1 Reflection seismic data

Reflection seismic data from the western Black Sea from various sources, recorded with a variety of instruments between the 1980s and 2002, were available to the ASSEMBLAGE project. A part of them was used in this study (see the compilation of profile tracks in Fig. 4.1). A short overview of the different surveys and their main recording parameters – as far as they are publicly known – is given below.

4.1.1.1 BLASON

In the French-Romanian research project BLASON, two reflection seismic surveys were carried out covering almost the entire western Black Sea (Fig. 4.1). During the cruise BLASON I in 1998, approximately 4,500 km of seismic profiles were recorded; another 4,500 km were added during the BLASON II cruise of 2002. The data were acquired using 'mini-GI' guns as seismic sources (generator/ injector volume configuration: 13/35 inch^3 during BLASON I, 24/24 inch^3 during BLASON II; operating pressure: 110-130 bar) and a 'Triton-Elics DELPH2' system with a 300 m long 24-channel analogue streamer (receiver interval 12.5 m) for recording at a sample interval of 1 ms. Parallel to the reflection seismic measurements described above, chirp sonar profiling was carried out during the BLASON cruises using a hull-mounted system with signal frequencies in the range of 1.8 kHz to 5 kHz and a power output of up to 9 kW. Not all acquired chirp sonar profiles were available for this study, their locations are given separately below.

4.1.1.2 GHOSTDABS

During the cruise of the German-Russian cooperative project GHOSTDABS in 2001, about 50 reflection seismic profiles with a total of 1,130 line-km were acquired on the Ukrainian shelf and on the continental slope off the Crimean Peninsula (Fig. 4.1).
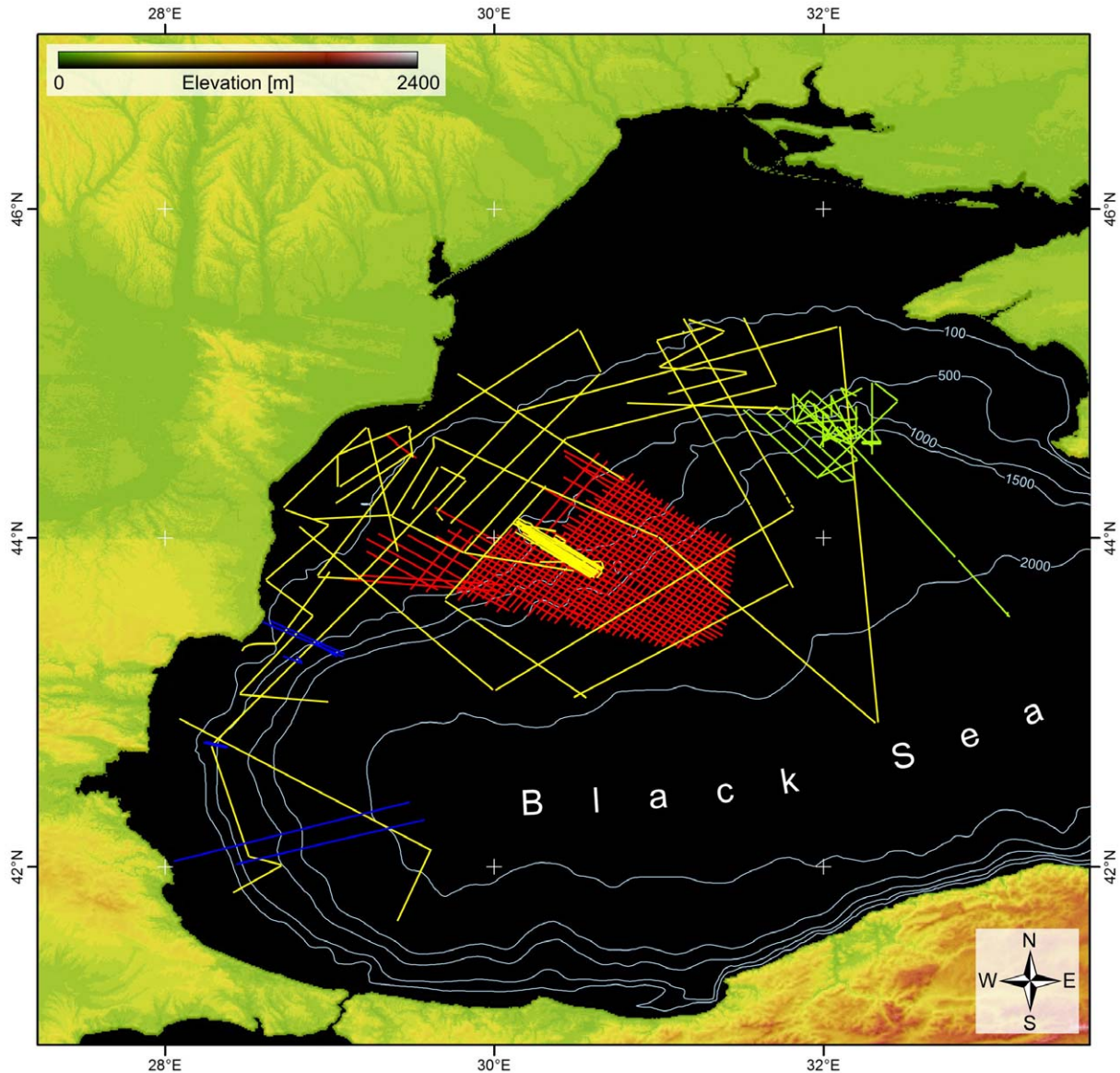
Fig. 4.1: Map of the reflection seismic profiles in the western Black Sea available for this study in the framework of the ASSEMBLAGE project. The data are compiled from various sources: Yellow lines – high-resolution seismic lines and chirp sonar data (not all lines are available) acquired during the BLASON I and II cruises. Green lines – high-resolution reflection seismic profiles acquired during the GHOSTDABS cruise. Red lines – industrial seismic data acquired under the supervision of Total SA of France, available at the University of Bucharest. Blue lines – very high-resolution reflection seismic lines acquired by the Institute of Oceanology of the Bulgarian Academy of Sciences (IO-BAS).

An array of one 'mini-GI' and one standard GI gun was used as seismic source. A 300 m long 'GECO Prakla' analogue streamer with 4 channels and a receiver interval of 50 m together with a custom-made digitizing/storage system were used for data recording. The data sampling interval was 1 ms.

4.1.1.3 Total

In 1994 and 2001, seismic surveys covering the outer shelf and large areas of the Danube deepsea fan were carried out on behalf of the French company TotalFinaElf (today: Total) in the Romanian sector of the Black Sea for oil and gas exploration (Fig. 4.1). These data were available at the University of Bucharest for additional interpretation. The technical specifications of the equipment used during acquisition as well as the processing routines applied are not known exactly; the data have a sampling interval of 4 ms.

4.1.1.4 IO-BAS

The Institute of Oceanology of the Bulgarian Academy of Sciences has been carrying out seismic surveys in the Bulgarian sector of the Black Sea since the early 1980s. Various pieces of equipment (such as boomer, sparker and chirp-sonar systems) were used, mostly with a very high data resolution. Nine profiles from different surveys were made available to the ASSEMBLAGE project (Fig. 4.1). More information on seismic surveying carried out by IO-BAS in the western Black Sea, such as cruise tracks or instrument descriptions, is available in the 'Seismics & Sonar' section of http://www.eu-seased.net.

The data available to this study consist of three sparker lines from the 'Sredetska' survey of 1988, one boomer line from the 'Godin' survey of 1990, two sparker lines from the 'Kaliakra' survey of 1990 and three boomer lines from the 'PP 2' survey of 1998. All data were recorded analogue using thermal printers. They were scanned from paper rolls and transformed into standard digital seismic data formats using custom-made software (available under http://www.kogeo.de). Slight image-enhancing reprocessing was applied to the data after the digitalization.

4.1.2 Gravity core and borehole data

In order to tie the results of the interpretation of the seismic profiles to lithologic and stratigraphic models, information from gravity cores and boreholes compiled from various sources was taken into account. A map of borehole and core locations is given in Fig. 4.2.
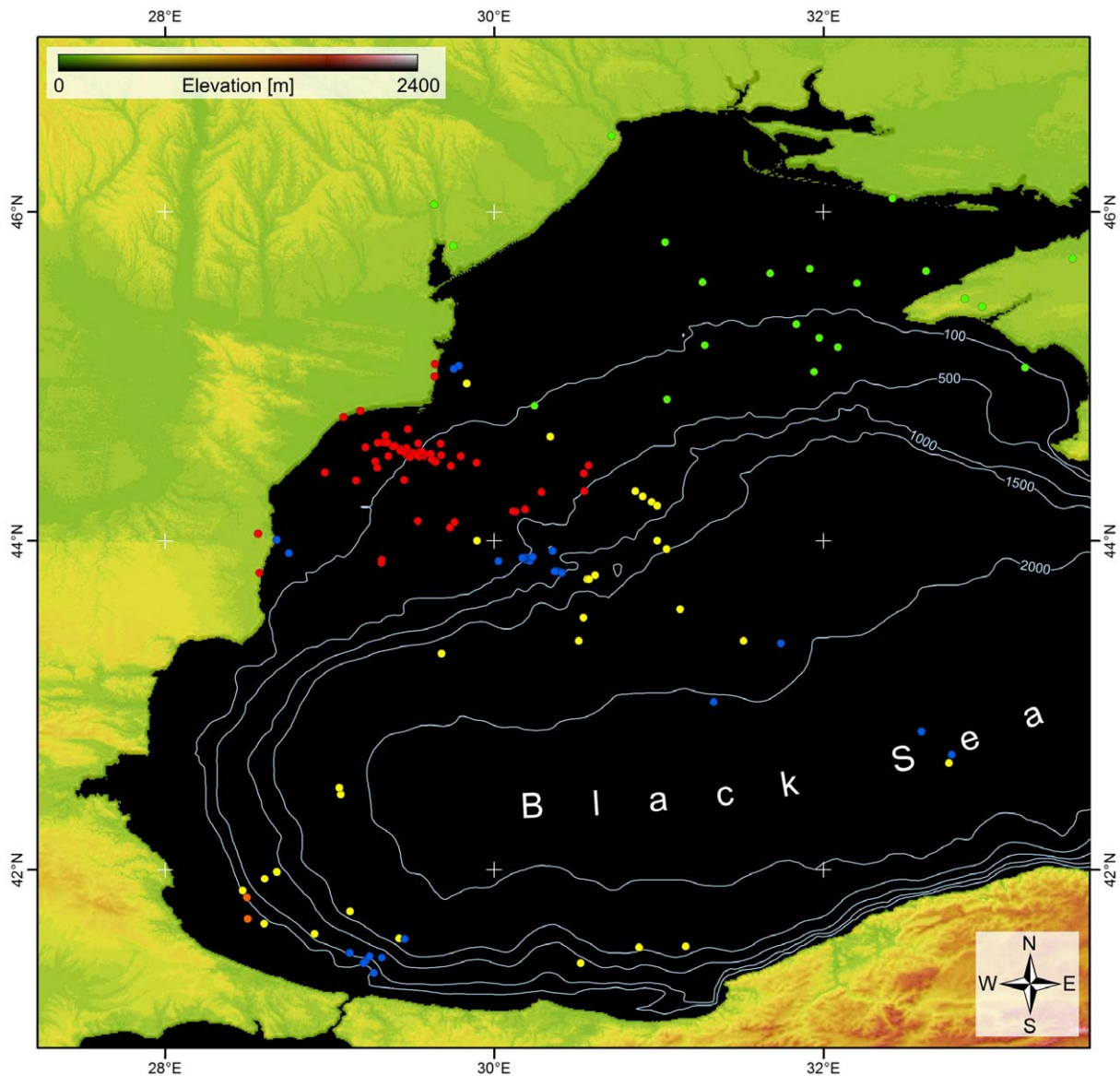
Fig. **4.2**: Map of the locations of gravity cores and boreholes with data available to this study. Yellow dots: Long gravity cores recovered during cruise 'MD139 – ASSEMBLAGE 1' on board the French R/V 'Le Marion Dufresne' in 2004. Blue dots: Gravity cores recovered during cruise 'BLASON II' in 2001. Red dots: Locations of oil and gas exploration wells drilled in the Romanian sector of the Black Sea on behalf of Petrom SA. Green dots: Oil and gas exploration wells in the Bulgarian sector of the Black Sea. Orange dots: Oil and gas exploration wells drilled on behalf of the Turkish TPAO and Turkey Westates Petroleum (e.g., Gillet, 2004).

4.1.2.1 Gravity cores

A research cruise on board the French research vessel 'Le Marion Dufresne' was carried out in the ASSEMBLAGE project in 2004 ('MD139 – ASSEMBLAGE 1'). A copy of the cruise report can be obtained online under: http://www.ifremer.fr/assemblage/documents/ ASSEMBLAGE1-Mission_Rapport.pdf

The 'Marion Dufresne' features the dedicated giant piston coring system 'Calypso' that allows deployment of gravity corers with coring tubes up to a total length of 75 m (this limitation is due to the length of the gangway where the coring system is installed). During the ASSEMBLAGE 1 cruise, tube lengths of up to 55 m were used to recover sediment cores from 45 coring stations. Lithostratigraphic descriptions and photographic documentation are available for every core. The stratigraphic log contains information on sedimentary structures, standard lithology, sediment colour and other specific observations such as clasts or erosion surfaces found in the cores. Sediment samples from some cores were also dated for stratigraphic correlation using AMS-^{14}C measurements.

More than 50 shorter gravity cores (length up to 5 m) were recovered during the BLASON II cruise of 2001 (Fig. 4.2). Limited age dating was carried out on these cores as well.

4.1.2.2 Industrial borehole data

Numerous deep industrial oil and gas exploration wells have been drilled in the western Black Sea, especially in the Romanian and Ukrainian sectors. Due to the mostly disappointing exploration results, data from many of them have been made available for scientific research.

Stratigraphic, depth and to a minor extent also lithological information from 60 boreholes in Romania and the Romanian Black Sea were available for interpretation. Additionally, stratigraphic and lithologic depth profiles from more than 20 boreholes in the Ukraine and the Ukrainian Black Sea could be evaluated for this study (Fig. 4.2).

Important information could also be retrieved from two boreholes (Igneada and Karadeniz) in Turkish waters in the southwestern Black Sea for stratigraphic correlation (Fig. 4.2).

4.1.3 Bathymetry

The bathymetric data used to create the maps and terrain models presented in this study are compiled from various public sources, such as the ETOPO2 global relief dataset derived from satellite altimetry observations and shipboard echo-sounding (Smith & Sandwell, 1997) (grid accuracy: 2 minutes; data can be obtained online at: http://www.ngdc.noaa.gov/mgg/

gdas/gd_designagrid.html). These data have been refined using depth measurements (derived from echo-sounding or reflection seismic data) obtained during the various research cruises that contributed to the database of this study. In addition, very-high resolving bathymetrical data were acquired using the hull-mounted multibeam echo-sounders onboard the French research vessels 'Le Suroît' (Simrad EM300) and 'Marion Dufresne' (Thomson Seafalcon 11) during the BLASON and ASSEMBLAGE cruises. These cover a number of spatially limited areas off the Bosphorus Strait, in the Viteaz Canyon, on the Danube fan and on the Romanian shelf.

4.2 Methods

4.2.1 Seismic stratigraphy

To establish a model of the stratigraphic relationships between depositional bodies identified by means of seismic interpretation, seismic stratigraphic techniques were used. Seismic stratigraphy is based on the principles of seismic sequence and seismic facies analyses that were originally introduced by Vail, Mitchum and co-workers (Vail et al., 1977; Mitchum, 1977) to integrate seismic interpretation into a sequence stratigraphic framework. Sequence stratigraphy itself tries to correlate genetically related facies within models of chronostratigraphically significant depositional surfaces (Van Wagoner et al., 1990).
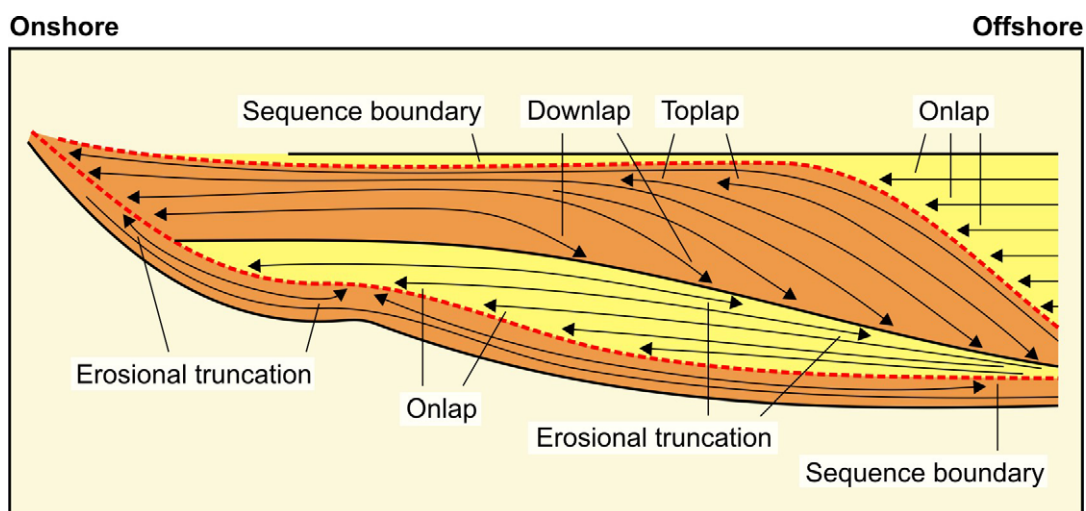

Fig. 4.3: Model of the different reflection terminations that determine the type of an unconformity or sequence boundary; after Vail et al. (1991).

According to the definition of Mitchum (1977), a stratigraphic 'sequence' is a relatively conformable succession of genetically related strata bounded by unconformities or their

correlative conformities. An 'unconformity' in the sense of seismic stratigraphy is a surface separating older from younger strata along which there is evidence of subaerial exposure and erosion resulting in a significant hiatus. A 'conformity' on the other hand shows no sign of erosion or non-deposition (Van Wagoner, 1988). By interpreting the terminations of reflectors, the type of an unconformity can be identified from seismic data: Onlap, downlap or toplap mark unconformities due to non-deposition, while erosional unconformities are charac-terized by truncated reflectors (Fig. 4.3, Vail et al., 1991).

The development of seismic stratigraphic sequences and their relative spatial geometry reflect the cycles of relative sea-level. During periods of rising or falling sea-levels, characteristic successions of depositional systems (so-called systems tracts) are formed; these are divided by major marker surfaces (Van Wagoner et al., 1990; Brown & Fisher, 1977). One seismic stratigraphic sequence corresponds to one complete sea-level cycle and is made up of the following elements: the basal sequence boundary, lowstand systems tract, transgressive surface, transgressive systems tract, maximum flooding surface, highstand systems tract and the concluding upper sequence boundary. A short description of the depositional characteristics of these elements according to Van Wagoner et al. (1990) is given below. Figure 4.4 shows their spatial composition at a model continental margin with a shelfbreak.

A sequence begins with the **lowstand systems tract** formed during periods of relatively low sea-levels above the **basal sequence boundary** (Fig. 4.4). Depending on the nature of the shelfbreak in the observed depositional space, the lowstand systems tract might be composed of one or two distinct units: the lowstand fan and the lowstand wedge. If a well-defined shelfbreak exists and the sea-level fall is sufficiently large, a lowstand fan develops which may be composed of a number of slope and basin-floor sedimentary fans. A lowstand wedge develops also where a distinct shelf-edge is absent or if the sea-level fall is not large enough. This wedge is built up by a progradational set of parasequences. The prograding depositional pattern might continue also if the falling sea-level reaches a stillstand (or even begins to rise slowly) because of the at best small increase in accommodation space in combination with a relatively high sediment input.

Retrogradational deposited parasequences characterize the **transgressive systems tract** that forms above the **transgressive surface** which marks its lower boundary (Fig. 4.4). The deposition of a transgressive systems tract is controlled by the additional accommodation space that is created when the sea-level rises at a rate faster than it could

be compensated by sedimentation. At the top of the transgressive systems tract, the **maximum flooding surface** forms, it marks the period of the fastest sea-level rise.
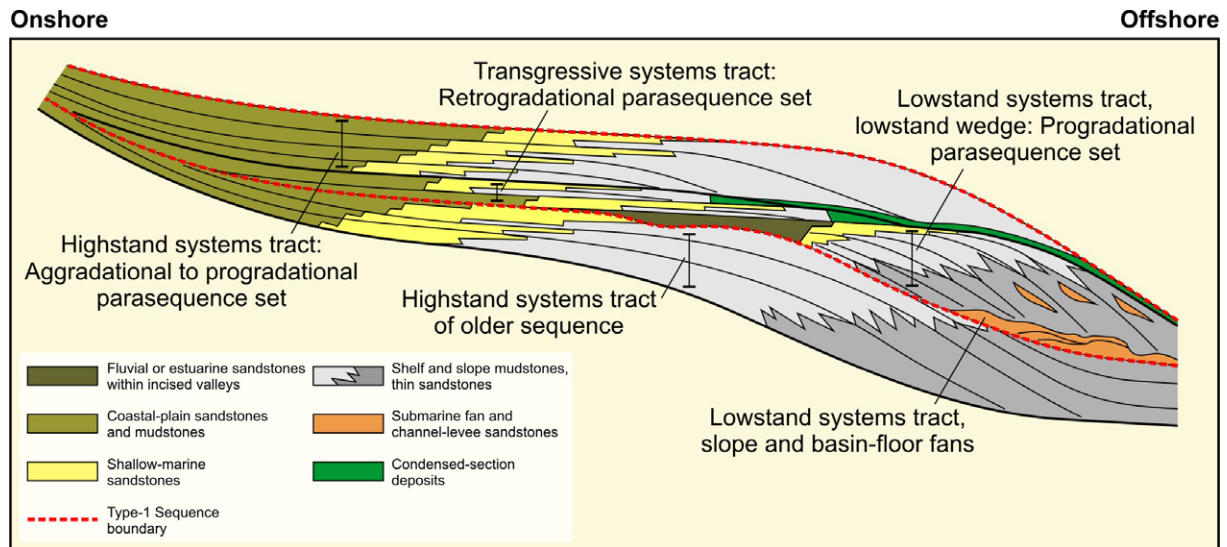

Fig. 4.4: Stratal patterns in a depositional sequence that develops in a basin with a shelfbreak. From Van Wagoner et al. (1990). The sequence is composed of lowstand, transgressive and highstand systems tracts bounded by unconformities and their correlative conformities (a 'Type-1' sequence in the sense of Van Wagoner et al., 1988).

When the rate of sea-level rise slows down, the **highstand systems tract** begins to form (Fig. 4.4). It develops above the maximum flooding surface until the sea-level cycle reaches its upper peak or even slowly begins to fall again. During this period, the available accommodation space is more-or-less constant, resulting in the deposition of aggradational to progradational parasequences. When the sea-level starts to fall at a faster rate, the **upper sequence boundary** is formed and the development of the sequence is complete.

4.2.2 Subsidence Analysis

The sequence stratigraphic interpretation of the depositional patterns in the western Black Sea requires reconstructing the 'geohistory' of the region (Van Hinte, 1978): Strata that are found in a certain present-day depth and with certain present-day lithological parameters need to be transformed to their state at the time of deposition to allow drawing conclusions about the paleo-depo-environment.

By carrying out a geohistory analysis, subsidence and sediment accumulation can be quantified as a function of time. To do so, three corrections need to be applied to the present stratigraphic thickness of a sediment layer (Allen & Allen, 1990):

- **Decompaction**: Correction for the compaction of layers due to the progressive loss of porosity with increasing burial depth.

- **Paleobathymetry**: The water depth at the time of deposition must be referenced to a constant datum (such as the present-day sea-level).

- **Absolute sea-level fluctuations**: Sea-level changes through time must be considered relative to the present sea-level.
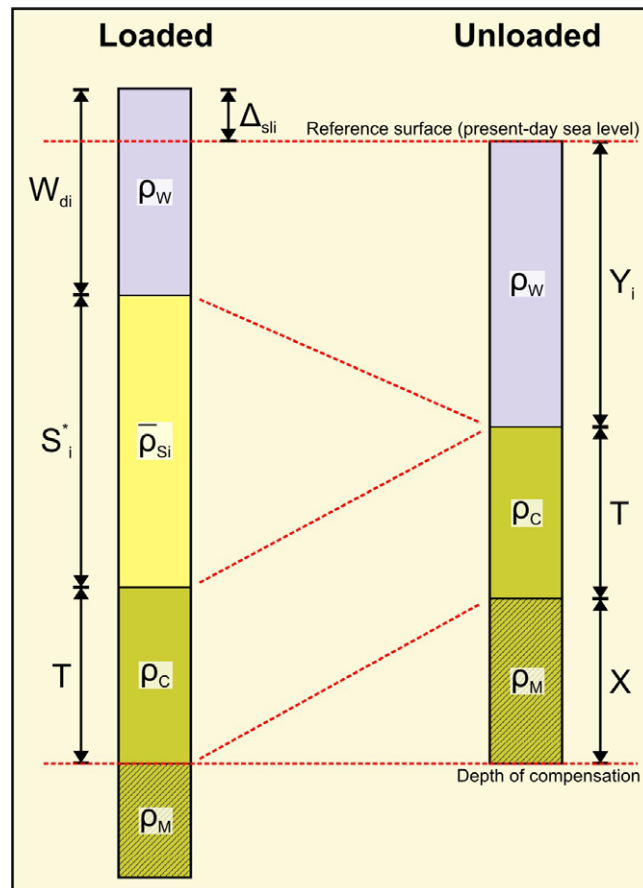
**Fig. 4.5**: 1D-Airy backstripping (e.g., Steckler & Watts, 1978) of two columns of crust (C) and upper mantle (M) in isostatic equilibrium before (loaded) and after (unloaded) backstripping. See text for an explanation of the abbreviations.

Added load due to sedimentation in a basin causes additional subsidence of the basement, because seawater (ρ_{water} = 1.03 kg m^{-3}), or less commonly air, is replaced by

sediments with a much higher density ($\rho_{avg.\ sediment}$ = 2.5 kg m^{-3}). The total subsidence that affected the basement is thus partitioned into subsidence due to sediment load on the one hand and tectonically driven subsidence on the other (Allen & Allen, 1990). The separation between the two depends on the assumption of the lithospheric isostatic response: In simple models, any load is compensated locally (Airy isostasy; e.g., Steckler & Watts, 1978), whereas more complex calculations consider a lateral transmission of stress and deformation through a regional flexure of the lithosphere (Watts et al., 1982).

To remove the effect of sediment load from the total subsidence and thus to quantify the amount of subsidence that can be assigned to tectonic activity, a technique called 'backstripping' is applied (Fig. 4.5). Hereby the stratigraphic record is used to quantify layer-by-layer (form younger to older layers) the depth in which the basement would be in the absence of the load that is represented by the respective layer. A commercial software package for geohistory analysis ('Basin Works', for Apple Macintosh computers) was used to perform the backstripping calculations in this study.

Figure 4.5 shows the simple case of backstripping under the assumption of Airy-isostasy with two lithospheric columns loaded and unloaded with a sediment layer. Balancing the pressure at the base of the two columns gives:

$$\rho_w\ g\ W_{di} + \overline{\rho}_{si}\ g\ S_i^* + \rho_c\ g\ T = Y_i\ \rho_w\ g + \rho_c\ g\ T + x\ \rho_m\ g \qquad (1)$$

where W_{di}, S_i^*, Y_i are the water depth, decompacted sediment thickness and tectonic subsidence of the ith stratigraphic layer, g is average gravity, T and ρ_c the mean crustal thickness and density respectively, ρ_m the mantle density and ρ_w and ρ_{si} the densities of water and decompacted sediments. Equation (1) can also be written as:

$$x = W_{di} + S_i^* + T - (Y_i + \Delta_{sli} + T) \qquad (2)$$

where Δ_{sli} is the sea-level change. Given equations (1) and (2), the following 'backstripping equation' can be derived:

$$Y_i = W_{di} + S_i^* \left[\frac{\left(\rho_m - \overline{\rho}_{si} \right)}{\left(\rho_m - \rho_w \right)} \right] - \Delta_{sli} \left[\frac{\rho_m}{\left(\rho_m - \rho_w \right)} \right] \qquad (3)$$

In this way, the tectonic subsidence Y_i can be determined directly from the observed stratigraphic data. The first term in equation (3) is a water depth term, the second is a sediment loading term and the third a sea-level loading term.

The equations above describe the simplified case of one (the ith) sediment layer. In practice, the procedure needs to be carried out for a number of layers. A sequence of stratigraphic units needs to be restored for each time step by decompacting the younger units and compacting the older ones. In this case, the tectonic subsidence is calculated from the total sediment thickness and the average density of the entire sedimentary column at a particular time. The mass of the total sediment column must equal the sum of the masses of all the individual stratigraphic layers, so that:

$$\overline{\rho_s}\, S^* = \sum_{i=1}^{n} \left[\rho_w\, \phi_i^* + \rho_{gi} \left(1 - \phi_i^*\right) \right] S_i^* \qquad (4)$$

where n is the number of stratigraphic units in the sequence at any one time. It follows then that:

$$\overline{\rho_s} = \frac{\sum_{i=1}^{n} \left[\rho_w\, \phi_i^* + \rho_{gi} \left(1 - \phi_i^*\right) \right] S_i^*}{S^*} \qquad (5)$$

The total tectonic subsidence Y can then be obtained by substitution in the backstripping equation (3):

$$Y = W_d + S^* \left[\frac{\left(\rho_m - \overline{\rho_s}\right)}{\left(\rho_m - \rho_w\right)} \right] - \Delta_{sl} \frac{\rho_m}{\left(\rho_m - \rho_w\right)} \qquad (6)$$

Backstripping attempts to correct the stratigraphic record for the effects of loading in the past, so that the thickness and density of a stratigraphic layer measured today must be adjusted to the effects of post-depositional processes such as compaction. The compaction of sediments is a function of the burial depth and has an immediate impact on the porosity φ. For normally pressured sediments, the depth-porosity curve is given by an exponential relationship (Athy, 1930; Hedberg, 1936; Rubey and Hubbert, 1960; Allen and Allen, 1990):

$$\phi = \phi_0 * e^{-cy} \tag{7}$$

where c is a coefficient determining the slope of the ϕ-depth curve, y is the burial depth and ϕ_0 is the is porosity at the surface (Rubey & Hubbert, 1960; Hedberg, 1936; Athy, 1930). To calculate the thickness of a sediment layer at a time in the past, it must be moved up the depth-porosity curve. If a layer at the present depths of y_1 and y_2 is moved to shallower depths y'_1 and y'_2, the amount of water-filled pore space can be calculated from equation (7) by integrating the porosity over the depth interval (Allen & Allen, 1990):

$$V_W = \int_{y_1}^{y_2} \phi_0\, e^{-cy}\, dy \tag{8}$$

which gives on integration

$$V_W = \frac{\phi_0}{c}\left\{ \exp\left(-cy_1\right) - \exp\left(-cy_2\right) \right\} \tag{9}$$

The total volume of a sediment layer (V_t) results from the addition of the volumes of the sediment grains (V_s) and the pore-filling water (V_w) respectively, so that

$$V_s = V_t - V_w \tag{10}$$

Considering a unity cross-sectional area, it follows from (9) and (10) that

$$y_s = y_2 - y_1 - V_W = y_2 - y_1 - \frac{\phi_0}{c}\left\{ \exp\left(-cy_1\right) - \exp\left(-cy_2\right) \right\} \tag{11}$$

If a sediment layer is decompacted the sediment volume remains constant, only the water volume is increased. From (11), it follows that in a unit area sedimentary column between y'_1 and y'_2 the thickness of water is

$$y'_w = \frac{\phi_0}{c}\left\{ \exp\left(-cy'_1\right) - \exp\left(-cy'_2\right) \right\} \tag{12}$$

After decompaction, the thickness of the sediment layer is the sum of the thickness of the sediment grains (11) and the thickness of the water (12). That is:

$$y'_2 - y'_1 = y_s - y'_w \tag{13}$$

Therefore,

$$
\begin{aligned}
y'_2 - y'_1 &= y_2 - y_1 - \frac{\phi_0}{c} \times \left\{ \exp\left(-cy_1\right) - \exp\left(-cy_2\right) \right\} \\
&\quad + \frac{\phi_0}{c} \left\{ \exp\left(-cy'_1\right) - \exp\left(-cy'_2\right) \right\}
\end{aligned}
\tag{14}
$$

This is the general decompaction equation corresponding to an upward displacement of a sediment layer on an exponential depth-porosity curve; it can be solved by numerical iteration, making it well-suited for computer-based calculations (Allen & Allen, 1990).

5. Interpretation of reflection seismic profiles from the western Black Sea

5.1. Introduction

The sea-level of the global oceans varied during the Quaternary between approximately -125 m and +10 m, following the advance and retreat of continental ice covers (Martinson et al., 1987; Shackleton, 1987; Imbrie et al., 1984; van Andel & Lianos, 1984). In contrast to all other marine areas, the Black Sea is linked to the global oceans only through a chain of narrow and shallow sea straits. These connect first the Atlantic Ocean with the Mediterranean Sea (Strait of Gibraltar), then the Mediterranean and Marmara Seas (Dardanelles) and finally the Marmara Sea with the Black Sea (Bosporus Strait). The Bosporus Strait is particularly shallow, with a present-day sill depth of not more than -32 m. Whenever the global sea-level drops below this level, the Black Sea is decoupled from the global ocean and transformed into an inland lake. During such lake stages, a potentially independent sea-level can develop, so that the global sea-level estimations cannot automatically be assigned to the Black Sea.

A collection of reflection seismic profiles, borehole information and sediment core data was available to this study of the sea-level history of the Black Sea (see section 4.1 for a detailed description of the database and data sources). Reflection seismic profiles of high and very high resolution from cruises carried out by various institutions for both scientific and commercial purposes were interpreted and calibrated with borehole and core information to study fluctuations of the Black Sea-level during the Quaternary and the Holocene transgression after the last glacial maximum.

5.2. South western Black Sea shelf

The study area on the south western Black Sea shelf has a more-or-less uniform width of around 30-50 km. The continental slope is moderately steep with the highest gradients found in the westernmost parts of the Black Sea off central Bulgaria. More to the north, close to the neighboring Romanian Black Sea sector, the shelf becomes notably narrower and the continental slope steeper (Fig. 5.1).

The map shown in Fig. 5.1 gives the location of the available seismic profiles from the BLASON 1, BLASON 2 and several IO-BAS cruises in this area. The examples presented in this chapter are also marked.
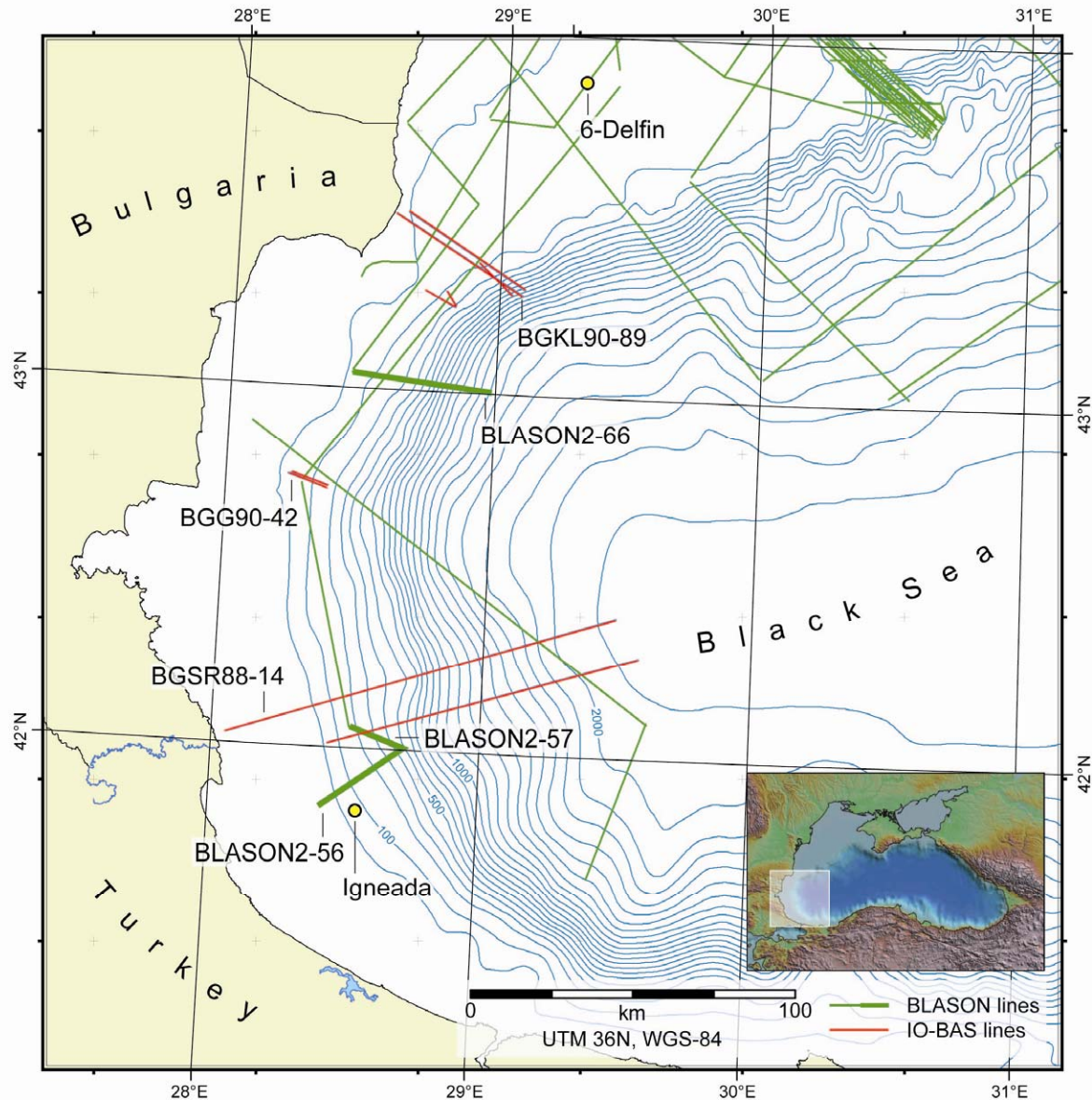
Fig. 5.1: Map of the southwestern Black Sea; the inset gives the map location. Given are the positions of reflection seismic lines acquired during the BLASON 1 and 2 cruises (green lines; bold green lines denote that both multi-channel and Chirp data are available) as well as lines acquired by the Institute of Oceanology of the Bulgarian Academy of sciences (IO-BAS). The yellow dots give the position of the exploration wells *Igneada* and *6-Delfin*. Isobaths are in meters. The line labels refer to the examples shown in this chapter. Survey abbreviations in profile labels: B2 – Blason 2; BGSR88 – Sredetska 1988; BGG90 – Godin 1990; BGKL90 – Kaliakra 1990; see section 4.1.1 for detailed survey descriptions.

Stratigraphic calibration of the reflection seismic profiles was based on Gillet (2004), in which two BLASON 2 profiles were correlated to the Turkish exploration borehole 'Igneada' (Fig. 5.2) on the southwestern Black Sea shelf. This correlation permitted the delineation of an erosional unconformity attributed to sea-level lowstands during a time period that correlated to the Messinian event in the Mediterranean as well as the Mio-Pliocene and the

Pliocene/Quaternary boundaries (Gillet, 2004). These are shown exemplarily on BLASON 2 line 56 (Fig. 5.3). For the purpose of this study, the Pliocene/Quaternary boundary is considered to be the baseline for tectonic and sedimentary estimates derived from the seismic stratigraphic interpretation presented in this chapter; every younger horizon will be normalized using this boundary, both spatially and in geological time.
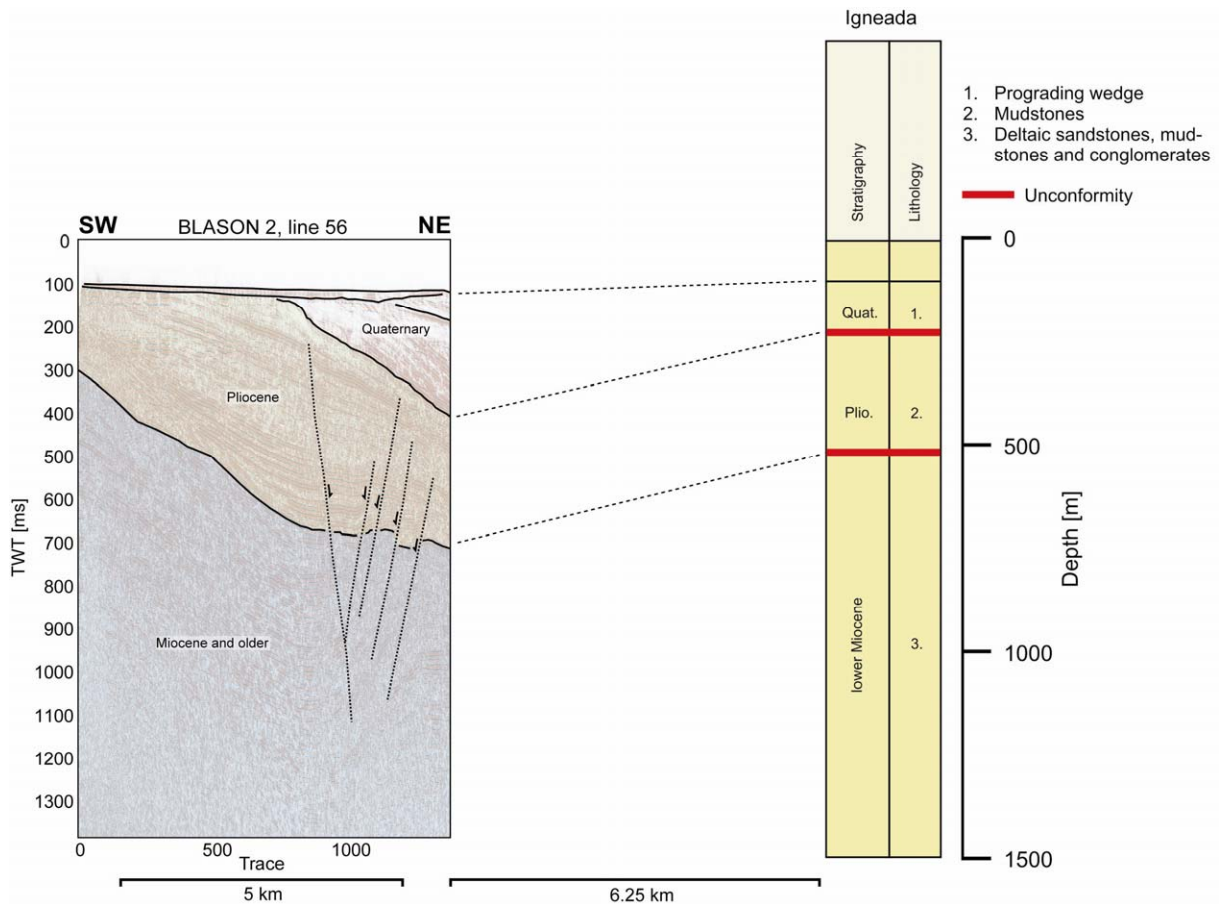

Fig. **5.2**: Correlation of the BLASON 2 profile 56 (compare with a larger section of this profile shown in Fig. 5.3) with the Turkish exploration well *Igneada* as presented by Gillet (2004; modified). This correlation allows the Mio-Pliocene and Pliocene/Quaternary boundaries to be established on the example reflection seismic line and through extrapolation in wide areas of the south western Black Sea. The Pliocene/Quaternary boundary serves as the 'baseline' for the tectonic and sedimentary reconstruction in this study.

The typical profiles BLASON 2-56 (Fig. 5.3) and BGSR 88-14 (Fig. 5.4) clearly document the influence of tectonic subsidence on the southwestern Black Sea shelf. Buried graben structures occur on the inner shelf within the Miocene and Pliocene formations, while the middle shelf is affected by normal faulting that was active at least until the mid-Quaternary. Large slump deposits in the adjacent sediments might
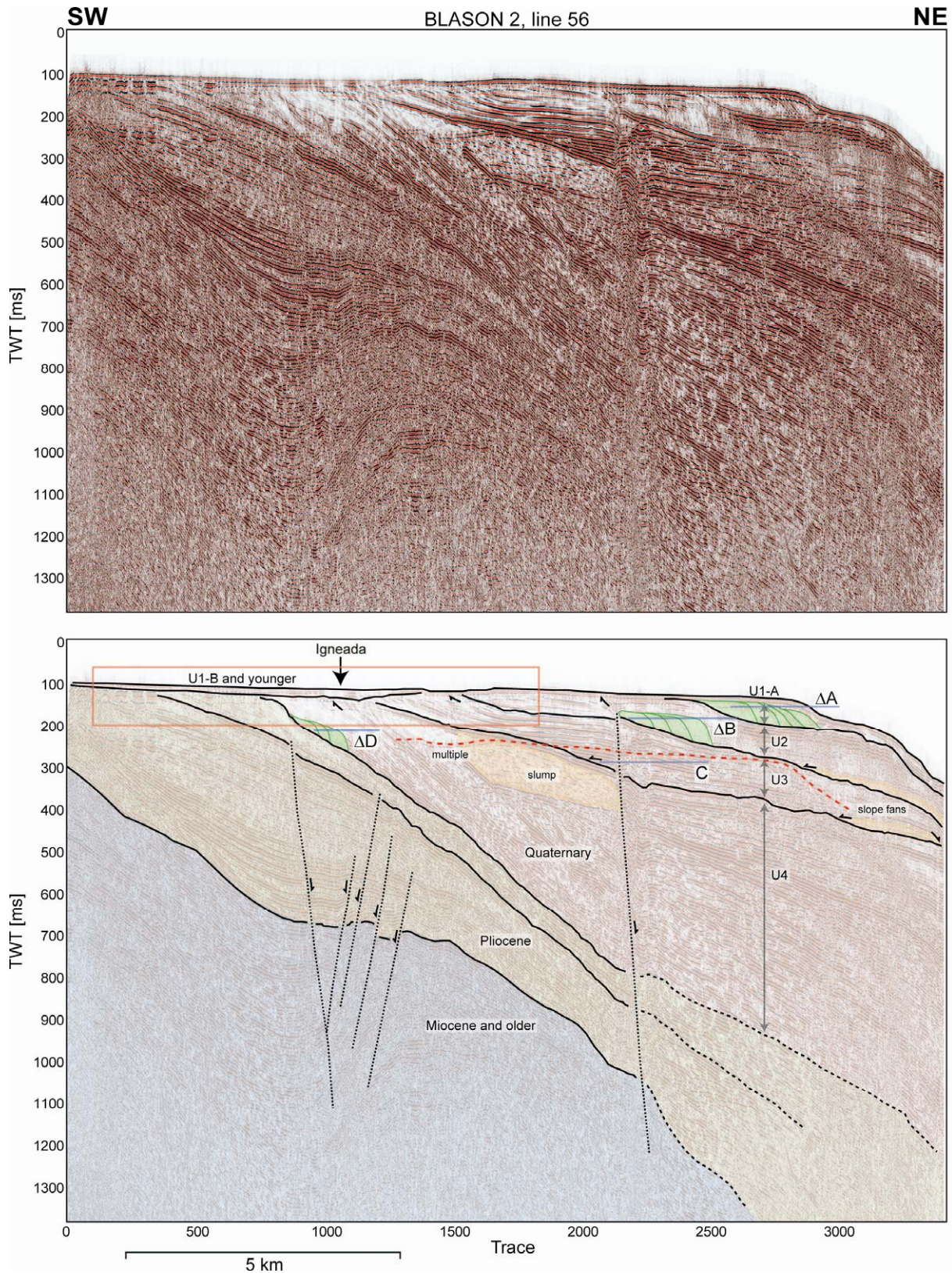
Fig. 5.3: Multi-channel high-resolution (mini GI-gun) line 56 of the BLASON 2 cruise. The lower stratigraphic boundaries between the Miocene, Pliocene and the Quaternary were identified using the correlation to the industrial borehole *Igneada* (Fig. 5.2; Gillet, 2004). The seismic-stratigraphic units U4 to U1 follow the nomenclature of Aksu et al. (2002a). The red rectangle shows the position of Fig. 5.4; the deltaic systems ΔB (U2) and ΔA (U1-A) are shown in detail in Fig. 5.6 and 5.7.
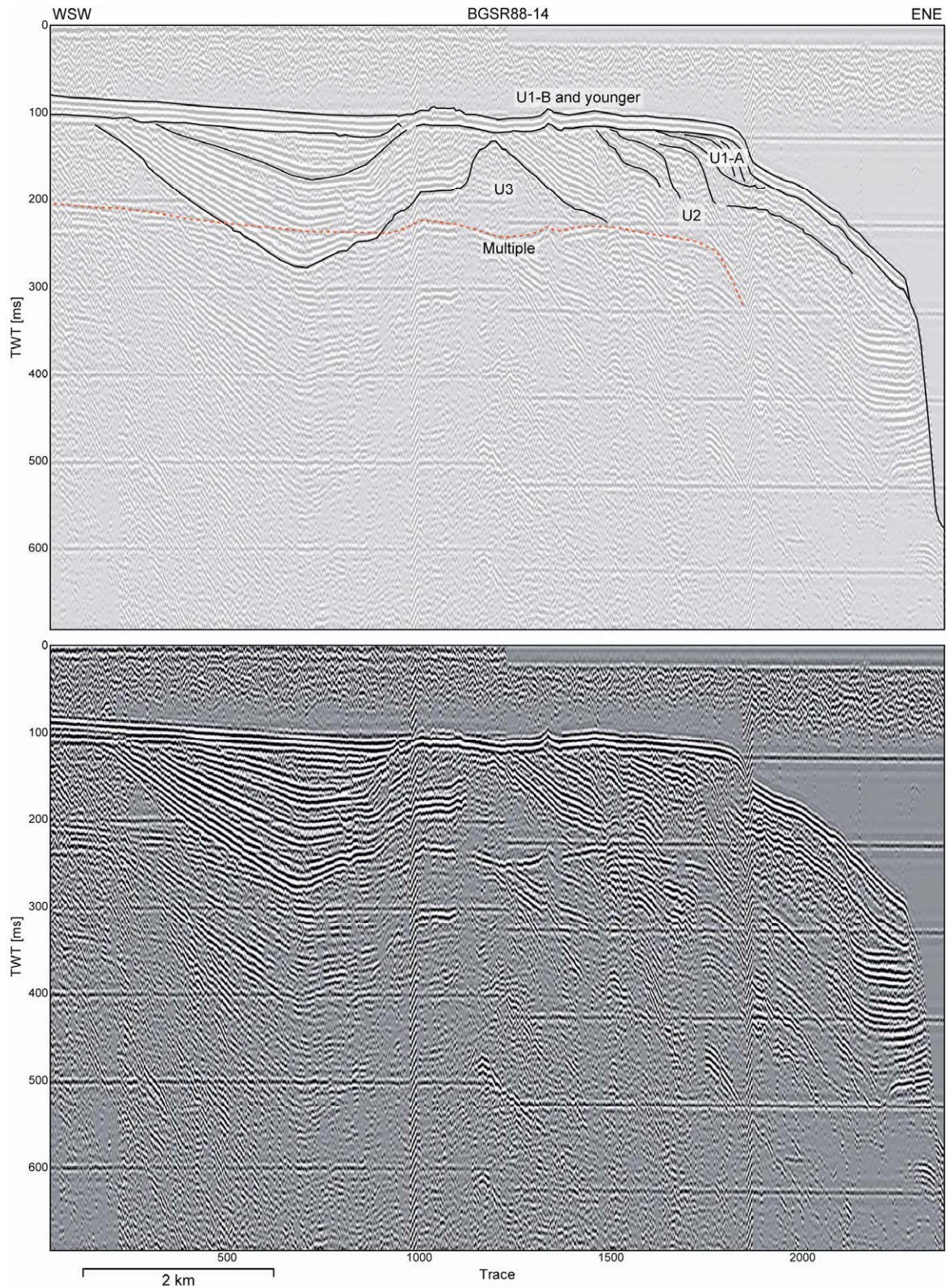
Fig. 5.4: IO-BAS sparker profile BGSR 88-14, recorded on the southern Bulgarian shelf. This example shows the influence of extensional tectonics on Mid-Quaternary sediments on the middle shelf. The profile is located approximately 25 km north of BLASON 2-56 (Fig. 5.3), indicating the strong lateral variability of tectonic structures in this region.

also indicate Quaternary tectonic movements (Fig. 5.4). The higher resolving sparker profile BGSR 88-14 shows that synclinal structures are also present in Mid-Quaternary deposits about 25 km north of the previous example.

These findings suggest that the southwestern Black Sea shelf was, at least during Late Tertiary and up to the Mid-Quaternary, under a long-lasting extensional tectonic regime, and that this area was affected by a subsidence that is temporally and spatially highly variable. The strongest movements seem to be confined to the middle shelf; on the outer and inner shelf the tectonic influence is less obvious. Thus, for a reconstruction of the depositional history of the region and its implications for the sea-level development, the role of differential vertical tectonics must be evaluated and taken into account.

Aksu et al. (2002)				This study			
Sedimentary units			Systems tract	Sedimentary units		Systems tract	Series
Unit 1	D		HST	Unit 1	C	TST	Quaternary
	C		TST		B	TST	
	B		TST				
	A	Δ1	LST		A (ΔA)	LST	
		Δ2		Unit 2 (ΔB)		LST	
		Δ3		Unit 3 (C)		LST	
		Δ4		Unit 4 (ΔD)		LST	
Unit 2							Pliocene

Tab. **5.1**: Comparison of the seismic stratigraphic model of Aksu et al. (2002) and the model presented in this study. Please note that the time axis is linear. Unit 1 in the sense of Aksu et al. (2002) is supposedly Late Pliocene to Quaternary in age, and the equivalent Unit 4 in this study is Quaternary in its entirety.

5.2.1. Late Pliocene-Quaternary sedimentary units

Four seismic stratigraphic units (named U4 to U1 in chronological order) have been identified on seismic profiles from the southwestern Black Sea. These rest on a Late Pliocene 'basement' and represent therefore the time span Early Quaternary to present.

Aksu et al. (2002a) presented a stratigraphic and sedimentary model for the southwestern Black Sea in which the slightly longer period from the Mio-Pliocene the present-day is subdivided into five seismic-stratigraphic units; a detailed description of their classification is given in section 3.5.3. Correlating this model with the seismic-stratigraphic reconstruction presented in this study gives the following results:

- The upper (Quaternary) part of the Late Pliocene to Quaternary Unit 1 in the sense of Aksu et al. (2002a) is equivalent to Unit 4 (U4) herein.

- U4 is the oldest of four seismic-stratigraphic unit interpreted in this study. Together with the younger units 3 to 1-A they represent the glacial periods of the Upper Quaternary characterized by low global sea-levels. Aksu et al. (2002b) assign these units to a single larger unit A that is then subdivided into four glacial episodes called Δ4-Δ1 in accordance with the occurrence of deltaic sedimentary systems.

- The youngest sedimentation after the last glacial maximum is divided into the sub-units U1-B and U1-C in this study, while Aksu et al. (2002a) presented a sequence of three divisions B to D. Table 5.1 shows a graphical comparison of the two models.

Based on the stratigraphic correlation described in section 5.2, the Pliocene-Quaternary depositional succession could be identified throughout large areas of the southwestern Black Sea shelf. Figures 5.6 and 5.7 show how the stratigraphic pattern is developed in the northern Turkish sector and the central Bulgarian sector: The overall arrangement of the four seismic stratigraphic units remains similar, but the sedimentary packages on the middle and outer shelf dip at a slightly smaller angle basinward (compare Figs. 5.6 and 5.7). As a result, the older units U3 and U4 occur at the shelf surface (except for a thin cover of very young - U1-B to Recent - sediments) in landward-shifted positions.

The northern profile BGSR 88-14 (Fig. 5.4) suffers from a typical, notably diminished quality of the seismic image. The map of Fig. 5.5 (after Gillet, 2005) shows the spatial extent of the affected areas: A large part of the outer shelf in the Romanian sector show a strong attenuation of the seismic signal, areas off the Danube delta and the Bulgarian coast show moderate to strong attenuation.

The degree of signal attenuation varies from moderate to complete. A high content of free gas in shallow sediments is most likely responsible for these effects, since many very-

high resolution seismic profiles show clearly-defined shallow gas fronts. To what degree the occurrence of free gas in the sediments affects the quality of the seismic image depends on the type of equipment used for data acquisition. Large-scale industrial seismic profiling suffers to a much lesser extent than seismic measurements carried out with scientific equipment aimed particularly at a high resolution in shallow sediments, rather than at a high penetration.
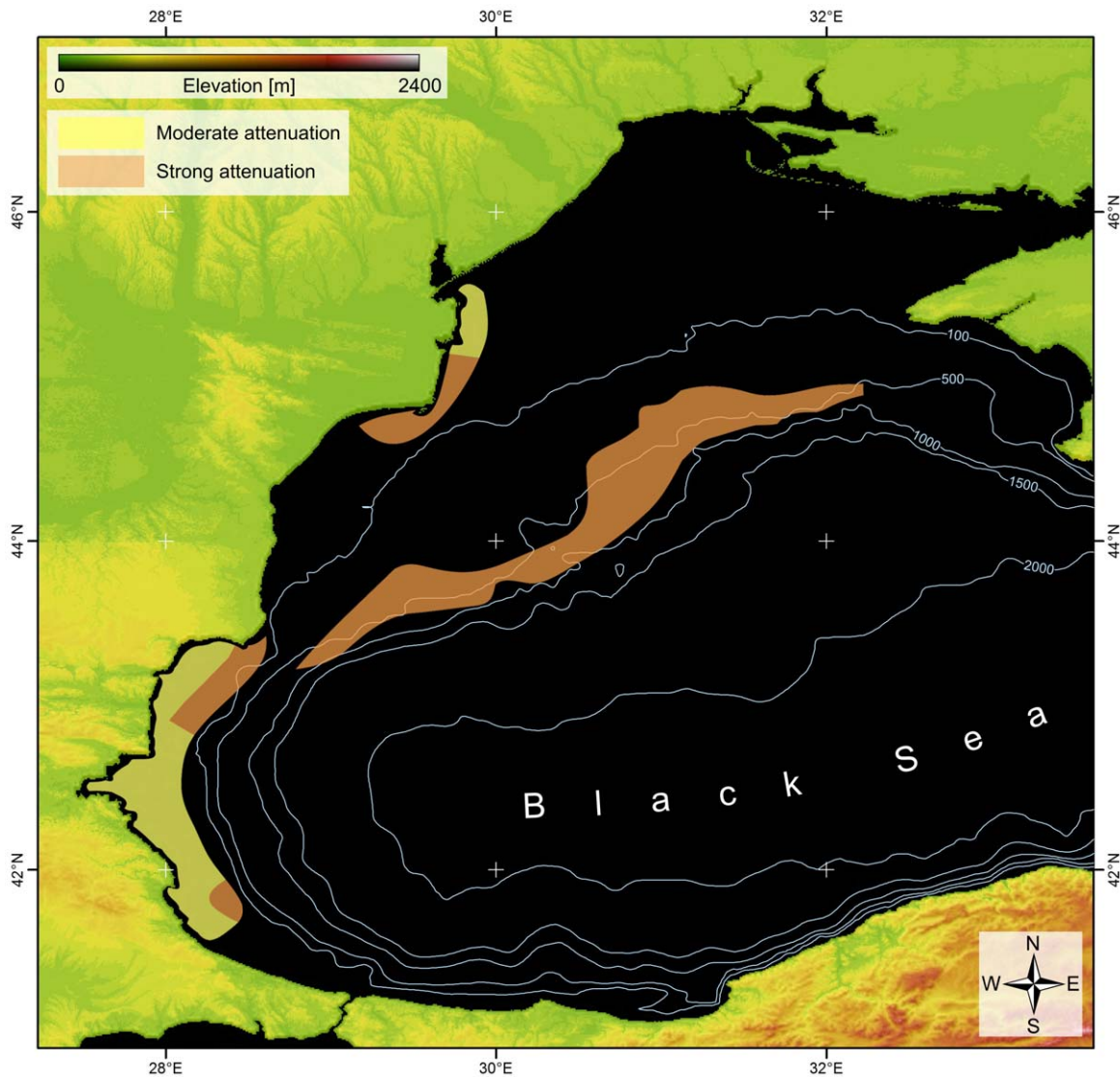

Fig. 5.5: Areas of the Western Black Sea shelf with noticeable to strong attenuation of seismic signals and subsequently diminished seismic imaging quality. Mapping is based on findings presented by Gillet (2005).
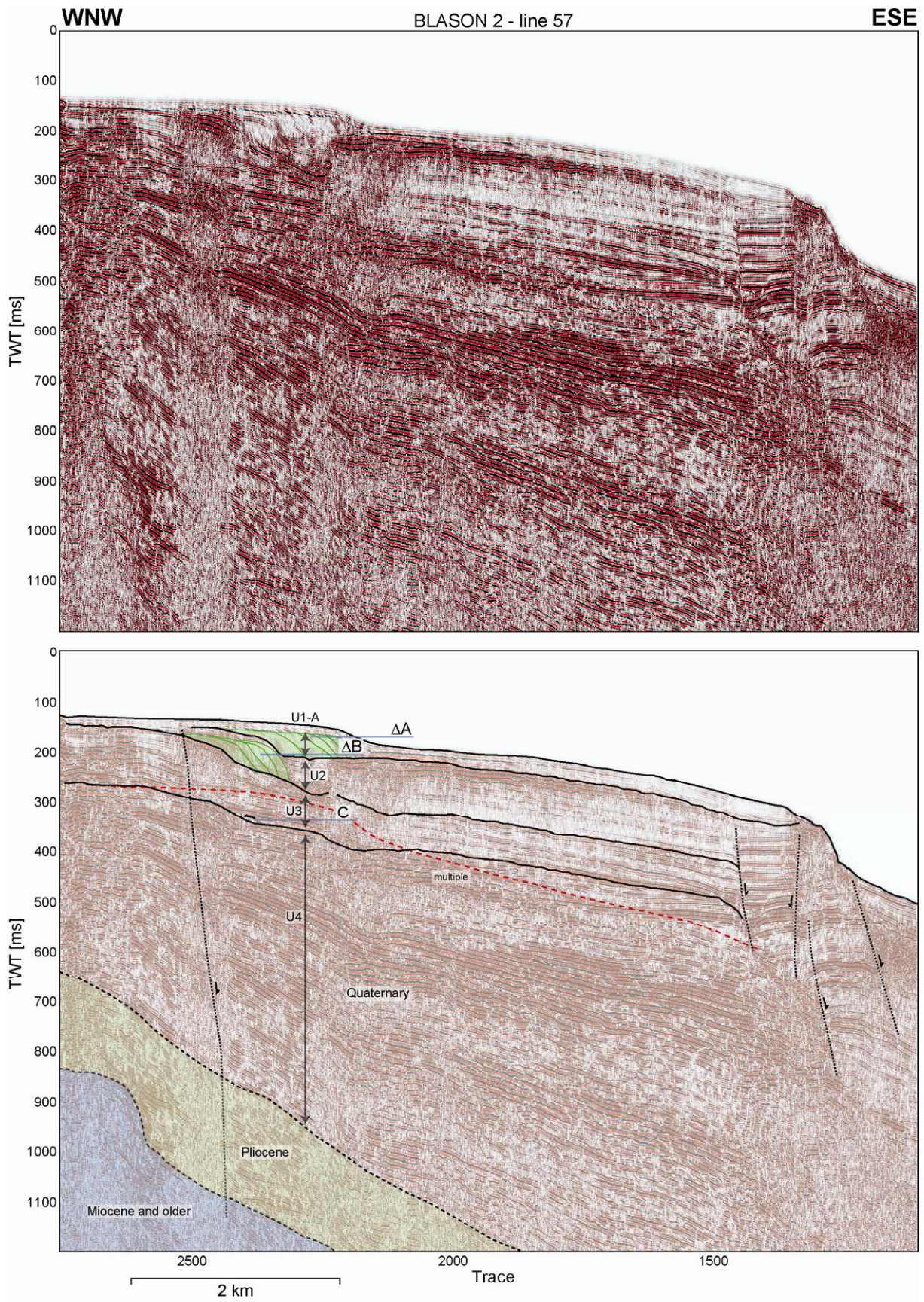
Fig. 5.6: Multi-channel high-resolution (mini GI-gun) line 57 of the BLASON 2 cruise showing the seismic-stratigraphic units U4 to U1 on the northern Turkish shelf. The Miocene to Quaternary boundaries are extrapolated from line BLASON 2 – 56 (Fig. 5.3).

5.2.1.1. Late Pliocene

Late Pliocene sediments form the 'baseline' for the seismic stratigraphic interpretation described below. Profiles that reach far landwards (such as BLASON 2-56; Fig. 5.3) show that Pliocene deposits can be found at the seafloor of the inner southwestern Black Sea shelf where it is shallower than approximately 75 m. The thin Pliocene succession is characterized by a slower sedimentation rates and/or slower subsidence than in the Quaternary. Its thickness across the shelf is relatively uniform, in contrast to the younger Quaternary deposits which thickens rapidly toward the outer shelf and slope.

Figure 5.6 shows signs of extensional faulting that displaced the Pliocene and older sediments of the inner and middle shelf and formed buried graben structures. Tectonic activity apparently ceased during the Upper Pliocene, leaving the youngest Pliocene sediments, the Plio-Quaternary boundary, as well as the Quaternary section unaffected.

The Pliocene deposits are represented by a series of mostly continuous reflectors of relatively strong amplitudes. Very-high resolution Chirp sonar data (Fig. 5.8) show that the layer thickness is much larger and the dip towards the basin is smaller in the Pliocene than in the Quaternary. On the inner and middle shelves, the Pliocene is strongly eroded and is overlain only by a thin, Late Quaternary to Holocene layer. Emerged layer boundaries give the erosional surface a characteristically uneven appearance, which is probably a result of tectonic tilting and subsequent e stratal rosion. Aksu et al. (2002a) described the same erosional pattern. However, they rejected a tectonic origin and preferred the interpretation of erosional oblique-progradational clinoforms. The unconformity rapidly deepens on the outer shelf towards the shelfedge, where it is buried underneath a Quaternary section some 1,000 ms TWT in thickness (Fig. 5.6).

5.2.1.2. Quaternary

5.2.1.2.1. Unit 4

The oldest seismic sequence above the Late Pliocene baseline is unit 4 (U4). It overlies in the southern part of the study area (northern Turkish shelf) the Pliocene-Quaternary unconformity described in the last section. The Figures 5.3 and 5.6 show this unconformity and U4 in two different resolutions.
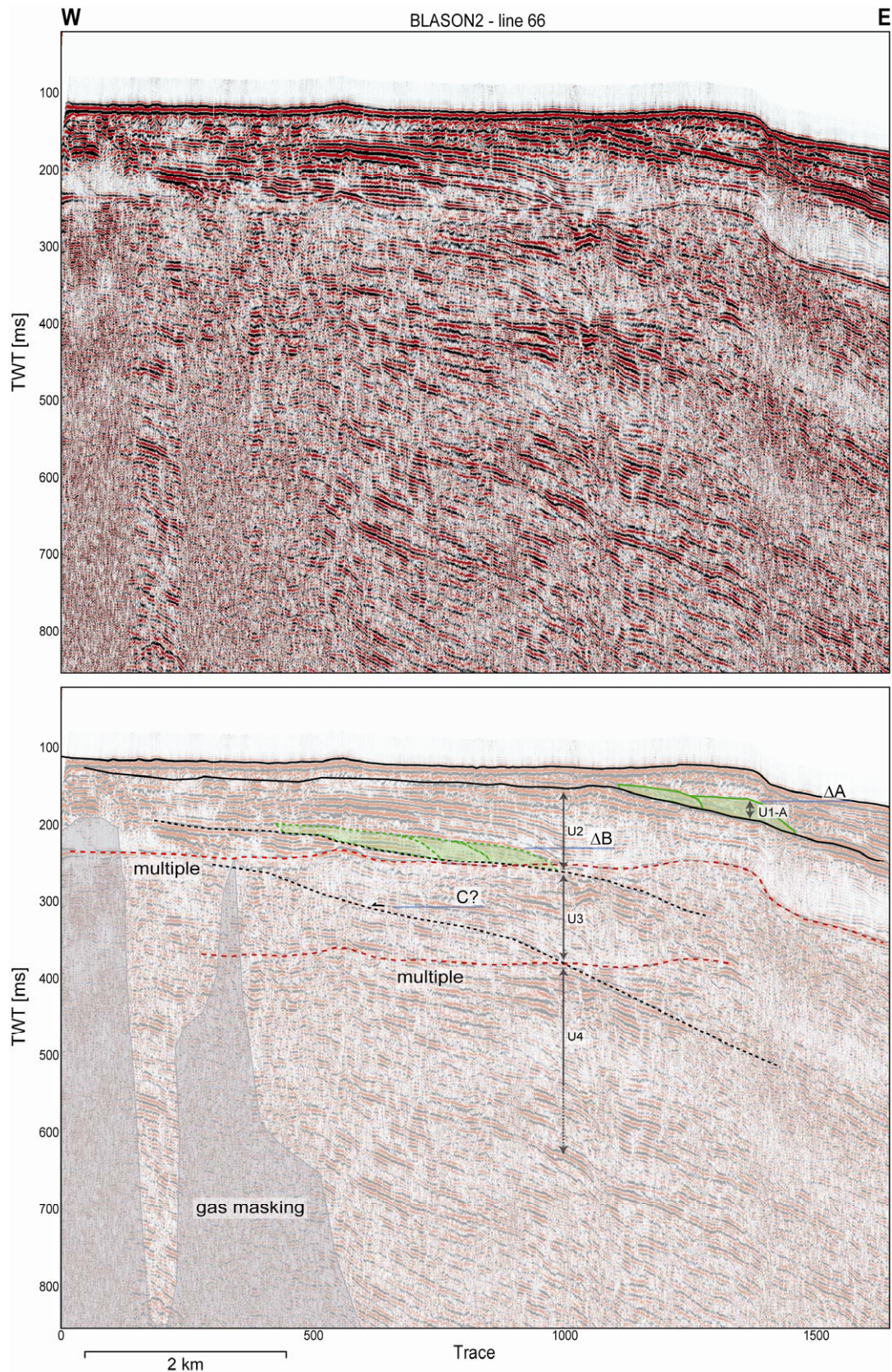
Fig. 5.7: Multi-channel high-resolution (mini GI-gun) line 66 of the BLASON 2 cruise showing the seismic-stratigraphic units U4 to U1 off Bulgaria. Compared to the more southerly profiles 56 and 57 (Figs. 5.3 and 5.6), the data quality is significantly diminished due to high concentrations of free gas in the sediments.
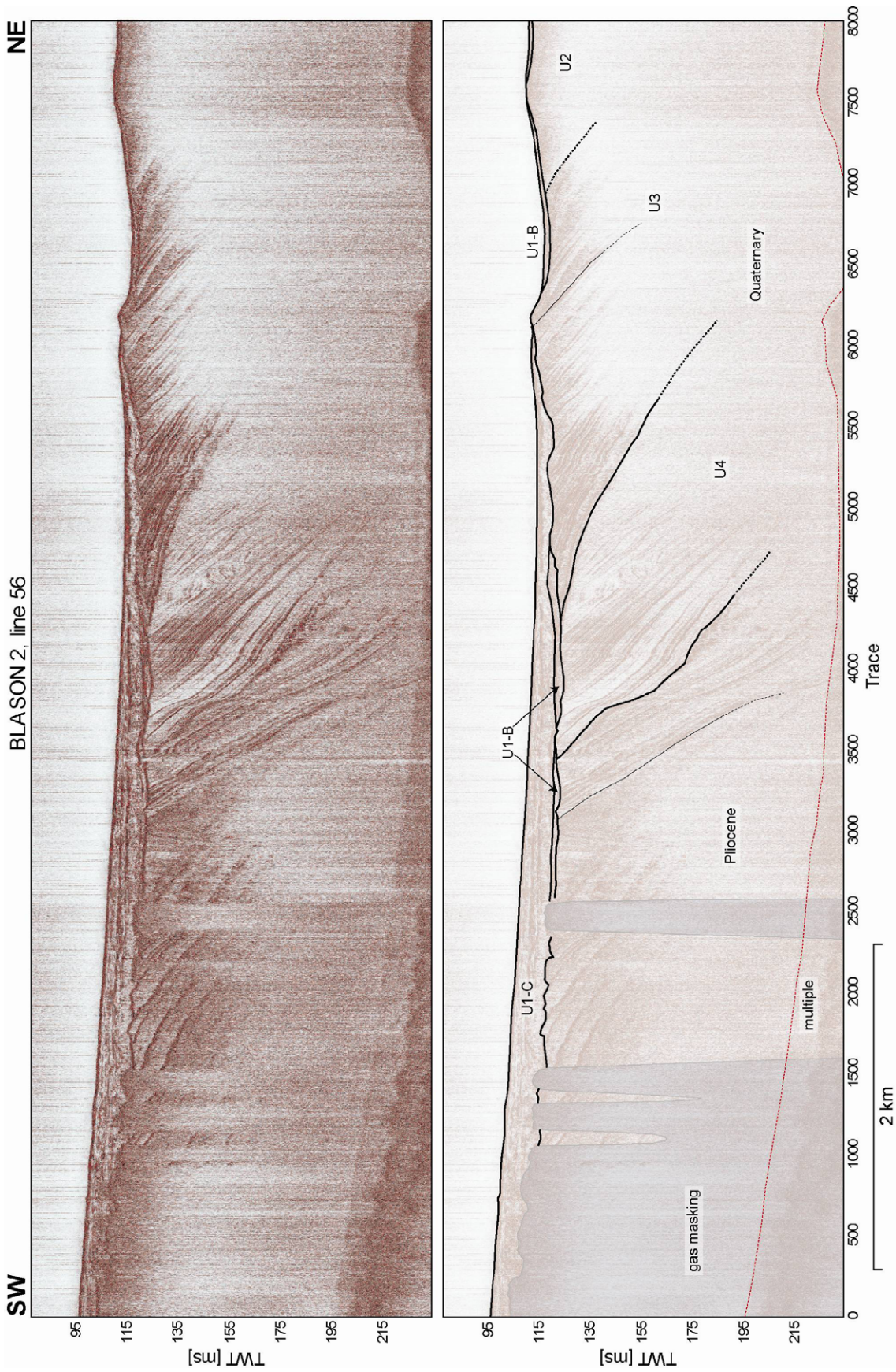
Fig. 5.8: Details of Chirp profile 56 from the BLASON 2 cruise. This example shows the relationship between U3, U2 and U1 on the middle and inner shelves off northern Turkey. Clearly visible is the erosional unconformity that delimits U3 and U2 against the different subunits of U1. The red box in Fig. 5.3 marks the position of this section relative to the reflection seismic profile.

The distinct character of the Plio-Quaternary boundary appears to have developed only locally on the northern Turkish shelf. It is not well recognizable on other profiles and has not been described by other authors (e.g., Aksu et al., 2002a).

The surface distribution of U4 is shown in Fig. 5.9. This unit is covered over large areas by a thin layer of Holocene to Recent sediments (Unit 1, Chapter 5.2.1.2.4). Along the southwestern shelf, U4 is distributed in a narrow band on the inner shelf between the 50 m isobath and the coast line. Father north where the shelf starts to widen, it occurs in a broader area also at greater water depths of up to around 150 m.

Unit 4 comprises a uniform, gently basinward-dipping sequence of mostly continuous reflectors. Multi-channel seismic profiles show the divergent character of the reflectors on the shelf, leading to an increase in thickness towards the deep basin. The maximum thickness of U3 is reached close to the present-day shelfedge (Fig. 5.3, Fig. 5.6).

Within U4, just above the Plio-Quaternary unconformity, a deltaic system (ΔD in Fig. 5.3) built up by sedimentation close to a paleo-shelfedge during an early Quaternary sea-level lowstand can be recognized. Based on the seismic data available for this study, the spatial extent of ΔD cannot be determined, because the profiles do not reach the its landward termination and the density of seismic lines in the vicinity is low.

The internal sedimentary configuration of U4 is imaged in detail on very high resolution Chirp profiles (Fig. 5.8). It consists of a set of progradationally-stacked reflectors with high amplitudes and good continuity. Individual layers can be of varying thickness and external form. Reflector dips decrease towards the basin to slightly lower angles than those observed in the older units.

The top of U4 is truncated by an erosional angular unconformity that divides U4 deposits from the overlying younger seismic unit 3 (U3). It runs subparallel to the basal unconformity. In addition to these regional unconformities that can be observed throughout the entire southwestern part of the study area, a number of minor internal unconformities subdivide the sedimentary succession of U4. These secondary unconformities appear to be developed only locally as they cannot be traced between adjacent seismic lines. They suggest clearly that differential tectonics and sedimentary environment variability affected the development of the western Black Sea shelf only on a local scale. For a quantitative description of the

factors that lead to their formation a much denser seismic database would be necessary though.
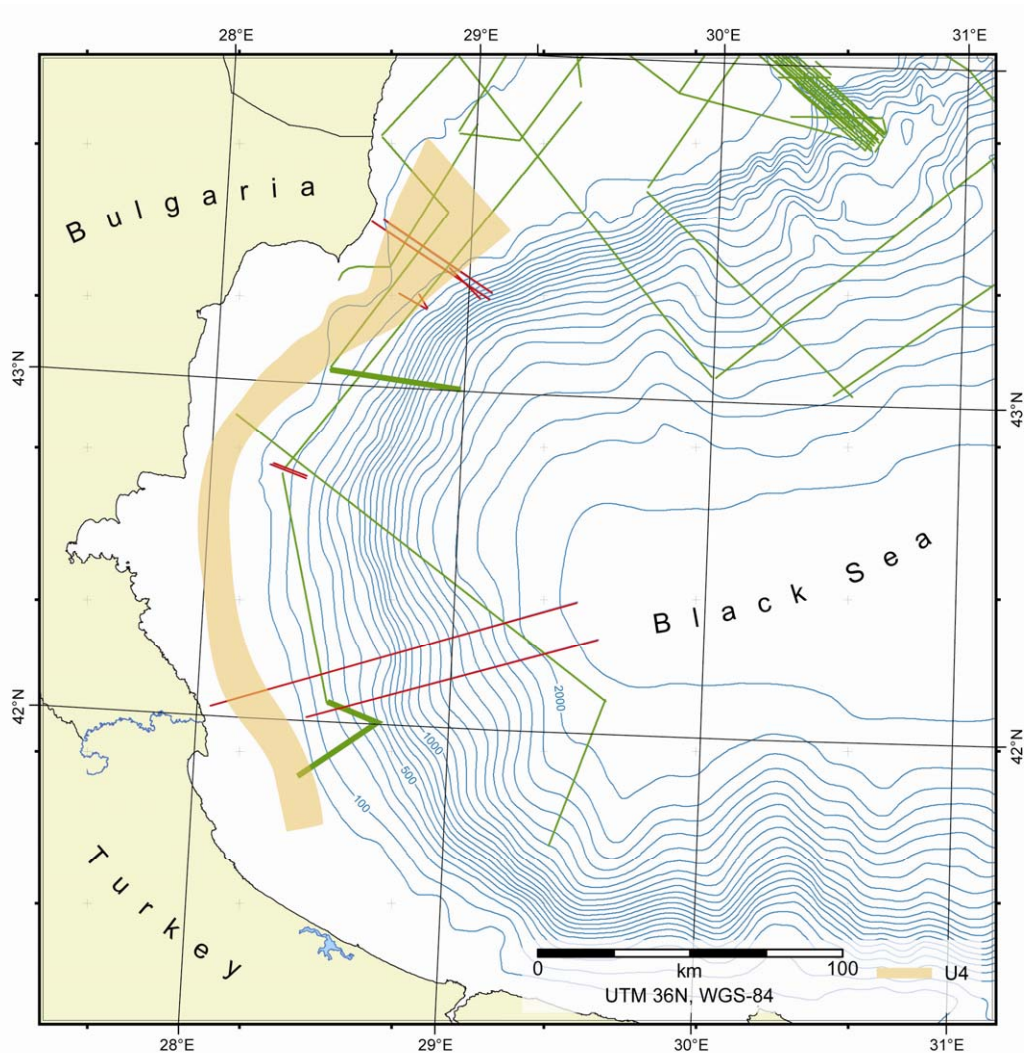
Fig. 5.9: Map showing the spatial distribution of the seismic stratigraphic Unit 4 (U4) projected to the present-day surface of the southwestern Black Sea shelf. The figure does not account for the thin layer of Holocene toRecent sediments that cover most of the seafloor in the study area.

5.2.1.2.2. Unit 3

Above the angular unconformity that separates the U4 and the younger Unit 3 (U3; Fig. 5.3) a set of progradationally-stacked reflectors with high amplitudes and good continuity makes up Unit 3 (U3). Its seismic configuration is best seen on very high resolution Chirp sonar data such as the profile shown in Fig. 5.8.

The depositional pattern of the strata of U3 is more uniform than those of U4; they do not vary much in thickness and are mostly parallel. The average layer thickness is less than in U4, although the structural composition is comparable.
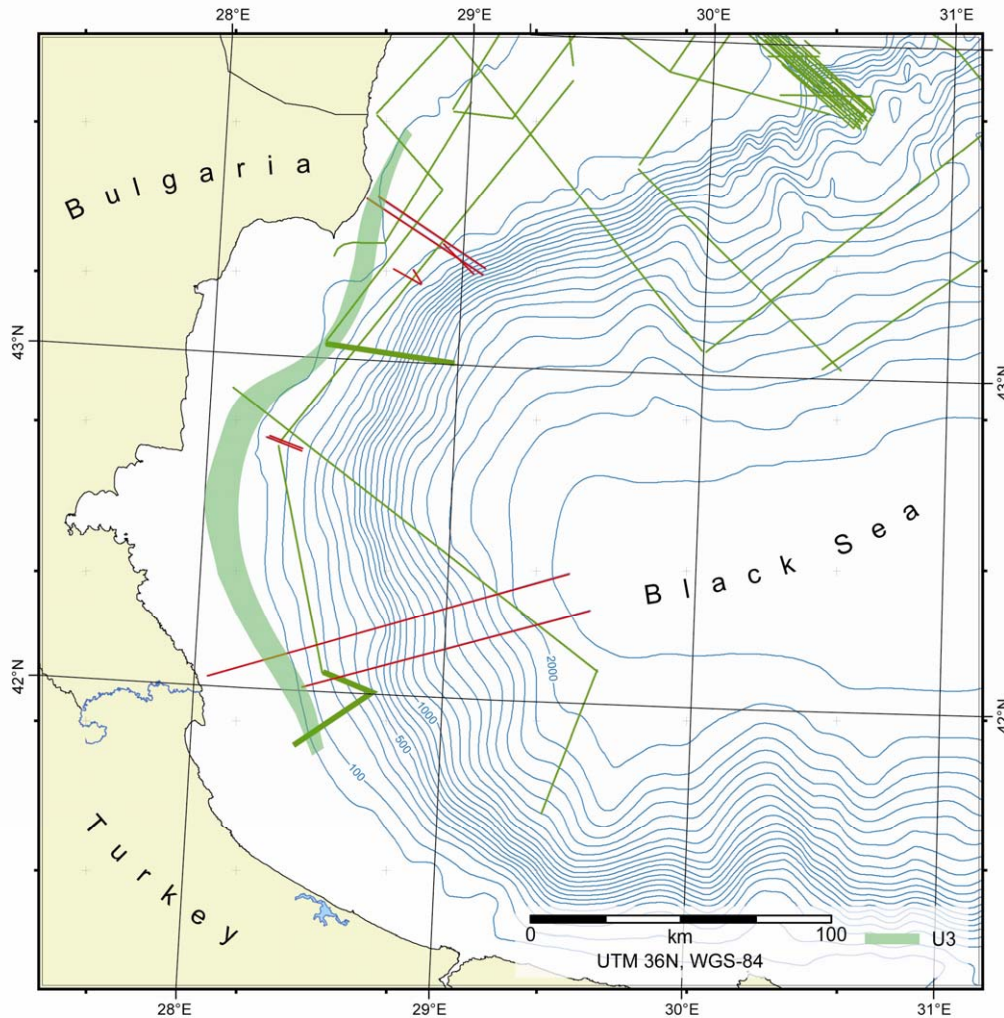
Fig. **5.10**: Map showing the spatial distribution of the seismic stratigraphic Unit 3 (U3) on the southwestern Black Sea shelf. The figure does not account for the thin layer of Holocene to Recent sediments that covers most of the seafloor in the study area.

The penetration depth reached by the very high frequency Chirp signals is less than in the previous units and decreases upwards in the vicinity of the present-day shelfedge. Since the signal near the penetration limit decreases gradually with depth, it must be a result of changes in sediment composition rather than the occurrence of free gas in the sediments. This is also corroborated by the finer stratification of U3 compared to U4, the finer average grain size and the overall lower sedimentation rate.

Lower-resolution reflection seismic profiles show the stratigraphic context of U3 and the sea-levelimplications during this period. Coastal onlaps (C in Figs. 5.3, 5.6 and 5.7) mark the sea-level lowstand during the time of deposition of the lower part of U3. The upper part of U3 was deposited during the subsequent sea-level rise and highstand, leading to a significant amount of aggradation on the present-day outer shelf. Unit 3 is concluded by a major unconformity that marks a phase of non-deposition and erosion after the sea level has lowered again.

In the southern and central Bulgarian sectors of the study area, the occurrence of Unit 3 is limited to the outer and middle shelves. On the northern Bulgarian shelf, it is found in a more landward position, nearly reaching the present-day coastline in some areas (Fig. 5.10).

5.2.1.2.3. Unit 2

The deposition of Unit 2 (U2) started during a sea-level lowstand which led to the development of the unconformity separating it from the preceding Unit 3. While the sea level remained at or close to the paleo-shelfedge, a deltaic system comprising the oldest parts of U2 developed (ΔB in Figs. 5.3, 5.6 and 5.7) .

The delta system ΔB is built up by characteristic sigmoidal sedimentary bodies shown in detail in Fig. 5.11. Here 11 individual bodies could be identified. Their internal reflection termination characteristics and their relative spatial geometry potentially give insight into small-scale high-order sea-level variations during the time of the formation of the delta system.

An analysis of the spatial geometry of the sedimentary bodies within ΔB implies relatively stable sea levels during the early stages (1-2; Fig. 5.11) of the delta system development, a falling sea level at the transition from stage 2 to 3, stable conditions during stages 3 through 6, rising sea levels during stages 7 and 8, followed again by falling sea levels (stages 9 and 10) and a final sea-level rise at the youngest stage 11. Given the small number of profile that actually image this delta system, a generalized quantitative interpretation of such subtle features would be questionable.
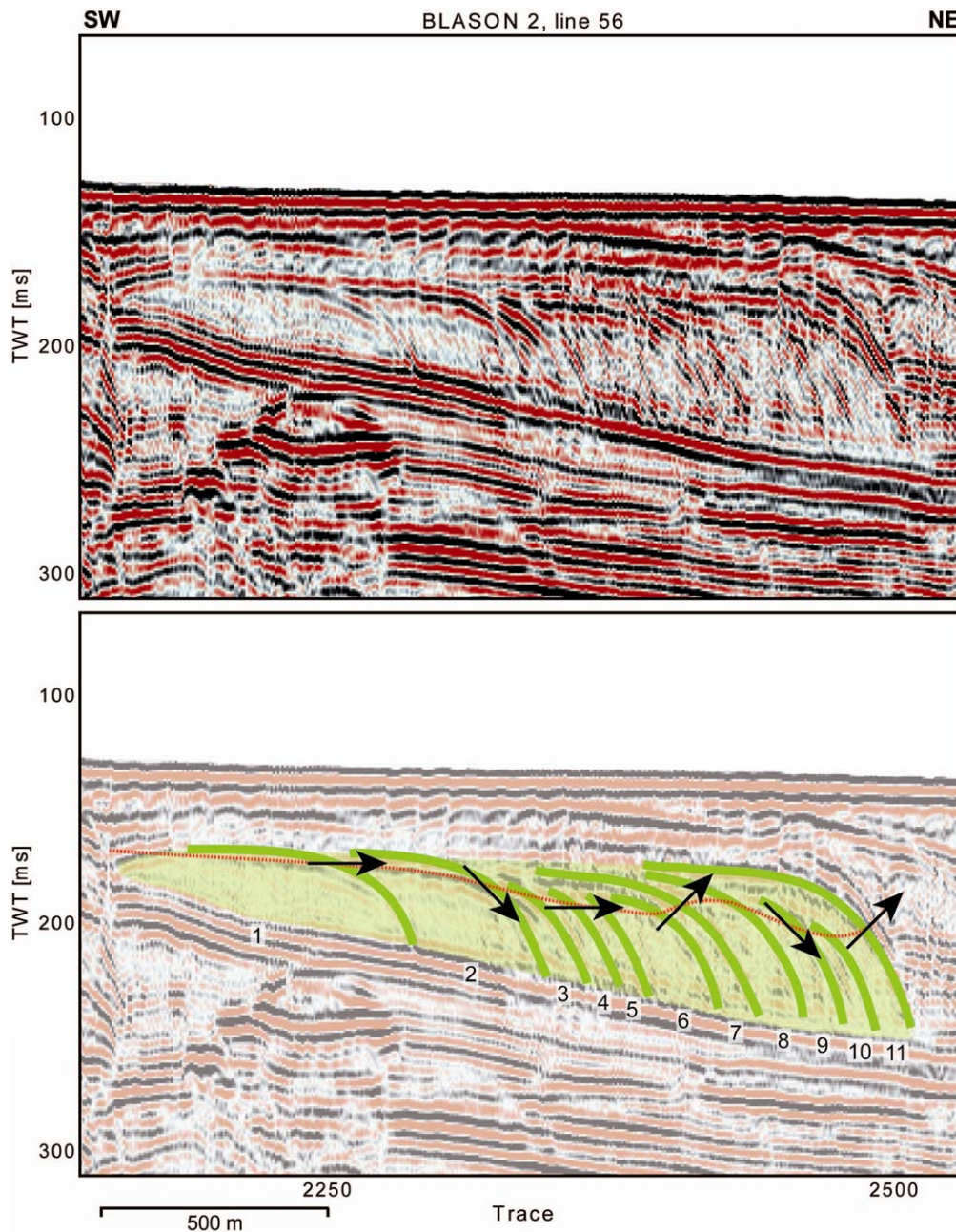
Fig. 5.11: Details from BLASON 2 line 56 showing the deltaic system ΔB found at the base of Unit 2. Eleven individual sedimentary bodies were identified that together make up ΔB. Their relative positions (as indicated by the red dotted line that connects the location of the topset-to-foreset transitions during the different stages) show small-scale variability of the sea level while the delta system formed. Black arrows indicate the corresponding sea-level trends. See Fig. 5.3 for the location within profile BLASON 2-56.

The shelfedge delta system ΔB is followed by a set of gently-dipping, prograding reflectors that reach the present-day seafloor in a narrow, coast-parallel stripe on the outer shelf in parts of the southern study area. This occurrence is situated around the 100 m isobath off southern and central Bulgaria, and slightly deeper towards the north.
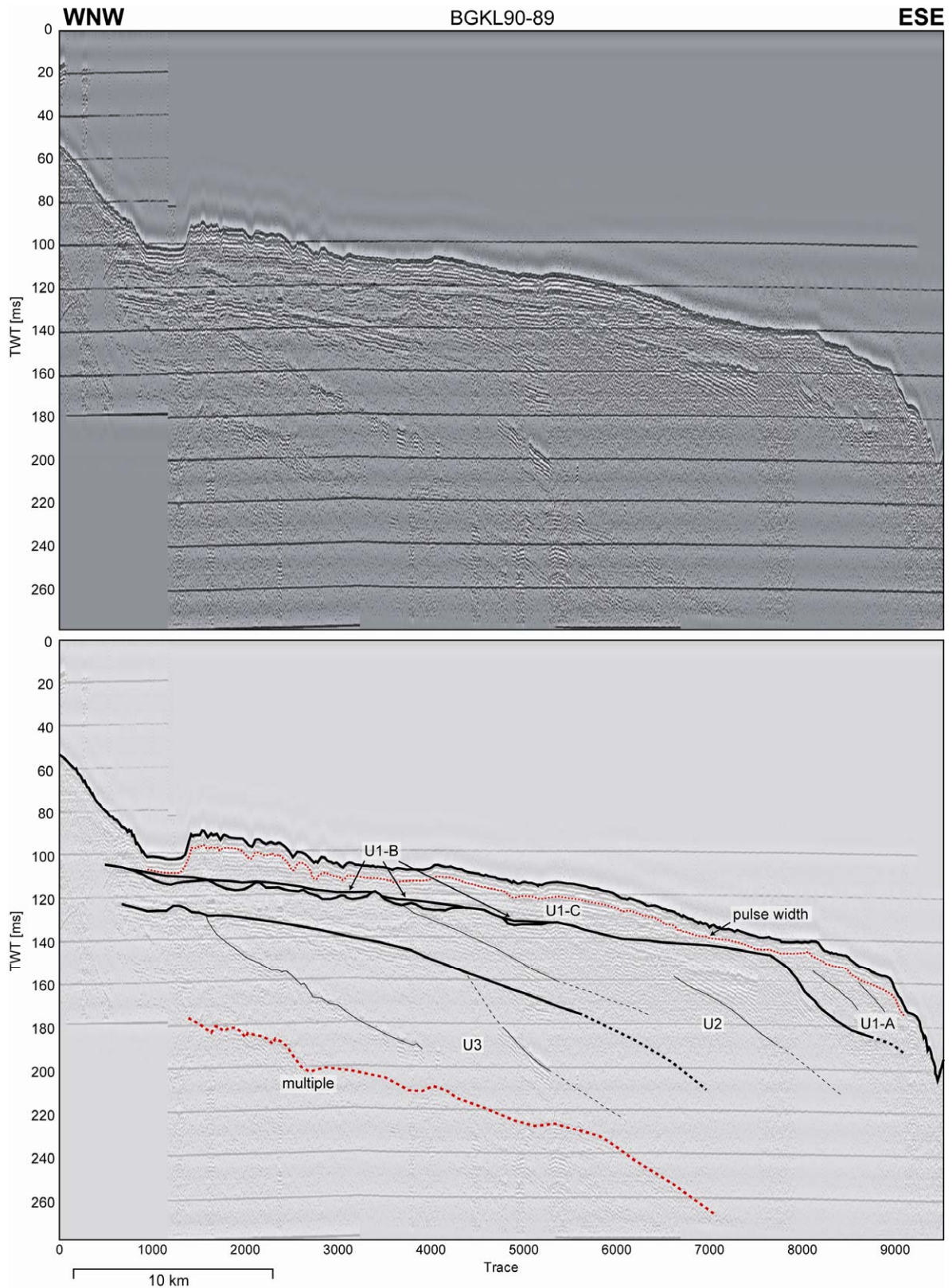
Fig. 5.12: IO-BAS Boomer profile BGKL90-89, showing unit 2 (U2) on the northern Bulgarian shelf. The overlying unit 1 shows a typical arrangement of its subunits U1-A to U1-C.

On the northern Bulgarian shelf, U2 is broader across the shelf; at the boundary between the Bulgarian and the Romanian Black Sea sectors, U2 covers almost the entire shelf between the 50 m and the 200 m isobaths (Fig. 5.13).
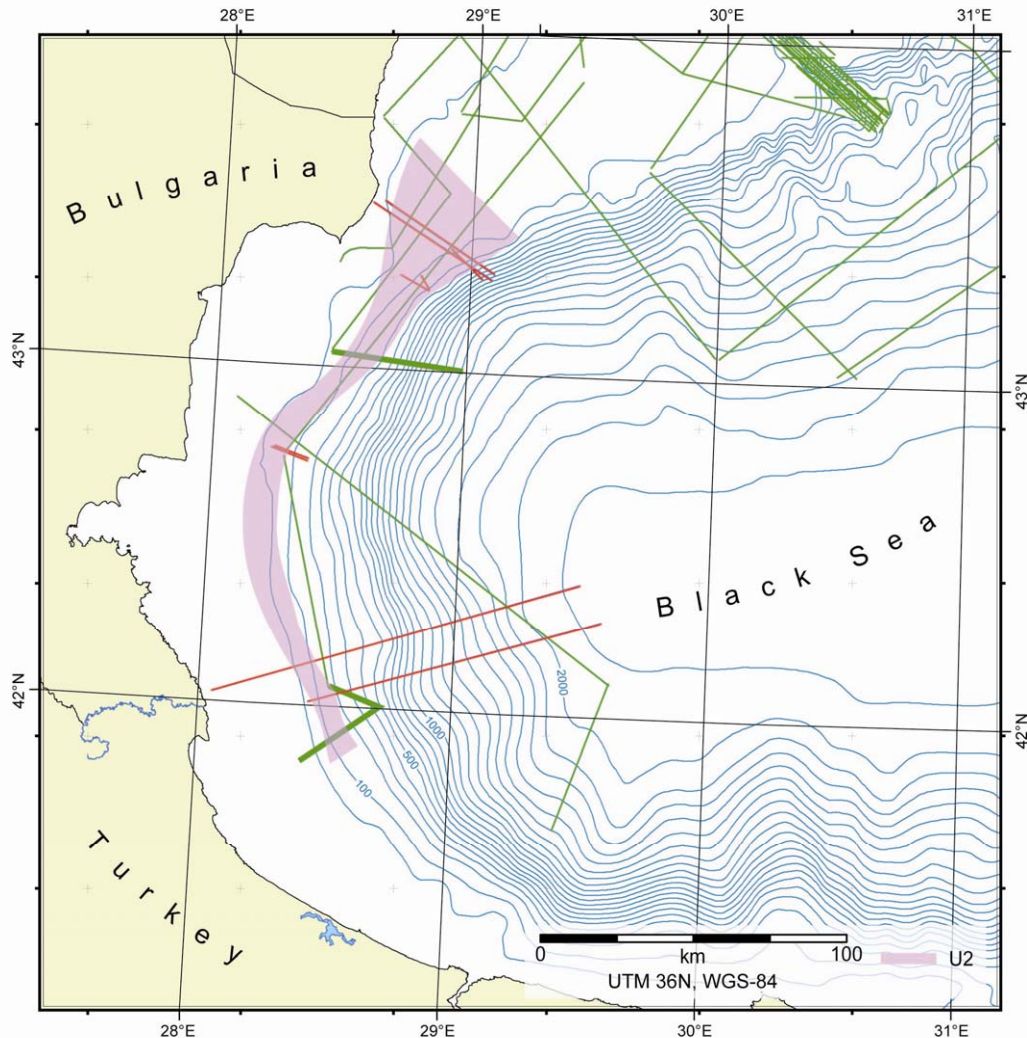
Fig. 5.13: Map showing the spatial distribution of the seismic stratigraphic Unit 2 (U2) at the surface of the southwestern Black Sea shelf. The thin Holocene to Recent sediment cover over most of the seafloor in the study area has been backstripped.

A thin, discordant layer of youngest sediments (Holocene to Recent) overlies U2 in most areas (Fig. 5.11). Only in small, probably isolated spots does U2 crop out at the seafloor (one example is shown in Fig. 5.8); absence of the younger drape cover is probably due to post-depositional erosion.

Chirp sonar data show significant differences between the seismic response of U2 and U3. In U3, there is a trend to lower penetration in its upper part, but even in the uppermost

94

section, a reflection pattern is still recognizable. Unit 2 in contrast is from the beginning completely transparent (Fig. 5.8). Coherent reflections other than from the seafloor itself are absent.

5.2.1.2.4. Unit 1

All the older seismic stratigraphic units starting with the Pliocene 'baseline' are truncated by a shallow, almost horizontal unconformity that marks the onset of the youngest seismic stratigraphic unit 1. This unit (U1) was presumably deposited during and since the last global sea-level lowstand (Latest Quaternary to Holocene).

A number of minor internal unconformities within U1 mark small, high-order sea-level fluctuations at the Quaternary-Holocene boundary and within the Holocene. These unconformities divide U1 into three stratigraphic subunits with distinct depositional characteristics (U1-A, U1-B, and U1-C in chronological order). Figure 5.14 shows their stratal relationship on a Boomer profile off Bulgaria.

5.2.1.2.4.1. Subunit U1-A

The oldest subdivision of unit 1 (U1-A) represents sedimentation during the last glacial maximum, when the sea level remained at a level close to or below the paleo-shelfedge during the time of deposition. As the location of the shelfedge did not change significantly since the last glacial maximum, the spatial occurrence of sediments attributed to U1-A is restricted to an area close to the present-day shelfedge. It follows a narrow band centered roughly at the 100 m isobath (Fig. 5.15).

Although the depositional characteristics of subunit U1-A vary somewhat across the western Black Sea shelf, they always comprise stacked, significantly aggrading, sigmoidal sediment bodies characteristic of a shelfedge delta complex.
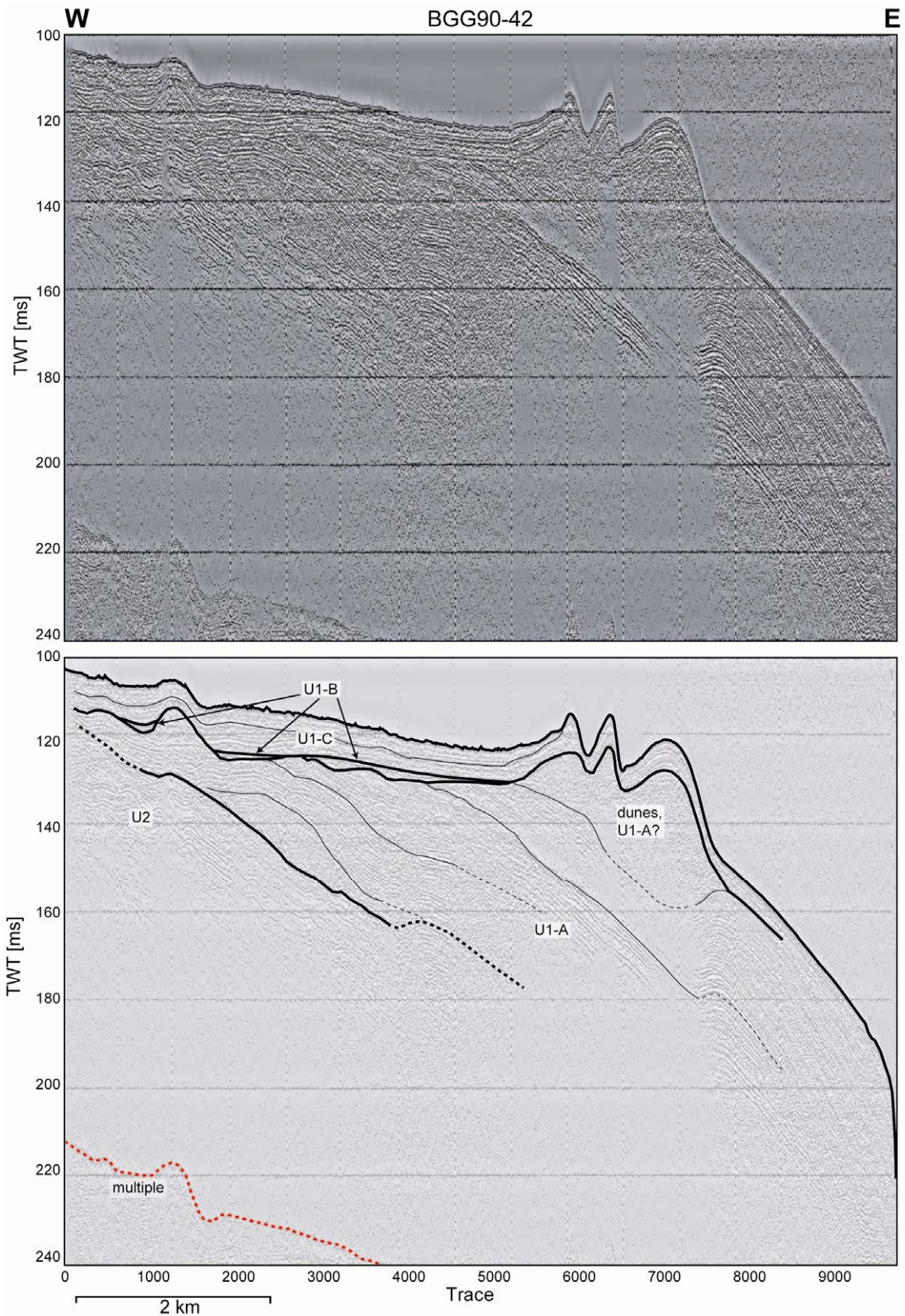
Fig. 5.14: IO-BAS Boomer profile BGG90-42, showing the stacking relationship between the subunits of U1 on the Black Sea shelf off central Bulgaria. Here, dune-like structures that might be interpreted as coastal dunes are developed. These features are assigned stratigraphically to subunit U1-A. See text for discussions.
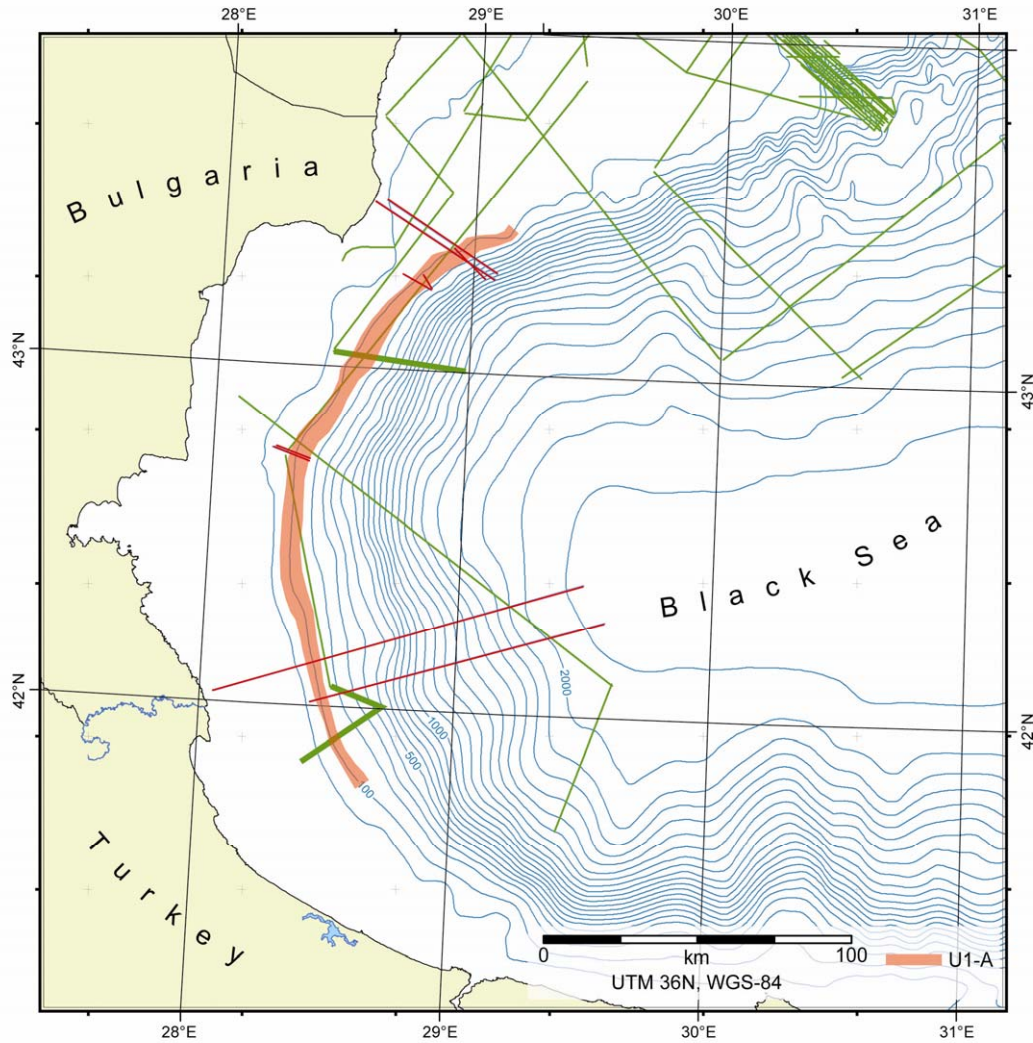
Fig. **5.15**: Map showing the spatial distribution of the seismic stratigraphic Unit 1-A (U1-A) on the southwestern Black Sea shelf.

In the southernmost part of the study area, subunit U1-A form a distinct shelf-edge deltaic system similar to those found within U4 and U2 (ΔA in Figs. 5.3, 5.6 and 5.7). Figure 5.16 shows that this system consists of eight separate sedimentary bodies. The relative positions of their foreset-to-topset transitions (see discussion for ΔB in section 5.2.1.2.3) suggest a stable sea level, during the older stages 1 and 2, a falling level at the transition to stage 3, followed by a short interval of a constant level (stages 3 and 4). Stages 5 and 6 suffered a falling sea level, whereas stage 7 and the concluding stage 8 are characterized by a final sea-level rise.
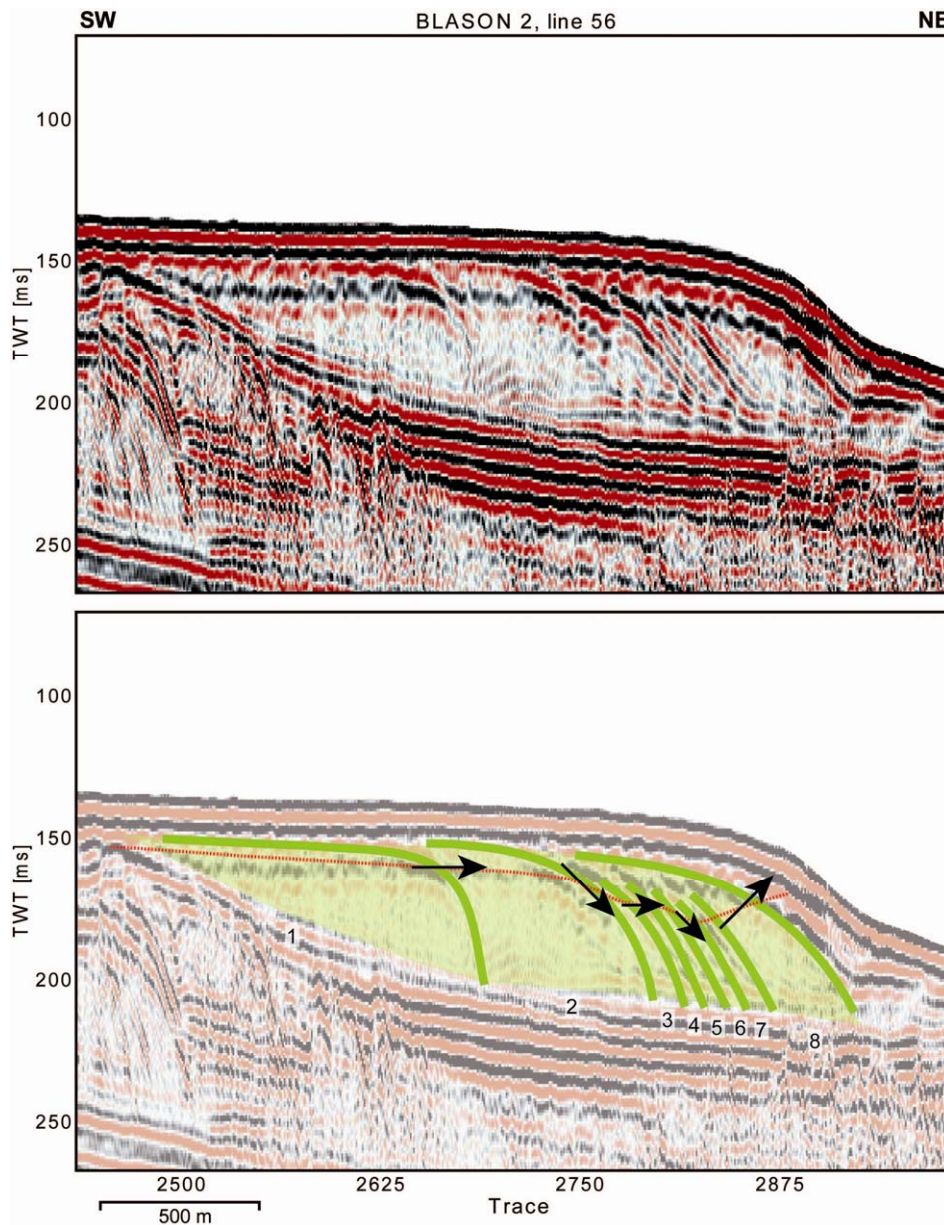
Fig. 5.16: Details from BLASON 2 line 56 showing the deltaic system ΔA in subunit A of unit 1 with its eight individual sedimentary bodies. Their relative positions (as indicated by the red dotted line that connects the location of the topset-to-foreset transitions during the different stages) show a small-scale variability of the sea level while the delta system formed. Black arrows indicate the corresponding sea-level trends. See Fig. 5.3 for position within profile BLASON 2-56.

Farther to the north on the shelf off central Bulgaria, the development of a shelfedge deltaic system is less obvious. Instead, shore-parallel dunes overlie the prograding strata of U1-A (Fig. 5.14). They have a maximum thickness of around 10 ms TWT and are interpreted to represent aeolian dune fields that might mark a paleo-coastal environment (Wilson, 1972). Sediments from dunes on the Romanian shelf cored during the BLASON 1 cruise yielded an age of around 9 ka. That a thin (~5 ms TWT) sediment drape covers these dunes suggests that dune formation is no longer active.
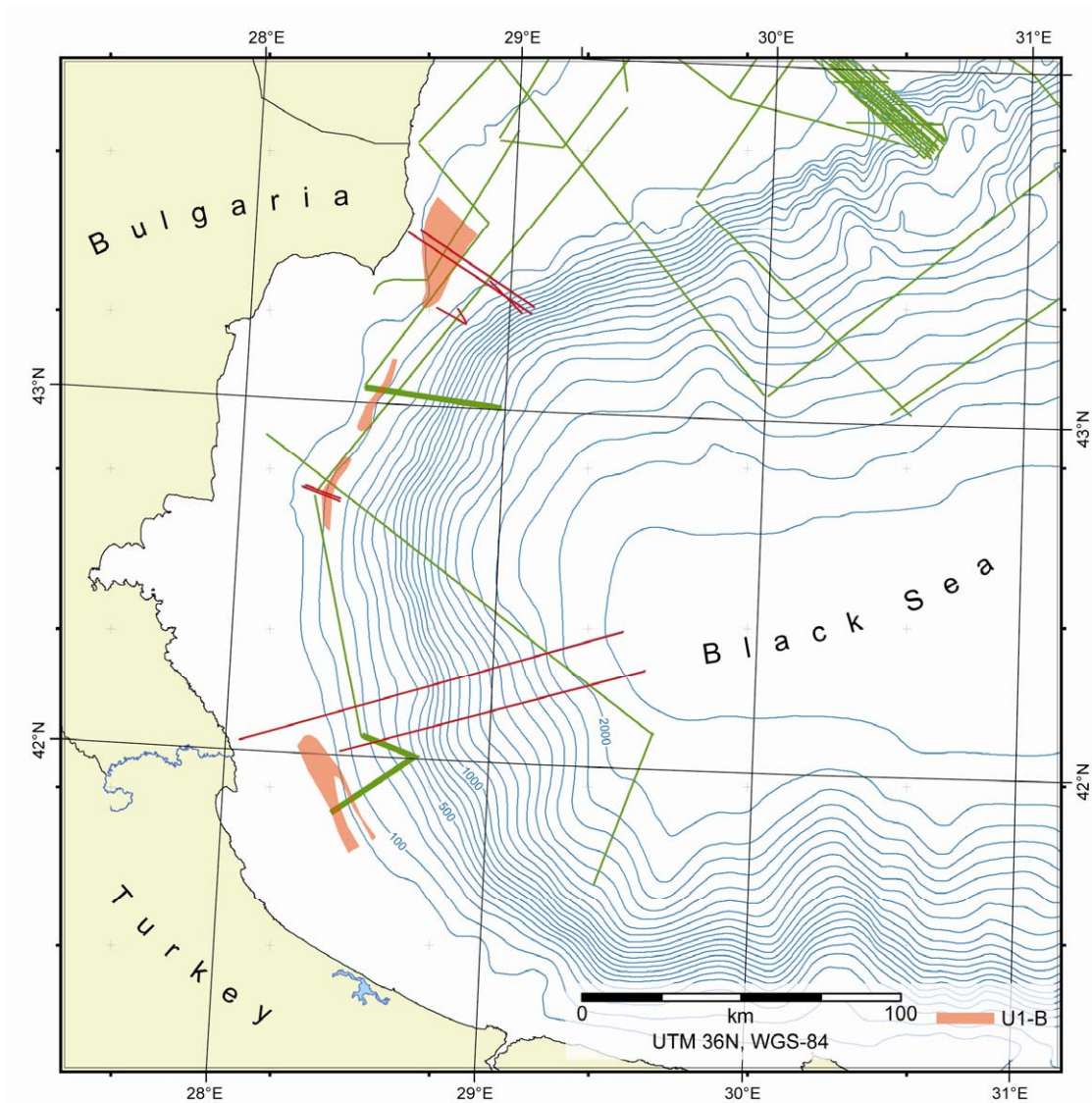
Fig. **5.17**: Map showing the spatial distribution of the seismic stratigraphic Unit 1-B (U1-B) on the southwestern Black Sea shelf.

Dune fields are wind-dominated deposits and their occurrence points to sedimentation in a dry climate, probably during the last glacial maximum. Thus, these deposits are considered a part of U1-A. The dunes are well-preserved, indicating that erosion during the Holocene transgression was negligible. They occur at a present-day water depth of 80-90 m. Assuming a mean storm wave-base of -30 m (Shcherbakov, 1979), the sea-level rise from about -85 m to at least -55 m must have been very rapid. Similar dunes at comparable water depths have been described on the Ukrainian shelf (Ryan et al., 2003), attesting to the widespread occurrence of these features. Coastal dunes, however, are absent on profiles from the southernmost and northern Bulgarian shelves (Fig. 5.4, Fig. 5.12), as well as the Turkish shelf (Fig. 5.3). Since the formation of these features on the outer shelf requires a

sufficiently low relative sea level, their absence might be another indication for differential vertical tectonic movements, which in this case would imply a smaller subsidence.

5.2.1.2.4.2. Subunit U1-B

The younger subdivisions of unit 1 (subunits U1-B and U1-C) were deposited during the postglacial sea-level rise and the Recent highstand. The areas in which sediments assigned to U1-B occur are shown in Fig. 5.17. At the southwestern end of the study area and off northern Bulgaria, U1-B occurs at subbottom depth of around 50 m, while it reaches >100 m offshore central Bulgaria.

Very high-resolution Boomer and Chirp sonar data show that sediments of subunit U1-B fill the small topographic lows on the rugged erosional top surface of the older units U2 to U4 (Figs. 5.8, 5.12, 5.14 and 5.18). Since the total thickness of U1-B is never over 5 ms TWT, it cannot be distinguished on lower resolution conventional seismic data.

U1-B is characterized by a landward-prograding internal configuration, suggesting spillover sedimentation during the initial phase of the postglacial transgression or during a time when the sea level remained close to the present-day shelfedge for a significant period of time.

The existence of shelf-edge perched deltas younger than U1-A implies that the postglacial sea-level rise was not continuous but was interrupted after the deposition of subunit U1-A by minor fluctuations that led to the formation of the unconformity between U1-B and U1-C as well as the subsequent buildup of coastal dunes.

5.2.1.2.4.3. Subunit U1-C

The youngest among the three subunits of unit 1 is U1-C. This is a landward-thickening package comprising retrogradationally stacked wedges (Fig. 5.8) that cover large parts of the shelf (Fig. 5.19). It reaches a thickness of 20 ms TWT, with a thickening tendency towards the north, making it barely recognizable on conventional seismic records.
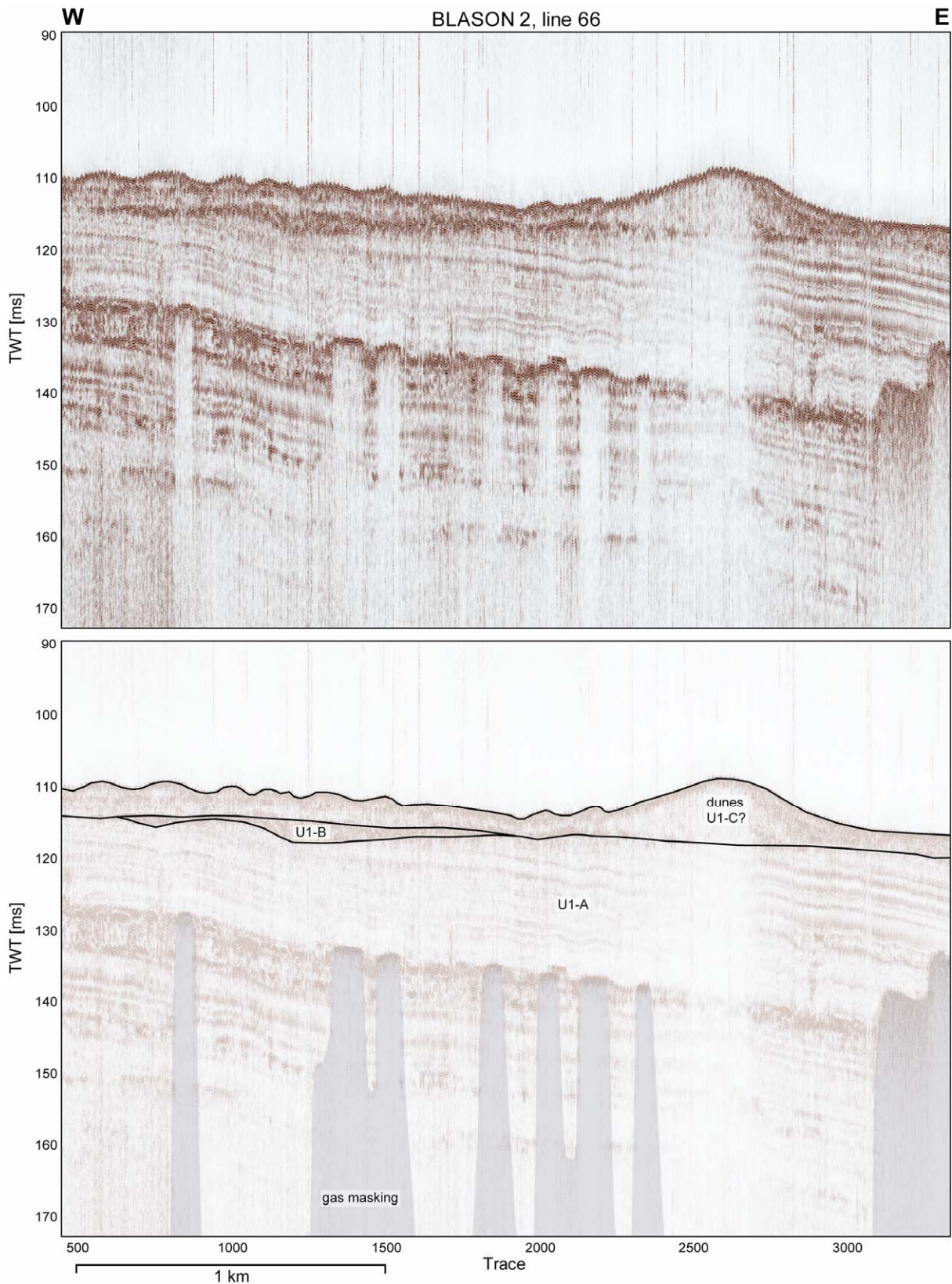
Fig. 5.18: Details of Chirp profile 66 recorded during the BLASON 2 cruise. Interpreting these features in this profile and in profile BGG90-42 (Fig. 5.14) as coastal dunes would imply that sea-level rise in the Black Sea during the Holocene was not uniform, but underwent fifth order cycles of fluctuations.

Figure 5.18 shows dune-like structures in subunit U1-C that resemble in shape and size the coastal dunes of U1-A. They overlie a well-developed angular unconformity that separates U1-A from the younger subunits. The assignment of these dunes to U1-C implies that they have a post-Early Holocene age. A thin sediment drape overlies the dunes found in U1-A (Fig. 5.14); it is however absent over the younger dunes in U1-C. Thus, whether the sedimentary system that constructed these dunes is now no longer active must remain uncertain.
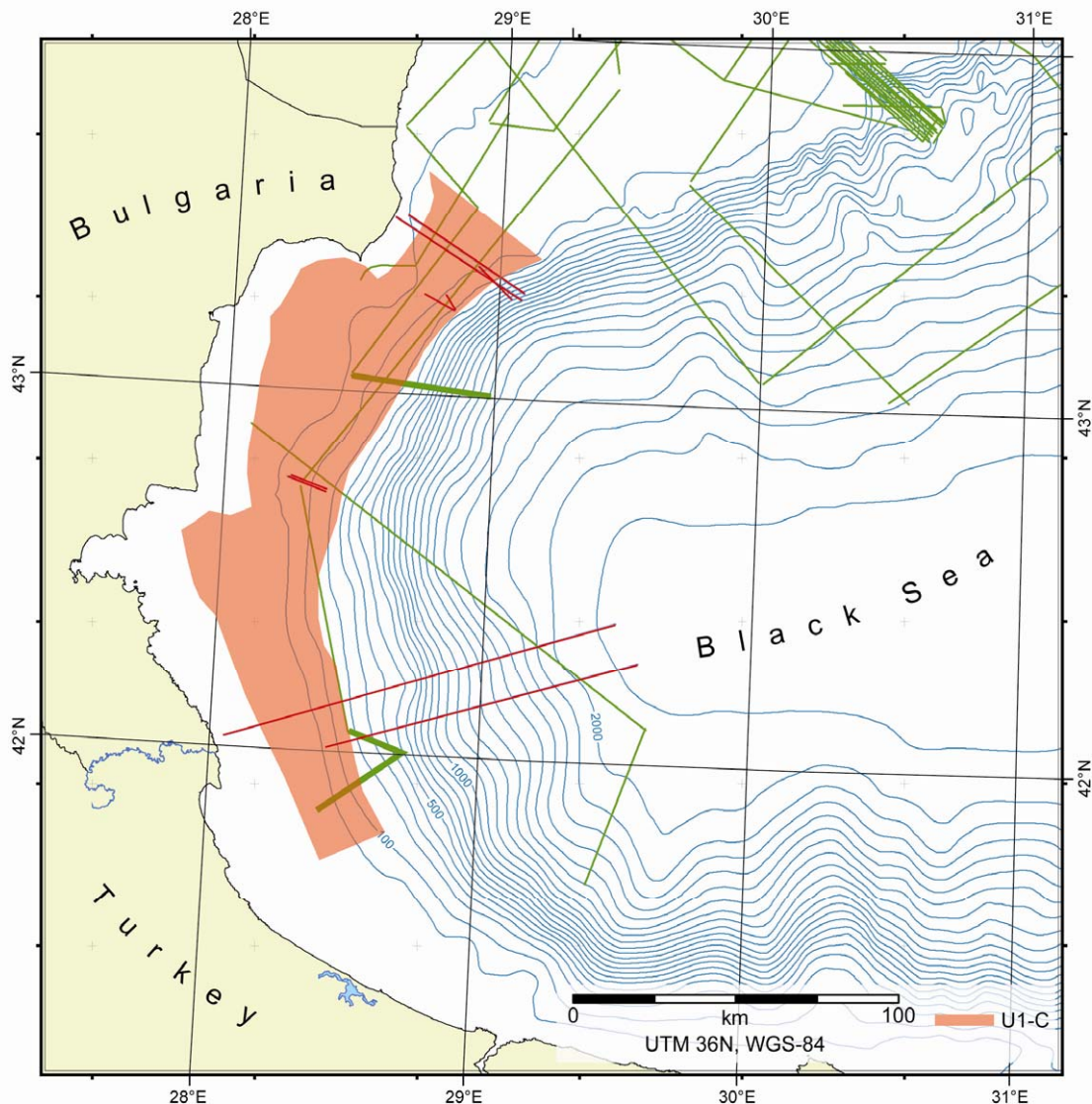
Fig. **5.19**: Map showing the spatial distribution of the seismic stratigraphic Unit 1-C (U1-C) on the southwestern Black Sea shelf.

The buildup of the dune-like features observed in the subunits of U1 must have taken place during times of subaerial exposure and low sea levels. A development during at least

two different phases of sea-level lowstand must be assumed: the first during and shortly after the last glacial maximum (Fig. 5.14) and the second during the post-Early Holocene after the sedimentation of subunit U1-B (Fig. 5.18).

5.3. Northwestern shelf

In contrast to the relatively narrow shelf of the southwestern Black Sea, the shelf broadens significantly in the northwest and reaches a width of almost 200 km. The slope gradient in the northwest is generally smaller than in the southwest.

Even though a comparatively dense network of reflection seismic lines was available, an application of the Quaternary seismic stratigraphic model described in the preceeding sections to the northwest turns out to be difficult. Fig. 5.20 shows exemplarily interpretation and data quality on three profiles from this area. Two factors made seismo-stratigraphic interpretation on the northwestern Black Sea shelf difficult:

- The lack of very high-resolution data covering the shelf of the Romanian sector (the majority of such data available for this study was provided by the Bulgarian National Institute of Oceanology, IO-BAS). Most of the available seismic lines consist of conventional air gun/streamer data, some acquired for industrial exploration and have a comparatively low resolution in the youngest stratigraphic units. These data cannot resolve the subtle seismic stratigraphic details necessary for a reconstruction of the youngest geological history.

- The problematic data quality in widespread areas across the northwestern Black Sea. Figure 5.5 shows that in particular the areas close to the shelfedge are affected by a severe attenuation of the seismic signal. Deeper penetration here is, however, critical for our seismic stratigraphic analysis.

Even if the detailed intra-Quaternary seismic stratigraphic classification of the south-western shelf could not be extended northward, interpretation of the available seismic data, seismic velocity information in combination with borehole data acquired for oil and gas exploration permit mapping of the base of the Quaternary for the shelf of the entire northwestern Black Sea. This in turn yields valuable information on the regional subsidence history and its control by tectonic activity.
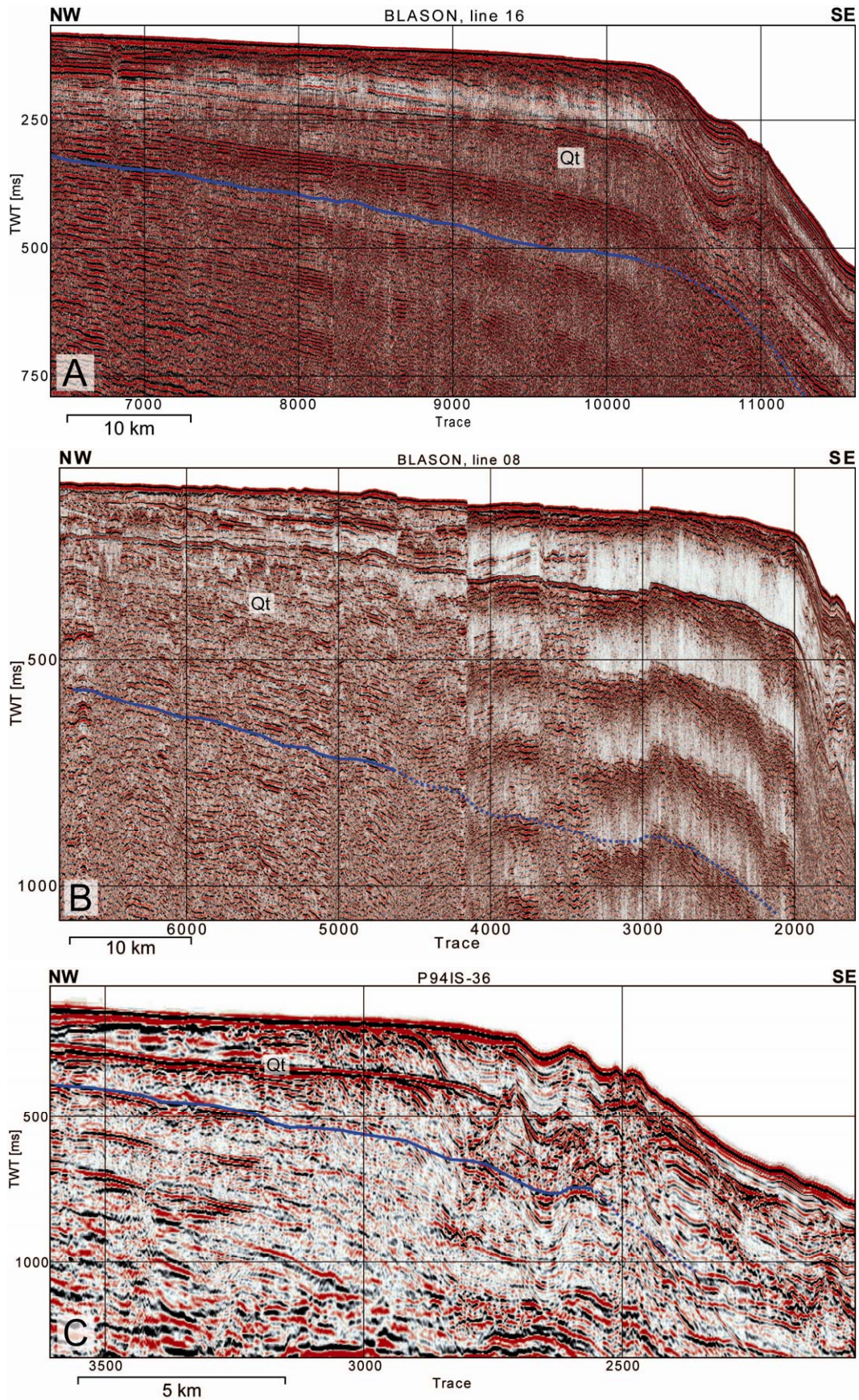
Fig. 5.20: Three typical profiles from the outer northwestern Black Sea shelf, showing the seismic characteristics of Quaternary deposits in this region. The profiles are sorted from south to north: A - Line 16 from cruise BLASON 1; B - BLASON 1, line 8. C - Line 36 of the 1994 survey for Total. See Fig. 5.21 for profile locations.
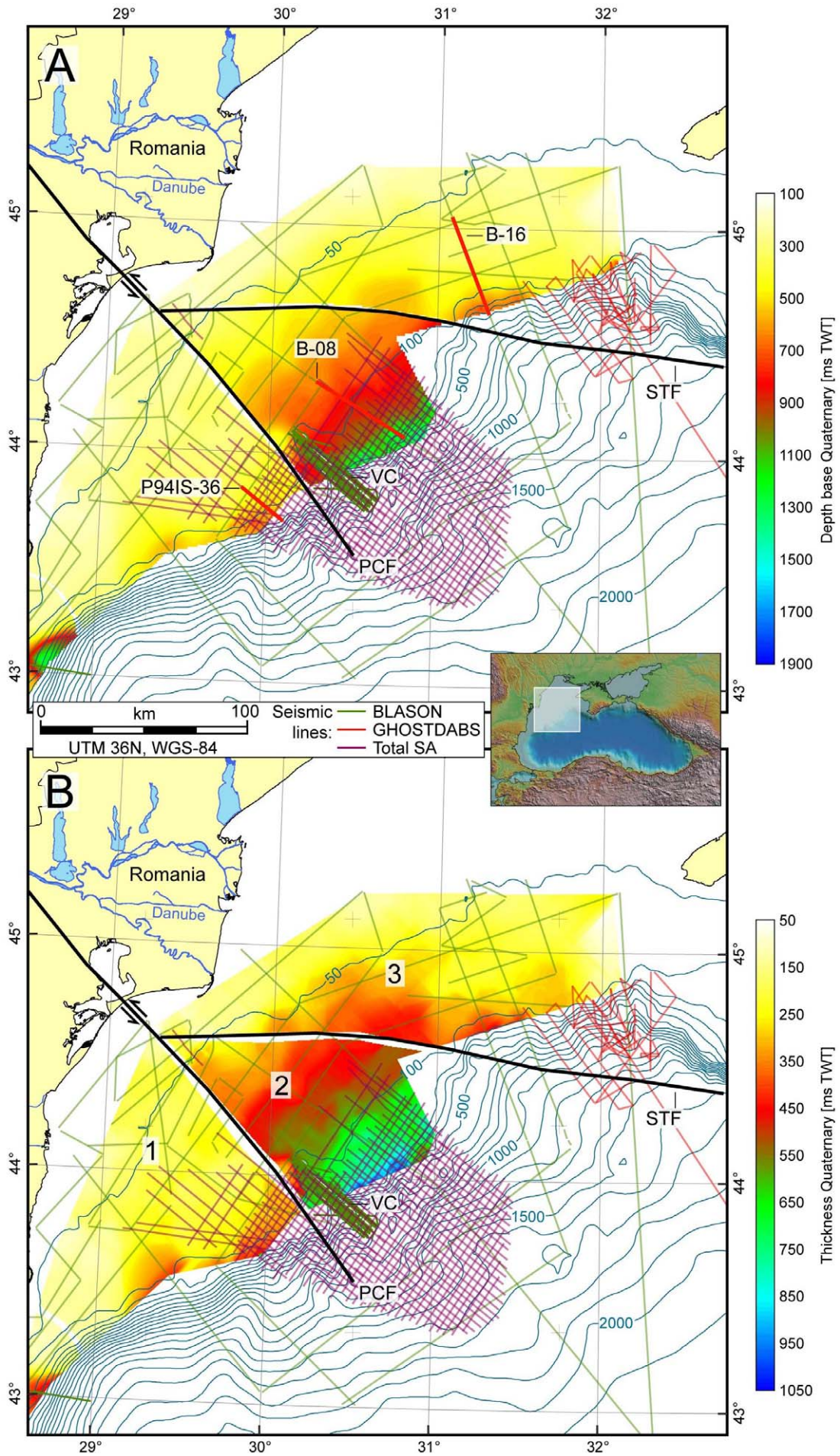
Fig. 5.21 (previous page): Two maps of the northwestern Black Sea shelf; location is shown in the inset. Map A shows the color-coded depth distribution (in ms TWT) of the base of the Quaternary interpolated from mapping results using the seismic lines shown in green (BLASON), red (GHOST-DABS), and purple (Total). Map B shows the distribution of thickness of the Quaternary section derived from map A color-coded in ms TWT. Bold black lines give the location of major fault systems (from Dinu et al., 2005). Abbreviations: VC – Viteaz Canyon, PCF – Peceneaga Camena Fault, STF – Sulina Tarkinkut Fault. Bold red lines in panel A mark the position of the profile in Fig. 5.20; numbers 1 to 3 in panel B give the major structural subdivisions on the northwestern Black Sea shelf as described in the text (see below).

The resulting depth distribution of the base of the Quaternary sediments on the northwestern Black Sea shelf and the corresponding thickness of the Quaternary section are shown in Fig. 5.21. Clearly visible is the three-tiered structural division in this part of the study area controlled by the major regional fault systems.

In the south (southern Romanian to Bulgarian Sector; 1 in Fig. 5.21-B), the Quaternary section is thin with a thickness of not more than 400 ms TWT even on the outermost shelf. This thickness is uniform, averaging approximately 150 ms TWT.

The central part (Romanian sector in the vicinity of the Viteaz Canyon; 2 in Fig. 5.21-B) in contrast shows the highest observed thickness of Quaternary sediments in the entire western Black Sea, reaching values of around 600 ms TWT close to the present-day shelfedge. In this area, mapping could be extended well below the shelfedge onto the continental slope where the Quaternary can reach a thickness of more than one second TWT.

In the northeastern segment (Romanian to Ukrainian Black Sea sectors; 3 in Fig. 5.21 -B), the average thickness is again smaller, but more variable than to the south. Large thickness values of 450–500 ms TWT occur at the transition to the central area. They decrease gradually to the north and to the east. In the easternmost study area, the Quaternary thickness does not exeed 200–250 ms even at the shelf break.

The depth and thickness distributions in Figure 5.21 show a good match between the implied structural segmentation of the northwestern shelf (as described above) and the location (mapped by Dinu et al., 2005) of the two most important fault systems in this region: The Peceneaga Camena Fault system (PCF) which stretches from the Romanian mainland across the shelf to the southeast onto the continental slope south of the Viteaz Canyon, and the Sulina Tarkankut Fault system (STF) that originates at the PCF on the inner shelf and extends towards the east into the Ukrainian sector of the Black Sea. These systems

had a significant influence on local subsidence at least until the Lower Quaternary and this influence might even persist until today. The subdivision of the northwestern shelf into three major zones is controlled by the location of the fault systems: The southwestern zone (1) off northern Bulgaria and southern Romania lies south of the PCF and is characterized by relatively thin Quaternary deposits. The area around and to the northeast of the Viteaz Canyon (2) is situated between the PCF and STF and comprises the thickest Quaternary succession. The wide shelf areas in the northern Black Sea belong to zone 3 and are limited by the STF to the south. Quaternary sediments of this zone reach a low to intermediate thickness.

6. Seismic stratigraphic model and subsidence analysis

6.1. Timing of Upper Quaternary sea-level fluctuations in the Black Sea

The stacked prograding deltaic successions in the seismic unit U4 on the middle shelf and in U2 and U1 close to the present-day shelfedge (ΔD, ΔB and ΔA e.g. in Fig. 5.3) are interpreted to have developed during sea-level lowstands of fourth order sea-level cycles, in analogy to similar observations from the eastern Mediterranean, Aegean and Marmara Seas (Aksu et al., 1999; Piper and Aksu, 1992; Aksu et al. 1992 a,b; Piper and Perissoratis, 1991; Aksu et al., 1987).
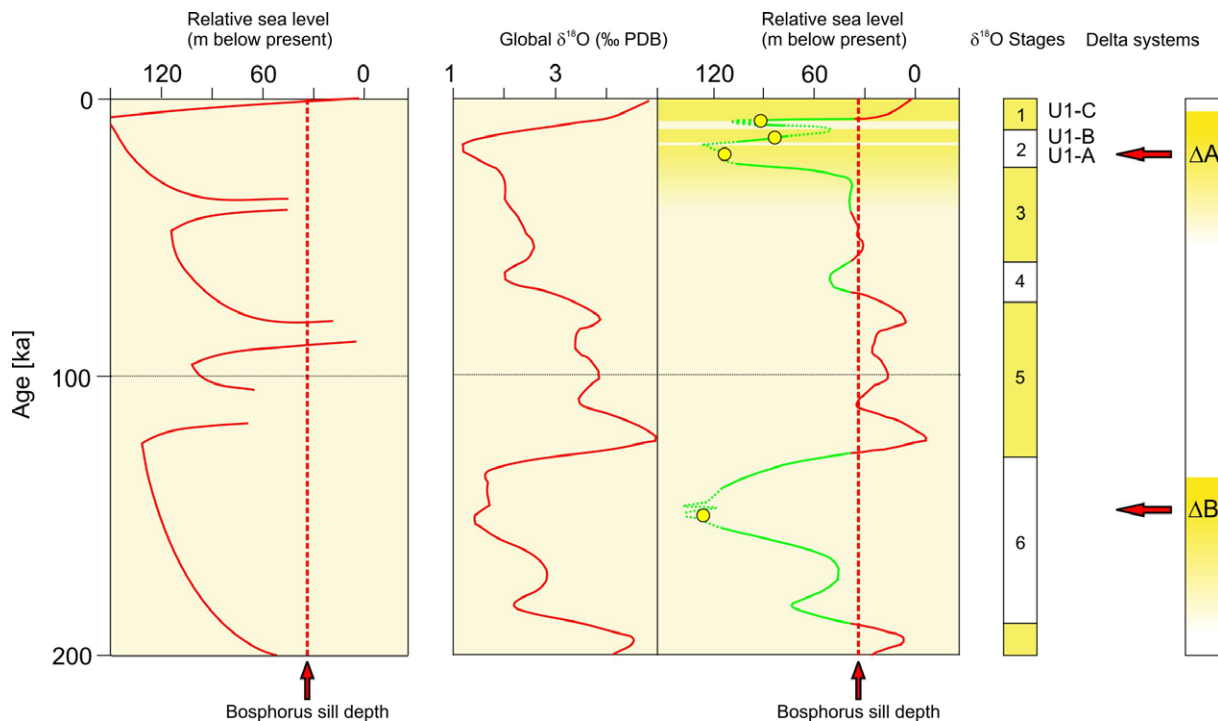
Fig. 6.1: Sea-level curves of the Black Sea for the past 200 kyr. The left panel shows the curve of Winguth et al. (1997; 2000). The centre panels give the sea-level curve constructed from the observed depths of the shelfedge deltaic systems (this study, green lines) and the global δ^{18}O curve of Skene et al. (1998, red lines). Global δ^{18}O stages are shown in the right panels for comparison. The yellow dots on the sea-level curve in the middle panel indicate fixed points in the sea level reconstruction according to the results of this study. High-frequency sea-level changes close to the deltaic systems ΔB and ΔA are exemplarily deduced from a detailed analysis of their internal depositional characteristics (Fig. 5.11, Fig. 5.16).

Past sea-levels lowstands can be deduced from changing elevations of the deltaic topset-to-foreset transition. The present-day depths of these transitions were determined assuming an average seismic velocity of 1,700 m/s for the overlying sediments. Corrections were made

assuming that the deltaic topset-to-foreset transition occurs in 15 m water depth (Aksu et al., 1999) and that the isostatic subsidence due to a water load of 90 m following postglacial sea-level rise is about 20 m (Smith et al., 1995). The corrected depths of the topset-to-foreset transitions of the deltaic systems give the paleo-sea level at the corresponding ages (Table 6.1). The results obtained were then integrated into the global $\delta^{18}O$ curve of Skene et al. (1998) (which provides sea-level estimates when the Black Sea was connected to the global oceans) to produce a regional sea-level curve for the Black Sea (Fig. 6.1).

Another indicator for a sea-level lowstand occurs at the base of unit U2, where coastal onlap (C in Fig. 5.3, Fig. 5.6) has been observed. These are supposedly formed in a coastal environment under very shallow water conditions (Vail et al., 1977). The deepest coastal onlap found within a sequence therefore gives the lowest water level reached during the time period represented provided that the entire sequence is preserved.

Lowstand indicator	Glacial	Age [ka]	Seismic unit	Depth [ms TWT]	Uncorrected depth [m]	Corrected depth [m]
ΔA	Würm	20	U1-A	170	144.5	109.5
ΔB	Riss	150	U2	195	165.8	130.8
C	Mindel	500	U3	285	242.3	222.3
ΔD	Günz (?)	900	U4	205	174.3	139.3

Tab. 6.1: Position of sea-level lowstands in the southwestern Black Sea deduced from topset-to-foreset transitions of paleo-deltaic systems (ΔA, ΔB, ΔD, labels same as in Fig. 5.3) and coastal onlaps (C). The corrected depths account for an estimated water depth of ~15 m in which the topset-to-foreset transitions were laid down and an isostatic subsidence of ~20 m due to a postglacial sea-level rise of ~90 m.

The deltaic system found above the Pliocene/Quaternary unconformity is interpreted to be of mid-Quaternary age, probably representing sedimentation during the first of the major Quaternary glaciations (Günz, age around 1 ma) after a long phase of a relatively continuous decrease of global temperatures during the Early Quarternary. The two younger deltaic systems are presumably laid down during the last two global glacial epochs, namely during Riss (ΔB, 180-125 ka) and Würm (ΔA, ca. 65-12 ka). This age assignment for the delta systems suggests an age of around 500 ka (Mindel glacial) for lowstand C at the base of unit 2.

6.2 Subsidence analysis

The depth values deduced from the interpretation of lowstand indicators during the Quaternary need to be corrected for the influence of tectonic subsidence as suggested by the recognition of young tectonic features on the seismic profiles. To quantify possible lateral variations in tectonic subsidence, the effects of sediment compaction, subsidence due to sediment load and thermal subsidence must first be removed.
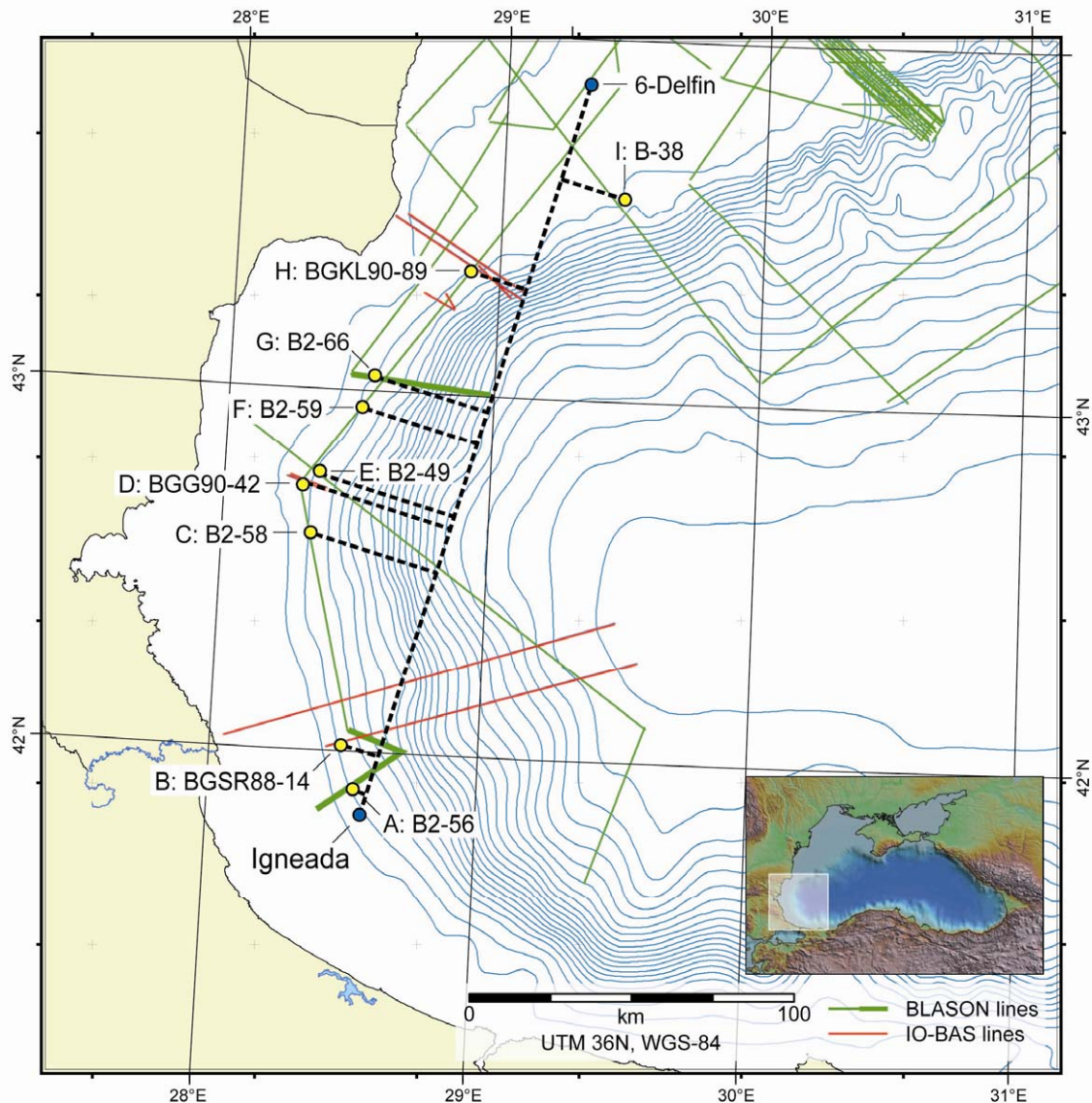
Fig. 6.2: Idealized subsidence analysis profile across the southwestern Black Sea shelf (dashed black line) between the exploration wells *Igneada* in the southwest and *6-Delfin* in the northeast (blue dots); the inset gives the map location. Yellow dots mark the measurement locations A-I (labels give the corresponding seismic profiles) at intersections of seismic profiles and the 100 m isobath. Survey abbreviations in profile labels: B2 – Blason 2; BGSR88 – Sredetska 1988; BGG90 – Godin 1990; BGKL90 – Kaliakra 1990; see section 4.1.1 for detailed survey descriptions.

A first estimate shows that the effect of thermal subsidence is small (<2 m) for the time interval considered here, it will thus not be taken into account in the following. To assess systematic lateral changes in tectonic subsidence (or differential tectonic subsidence), the subsidence analysis method developed and refined by Bond et al. (1989), Bond & Kominz (1984), and Sclater & Christie (1980) was applied.

On the southwestern shelf off Turkey and Bulgaria, two-way travel times (TWT) to the base of the Quaternary and of the units U2 and U1 at a water depth of 100 m on a number of high-resolution seismic profiles served as input data (see Fig. 6.2 for profiles and section 4.1.1 for survey description). The measurement locations were projected onto a NNE-SSW-striking idealized profile constructed by joining the boreholes *6-Delfin* in the north with *Igneada* in the south by a straight line (Fig. 6.2). The results of the subsidence analysis are described in section 6.2.1.

The initially measured seismic two-way-travel times in milliseconds were converted to depths using interpolated interval velocities for the Quaternary at each projected point. These velocities were calculated using values deduced from a correlation of mapped seismic horizons with borehole information, and (for interpolation) assuming that the velocity gradient between the two boreholes is linear. Figure 6.3 shows the initially measured travel times used for the subsidence analysis.

To extend the subsidence measurements in the south onto the northeastern shelf, a second profile was constructed using the same basic principle as described above. This profile is located on the shelf in the northern part of the study area off Romania and the Ukraine. The results of the subsidence analysis along this second profile are described in section 6.2.2.

Because of the lack of very high resolution seismic data and and inferior data quality throughout large areas of this region (most likely due to high gas content and coarse-grained sediments, see section 5.2.1), the intra-Quaternary units mapped in the southwest could not be extended to the northeastern Black Sea shelf with confidence. Consequently, only the depth to the base of the Quaternary was available for subsidence analysis along this profile.

The available data for the northwestern subsidence analysis profile include information from a large number of boreholes. Thus, the lithology along the profile is known in great detail and the results are very reliable.

For subsidence analysis study on the northwestern Black Sea shelf, data from the following Romanian and Ukrainian exploration boreholes were evaluated: *6-Delfin*, *12-Midia*, *1-Ovidiu* and *75-Cobalcscu* from the Romanian sector, and *1-Desantna*, *2-Iliechevska*, and *1-Zentralna* fromn the Ukrainian sector. The true depth of the base of the Quaternary deduced from the borehole information was used to calculate the interval velocity of the Quaternary sediments.
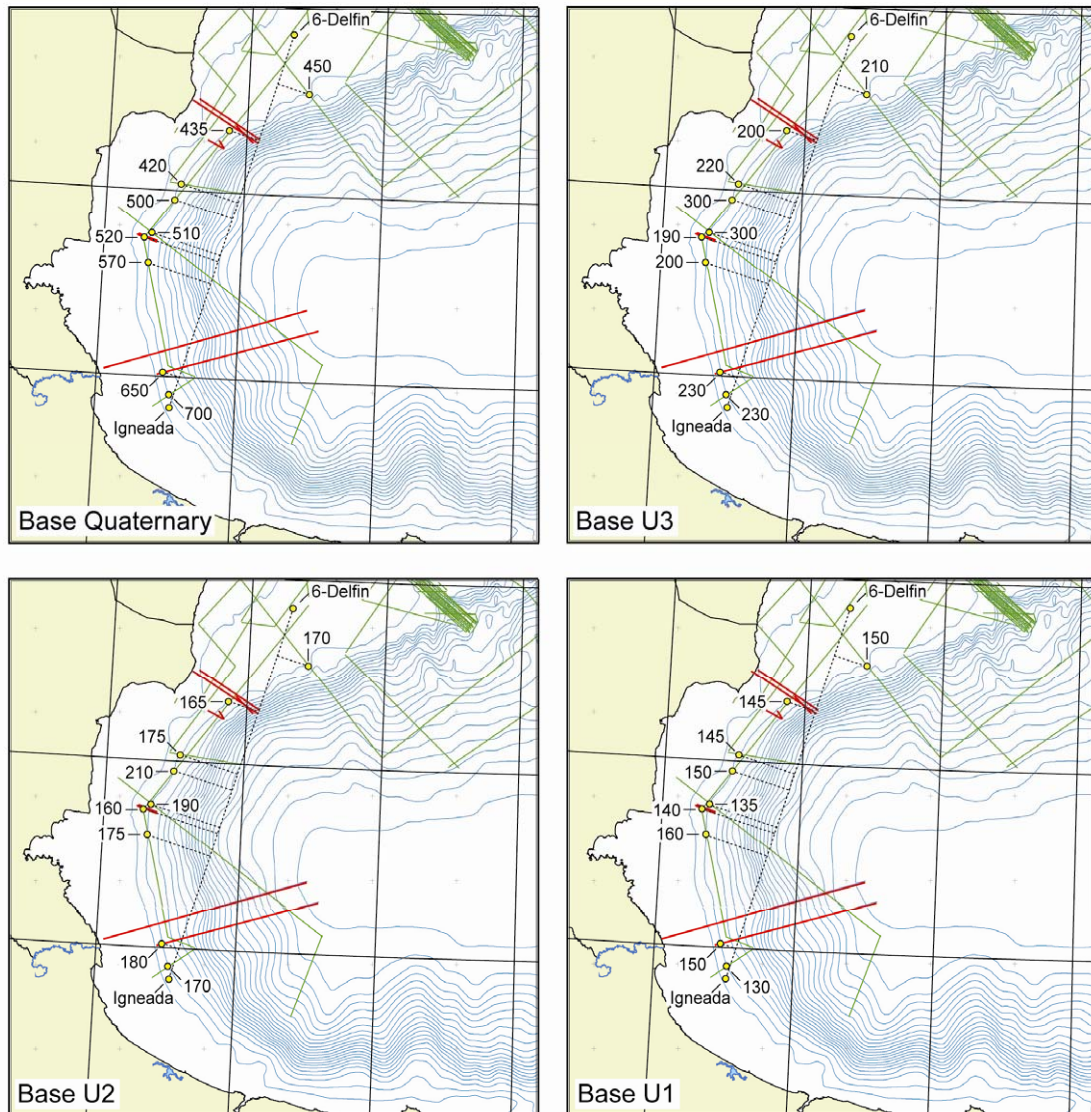
Fig. **6.3**: Input data for the subsidence analysis to quantify tectonic and sedimentary subsidence. Yellow dots give the measurement points, and the associated numbers denote TWT in ms to the horizon under consideration. The black dotted line is the NNE-SSW-striking idealized profile made by connecting the wells *6-Delfin* and *Igneada*. The projected positions of the measurement points on this profile are also shown. Map extent is the same as in Fig. 6.2.

112

6.2.1 Subsidence analysis profile 1: Turkish and Bulgarian sectors

The subsidence analysis along an idealized profile through the Turkish and Bulgarian shelves between the two exploration boreholes *Igneada* in the southwest and *6-Delfin* in the northeast yielded the amount of tectonic subsidence and subsidence due to sediment loading at nine different measurement locations (Fig. 6.3). The input model was created using mapping results for the seismic horizons representing the base of the following seccessions: Quaternary, U3, U2 and U1. The curves shown in Fig. 6.4 depict the depth (converted to meters) of the horizons and the tectonic, sedimentary and total subsidence of these four horizons from their formation to the present-day. In Fig. 6.5, the subsidence history of the western Black Sea shelf is shown by the plots of tectonic and total subsidence against time at the measurement locations.

The results presented herein suggest that tectonic subsidence in the Bulgarian sector of the western Black Sea varied more-or-less linearly during the Quaternary, increasing generally from NNE to SSW (Fig. 6.4). The only exception is during the Upper Quaternary, when it increased abruptly in the central segment of the idealized profile off central Bulgaria (D and E in Fig. 6.4), but kept to the general trend in both the northern and southern segments (A to C and F to I in Fig. 6.4). This suggests enhanced tectonic activities off central Bulgaria during the deposition of unit 1 in the Upper Quaternary. If the sedimentary sequences were laid down on a stable or tectonically uniformly subsiding shelf, they would form a succession in which the lowstand indicators shift up-sequence steadily basinwards and the shelfedge progrades (Aksu et al., 1992a, b). The profile Blason 2-56 (Fig. 5.3) shows that this is the case for the period between the lowstand indicators C and B, as well as B and A. Between the lowstands D and C, a large seaward shift of the coastline accompanied by an increase in depth of the indicators occurred. This suggests that during the Quaternary after the formation of onlap C, tectonic subsidence must have proceeded in a manner different from that of the preceding period.

The Tables 6.2 through 6.5 summarize the results of the subsidence analysis along the idealized profile shown in Fig. 6.2. Table 6.2 shows the relative importance of tectonic and sedimentary subsidence in the observed total subsidence of a seismic stratigraphic interface at the different measurement stations A-I (see also Fig. 6.4). Table 6.3 gives the corresponding initial decompacted thickness values for the individual layers. With these values, the subsidence rates (Tab. 6.4) and decompacted sedimentation rates (Tab. 6.5) can be estimated.
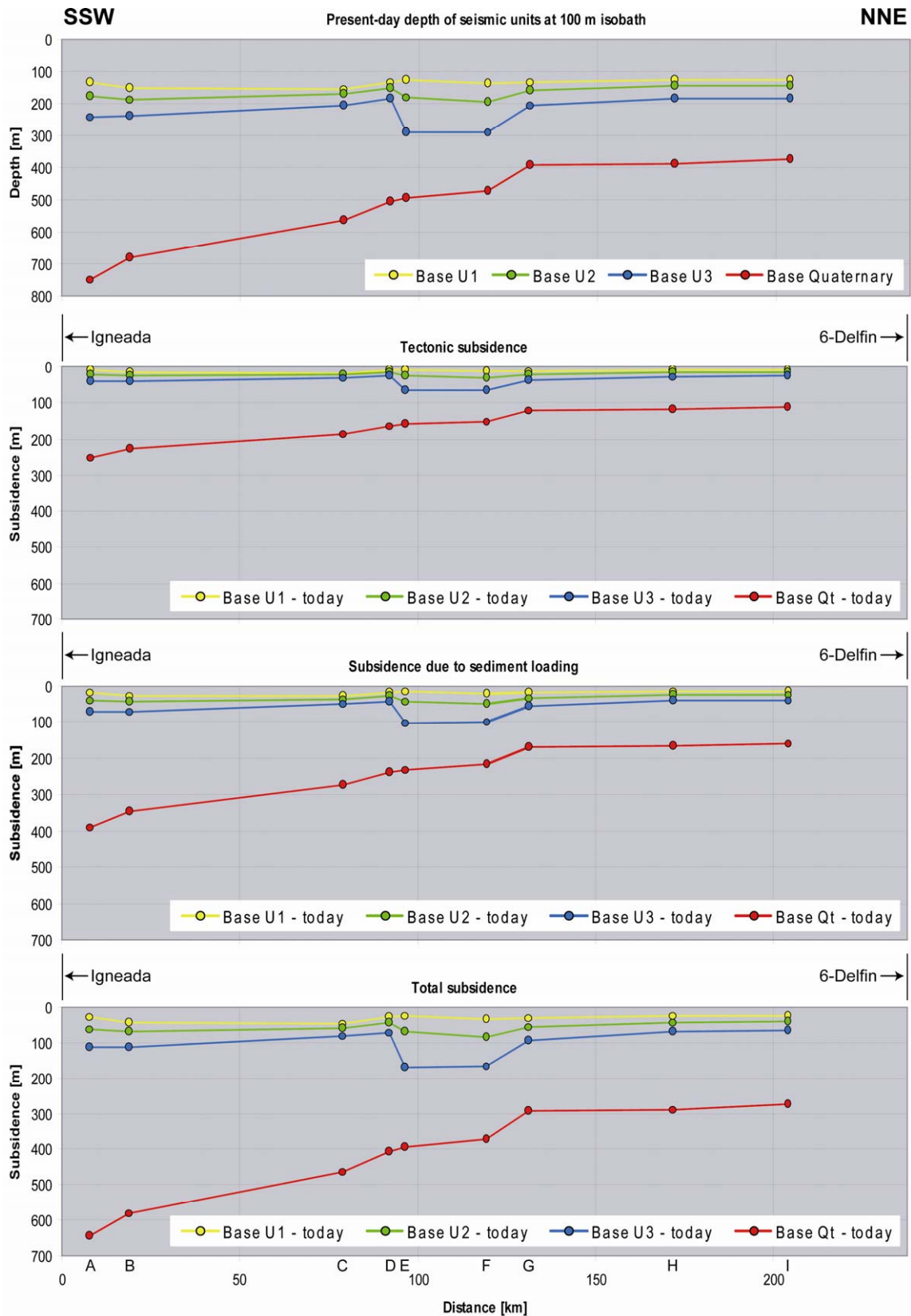
**Fig. 6.4:** Upper panel: Present-day depth in meters of the four horizons considered in the subsidence analysis (base of Quaternary, base of U3, base of U2 and base of U1) projected onto a profile connecting the boreholes *Igneada* in the SSW and *6-Delfin* in the NNE. The lower three panels give the amounts of tectonic, sedimentary and total subsidence of these four horizons from their formation to the present-day.

Location	Total subsidence [m]			
	bQt-U3	U3-U2	U2-U1	U1-Recent
A	529	53	34	28
B	465	43	27	44
C	381	21	13	47
D	334	26	16	30
E	223	101	45	25
F	207	81	50	35
G	197	40	25	31
H	219	27	18	25
I	208	25	16	26

Location	Tectonic subsidence [m]			
	bQt-U3	U3-U2	U2-U1	U1-Recent
A	212	20	12	10
B	189	16	10	16
C	157	8	5	18
D	139	10	6	11
E	94	41	17	10
F	88	33	20	13
G	84	16	10	12
H	93	11	7	10
I	88	10	7	10

Location	Sedimentary subsidence [m]			
	bQt-U3	U3-U2	U2-U1	U1-Recent
A	317	33	22	18
B	276	27	17	28
C	224	13	8	29
D	195	16	10	19
E	129	60	28	15
F	119	48	30	22
G	113	24	15	19
H	126	16	11	15
I	120	15	9	16

Tab. 6.2: Results of the subsidence analysis for the Quaternary of the Bulgarian sector of the western Black Sea shelf: Total, tectonic and sedimentary subsidence in meters for the four intervals base of Quaternary-base of U3 (bQt-U3), base of U3 to base of U2 (U3-U2), base U2 to base of U1 (U2-U1) and base of U1-Recent (U1-Recent) at the locations A to I (Fig. 6.2).

Location	Initial decompacted thickness [m]			
	bQt-U3	U3-U2	U2-U1	U1-Recent
A	529	67	44	37
B	465	53	35	57
C	381	25	16	58
D	334	30	20	36
E	223	113	53	31
F	207	90	58	42
G	198	44	29	36
H	219	31	20	30
I	208	28	29	30

Tab. 6.3: Results of the subsidence analysis for the Quaternary of the Bulgarian sector of the western Black Sea shelf: Initial decompacted thickness for the four intervals (bQt-U3), base of U3 to base of U2 (U3-U2), base U2 to base of U1 (U2-U1) and base of U1-Recent (U1-Recent) at the locations A to I (Fig. 6.2).

Location	Decompacted total subsidence rate [m/ka]			
	bQt-U3	U3-U2	U2-U1	U1-Recent
A	0.48	0.21	0.12	1.38
B	0.42	0.17	0.1	2.18
C	0.35	0.08	0.05	2.34
D	0.3	0.1	0.06	1.49
E	0.2	0.4	0.16	1.26
F	0.19	0.32	0.18	1.74
G	0.18	0.16	0.09	1.53
H	0.2	0.11	0.06	1.29
I	0.19	0.1	0.06	1.29

Location	Decompacted tectonic subsidence rate [m/ka]			
	bQt-U3	U3-U2	U2-U1	U1-Recent
A	0.19	0.08	0.04	0.49
B	0.17	0.06	0.04	0.79
C	0.14	0.03	0.02	0.89
D	0.13	0.04	0.02	0.57
E	0.09	0.16	0.06	0.48
F	0.08	0.13	0.07	0.67
G	0.08	0.06	0.04	0.61
H	0.08	0.04	0.03	0.51
I	0.08	0.04	0.02	0.52

Location	Decompacted sedimentary subsidence rate [m/ka]			
	bQt-U3	U3-U2	U2-U1	U1-Recent
A	0.29	0.13	0.08	0.89
B	0.25	0.11	0.06	1.39
C	0.21	0.05	0.03	1.45
D	0.17	0.06	0.04	0.92
E	0.11	0.24	0.1	0.78
F	0.11	0.19	0.11	1.07
G	0.1	0.1	0.05	0.92
H	0.12	0.07	0.03	0.78
I	0.11	0.06	0.04	0.77

Tab. 6.4: Results of the subsidence analysis for the Quaternary of the Bulgarian sector of the western Black Sea shelf: Total, tectonic and sedimentary subsidence rates in meters per 1000 years for the four intervals base of Qaternary-base of U3 (bQt-U3), base of U3 to base of U2 (U3-U2), base U2 to base of U1 (U2-U1) and base of U1-Recent (U1-Recent) at the locations A to I (Fig. 6.2).

Location	Decompacted sedimentation rates [m/ka]			
	bQt-U3	U3-U2	U2-U1	U1-Recent
A	0.48	0.27	0.16	1.86
B	0.42	0.21	0.12	2.83
C	0.35	0.1	0.06	2.88
D	0.3	0.12	0.07	1.81
E	0.2	0.45	0.19	1.54
F	0.19	0.36	0.21	2.1
G	0.18	0.17	0.1	1.78
H	0.2	0.12	0.07	1.49
I	0.19	0.11	0.07	1.48

Tab. 6.5: Results of the subsidence analysis for the Quaternary of the Bulgarian sector of the western Black Sea shelf: Decompacted sedimentation rates in meters per 1000 years for the four intervals base of Qaternary-base of U3 (bQt-U3), base of U3 to base of U2 (U3-U2), base U2 to base of U1 (U2-U1) and base of U1-Recent (U1-Recent) at the locations A to I (Fig. 6.2).
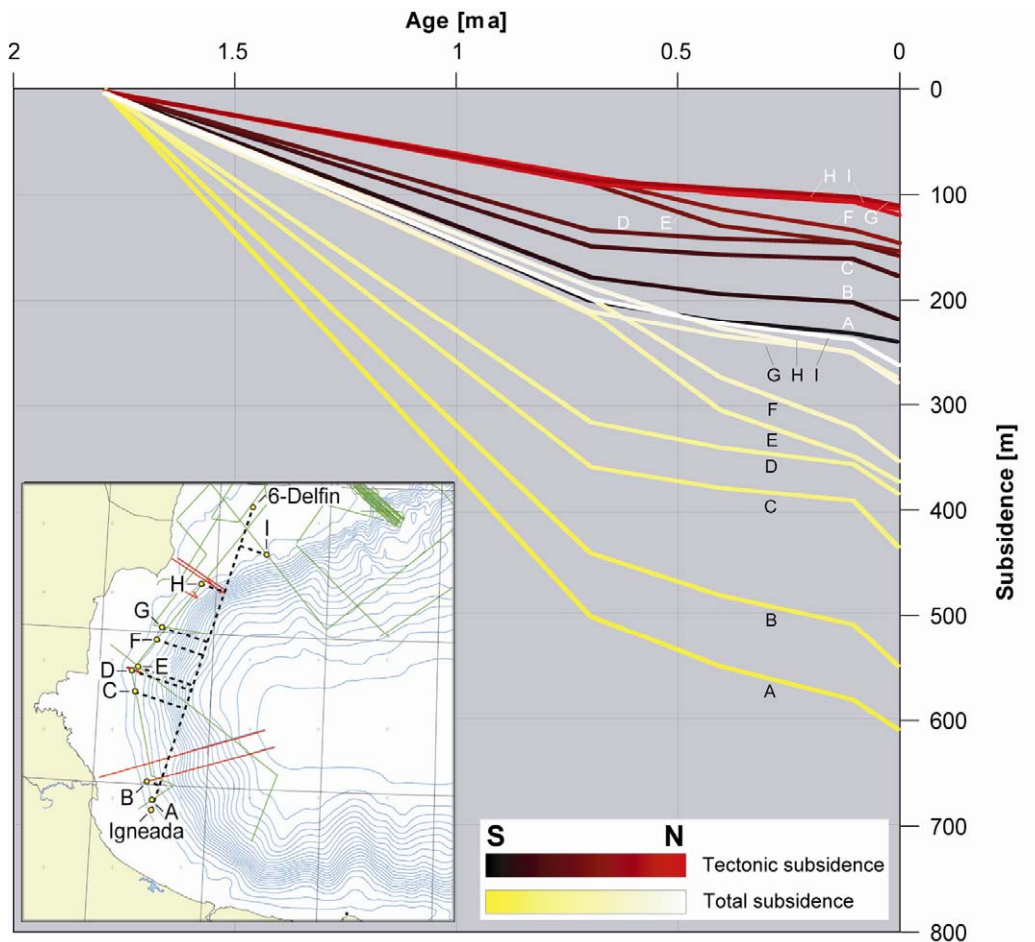
Fig. 6.5: Quaternary subsidence history at the measurement locations (yellow dots on the map; map extent same as in Fig. 6.2). The darker curves (black to red) give the tectonic subsidence through time for each location, while the lighter curves (yellow to white) depict total subsidence (tectonic subsidence + subsidence due to sediment loading).

6.2.2 Subsidence analysis profile 2: Romanian and Ukrainian sectors

The subsidence analysis along profile 2 on the northwestern Black Sea shelf (Fig. 6.6) is based on mapping of the base of the Quaternary. The underlying depth and thickness distributions on the northwestern Black Sea shelf (measured in ms TWT) are shown in Fig. 5.21. The extent of the mapped area is limited towards the deeper basin by the traceability of the corresponding horizon on the seismic profiles as this stratigraphic boundary is not necessarily marked by a coherent reflection and the area around the northwestern shelfedge is particularly prone to strong attenuation of seismic signals. Laterally on the shelf, however, the base of the Quaternary could be mapped throughout a continuous area that covers most of the Romanian and western Ukrainian Black Sea sectors.
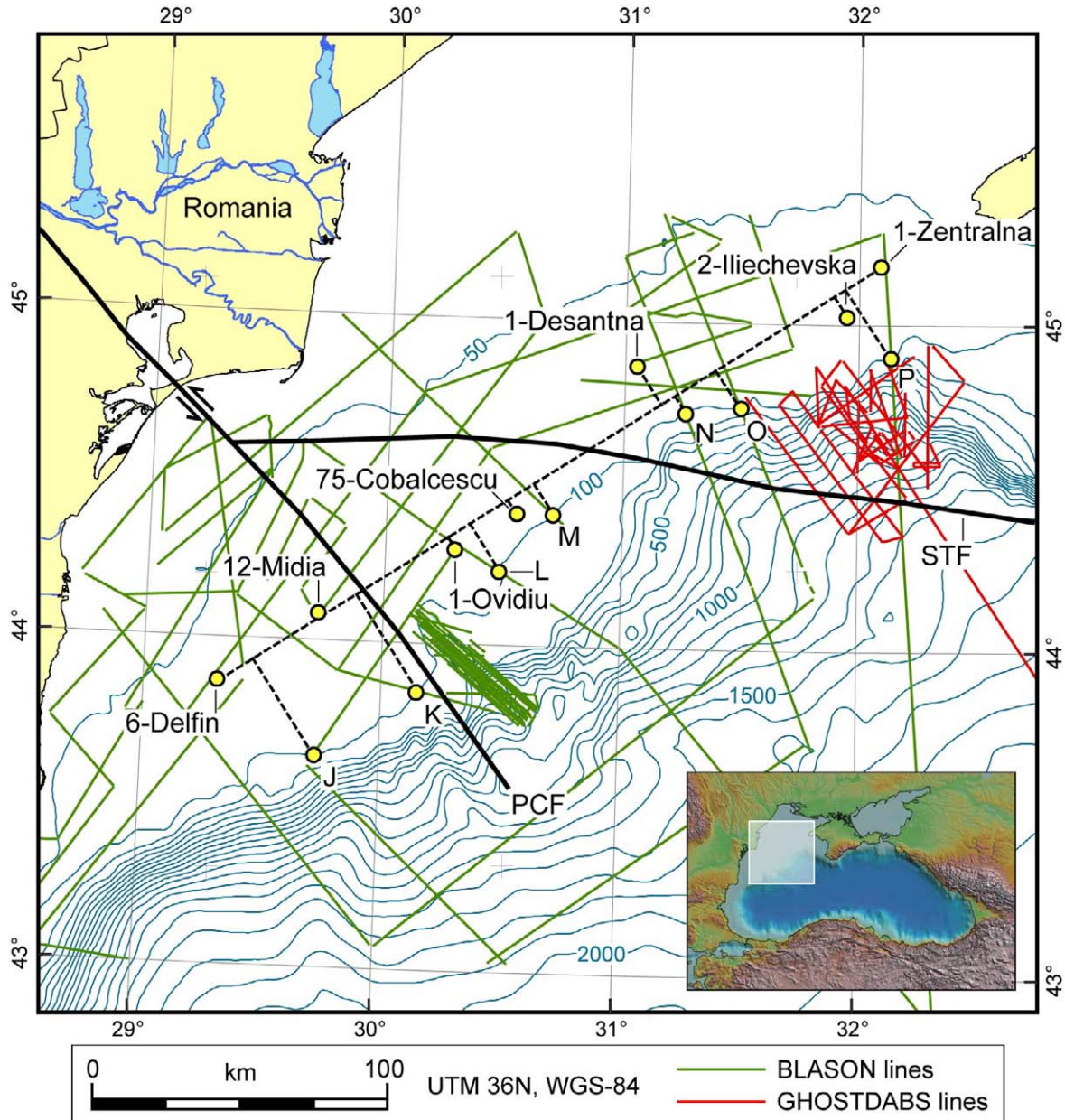
Fig. 6.6: Map showing the position of the subsidence analysis profile 2 in the Romanian and Ukrainian sectors of the northwestern Black Sea (dashed black line). Yellow dots give the measurement locations (J-P) and borehole positions. Bold black lines mark major regional tectonic elements, namely the Peceneaga Camena fault (PCF) and the Sulina Tarkinkut fault (STF). Inset gives the map location.

In the northern part of the study area, data from a number of oil and gas exploration wells provided a detailed lithology long the idealized profile shown in Fig. 6.7. These data in combination with the seismic stratigraphic interpretation already described provide the basis for subsidence analysis along the northwestern profile.
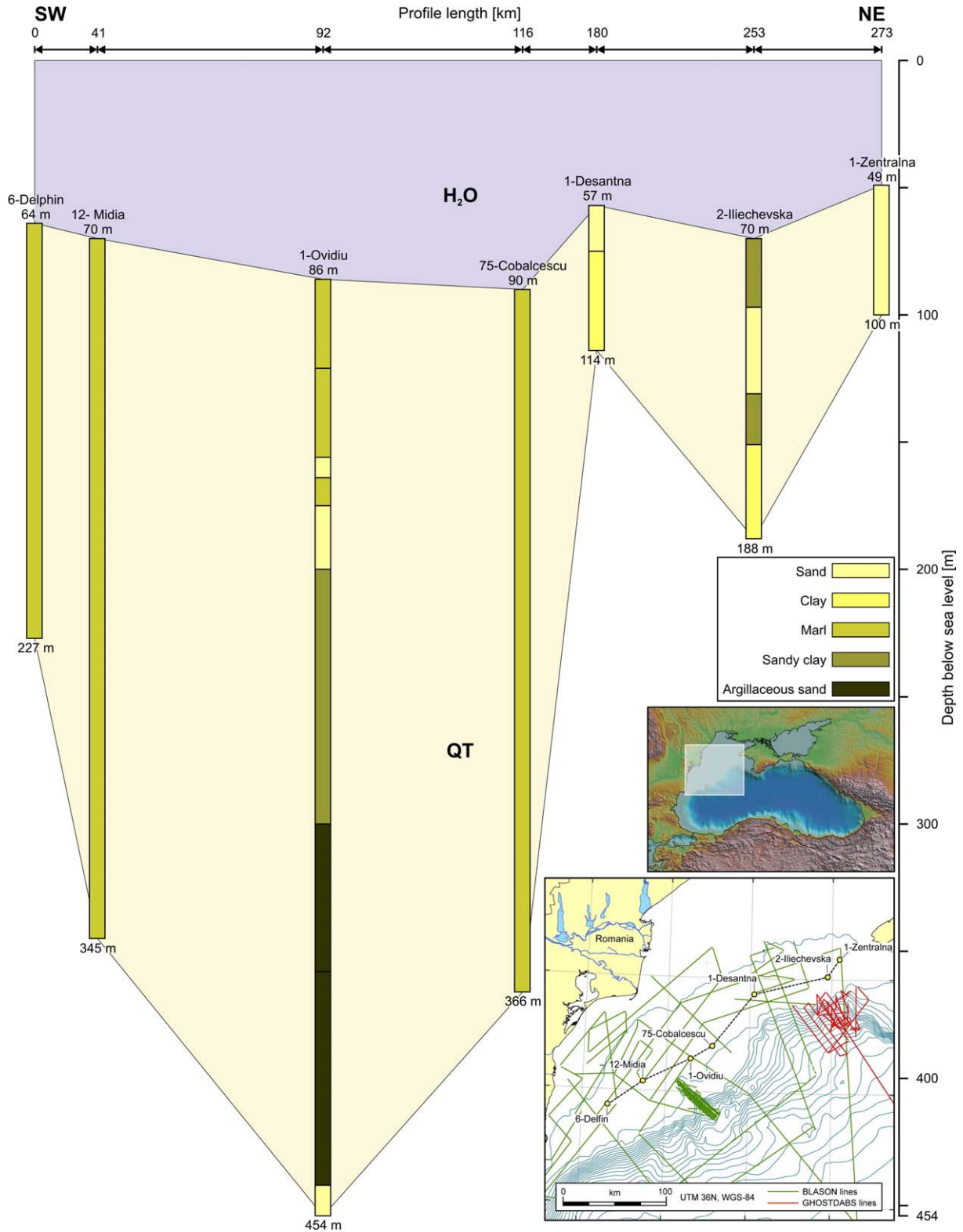
Fig. **6.7**: Lithology of the Quaternary sediments along a profile on the northwestern Black Sea shelf derived from Romanian and Ukrainian borehole data. The dashed line on the map in the lower right (same extent as in Fig. 6.6) gives the profile through the wells *6-Delfin*, *12-Midia*, *1-Ovidiu*, *75-Cobalcescu*, *1-Desantna*, *2-Iliechevska*, and *1-Zentralna* (the first four wells are situated in the Romanian sector, the latter three in the Ukrainian sector).
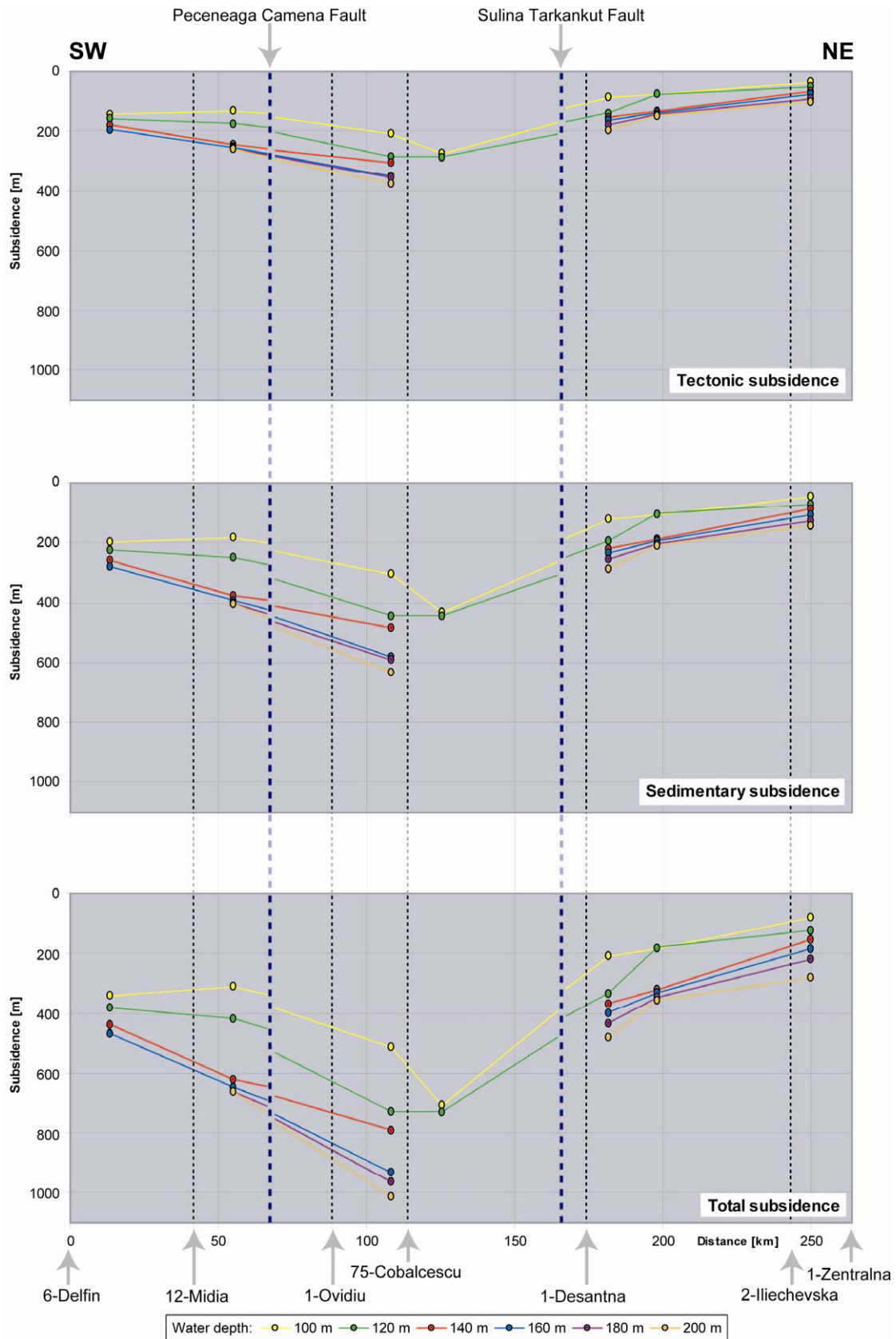
Fig. **6.8**: Three panels showing the amounts of tectonic, sedimentary, and total subsidence along the profile of Fig. 6.6. Each colour gives the measurements at a constant water depth. Grey arrows above the panels give the approximate locations of the major faults; grey arrows below the panels mark the location of boreholes.

A lateral correlation shows clearly how the two major regional fault systems divide the shelf into large isolated blocks that have significantly different Quaternary thicknesses (Figs. 5.21 and 6.6): the Peceneaga Camena Fault system (PCF) extending from the Romanian onshore south of the Danube delta to the southeast in the southern vicinity of the Viteaz Canyon), and the Sulina Tarkinkut Fault system (STF) stretching from the PCF on the inner Romanian shelf to the east.

A: 100 m

Location	Total subsidence [m]	Tectonic subsidence [m]	Sedimentary subsidence [m]
J	341	141	200
K	311	130	181
L	515	207	308
M	710	277	433
N	208	88	120
O	185	78	107
P	80	34	46

| Location	Decompacted total subsidence rate [m/ka]	Decompacted tectonic subsidence rate [m/ka]	Decompacted sedimentary subsidence rate [m/ka]
J	0.19	0.08	0.11
K	0.17	0.07	0.1
L	0.29	0.12	0.17
M	0.39	0.15	0.24
N	0.12	0.05	0.07
O	0.1	0.04	0.07
P	0.04	0.02	0.02

B: 120 m

Location	Total subsidence [m]	Tectonic subsidence [m]	Sedimentary subsidence [m]
J	382	157	225
K	418	171	247
L	729	284	445
M	729	284	445
N	331	137	194
O	179	76	103
P	124	53	71

Location	Decompacted total subsidence rate [m/ka]	Decompacted tectonic subsidence rate [m/ka]	Decompacted sedimentary subsidence rate [m/ka]
J	0.21	0.08	0.13
K	0.23	0.09	0.14
L	0.41	0.16	0.25
M	0.41	0.16	0.25
N	0.18	0.08	0.1
O	0.1	0.04	0.06
P	0.07	0.03	0.04

Tab. 6.6: See next page for caption.

C: 140 m

Location	Total subsidence [m]	Tectonic subsidence [m]	Sedimentary subsidence [m]
J	438	179	259
K	622	246	376
L	789	304	485
M			
N	369	152	217
O	322	134	188
P	153	65	88

Location	Decompacted total subsidence rate [m/ka]	Decompacted tectonic subsidence rate [m/ka]	Decompacted sedimentary subsidence rate [m/ka]
J	0.24	0.1	0.14
K	0.35	0.14	0.21
L	0.44	0.17	0.27
M			
N	0.21	0.08	0.13
O	0.18	0.07	0.11
P	0.09	0.04	0.05

D: 160 m

Location	Total subsidence [m]	Tectonic subsidence [m]	Sedimentary subsidence [m]
J	470	191	279
K	645	254	391
L	934	352	582
M			
N	399	163	236
O	332	137	195
P	184	78	106

Location	Decompacted total subsidence rate [m/ka]	Decompacted tectonic subsidence rate [m/ka]	Decompacted sedimentary subsidence rate [m/ka]
J	0.26	0.11	0.15
K	0.36	0.14	0.22
L	0.52	0.2	0.32
M			
N	0.22	0.09	0.13
O	0.18	0.08	0.1
P	0.1	0.04	0.06

Tab. 6.6 (continued): Summary of results of subsidence analysis along the idealized profile 2 on the Romanian and Ukrainian shelves of the Black Sea between measurement points J (6-Delfin) and P (1-Zentralna). See Fig. 6.6 for profile location. Measurements were made at six different water depths ranging from 100 m (A) to 200 m (F) in 20 m intervals. The upper panel in the panel-pairs A to F gives subsidence values (tectonic, sedimentary, and total) in meters, the lower panel the corresponding subsidence rates in meters per kyr. Missing values are due to the fact that the seismic data quality did not allow the interpretation of the base of the Quaternary at all water depths at a measurement point.

E: 180 m

Location	Total subsidence [m]	Tectonic subsidence [m]	Sedimentary subsidence [m]
J			
K	663	260	403
L	949	357	592
M			
N	432	176	256
O	346	143	203
P	219	92	127

Location	Decompacted total subsidence rate [m/ka]	Decompacted tectonic subsidence rate [m/ka]	Decompacted sedimentary subsidence rate [m/ka]
J			
K	0.37	0.14	0.23
L	0.53	0.2	0.33
M			
N	0.24	0.1	0.14
O	0.19	0.08	0.11
P	0.12	0.05	0.07

F: 200 m

Location	Total subsidence [m]	Tectonic subsidence [m]	Sedimentary subsidence [m]
J			
K	663	260	403
L	1011	377	634
M			
N	479	194	285
O	356	147	209
P	249	104	145

Location	Decompacted total subsidence rate [m/ka]	Decompacted tectonic subsidence rate [m/ka]	Decompacted sedimentary subsidence rate [m/ka]
J			
K	0.37	0.14	0.23
L	0.56	0.21	0.35
M			
N	0.27	0.11	0.16
O	0.2	0.08	0.12
P	0.14	0.06	0.08

Tab. 6.6 (continued): See previous page for caption.

For the subsidence analysis, TWT of the base of the Quaternary were measured at water depths of 100-200 m in steps of 20 m at the locations J-P (Fig. 6.6). These times were then converted to depths using interpolated interval velocities derived from the borehole data. The resulting amounts and rates of Quaternary subsidence are summarized in Tables 6.6 A-F.

The highest subsidence is found in the vicinity of the Viteaz Canyon (VC; Fig. 14) in the tectonic depression between the Peceneaga Camena and Sulina Tarkinkut faults. The southwestern and northeastern segments of the profile (south of the PCF and north of the STF, respectively) show smaller amounts of subsidence generally increasing to the southwest. Figure 6.8 summarizes the derived total, tectonic and sedimentary subsidence for the northwestern Black Sea shelf at the different measurement points along the analysis profile.

This study attests to an underlying trend of increasing subsidence towards the deeper basin. This observation agrees with the model of an Atlantic-type margin subsiding at a constant rate about a fixed hinge line (Pitman, 1978; Watts and Ryan, 1976).

7. Quaternary development of the Black Sea level

7.1 Sea-level reconstruction

In the following, an attempt will be made to reconstruct the sea-level history in the western Black Sea. Firstly, the underlying larger-scale Quaternary climate fluctuations will be described. These fluctuations give rise to glacial and interglacial periods as well as fourth order sea-level cycles. Secondly, sea-level change during the past 25 kyr (the time period since the last glacial maximum) will be analyzed in detail. In particular, fifth and possibly sixth order sea-level fluctuations will be discussed, as the youngest geological history is imaged at a higher resolution in the data available.

7.1.1 Large-scale sea-level fluctuations during the Quaternary

Past sea-levels during the Quaternary in the Black Sea region can be deduced from seismic stratigraphic interpretation (depth levels at which a particular stratigraphic boundary occurs) combined with subsidence analysis results to account for the displacements that the boundary has experienced after its formation.

Reconstruction of sea-level lowstands provides the framework for the following classification of the seismic stratigraphic units mapped in the western Black Sea and their implications to regional sea-level fluctuations. The oldest seismic stratigraphic unit U4 mapped in the study area is dated to Early Quaternary times. It was deposited onto a 'baseline' (in the sense of this study) of Miocene-Pliocene units strongly affected by extensional tectonics and subsidence. It is assumed that during the past 250 kyr regressive phases in the Black Sea correspond to the main glacial periods in Eurasia (Winguth et al., 1997, 2000; Wong, 1994). Consequently, the development of the oldest of the four significant sea-level lowstand indicators, a deltaic complex found in U4 (lowstand indicator ΔD), might be Günz glacial in age. The subsequent lowstand observed in U3 (lowstand indicator C) would then correspond to the Mindel glacial. The deltaic sequence found in unit U2 is assigned to the sea-level lowstand during the Riss glacial. This lowstand may have reached -100 m (Fedorov, 1978) or even around -125 m (this study, see text below). The lowstands of the Riss and Würm glacials are separated by an interglacial with a sea level that exceeded the present-day level by up to 12 m (Chepalyga, 1984; Fedorov, 1978; Shercheglov et al., 1977; Ostrovskiy et al., 1977; Izmaylov, 1977).

125

The depth converted measurements for the sea-level indicators of lowstand D is 174.3 m and of lowstand C is 242.3 m, a difference of 63 m. This apparently deeper position of the younger lowstand C can be attributed to the more proximal position of the deltaic succession that marks lowstand D and the subsequently smaller amount of subsidence that occurred at this position.

Subsidence analysis at location A with a water depth of 100 m yielded 644 m of total subsidence since the beginning of the Quaternary (Tab. 6.2). The subsidence curves of Fig. 6.5 suggest that approximately 550 m remain for the time since the development of lowstand D. A subsidence that decreases linearly landwards is typical of a shelf region that can be described by the fixed hinge line model (Pitman, 1978; Watts and Ryan, 1976). Since the northern part of the western Black Sea subsides linearly (profile 2; section 6.2.2), subsidence at the location of the lowstand D indicator (ΔC; e.g. Fig. 5.3) must be on the order of 25 % of the measured subsidence at 100 m water depth. Given an uncorrected depth for lowstand D of 174 m, the estimated paleo-sea level would be slightly lower than the present-day level (-13 m).

The observed uncorrected depth values for lowstands C and B are 242.3 and 165.8 m respectively, giving an apparent difference of 76.5 m. Subsidence analysis for location A (Tab. 6.2) yielded a total subsidence of 53 m for the 350 kyr (500 - 150 ka) during which unit U3 was deposited. Lowstand B, with an assigned age of 150 ka, lies within U2 just on top of the unconformity that divides the two units. If one assumes that the subsidence history of U3 and the oldest parts of U2 is approximately linear, then the total subsidence in the time interval base of U2 to base of ΔB is by interpolation 75 m. This amount is comparable to the apparent difference of 76.5 m between the lowstands C and B, suggesting that the apparent sea levels at the two lowstands are more-or-less identical, and that the depth difference can be attributed to subsidence in the time interval between the two lowstands alone. However, Aksu et al. (1999) showed that the deltaic system formed during lowstand B originated at about 15 m water depth, whereas the coastal onlap of lowstand C was presumably formed at sea level. Therefore the sea level during lowstand B was probably around 15 m higher than that during lowstand C. Lowstand D needs to be corrected in the same way to +2 m, moving it even closer to the present-day level.

Lowstand A is interpreted to have formed during the Würm glacial around 20 ka. The total subsidence between lowstands B and A is presumably 12 m (difference between 87 and 75 m, see above). This is less than the apparent difference of 21.3 m between the present-

day depths of the lowstand indicators. Thus, sea-level during lowstand A must have been approximately 9 m higher than that during lowstand B.

If the correction of 28 m total subsidence since lowstand A (Tab. 6.1) is subtracted from the uncorrected depth of the lowstand deltaic system ΔA of 144.5 m, then the calculated sea-level at lowstand A (Würm) after subsidence correction is 116 m below present sea level. In turn, the sea levels at lowstands B (Riss) and C (Mindel) must have been -125 and -140 m respectively.

7.1.2. Small-scale sea-level fluctuations during the past 25 ka

The sea-level curve compiled by Chepalyga (1984; red curve in Fig. 7.1) from fossil and microfossil data, strandlines, as well as lithostratigraphic and mineralogical information shows high-order sea-level fluctuations during the Holocene. His smoothed curve (red curve in Fig. 7.1) implies two phases of rapid sea-level rise, each succeeding a significant regression, at about 10.5 and 7.5 ka. The regressions, however, must have been more severe than suggested by Chepalyga (1984): The interpretation of seismic data presented here yielded sea-level lowstands of around -110 and -115 m (Fig. 6.1). These values are closer to those suggested by Ryan et al. (2003; orange curve in Fig. 7.1). In contrast to the results of this study that indicate a relatively slow sea-level rise over a longer period within the Holocene, both curves (red and orange curves in Fig. 7.1) imply that the last transgression led rapidly to sea levels close to the present and remained there with only minor fluctuations over the past 7 to 8 kyr. Other authors presented sea-level curves that feature a slower sea-level rise during the younger Holocene (Konikov et al., 2007, light blue line in Fig. 7.1; Ostrovskiy et al., 1977; green line in Fig. 7.1), but their models do not support strong regressions during the Holocene.

At the last glacial maximum (LGM) around 20 ka, the Black Sea level reached a distinct lowstand. Different values for this lowstand have been reported by various authors: -90 m to -110 m (Fig. 7.1; Chepalyga, 1984), -98 m to -115 m (Popescu et al., 2004), - 100 m to -110 m (Görür et al., 2001; Demirbag et al., 1999), -110 m (Ryan et al., 1997) and -110 m to -130 m (Ostrovskiy et al., 1977). In this study, a sea level of -116 m is calculated from the depth of the topset-to-foreset transition of the delta system ΔA developed during this lowstand (Tab. 6.1).
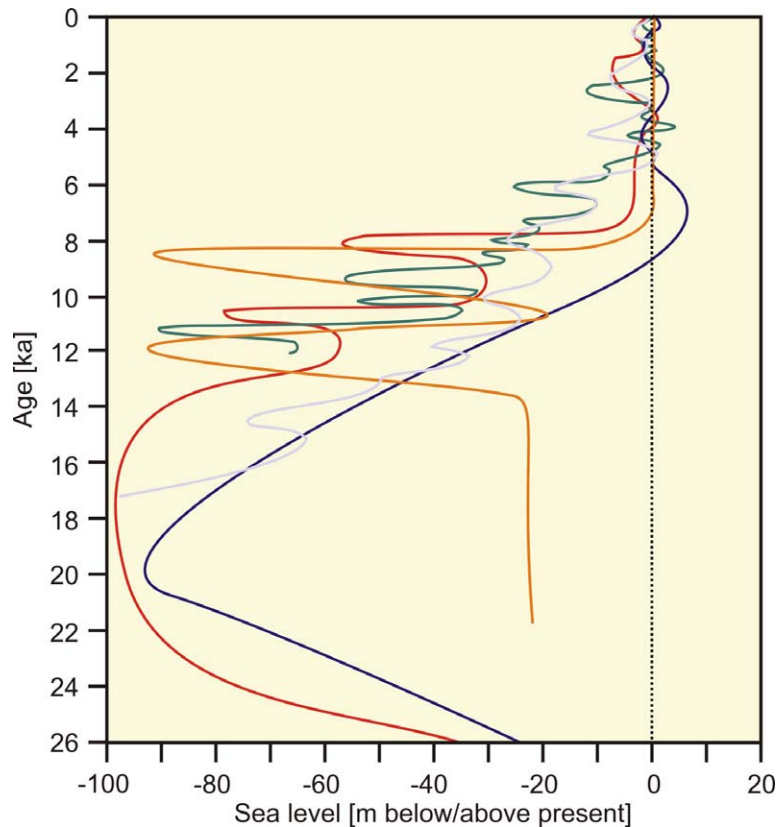
Fig. **7.1**: Different sea-level curves for the Black Sea during the past 26 kyr as presented in the literature. The green and red curves (the former is based on data from Ostrovskiy et al., 1977) are from Chepalyga (1984); the blue curve is from Wong et al. (1994), the orange curve from Ryan et al. (2003), and the light blue curve from Konikov et al. (2007).

The late glacial and Holocene times after the LGM are characterized by an overall global warming interspersed with several cooling phases (Tab. 7.1; Klimanov, 1997). The response of the level of the Black Sea in to this climatic trend is generally an increase.

Details of the sea-level rise in the Black Sea since the last glacial maximum are still under debate. Some authors suggest that the Black Sea was a giant freshwater lake during the last glacial maximum with a water level close to the low values (around -150 m) quoted above. It remained low until the dramatic rise ('catastrophic flooding') occurred when the global sea level reached the Bosphorus sill at around 8.4 ka (Ryan et al., 2003, 1997a, b; Ballard et al., 2000). Others argue that it was in fact the Black Sea that overflowed the Strait of Bosphorus and expelled freshwater into the Marmara Sea during the Early Holocene (Görür et al., 2001; Aksu et al., 1999).

The initial post-LGM sea-level rise was a response to retreat of the Fennoscandian and Alpine ice shields, which reached a maximum between 15 and 14 ka. During this time, melt-

water increased river discharge into the Black Sea by a factor of 2 (Tab. 7.1; Sidorchuk et al., 2002), driving its sea level towards the depth of the Bosphorus sill. Knowledge on this depth is important, since it limits the Black Sea level as long as the global sea level is lower.

The deposition of subunit U1-B, interpreted to have formed during a temporary stillstand in the course of the post-glacial sea-level rise, is restricted on the interpreted profiles to an area with an uncorrected depth below 100 ms TWT which corresponds to approximately -75 m. This implies that the Bosphorus sill was not deeper than -75 m at the time of the deposition of subunit U1-B, probably even shallower since morphologically higher parts of U1-B might have been eroded. It is likely that the deposition of U1-B is related to the possible meltwater pulses between 18 and 15.5 ka reported by Bahr et al. (2005).

Age [ka]	Subdivision	Temperature	Precipitation	Evaporation	Salinity	Reference	Sea Level [m]	Seismic unit
6-0	Mid-Holocene	+	+	+	+	Tarasov et al., 1999		U1-C (7-0 ka)
10.3-8	Preboreal	++	–			Velichko et al., 2002	below -90	
10.7-10.3	Younger Dryas	––	––	––	––	Klimanov, 1997 Velichko et al., 2002		
12-10.7	Allerød	+	+	0	–	Klimanov, 1997 Velichko et al., 2002	above -85	U1-B (18-10.7 ka)
12.5-12	Bølling	0	–	––	–	Sidorchuk et al., 2002		
18-15.5	Fresh water pulses	+	–	–	––	Bahr et al., 2005		
28.5-18	Last glaciation	––	––	––	–	Tarasov et al., 1998	-116	U1-A (29-18 ka)
40-25	Surozhskian				++	Fedorov, 1978 Ostrovskiy et al., 1977	12	

Tab. **7.1** Summary of the climatic evolution of the Black Sea area during the past 25 kyr compiled from the literature. The sea-level values and assigned seismic stratigraphic units are from this study. The temperature, precipitation, evaporation and salinity are given qualitatively from very high to very low (++, +, 0, –, ––).

The global ocean is thought be connected to the Marmara Sea through the Dardanelles since 12 ka (Cagatay et al., 2000). When the subsequent re-connection to the Black Sea occurred depends on the depth of the Bosphorus sill. Major et al. (2006, 2002) presented models with either a deep (-80 m, equivalent to the depth of the Dardanelles) or a shallow sill level of less than -35 m (Major et al., 2002), or around -30 m (Major et al., 2006). In the deep sill scenario, the Black Sea level would follow the global sea level starting at about 12 ka, whereas the shallow sill models would predict a re-connection between the Black and Marmara seas around 8.4 ka (Major et al., 2002), or around 9.4 ka (Major et al., 2006). The

idea of a shallow sill is favored here, as the implied timing matches proposed dates for the appearance of brackish-marine mollusk species (Ryan et al., 1997; Sherbakov & Babak, 1979; Popov, 1973) and dinoflagellates (Wall & Dale, 1974), as well as to oxygen isotope measurements (Major et al., 2002; Deuser, 1972).

Behind a shallow sill, the Black Sea could operate independently of the global oceans, responding only to changes in water balance in its drainage basin. This balance may have become negative as a result of increased evaporation in warmer climates and meltwater input via rivers after 14 ka, in particular around 12 ka and 9.5 ka (uncorrected radiocarbon years; Major et al., 2003). In contrast, evaporation during the Younger Dryas cold stage was low; freshwater discharged from the Black Sea into the Marmara Sea (Major et al., 2003), probably initiating sapropel sedimentation and the formation of deltas (Ryan et al., 2003).

For the isolated Caspian Sea, warm phases with high evaporation coincide with low sea levels and cold phases correlate with high sea levels (Svitoch, 1999; Chepalyga, 1984). The Black Sea must have behaved analogously during the Late Pleistocene-to-Holocene transition, so that after the late glacial transgression, the level of the Black Sea lowered as the water balance in its drainage basin experienced a negative shift. During the subsequent Younger Dryas cold period, the water level rose above the Bosphorus sill, only to retreat under the warmer climate of the Early Holocene.

Deposition of subunit U1-B stopped after the sea level had fallen sufficiently (below -90 m), presumably during phases of warmer climate (Ryan et al., 2003). U1-B was subsequently partially eroded, so that only small in-fill remnants exist today. The relatively short Younger Dryas probably left little record in the seismic sequences.

The post-glacial sea-level fall reached a minimum that allowed the formation of the coastal sedimentary features found today on the outer shelf at a depth of around 90 m. Cardiid shells retrieved from a depth of 55 m have been AMS radiocarbon dated to this interval (Lericolais et al., 2002). These shells are indicators for saline ponds, strongly suggesting that the shelf was subaerially exposed.

The Black Sea was reconnected to the global ocean after its level reached the Bosphorus sill and marine water entered the Black Sea at a time between 9.4 ka (Major et al., 2006), 8.4 ka (Sherbakov & Babak, 1979), or up to 7.6 ka (Ryan et al., 1997). Even if the 'catastrophic' character of this event cannot be demonstrated, it must have been rapid

enough to preserve the coastal features developed during the preceding lowstand. The sediments deposited from the onset of this rapid transgression to the present-day are assigned to subunit U1-C which shows a retrogradational stacking pattern. This retrogradation indicates that sedimentation occurred during the transgression as well as during the highstand that still persists, probably reflecting the complex pattern of five distinct regressive phases proposed by Konikov et al. (2007; light blue curve in Fig. 7.1). If the scenario is correct, then the rapid transgression could not have reached the present sea level, in contrast to the suggestion of Ryan et al. (2003; orange curve in Fig. 7.1), but must have been falling over a significant period, allowing subunit U1-C to form.

These results suggest that the development of the Black Sea level during the past 25 kyr is in general compatible with the models of Chepalyga (1984) and Ryan et al. (2003; Fig. 7.1) as well as the shallow-sill model of Major et al. (2002, 2006), but are insufficient to resolve the question of catastrophic or gradual rise after in the Holocene.

8. Conclusions and recommendations for future research

8.1 Conclusions

Interpretation of high and very high resolution seismic reflection data yielded a seismic stratigraphic model for the southwestern Black Sea shelf with four Quarternary units (U4 to U1 in chronological order). The Mio-Pliocene section is taken to be the 'baseline' for the Quaternary subsidence analysis. On the inner shelf of the southwestern Black Sea, the development of normal faults suggests an extensional tectonic regime at this time. These fault systems stayed active at least until the Upper Pliocene. Figure 8.1 shows a schematic model of the Miocene to Pliocene deposition on the western Black Sea shelf: Gradually increasing subsidence towards the outer shelf led to a basinward increase in thickness of the Pliocene and extensional faulting on the inner shelf.
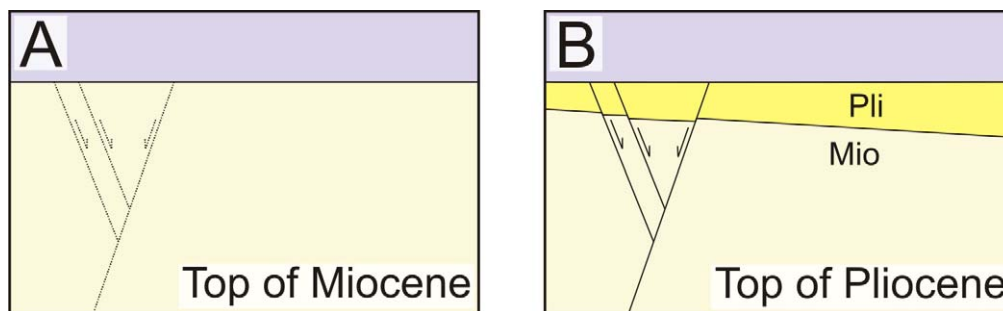
Fig. 8.1: Schematic development of the Miocene and Pliocene on the western Black Sea shelf. The inner shelf underwent extensional faulting during the Miocene (panel A) that stayed active at least until the Upper Pliocene. Subsidence of the top of Miocene increased gradually towards the outer shelf (panel B). Abbreviations: Mio – Miocene; Pli – Pliocene.

During the Quaternary, the seismic stratigraphic model proposed is controlled by the most distinct climatic events of this period, namely the four major glaciations Günz, Mindel, Riss, and Würm. They led to sea-level lowstands and in turn to the formation of erosional unconformities as well as the subsequent transitions from one seismic stratigraphic unit to the one overlying it.

The oldest seismic sequence mapped (U4) is of Early Quaternary age and comprises a succession of gently basinward-dipping strata. These were deposited above an unconformity separating the Pliocene from the Quaternary. A deltaic complex (ΔD) developed on the present-day inner shelf in this unit, probably during an early phase of low sea level during

the Quaternary, presumably the Günz glacial at approximately 1 ma. Figure 8.2 shows the reconstruction of the western Black Sea shelf before and after the deposition of U4.
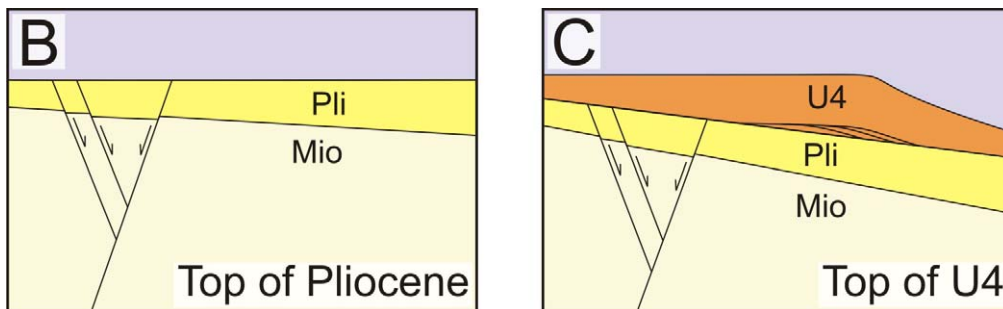

Fig. 8.2: Reconstruction of the western Black Sea shelf before (panel B) and after the deposition of the oldest Quaternary seismic stratigraphic unit mapped (U4; panel C). Within U4, a shelfedge delta system developed during the sea-level lowstand of the first major glaciation in the Quaternary (Günz glacial). Abbreviations: Mio – Miocene; Plio – Pliocene; U4 – Unit 4.

A second well-developed angular unconformity marks the transition from U4 to the succeeding unit U3. Unlike U4, a shelfedge delta system is absent in U3. However, interpreted coastal onlaps in its lower section could be assigned to the sea-level lowstand of the second major Quaternary galciation, the Mindel glacial (approximately 500 ka). The upper part of U3 attests to significant aggradation on the shelf; it was deposited during the subsequent sea-level rise and highstand (Fig. 8.3).
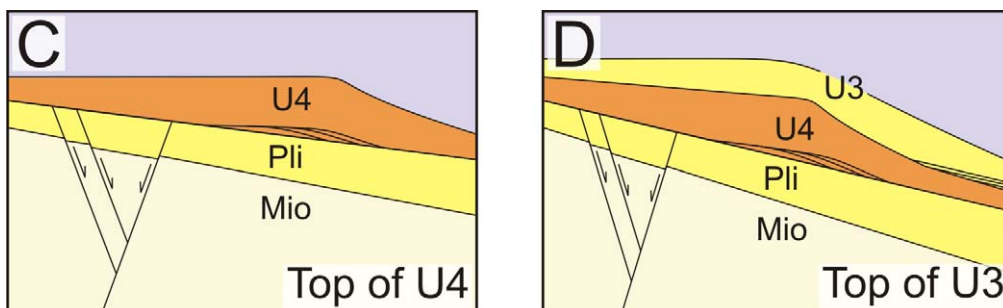
Fig. 8.3: Reconstruction of the western Black Sea shelf before (panel C) and after the deposition of seismic stratigraphic unit U3 (panel D). Although a shelfedge delta system is absent in U3, coastal onlaps mark a sea-level lowstand during its deposition. Abbreviations: Mio – Miocene; Plio – Pliocene; U4 – Unit 4; U3 – Unit 3.

Deposition of U3 was concluded when the sea-level rise came to an end and a subsequent falling sea level led to the development of an unconformity separating U3 from Unit 2 (U2). Analogous to U4, the lower part of U2 comprises a shelfedge delta system deposited during the sea-level lowstand presumably of the Riss Glacial at around 150 ka.

Aggradation on the inner and middle shelves during the deposition of U2 was less than in the case of U3. Instead, buildup of the shelfedge delta system and subsequent sedimentation on the outer shelf led to significant progradation and a basinward shift of the shelfedge (Fig. 8.4).
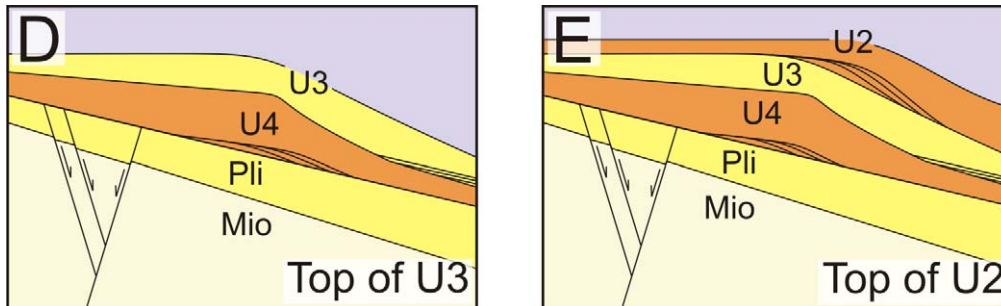
Fig. **8.4**: Reconstruction of the western Black Sea shelf before (panel D) and after the deposition of seismic stratigraphic unit U2 (panel E). The internal configuration and external geometry of U2 resemble that of the Early Quaternary U4 with a shelfedge delta system developed during a sea-level lowstand at the base of the unit. Abbreviations: Mio – Miocene; Plio – Pliocene; U4 – Unit 4; U3 – Unit 3; U2 – Unit 2.

The youngest seismic stratigraphic unit U1 was subdivided into three subunits (U1-A to U1-C in chronological order) using very-high resolution Boomer profiles (Fig. 8.5).
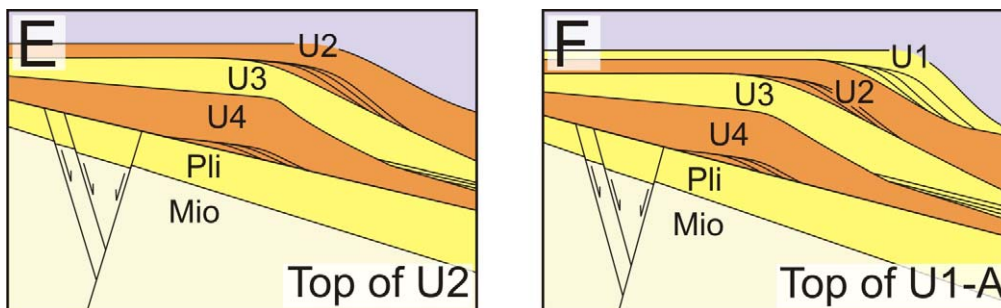

Fig. **8.5**: Reconstruction of the western Black Sea shelf before (panel E) and after the deposition of seismic stratigraphic unit U1 (panel F). The depositional environment of units U2 and U1 appears to be largely comparable. U1 also comprises a shelfedge delta system at its base and is characterized by relatively minor aggradiation but rather very significant progradation of the shelfedge. U1 is subdivided into small-scale seismic statigraphic subunits developed since the last glacial maximum, these are shown in detail in Fig. 8.6. Abbreviations: Mio – Miocene; Plio – Pliocene; U4 – Unit 4; U3 – Unit 3; U2 – Unit 2; U1 – Unit1.

Subunit U1-A consists of a prograding shelfedge delta system partially overlain by shore-parallel dunes (Fig. 8.6). The younger subunits U1-B (Fig. 8.7) and U1-C (Fig. 8.8) were deposited during the postglacial sea-level rise and the Recent highstand. Sediments of

subunit U1-B fill the small topographic lows on the rugged erosional top surface of the units U3 and U2, whereas U1-C forms a landward-thickening package of retrogradational wedges that cover large areas of the present-day shelf. Occasionally, dune-like features that resemble in shape and size the dunes already described are observed in subunit U1-C. We speculate that these features mark two phases of sea-level lowstand: the first during and shortly after the last glacial maximum, and the second during the post-Early Holocene after the sedimentation of subunit U1-B.
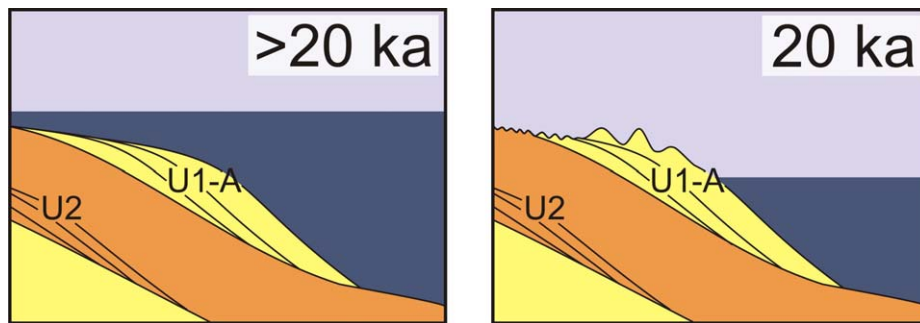
**Fig. 8.6**: Model for the development of the oldest subunit U1-A of unit U1 and the corresponding sea-level at the time of each snapshot. The left panel shows the western Black Sea shelf at a time close to the last glacial maximum, when the shelfedge delta system ΔA formed (>20 ka; see e.g. Fig. 5.3). The development of coastal dunes within U1-A suggests subaerial exposure of the outer shelf at times of an even lower sea level, most likely during the last glacial maximum itself (right panel; 20 ka).

Overall, the seismic stratigraphic model described above is in agreement with the model of Aksu et al. (2002; Tab. 5.1). Both models comprise four characteristic phases of sedimentation during sea-level lowstands in the Quaternary. These phases are marked by buried deltaic complexes deposited in the vicinity of the paleo-shelfedge (Δ4 to Δ1 of unit A in Aksu et al., 2002, corresponding to units U4 to U1A in this study). A sea-level lowstands might be marked by coastal onlaps when a shelfedge delta system is absent. The two models differ in the interpretation of the youngest seismic stratigraphic units subsequent to the development of the youngest deltaic complex: the three units B, C, and D of Aksu et al. (2002) correspond to the two units U1-B and U1-C of this study.

Lowstand seismic indicators such as topset-to-foreset transitions of shelfedge deltas or coastal onlaps in the seismic units mapped were interpreted to reconstruct uppermost Quaternary sea-level fluctuations in the Black Sea. The seismic data show that temporally- and spatially-varying tectonic activities affected the Black Sea shelf. Therefore, to deduce past sea levels from these lowstand indicators, the influence of tectonic and sedimentary subsidence must be taken into account.

To quantify the tectonic subsidence and to assess its regional trend, a subsidence analysis was carried out along an idealized profile (Sclater & Christie, 1980; Bond & Kominz, 1984; and Bond et al., 1989). The results of this study show that tectonic subsidence in the Bulgarian sector was more-or-less constant during the Quaternary, increasing generally from NNE to SSW. More intense tectonic activities characterize the shelf off central Bulgaria during the deposition of unit U1.
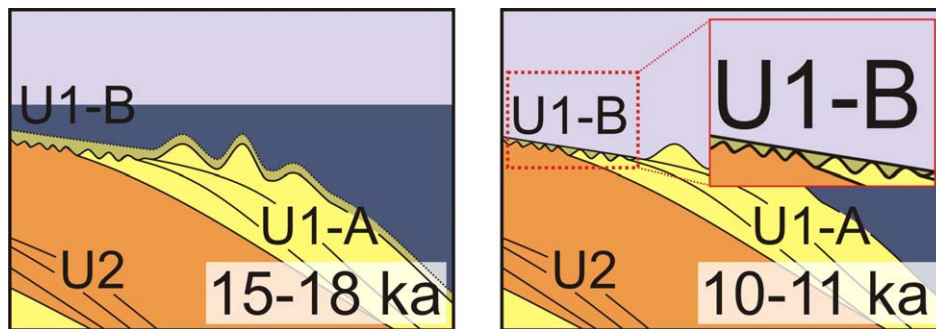

Fig. **8.7**: Model for the development of subunit B of U1 and the corresponding sea level. The left panel (15-18 ka) shows the western Black Sea shelf at a time when meltwater pulses from the retreating European and Asian ice shields lead to a sea-level highstand in the Black Sea and the deposition of U1-B. Most of this unit was later eroded when the sea level fell to a lower level (right panel; 10-11 ka), so that only small remnants of U1-B exist today.

The reconstruction of sea-level lowstands suggests that the oldest seismic stratigraphic unit U3 is of Late Pliocene to Quaternary age. The regressive phases in the Black Sea correspond to the main glacial periods in Eurasia (Wong, 1994; Winguth et al., 1997, 2000). The deltaic sequence found in unit U2 was formed during the Riss glacial sea-level lowstand of -125 m. A second lowstand at -116 m was reached around the LGM at 20 ka. It led to the deposition of the prograding delta in subunit U1-A (Fig. 8.6). During the subsequent global warming in late glacial and Holocene times, the Black Sea level rose in response to the climatic trend. Interruptions by several cooling phases (Klimanov, 1997) slowed down or even inverted the sea-level rise temporally.

Subunit U1-B (Fig. 8.7) is interpreted to have formed during a minor phase of sea-level stillstand and is found at water depths greater than 85 m. Its deposition was possibly related to meltwater pulses between 18 and 15.5 ka (Bahr et al., 2005) and stopped after the sea level had fallen to below -90 m. During this post-glacial lowstand, coastal sedimentary features formed on the outer shelf and saline ponds existed on the subaerially exposed inner shelf (Lericolais et al., 2005). The rising global sea level reached the Bosphorus sill around

8.4 ka and marine water entered the Black Sea (Sherbakov & Babak, 1979). The subsequent transgression must have been rapid enough to preserve the coastal features developed during the preceding lowstand but not necessarily 'catastrophic' in the sense of Ryan et al. (1997, 2003).

The retrogradationally-stacked packages of the youngest subunit U1-C formed during the Holocene transgression (Fig. 8.8). This geometry and the observation of coastal dunes within this subunit indicate at least slower phases of sea-level rise on the way to the present-day conditions.
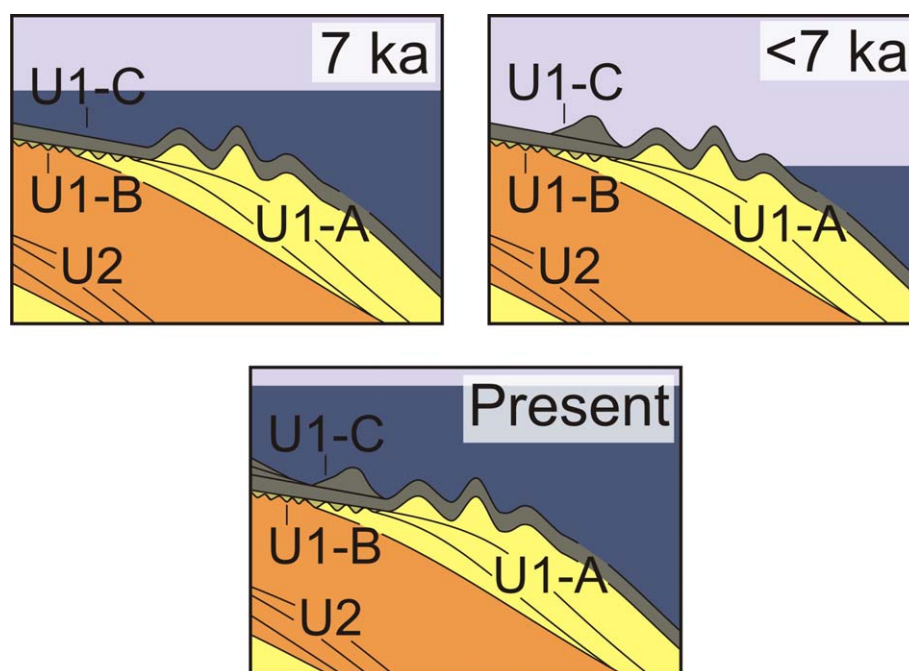
Fig. **8.8**: Qualitative reconstruction of the development of the youngest U1 subunit U1-C to the present-day, along with the corresponding sea-level. The deposition of U1-C started during the Early Holocene transgression (left panel; 7 ka). This transgression, however, must have been interrupted (and possibly temporarily inverted) as coastal dunes within U1-C suggest (middle panel; <7 ka), The sea level continued to rise towards the present-day level (right panel) and retrogradationally-stacked deposits formed on the western Black Sea shelf.

8.2 Recommendations for future research

This seismic stratigraphic study shows the importance of a careful match between the scientific questions to be addressed in a project and the types of data necessary to answer those questions. For the reconstruction of the youngest sea-level history in the Black Sea, the nature and quality of the data required are:

- The seismic profiles should cross the entire width of the shelf at least to a position beyond the present-day shelfedge.

- The resolution of the seismic data should be high enough to resolve high-order unconformities and internal configurations of the subunits bounded by them .

- The seismic data should also permit a reconstructf the relationship between the youngest sedimentary history and a deeper 'baseline' (in this study the base of the Quaternary), so that a subsidence analysis can be carried out to quantify the influence of tectonic movements and subsidence on sea-level change.

- The relative sea-level history derived from seismic stratigraphic interpretation needs to be calibrated against geological time and absolute depth. The necessary information on the position and age of certain intervals in the sedimentary column must be extracted from borehole data.

- Resolution issues similar to those for seismic data also apply to borehole information, for the entire stratigraphic column of interest and at the same time have a particularly high resolution for the analysis of the youngest geological history.

The seismic data available to the ASSEMBLAGE project consist mainly of profiles acquired during the projects BLASON1 and BLASON2, GHOSTDABS in combination with industrial seismic data, and at a time too late for this dissertation, data from the ASSEMBLAGE II and HyBlack-3D cruises (see section 4.1.1). The seismic data available to this dissertation cover almost the entire shelf area of the western and northwestern Black Sea and are oftentimes even available in different versions acquired with several types of equipment. The profile density is high enough for recommendations on promising areas for future data acquisition as well as on the preferred choice of acquisition tools. The comparison of these tools below shows that the impact of a wrong choice can be severe.

The biggest challenge for scientific seismic profiling in the western Black Sea is to avoid zones that are affected by the abundant occurrence of shallow free gas and thus show a strong, sometimes severe, attenuation of the seismic signal with depth (seismic blanking; see section 5.2.1). Generally free gas is seldom on the southwestern shelf off northern Turkey and southern Bulgaria, so that this area should be among the preferred geographical targets for future studies.
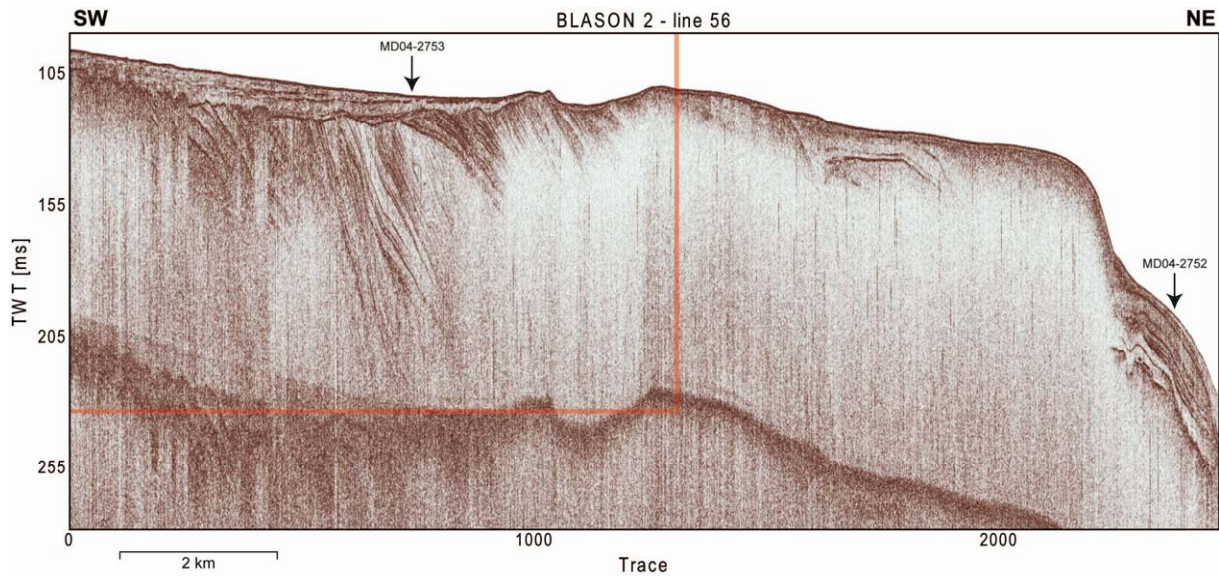
Fig. **8.9**: Chirp sonar profile acquired during the BLASON 2 cruise (profile 56) representing a basinward extension of the data shown in Fig 5.8. Even though lower-resolution air gun/streamer profiling suggests good resolution and good penetration at this location (Figs. 5.3 and 5.16), the Chirp system was not able to generate interpretable images in the vicinity of the shelfedge. The red box shows the approximate position of overlap with the data shown in Fig. 5.8. The black arrows give the locations for the sediment cores shown in Fig. 8.12 (MD04-2752) and Fig. 8.11 (MD04-2753).

Figures 5.3, 5.4, and 8.9 show an example of profiles acquired almost at the same location on the southwestern Black Sea shelf, but with three different seismic tools: A mini-GI air gun/streamer combination, a sparker source/streamer combination, and a hull-mounted Chirp sonar profiling system. When these three profiles are compared with one another, the importance of the availability of data with a range of resolution and penetration characteristics becomes obvious. Even though only a relatively low resolution is achieved with the mini-GI air gun source (Fig. 5.3), it still is a good choice to obtain images of the entire stratigrahic column to a chosen 'baseline' reflection that is not too deep (such as for instance the base of the Quaternary here). Larger air gun sources would likely be able to produce images to an even deeper level, but at the cost of a lower resolution.

The most subtle features can be extracted from Chirp sonar data (e.g., Figs. 5.8, 5.18 and 8.9). There are, however, areas where the sedimentary composition of the shallow deposits and/or gas occurrences makes Chirp sonar data not very useful although air gun/streamer profiles suggest a viable data quality. The example in Fig. 8.9 for instance shows that Chirp data acquisition could not generate useful images for the area in the vicinity of the shelfbreak where lower-resolving mini-GI air guns produced good results (Figs. 5.3 and 5.16). This fact is of particular importance as the internal reflection configuration

close to the shelfbreak is highly significant for sea-level research. Data acquired using a medium-resolution source such as a sparker or water gun system might be a good compromise: The examples shown here (e.g., Fig. 5.4) suggest that these data are much less affected by the factors hampering the very-high resolution Chirp sonar, and at the same time are enough to resolve small-scale structures needed for an interpretation of high-order cycles in seismic stratigraphy.

If the streamer and seismic recording system deployed are versatile enough to meet the requirements of both a mini-GI gun and a sparker source, it would be also possible to use both sources at the same time in parallel with only a minimum of additional effort. The Hydroscience Technologies SeaMUX streamer and NTRS recording system available at the IfBM, University of Hamburg, was constructed specially to operate simultaneously with a broad range of seismic sources. It constitutes a very good base tool for multiple streamer-based acquisition systems.

A major contribution to almost every research project is previously acquired data in the possession of the different project partners. At the project planning stage, an assessment of datasets that are desirable for the project should be made.and incentives for the participating institutions to contribute these data to the project database should be devised. Figure 8.10 shows exemplarily a basemap of the various very-high resolution seismic surveys carried out in the Bulgarian sector of the Black Sea acquired under the supervision of the Institute of Oceanology of the Bulgarian Academy of Sciences (IO-BAS; EUROSEISMIC database, survey maps and descriptions available at: http://www.eu-seased.net/welcome_flash.html). Only a very small selection of these data were available for the preparation of this study (see section 4.1.1), but they have nevertheless proven to be of great value.

An extensive use of pre-existing data in any future attempt to further clarify the youngest seismic and sequence stratigraphy in the western Black Sea is recommended. One might even consider to purchase selected datasets (the data shown in Fig. 8.10, for example, are commercially available). The necessary investment would most likely be much smaller than that needed to organize a new cruise to acquire similar data, although any new data would almost certainly have a superior quality. In addition, an analysis of pre-existing would greatly reduce the risk of acquiring new data 'at the wrong place'.
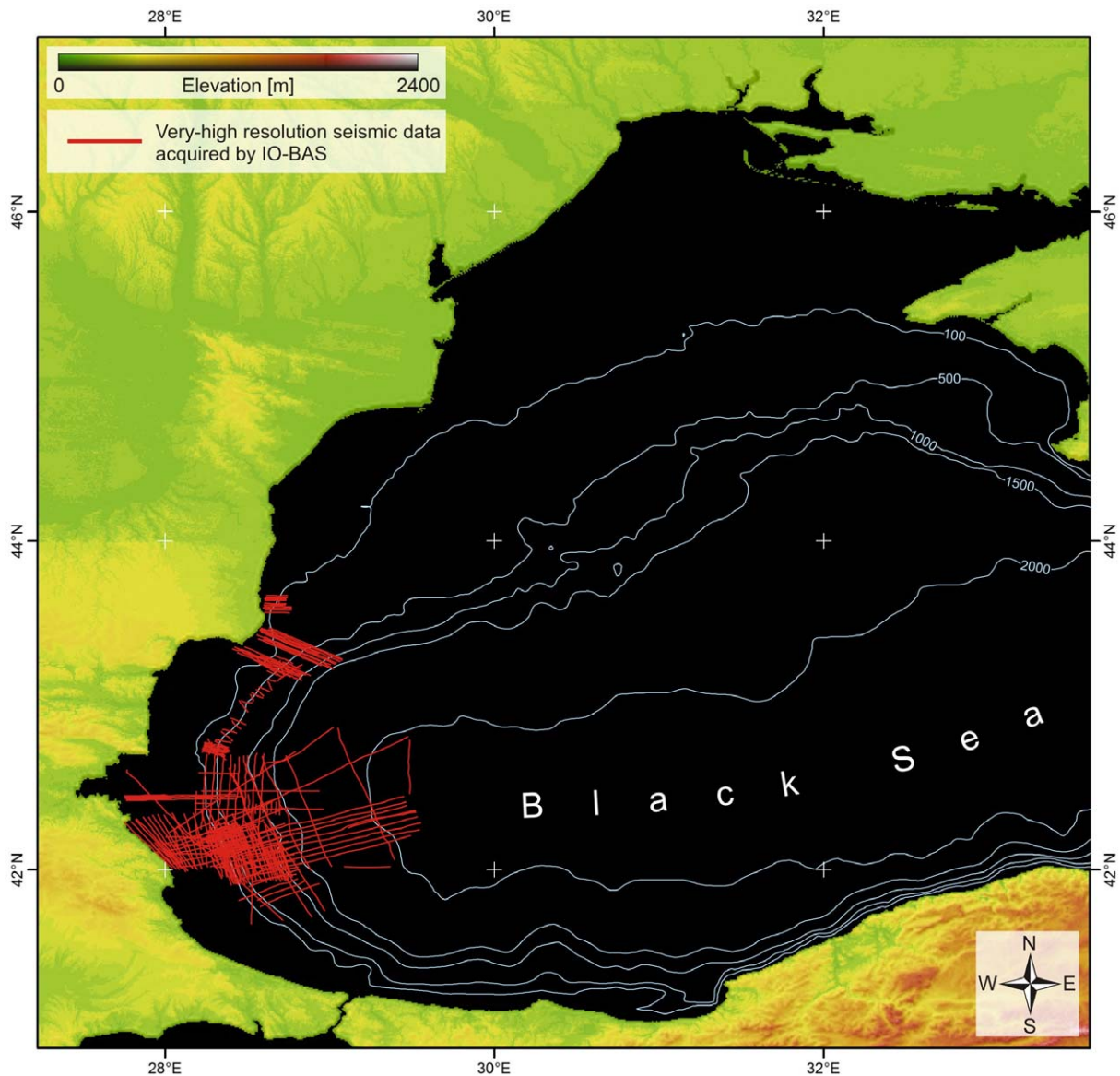
Fig. 8.10: Basemap of very-high resolution seismic surveys acquired by the Institute of Oceanology of the Bulgarian Academy of Sciences (IO-BAS) since the late 1980ies. The survey meta-data are available through the EU-SEASED project (http://www.eu-seased.net). The dense network of profiles in the southernmost Bulgarian Black Sea sector makes these data particularly interesting for future attempts to clarify the sea-level history of the Black Sea, as this area has proven to be one of the most promising targets for seismic stratigraphic research in the western Black Sea.

The incorporation of borehole information is necessary to calibrate the the seismic stratigraphic interpretation. As industrial exploration drilling and scientific drilling of a similar scale (such as ODP and IODP) are beyond the budget of projects like ASSEMBLAGE, sediment coring will always be the main source of directly measured subsurface data. Also, large-scale exploration drilling normally ignores the youngest/ shallowest parts of the stratigraphic column drilled as the exploration targets lie much deeper. Cores retrieved using

the dedicated French research vessel 'Le Marion Dufresne' in the ASSEMBLAGE project (see section 4.1.2) illustrate the capabilities available in the meantime using research equipment.
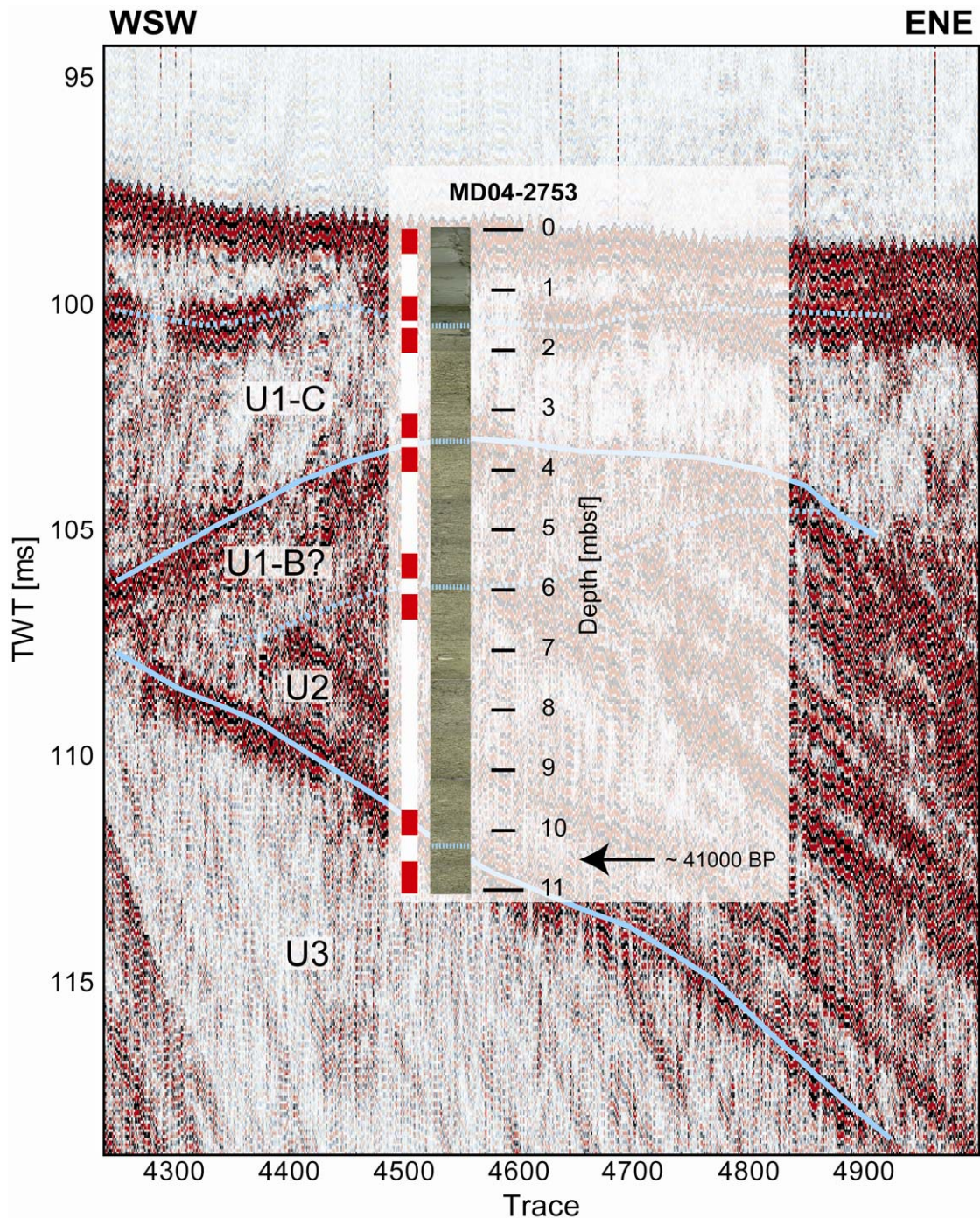
Fig. 8.11: Correlation of sediment core MD03-2753 with seismic profile BLASON2-56 (Fig. 8.9) which goes over the core location. This core is potentially very useful in any sequence stratigraphic reconstruction, as it penetrates several proposed seismic stratigraphic units. Red intervals on the left of the core image give intervals in which age estimations would be desirable; black arrow shows the location where the core has actually been dated and the AMS C^{14} age.

Any new research project aiming at seismic and sequence stratigraphy should include a dedicated cruise leg to collect sediment cores following the acquisition of seismic data. Coring stations should be selected only after a preliminary seismic stratigraphic framework is established, so that as many seismic stratigraphic units as possible can be sampled.

To calibrate the seismic stratigraphic framework developed from an interpretation of seismic reflection data, core samples from the different interpreted seismic stratigraphic units should be dated. These samples should be chosen at locations so as to minimize the uncertainties introduced by the uncertain phases of non-deposition and erosion for which a sedimentary record is missing.

Figures 8.11 and 8.12 show two examples of sediment cores recovered during the ASSEMBLAGE 1 cruise at locations chosen using seismic profiles of the BLASON 2 cruise. Core intervals were proposed for dating these cores and these samples were actually dated. This shows clearly the potential that is looming in pre-existing data, because for the first time, age dates become available directly above and below the interpreted unconformities of our model. In future projects aiming at recent sea-level reconstructions, the budget allocated to age determination of sediment samples should be large enough to permit sample dating at all critical core levels.

To summarize, we recommend the following for any future reconstructions of the Quaternary (in particular Holocene) sea-level history in the Black Sea:

- It should target particularly the southwestern shelf on either side of the offshore boundary between Turkey and Bulgaria. In this area, coarse sediments and free gas that deteriorate the data quality occur the least often.

- Close cooperation with local institutions is essential to provide possible access to to the enormous archives of previously acquired data. Even if such archives could not be made available to the project, they would be invaluable during the planning stage for target selection.

- Acquisition of new reflection seismic data should be carried out using a multiple source approach to cover as broad a range of resolution and penetration as possible. At the cost of transport and deployment of additional equipment, this would help to minimize the chance of acquire data that cannot be usefully interpreted, because

features are either not resolved or beyond the resolution limits of the acquisition tools. The choice of seismic sources depends on the target intervals (in terms of geological time): If the youngest (e.g., Holocene) history is of interest, the highest possible resolution would be desirable, and lower-resolution systems would be deployed with a lower priority. Older and with it deeper targets would imply a reversal in these priorities.
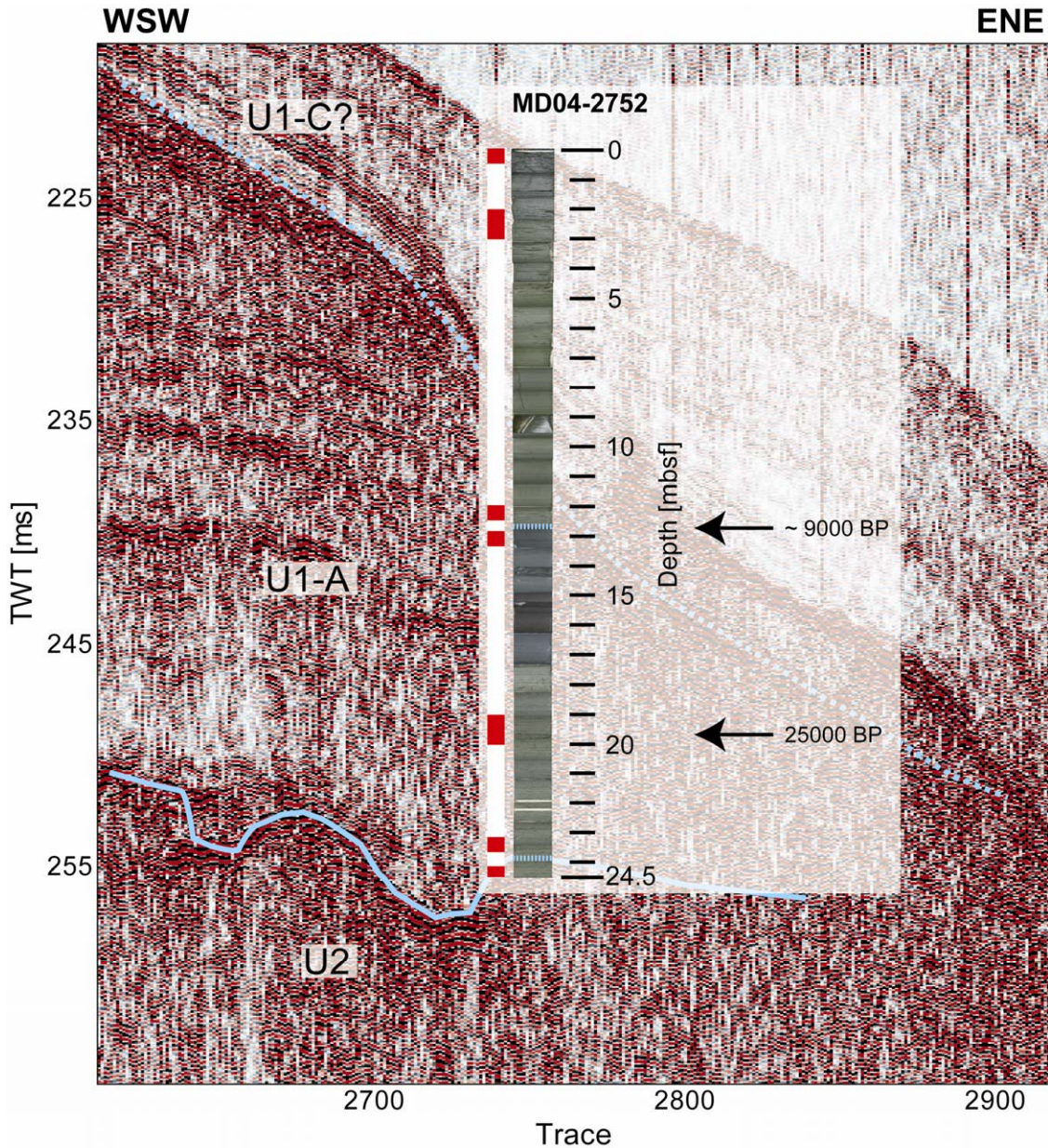
Fig. 8.12: Correlation of sediment core MD03-2752 with seismic profile BLASON2-56 (Fig. 8.9) which goes over the core location. This core is potentially very useful in any sequence stratigraphic reconstruction, as it penetrates several proposed seismic stratigraphic units. Red intervals on the left of the core image give intervals in which age estimates would be desirable; black arrows show the locations where the core has actually been dated and the AMS C[14] ages.

- After a preliminary interpretation (including mapping) of all the seismic data available, coring stations should be proposed and sediment sampling carried out. The station locations should match the equipment used with the target depths.

- Following sediment sampling, the seismic interpretation should be correlated with and calibrated against the sediment cores, so that core intervals to be dated can be chosen.

- The dated ages should be used to generate the final seismic stratigraphic model which should be base on absolute age and depth calibrations. Then a reconstruction of the sea-level history of the Black Sea can follow.

.

Acknowledgements

I would like to thank Prof Dr. H.K. Wong for his willingness to promote and support this PhD thesis, for discussions and suggestions, for guidance and advice, for reviewing the manuscript, and first and foremost for his patience since more than ten years.

Thanks to Dr. T. Lüdmann for friendship, support, and company during all the time I spend with the workgroup, and for taking care of 'business', both onshore and offshore.

Thanks to Thomas and Sebastian for helping to submit this thesis.

Thanks, Danke, Mulţumesc, Merci, Spaseeba, Blagodarya, Xie xie, Gracias, Grazie, to everyone I had the pleasure to work with. Thanks of course to all the usual suspects – too numerous to mention - that made studying Geology in Hamburg a truly unique and 'unregrettable' experience!

Without the love, support, encouragement, and understanding of my family this work would not have been possible: Cătălina, Sophia, and Iacob, my parents, brothers and all others, thank you.

References

ADAMIA, Sh. A., I. P. GAMKRELIDZE, G. S. ZAKARIADZE & M. B. LORDKIPANZE, 1974, Adjaro-Trialetsky depression and problem of formation of deep basin in the Black Sea: Geotektonika, 1974 (1), p. 78-94.

ALGAN, O., E. GÖKASAN, C. GAZIOĞLU, Z. Y. YÜCEL, B. ALPAR, C. GÜNEYSU, E. KIRCI, S. DEMIREL, E. SARI, D. ONGAN, 2002. A high-resolution seismic study in Sakarya Delta and submarine Canyon, southern Black Sea shelf: Continental Shelf Research 22 (10), p. 1511–1527.

ALLEN, P.A. & J.R. ALLEN, 1990, Basin Analysis: Principles and Applications: Blackwell Science Ltd, Oxford, UK, p. 263-277.

AKSU, A.E., D. YAŞAR & P.J. MUDIE, 1995a, Paleoclimatic and paleoceanographic conditions leading to development of sapropel layer S1 in the Aegean Sea basins: Palaeogeogr. Palaeoclimatol. Palaeoecol. 116, p. 71-101.

AKSU, A.E., D. YAŞAR, P.J. MUDIE & H. GILLESPIE, 1995b, Late glacial-Holocene paleoclimatic and paleoceanographic evolution of the Aegean Sea: micropaleontological and stable isotopic evidence: Mar. Micropaleontol. 25, p. 1-28.

AKSU, A.E., R.N. HISCOTT & D. YAŞAR, 1999, Oscillating Quaternary water levels of the Marmara Sea and vigorous outflow into the Aegean Sea from the Marmara Sea-Black Sea drainage corridor: Mar. Geol. 153, p. 275-302.

AKSU, A.E., R.N. HISCOTT, M.A. KAMINSKI, P.J. MUDIE, H. GILLESPIE, T. ABRAJANO & D. YAŞAR, 2002a, Last glacial - Holocene paleoceanography of the Black Sea and Marmara Sea: stable isotopic, foraminiferal and coccolith evidence: Mar. Geol. 190, p. 119-149.

AKSU, A.E., C. YALTIRAK & R.N. HISCOTT, 2002b, Quaternary paleoclimatic-paleoceano-graphic and tectonic evolution of the Marmara Sea and environs: Mar. Geol. 190, p. 9-18.

ANDERSON, J.B., K. ABDULAH, S. SARZALEJO, F. SIRINGAN & M.A. THOMAS, 1996, Late Quaternary sedimentation and highr-esolution sequence stratigraphy of the east Texas

shelf. In: M. De BATIST & P. JACOBS (Eds.), Geology of Siliciclastic Shelf Seas: Geological Society London, Special Publication 117, p. 95-124.

ALGAN, O., N. ÇAGATAY, A. L. TCHEPALYGA, D. ONGAN, C. EASTOE & E. GÖKASAN, 2001, Stratigraphy of the sediment infill in Bosphorus Strait: water exchange between the Black and Mediterranean Seas during the last glacial-Holocene: Geo-Marine Letters, v. 20, no. 4, p. 209-218.

ALLEN, P.A. & J.R. ALLEN, 1990, Basin Analysis: Principles and Applications: Blackwell Science Ltd, Oxford, UK, p. 263-277.

ANDRUSOV, N.L., 1890, Need for deep-water investigations in the Black Sea: Izv. Russk. Geogr. Obshch., vol. 26, p. 171-185.

ATANASSOVA, J., 1995, Palynological Data of Three Deep Water Cores from the Western Part of the Black Sea: Sofia, Pensoft, p. 68-93.

ATHY, L.F., 1930, Density, porosity and compaction of sedimentary rocks: Bull. AAPG, vol. 14, p. 1-24.

BAHR, A., F. LAMY, H. ARZ, H. KUHLMANN & G. WEFER, 2005, Late glacial to Holocene climate and sedimentation history in the NW Black Sea: Marine Geology 214, p. 309-322.

BALLARD, R.D., D.F. COLEMAN & G.D. ROSENBERG, 2000, Further evidence of abrupt Holocene drowning of the Black Sea shelf: Mar. Geol. 170, p. 253-261.

BANKS, C.J., 1997, Basins and thrust belts of the Balkan coast and the Black Sea. In: A.G. ROBINSON (Ed.), Regional and Petroleum Geology of the Black Sea and Surrounding Region: AAPG Memoir 68, p. 115-128, Tulsa, OK.

BANKS, C.J. & A.G. ROBINSON, 1997, Mesozoic strike-slip back-arc basin of the Western Black Sea region. In: A.G. Robinson (Ed.), Regional and Petroleum Geology of the Black Sea and Surrounding Region: AAPG Memoir 68, Tulsa, OK, p. 53-62.

BANU, C.A., 1967. Limnologia sectorului românesc al Dunării, Monograph Acad. RSR, Bucharest, 650 pp.

BARBER, K., B. ZOLITSCHKA, P. TARASOV & A.F. LOTTER, 2004, Atlantic to Urals - The Holocene climatic record of mid-latitude Europe. In: R.W. BATTARBEE et al. (Eds.), Past climate variability through Europe and Africa: Kluwer Dordrecht, p. 417–442.

BARBU, C., N. ALI MEHMED & C. PARASCHIV, 1969, The Paleozoic in the East Carpathian foreland between Buzău Valley and the northern border of Romania: Petrol şi Gaze XX, vol. 12, p. 863-868 (in Romanian).

BEŞIKTEPE, Ş., H.I. SUR, E. ÖZSOY, M.A. LATIF, T. OGUZ & Ü. ÜNLÜATA, 1994, The circulation and hydrography of the Marmara Sea: Prog. Oceanogr. 34, p. 285-334.

BOGDANOVA, C., 1969, Seasonal fluctuations in the inflow and the distribution of the Mediterranean waters in the Black Sea. In: L.M. FOMIN (Ed.), Basic Features of the Geological Structure, the Hydrological Regime and Biology of the Mediterranean Sea: Academy of Science, USSR, Moscow. English translation by Institute of Modern Languages, Washington, DC, p. 131-139.

BROWN, D., 1999, 'Great Flood' Theory passes science test: Dam! Where did all that water come from: AAPG Explorer, April, p. 47-67.

BROWN, L.F. & W.L. FISHER, 1977, Seismic-stratigraphic interpretation of depositional systems: examples from Brazil rift and pull-apart basins. In: C.E. PYATON (Ed.), Seismic Stratigraphy - Applications to Hydrocarbon Exploration: AAPG Memoir 26, p. 213-248.

BURG, J.-P., L.-E. RICOU, I. GODFRAUX, D. DIMOV & L. KLAIN, 1996, Syn-metamorphic nape complex in the Rhodope Massif. Structure and kinematics: Terra Nova 8, p. 6-15.

BOCCALETTI, M., P. GOCEV & P. MANETTI, 1974, Mesozoic zones in the Black Sea region: Boll. Soc. Geol. Ital., 96, p. 547-565.

BONDAR, C., I. STARE, D. CERNEA & E. HĂRĂBAGIU, 1991, Water flow and sediment transport of the Danube at its outlet into the Black Sea: Meteorol. Hydrol. 21, p. 21-25.

CARTER, R.M., S.T. ABBOTT, C.S. FULTHORPE, D.W. HAYWICK & R.A. HENDERSON, 1991, Application of global sea level and sequence-stratigraphic models in Southern Hemisphere Neogene strata from New Zealand. In: D.I.M. MacDONALD (Ed.).

Sedimentation, Tectonics, and Eustasy: Sea Level Changes at Active Margins, vol. 12. Int. Assoc. Sediment. Spec. Pub, p. 41-65.

CHATALOV, G., 1990, Geology of Strandzha Zone in Bulgaria: Geologica Balcanica, Series Operum Singulorum No. 4, Bulgarian Academy of Science.

CHEN, F., W. SIBEL, M. SATIR, M.N. TERZIOGLU & K. SAKA, 2002, Geochronology of the Karadere basement (NW Turkey) and implications for the geological evolution of the Istanbul Zone: Int. Journal of Earth Science 91, p. 469-481.

CHEPALYGA, A. L., 1984, Inland sea basins. In: A. A. VELICHKO, H. E. J. WRIGHT & W. BARNOSKY-CATHY (Eds.), Late Quaternary environments of the Soviet Union: Mineapolis, MN, United States, Univ. Minn. Press., p. 229-247.

CHEPALYGA, A.L., 2002. Chernoe more [Black Sea]. In: VELICHKO, A.A. (Ed.), Dinamika landshaftnykh komponentov i vnutrennikh morskikh basseinov severnoi Evrazii za poslednie 130 000 let [Dynamics of Terrestrial Landscape Components and Inner Marine Basins of Northern Eurasia during the Last 130,000 years]: Moscow, GEOS, p. 170–182.

CHIOCCI, F.L., G. ERCILLA & J. TORRES, 1997, Stratal architecture of western Mediterranean margins as the result of the stacking of Quaternary lowstand deposits below 'glaciao-eustatic fluctuation base': Sediment. Geol. 112, p. 195-217.

DABOVSKI, C., I. ZAGORCHEV & G. GEORGIEV, 2004, East European Craton - Scythian Platform - Dobrogea - Balkanides - Rhodope Massif - Hellenides - East Mediterranean - Cyrenaica, From the Moesian Platform to the Balkanides and East Rhodope Massif: TRANSMED Transect VII. In: CAVAZZA, W., et al. (eds). The TRANSMED Atlas - The Mediterranean region from crust to mantle: Springer Verlag, Berlin Heidelberg, 141pp.

DACHEV, C., V. STANEV & P. BOKOV, 1988, Structure of the Bulgarian Black Sea area: Bolletino di Geofisica Teorica e Applicata No. 117-118, vol. 30, p. 79-107.

DEAN, W.T., O. MONOD, R.B. RICKARDS, O. DEMIR & P. BULTYNCK, 2000, Lower Palaeozoic stratigraphy and palaeontology, Karadere-Zirze area, Pontus Mountains, northern Turkey: Geol. Mag. 137, p. 555-582.

DEGENS, E. T. & D. A. ROSS, 1970, Oceanographic Expedition in the Black Sea - A preliminary report: Die Naturwissenschaften, 7, p. 349-353.

DEGENS, E. T. & D. A. ROSS, 1972, Chronology of the Black Sea over the last 25,000 years: Chem. Geol., 10, p. 1-16.

DEGENS, E. T. & A. D. ROSS (Eds.), 1974, The Black Sea - Geology, Chemistry, and Biology: AAPG Memoir, 20. Tulsa, Oklahoma, 595 pp.

DEGENS, E.T., P., STOFFERS, S., GOLUBIC & M.D. DICKMAN, 1978, Varve chronology: estimated rates of sedimentation in the Black Sea deep basin. In: D.A. ROSS & Y.P. NEPROCHNOV (Eds.), Initial Reports of the Deep Sea Drilling Project, 42 (part 2): U.S. Govt. Printing Office, Washington, D.C., p. 499-508.

DEGENS, E. T., H. K. WONG & M. G. WIESNER, 1986, The Black Sea region: Sedimentary facies, tectonics and oil potential. In: E. T. DEGENS, P. A. MEYERS & S. C. BRASSEL (Eds.): Biochemistry of Black Shales: Mitt. Geol.-Paläont. Inst. Univ. Hamburg, SCOPE/UNEP Sonderband, 60, p. 127-149.

DEMIRBAG, E., E. GÖKASAN, F. Y. OKTAY, M. SIMSEK & H. YÜCE, 1999, The last sea level changes in the Black Sea: evidence from the seismic data: Marine Geology, v. 157, no. 3-4, p. 249-265.

DEN DULK, M., G.J. REICHART, S. VAN HEYST, G.J. VAN DER ZWAAN, 2000. Benthic foraminifera as proxies of organicmatter flux and bottomwater oxygenation? A case history from the northern Arabian Sea: Palaeogeogr. Palaeoclimatol. Palaeoecol. 161, p. 337–359.

DERCOURT, J., L. P. ZONENSHAIN, L.-E. RICOU, V. G. KAZMIN, X. Le PICHON, A. L. KNIPPER, C. GRANDJACQUET, I. M. SBORTSHIKOV, J. GEYSSANT, C. LEPVRIER, D. H. PECHERSKY, J. BOULIN, J.-C. SIBUET, L. A. SAVOSTIN, O. SOROKHTIN, M. WESTPHAL, M. L. BAZHENOV, J. P. LAUER & B. BIJU-DUVAL, 1986, Geological evolution of the Tethys belt from the Atlantic to the Pamirs since the Lias: Tectonophysics, 123, p. 241-315.

DERCOURT, J., L.E. RICOU & B. VRIELYNCK (Eds.), 1993, Atlas Tethys, Paleoenvironmental Maps: Gauthier-Villars, Paris, p. 307, maps 14, pl. 1.

DEUSER, W.G., 1972, Late-Pleistocene and Holocene history of the Black Sea as indicated by stable isotope studies: Journal of Geophysical Research 77, p. 1071-1077.

DIMITROV, P.S., 1982, Radiocarbon datings of bottom sediments from the Bulgarian Black Sea Shelf: Bulg. Acad. Sci. Oceanol. 9, p. 45-53.

DINU, C., H.K. WONG & D. ŢAMBREA, 2002, Stratigraphic and tectonic syntheses of the Romanian Black Sea shelf and correlation with major land structures: Bucharest Geoscience Forum, Special Volume No. 2, p. 101-117.

DINU, C., H.K. WONG, H.K., D. TAMBREA & L. MATENCO, 2005, Stratigraphic and structural characteristics of the Romanian Black Sea shelf: Tectonophysics 410 (1–4), 417–435.

ERIS, K.K., W.B.F. RYAN, M.N. ÇAGATAY, U. SANCAR, G. LERCOLAIS, G. MENOT, E. BARD, 2007. The timing and evolution of the post-glacial transgression across the Sea of Marmara shelf south of Istanbul: Marine Geology 243, p. 57–76.

EVSYLEKOV, Y. D. & K. M. SHIMKUS, 1995, Geomorphological and neotectonic development of outer part of continental margin to the south of Kerch Strait: Oceanology, v. 35, p. 623-628.

FEDEROV, P. V., 1978, The Pleistocene of the Ponto-Caspian: Moscow, Nauka Press.

FEDOROV, P. V., 1988, The problem of changes in the level of the Black Sea during the Pleistocene: International Geology Review, v. 30, no. 6, p. 635-641.

FILIPOVA-MARINOVA, M., 2004, Late quaternary palaeoenvironmental records from the southern Bulgarian Black Sea coast. In: ASSEMBLAGE first workshop, Varna, Bulgaria, 10 pp.

FINETTI, I., G. BRICCHI, A. Del BEN, M. PIPAN & Z. XUAN, 1988, Geophysical study of the Black Sea area: Bolletino di Geofisica Teorica e Applicata, v. 30, no. 117-118, p. 197-324.

FLOOD, R.D., P.L. MANLEY, R.O. KOWSMANN, C.J. APPI & C. PIRMEZ, 1991, Seismic facies and Late Quaternary growth of Amazon submarine fan. In: P. WEIMER & M.H. LINK

(Eds.), Seismic Facies and Sedimentary Pprocesses of Submarine Fans and Turbidite Systems: Springer, New York, p. 415-433.

FONTANIER, C., F.J. JORISSEN, L. LICARI, 2002. Live benthic foraminiferal faunas from the Bay of Biscay: faunal density, composition, and microhabitats: Deep Sea Res. I 49, p. 751–785.

FONTANIER, C., F.J. JORISSEN, G. CHAILLOU, 2003. Seasonal and interannual variability of benthic foraminiferal faunas at 550 m depth in the Bay of Biscay: Deep-Sea Res. I 50, p. 457–494.

FULTHORPE, C.S., 1991, Geological controls on seismic resolution: Geology v. 19, p. 61-65.

GILLET, H., G. LERICOLAIS, J.-P. REHAULT & C. DINU, 2003, La stratigraphie oligo-miocène et la surface d'érosion messinienne en mer Noire, stratigraphie sismique haute résolution : C. R. Geoscience 335, p. 907-916.

GILLET, H., 2004, La stratigraphie tertiaire et la surface d'erosion messinienne sur les marges occidentales de la Mer Noire: stratigraphie sismique haute resolution, L'universite de Bretagne Occidentale.

GIOSAN, L., Y. MART, C.M. MCHUGH, D. VACHTMAN, N.M. ÇAGATAY, E.K. KADIR, W.B. RYAN, 2005. Megafloods in marginal basins: new data from the Black Sea: EOS Trans. AGU 86 (52), PP32A-03.

GIOSAN, L., 2006, J. P. DONELLY, S. CONSTANTINESCU, F. FILIP, I. OVEJANU, A. VESPREMEANU-STROE, E. VESPREMENANU, G. A. T. DULLER, 2006, Young Danube delta documents stable Black Sea level since middle Holocene: Morphodynamic, paleogeographic, and archaeological implications: Geology v. 34, no. 9, p. 757-760.

GÖKASAN, E., E. DEMIRBAG, F. Y. OKTAY, B. ECEVITOGLU, M. SIMSEK & H. YÜCE, 1997, On the origin of the Bosphorus: Marine Geology, v. 140, no. 1-2, p. 183-199.

GÖRÜR, N., 1988, Timing of opening of the Black Sea basin: Tectonophysics, 147, p. 247-262.

GÖRÜR, N., O. MONOD, A.I. OKAY, A.M.C. SENGÖR, O. TÜYSÜZ, E. YIGITBAS, M. SAKINC & R. AKKÖK, 1997, Palaeogeographic and tectonic position of the Carboniferous rocks of the western Pontides (Turkey) in the frame of the Variscan belt: Bull. Soc. Géol. France 168, p. 197-205.

GÖRÜR, N., M. N. CAGATAY, O. EMRE, B. ALPAR, M. SAKINC, Y. ISLAMOGLU, O. ALGAN, T. ERKAL, M. KECER, R. AKKOK & G. KARLIK, 2001, Is the abrupt drowning of the Black Sea shelf at 7150 yr BP a myth?: Marine Geology, v. 176, no. 1-4, p. 65-73.

GROSSWALD, M.G. & T.J. HUGHES, 2002, The Russian component of an Artic ice sheet during the Last Glacial Maximum: Quat. Sci. Rev. 21, p. 121-146.

HAYDOUTOV, I. & S. YANEV, 1997, The Protomoesian microcontinent of the Balkan Peninsula - a peri-Gondwanaland piece: Tectonophysics, vol. 272, p. 303-313.

HEDBERG, H.D., 1936, Gravitational compaction of clays and shales: Am. J. Sci., vol. 31, p. 241-287.

HISCOTT, R.N., 2001, Depositional sequences controlled by high rates of sediment supply, sea-level variations, and growth faulting: the Quaternary Baram Delta of northwestern Borneo: Mar. Geol. 175, 67-102.

HISCOTT, R.N. & A.E. AKSU, 2002, Late Quaternary history of the Marmara Sea and Black Sea from high-resolution seismic and gravity-core studies: Mar. Geol. 190(1-2), 261-282.

HISCOTT, R.N., A.E. AKSU, D. YAŞAR, M.A. KAMINSKI, P.J. MUDIE, V. KOSTYLEV, J. MacDONALD, F.I. IŞLER & A.R. LORD, 2002, Deltas south of the Bosphorus Strait record persistent Black Sea outflow to the Marmara Sea since ~10 ka: Mar. Geol. 190(1-2), 95-118.

HISCOTT, R.N., A.E. AKSU, P.J. MUDIE, M.A. KAMINSKI, T. ABRAJANO, D. YAŞAR, A. ROCHON, 2007. The Marmara Sea gateway since ~16 ky BP: non-catastrophic causes of paleoceanographic events in the Black Sea at 8.4 and 7.15 ky BP. In: YANKO-HOMBACH, V., GILBERT, A.S., DOLUKHANOV, P.M. (Eds.), The Black Sea Flood Question: Springer, The Netherlands, p. 89–117.

IANOVICI, V., V. MIHĂILESCU, L. BADEA, T. MORARIU, V. TUFESCU, M. IANCU, C. HERBST & H. GRUMĂZESCU (Eds.), 1960, Geografia văii Dunării Românești: Acad. RSR, Bucharest, 783 pp.

ILIESCU, V., 1974, Preliminary results of the palyno-protistological study of the pre-Silurian deposits from the basement of the Moldavian Highland: D. S. Inst. Geol. LX/3, p. 225-234 (in Romanian).

IMBRIE, J., J.D. HAYS, D.G. MARTINSON, A. McINTYRE, A.C. MIX, J.J. MORLEY, N.G. PISIAS, W.L. PRELL & N.J. SHACKLETON, 1984, The orbital theory of Pleistocene climate: Support from a revised chronology of the marine $\delta^{18}O$ record. In: A.L. BERGER, J. IMBRIE, J. HAYS, G. KUKLA & B. SALTZMAN (Eds.): Milankovitch and Climate, Part I, Reidel, The Netherlands, p. 269-305.

KAMINSKI, M.A., A. AKSU, M. BOX, R.N. HISCOTT, S. FILIPESCU, M. AL-SALAMEEN, 2002. Late Glacial to Holocene benthic foraminifer in the Marmara Sea: implications for Black Sea–Mediterranean Sea connections following the last deglaciation: Marine Geology 19, p. 165–202.

KARANTSEV, Y.V., 1982, Tectonics of the Crimea: Nauka, Moskow.

KEREY, I.E., E. MERIÇ, C. TUNOĞOLU, G. KELLING, R.K. BRENNER, A.U. DOĞAN, 2004. Black sea-Marmara Sea Quaternary connections: new data from the Bosphorus, Istanbul, Turkey: Palaeogeogr. Palaeoclim. Palaeoecol. 204, p. 277–295.

KONERDING, C., 2006, Mio-Pleistocene sedimentation and structure of the Romanian shelf, northwestern Black Sea: University of Hamburg, Institute of Biogeochemy and Marine chemistry.

KONIKOV, E.G., 2004. Exzogeodinamicheskaya model sedimentatzii i formirovaniya beregovih sistem severo-zapadnoi chasti Chornogo moriya na protyazhenii poslednih 18000 let [Exzogeodynamic model of conditions sedimentation and shaping of coastal geosystems of a northwest part of the Black Sea for the last 18000 years]: Visnyk Odes'kogo Natsional'nogo Universitetu 4 (9), p. 161–179.

KONIKOV, E.G., 2005. Coastline migration and periodicity of sedimentation on the northwest shelf of Black Sea in late Pleistocene and Holocene. In: YANKO-HOMBACH, V., BUYNEVICH, I., CHIVAS, A., GILBERT, A., MARTIN, R., MUDIE, P. (Eds.), Extended Abstracts of the First Plenary and Field Trip of IGCP-521 Project 'Black Sea—Mediterranean corridor during the last 30 ky: Sea level change and human adaptation': October 8–15, 2005, Kadir Has University, Istanbul, Turkey, p. 87–89.

KORENEVA, E. V. & G. G. KARTASHOVA, 1978, Palynological study of samples from holes 379A, 380A, Leg 42B. In: D. A. ROSS, Yu. P. NEPROCHNOV et al. (Eds.), Initial Reports of the Deep Sea Drilling Project, 42 (2): U. S. Govt. Printing Office, Washington, D. C., p. 951-992.

KRAFT, J.C., M.J. CHRZASTOWSKI, D.F. BELKNAP, M.A. TOSCANO & C.H. FLECHER III, 1987, The transgressive barrier-lagoon coast of Delaware: morphostratigraphy, sedimentary sequences and response to relative sea level. In: D. NUMMEDAL, O.H. PILKEY & J.D. HOWARD (Eds.), Sea Level Fluctuation and Coastal Evolution: SEPM Special Publication 41, p. 129-143.

KROONENBERG, S.B., G.V. RUSAKOV & A.A. SVITOCH, 1997, The wandering of the Volga delta: a response to rapid Caspian sealevel change: Sediment. Geol. 107, p. 189-209.

KUPRIN, P.N., F.A. SCHERBAKOV & I.I. MORGUNOV, 1974, Correlation, age, and distribution of the postglacial continental terrace sediments of the Black Sea: Baltica 5, p. 241–249.

LANE-SERFF, G.F., E.J. ROHLING, H.J. BRYDEN & H. CHARNOCK, 1997, Postglacial connection of the Black Sea to the Mediterranean and its relation to the timing of sapropel formation: Paleoceanography 12 (2), p. 169-174.

LARCHENKOV, E. & S. KADURIN, 2005. Modelling of coastline position along north-western part of the Black Sea for the past 25 ky. In: YANKO-HOMBACH, V., BUYNEVICH, I., CHIVAS, A., GILBERT, A., MARTIN, R., MUDIE, P. (Eds.), Extended Abstracts of the First Plenary Meeting and Trip of IGCP-521 Project 'Black Sea—Mediterranean corridor during the last 30 ky: Sea level change and human adaptation': October 8–15, 2005, Kadir Has University, Istanbul, Turkey, p. 102–103.

LENG, M.J. & J.D. MARSHALL, 2004, Palaeoclimate interpretation of stable isotope data from lake sediment archives: Quat. Sci. Rev. 23, p. 811-831.

LERICOLAIS, G., I. POPESCU, F. GUICHARD, S.-M. POPESCU, M. MANOLAKAKIS, 2006. Water-level fluctuations in the Black Sea since the Last Glacial Maximum. In: YANKO-HOMBACH, V., GILBERT, A.S., PANIN, N., DOLUKHANOV, P.M. (Eds.), The Black Sea Flood Question: Changes in Coastline, Climate, and Human Settlement: Springer, Dordrecht, p. 437–452.

LETOUZEY, J., B. BIJU-DUVAL, A. DORKEL, R. GONNARD, K. KRISTCHEV, L. MONTADERT & O. SUNGURLU, 1977, The Black Sea: A marginal basin - Geophysical and geological data. In: B. Biju-Duval & L. Montadert (Eds.): International Symposium on the structural history of the Mediterranean basins: Split. Paris, p. 363-376.

MACAROVICI, N., 1971, La faune silurienne du fondament du Plateau Moldave (les forages de Jassy et de Todireni-Botosani): Anal. St. Univ. "Al. I. Cuza" s.n. (s. II, b. Geol.) XVII, p. 99-115.

MAJOR, C. O., 1994, Late Quaternary sedimentation in the Kerch area of the Black Sea shelf: response to sea level fluctuation [BA thesis]: Wesleyan University, 116 pp.

MAJOR, C., W. RYAN, G. LERICOLAIS & I. HAJDAS, 2002, Constraints on Black Sea outflow to the Sea of Marmara during the last glacial-interglacial transition: Mar. Geol. 190, p. 19-34.

MAJOR, C.O., S.L. GOLDSTEIN, W.B.F. RYAN, G. LERCOLAIS, A.M. PIOTROWSKI, I. HAJDAS, 2006. The co-evolution of Black Sea level and composition through the last deglaciation and its paleoclimatic significance: Quat. Sci. Rev. 25, p. 2031–2047.

MAMAEV, V. O. & O. R. MUSIN, 1997, Black Sea Geographic Information System, CD-ROM, In: Programme, B. S. E. P. - U. N. D. (Ed.): New York, United Nations Publications.

MANGERUD, J., V. ASTAKHOV, M. JAKOBSSON & J.I. SVENDSEN, 2001, Huge Ice-age lakes in Russia: J. Quat. Sci. 16 (8), p. 773-777.

MANGERUD, J., M. JAKOBSSON, H. ALEXANDERSON, V. ASTAKHOV, G.K.C. CLARKE, M. HENRIKSEN, C. HJORT, G. KRINNER, J.-P. LUNKKA, P. MFLLER, A. MURRAY, O. NIKOLSKAYA, M. SAARNISTO & J.I. SEVENDSEN, 2004, Ice-dammed lakes and rerouting of the drainage of northern Eurasia during the Last Glaciation: Quat. Sci. Rev. 23, p. 1313-1332.

MARKOV, K.K., G.I. LAZUKOV & V.A. NIKOLAYEV, 1965, The Quaternary Period (Glacial Period- Antropogen Period): Moscow, Moskov Univ., 371 pp.

MAROVIC, M., A. GRUBIC, I. DJOKOVIC, M. TOLJIC & V. VOJVODIC, 1997a, The genesis of Djerdap Gorge. In: Intern. Symp. on Geology in the Danube Gorges, Belgrade-Bucharest, p. 99-104.

MAROVIC, M., A. GRUBIC, I. DJOKOVIC, M. TOLJIC & V. VOJVODIC, 1997b, The neoalpine tectonic pattern of Djerdap region. In: Intern. Symp. on Geology in the Danube Gorges, Belgrade-Bucharest, p. 111-115.

McHUGH, C.M.G., D. GURUNG, L. GIOSAN, W.B.F. RYAN, Y. MART, U. SANCAR, L. BURCKLE, M.N. ÇAGATAY, 2008. The last reconnection of the Marmara Sea (Turkey) to the World Ocean: A paleoceanographic and paleoclimatic perspective: Marine Geology 255, p. 64–82.

MESTEL, R., 1997, Noah's flood: New Sci. 156, p. 24-27.

McINNIS, D., 1998, Two geologists trace Noah's Flood to the violent birth of the Black Sea: Earth August, p. 46-54.

MILANOVSKY, E.E., 1991, Geology of the URSS, Part 3: Moskow Univ. Press, Moskow, 272 pp.

MITCHUM, R.M., 1977, Seismic stratigraphy and global changes of sea level, Part 1: Glossary of terms used in seismic stratigraphy. In: C.E. PAYTON (Ed.), Seismic Stratigraphy - Applications to Hydrocarbon Exploration: AAPG Memoir 26, p. 205-212.

MURATOV, M.V, 1969, Geology of the URSS, Crimea, Part 1: Geology, vol. VIII, Nedra, Moscow, 576 pp.

MURRAY, J. W., 1991, The 1988 Black Sea oceanographic expedition: Introduction and summary: Deep-Sea Research, 38 (Suppl. 2), p. 655-661.

MURRAY, J., 2006. Ecology and Applications of Benthic Foraminifera: Cambridge University Press. 422 pp.

MYERS, P.G., C. WIELKI, S.B. GOLDSTEIN & E.J. ROHLING, 2003, Hydraulic calculations of postglacial connections between the Mediterranean and the Black Sea: Mar. Geol. 201, p. 253-267.

NEPROCHNOV, Y. P., 1980, Geologicheskaya istoriya Chernogo morya po rezultatam glubokovodnogo bureniya - (Translated Title: The geologic history of the Black Sea from the results of deep-sea drilling): Moscow, USSR, Nauka Press, 212 pp.

NEVESSKAYA, L.A., 1965, Late Quaternary bivalve mollusks of the Black Sea: their systematics and ecology: Acad. Nauk SSSR Paleont. Inst. Trudy 105, 1-390 pp.

NIKISHIN, A.M., P.A. ZIEGLER, D.I. PANOV, B.P. NAZAREVICH, M.-F. BRUNET, R.A. STEPHENSON, S.N. BOLOTOV, M.V. KOROTAEV & P.L. TIKHOMIROV, 2001, Mesozoic and Cenozoic evolution of the Scythian Platform-Black Sea-Caucasus domain. In: P.A., ZIEGLER, W. CAVAZZA, A.H.F. ROBERTSON & S. CRASQUIN-SOLEAU (Eds.), Peri-Tethys Memoir 6: Peri-Tethyan Rift/Wrench Basins and Passive Margins, Mémoires du Muséum national d'Histoire naturelle, Paris, vol. 186, p. 295-346.

NIKISHIN, A.M., M.V. KOROTAEV, A.V. ERSHOV & M.-F. BRUNET, 2003, The Black Sea basin: tectonic history and Neogene-Quaternary rapid subsidence modeling: Sedimentary Geology, vol. 156, p. 149-168.

NOAKES, J. E. & N. HERZ, 1983, University of Georgia Radiocarbon dates VII: Radiocarbon, vol. 25, no. 3, p. 919-929.

OĞUZ, T., V.S. LATUN, M.A. LATIF, V.V. VLADIMIROV, H.I. SUR, A.A. MARKOV, E. ÖZSOY, B.B. KOTOVSHCHIKOV, V.V. EREMEEV & Ü. ÜNLÜATA, 1993, Circulation in the surface and intermediate layers of the Black Sea: Deep-Sea Res. I 40, p. 1597-1612.

OKAY, A. I., A. M. C. SENGÖR & N. GÖRÜR, 1994, Kinematic history of the opening of the Black Sea and its effect on surrounding regions: Geology, 22, p. 267-270.

OSTROVSKIY, A. B., Y. A. IZMAYLOV, I. P. BALABANOV, S. I. SKIBA, N. G. SKRYABINA, S. A. ARSLANOV, N. A. GEY & N. I. SUPRUNOVA, 1977, New data on the paleohydrological regime of the Black Sea in the Upper Pleistocene and Holocene. In: P. A. KAPLIN & F. A. SHCHERBAKOV (Eds.), Paleogeography and Deposits of the Pleistocene of the Southern Seas of the USSR: Moscow, Nauka Press, p. 131-141.

ÖZSOY, E., M.A. LATIF, S. TUGFLRUL & Ü. ÜNLÜATA, 1995, Exchanges with the Mediterranean, fluxes and boundary mixing processes in the Black Sea. In: F. BRIAND (Ed.), Mediterranean Tributary Seas. Bulletin de l'Institut Oceanographique, Monaco, Special No. 15, CIESME Science Series 1, p. 1-25.

ÖZSOY, E., M.A. LATIF, H.I. SUR & Y. GORYACHKIN, 1996, A review of the exchange flow regimes and mixing in the Bosphorus Strait. In: F. BRIAND (Ed.), Mediterranean Tributary Seas: Bulletin de l'Institut Oceanographique, Monaco, Special No. 17, CIESME Science Series 2, p. 187-204.

PALUSKA, A. & E.T. DEGENS, 1979, Climatic and tectonic events controlling the Quaternary in the Black Sea region: Geol. Rundschau 68 (1), p. 284–301.

PANIN N., 1974, Evolution of the Danube delta during the Holocene: Geologia Cuaternarului, H(5), p. 107-121.

PANIN, N., S. PANIN, N. HERZ & J. E. NOAKES, 1983, Radiocarbon dating of Danube Delta deposits: Quaternary Research, v. 19, p. 249-255.

PANIN, N., 1989, Danube Delta. Genesis, evolution and sedimentology: Rev. Roum. Geol. Geophys. Geogr., Ser. Geogr. 33, p. 25-36.

PANIN, N., 1997, On the geomorphologic and geologic evolution of the river Danube: Black Sea interaction zone: Geo-Eco-Marina, v. 2, p. 31-40.

PANIN, N. & D. JIPA, 1998, Danube river sediment input and its interaction with the north-western Black Sea: results of EROS-2000 and EROS-21 projects: Geo-Eco-Marina, v. 3, p. 23-35.

PANIN, N. & D. JIPA, 2002, Danube river sediment input and its interaction with the northwestern Black Sea: Estuar. Coast. Shelf Sci. 54, p. 551-562.

PANIN, N. & S. PANIN, 1967, Regressive sand waves on the black sea shore: Marine Geology, v. 5, no. 3, p. 221-226.

PANIN, N. & I. POPESCU, 2007, The northwestern Black Bea: climatic and sea level changes in the Upper Quaternary. In: V. YANKO-HOMBACH, A. S. GILBERT, N. PANIN & P. M. DOLUKHANOV (Eds.), The Black Sea Flood Question: Changes in Coastline, Climate, and Human Settlement: Springer-Verlag Berlin Heidelberg, p. 387-404.

PANIN, N., S. PANIN, N. HERZ & J. E. NOAKES, 1983, Radiocarbon dating of Danube Delta deposits: Quaternary Research, v. 19, p. 249-255.

PARASCHIV, D., 1985, The present state of knowledge of Precambrian and Paleozoic formations from the Moldavian Platform: Mine, Petrol şi Gaze, vol. 11 (in Romanian).

PĂTRULIUŞ, D. & M. IORDAN, 1974, On the presence of the *Pogonophore Sabellidites cambriensis Ian*. and the algae *Vendotaenia antiqua Gnil*. in the pre-Silurian deposits from the Moldavian Highlands: D.S. LX/4 (in Romanian).

PĂTRUŢ I., C. PARASCHIV, T. DĂNEŢ, L. MOTAS, N. DĂNEŢ & N. BALTREŞ, 1983, The geological constitution of the Danube Delta: An. Inst. Geol. Geofiz. 59, Bucureşti, p. 55-61.

POPESCU, I., G. LERICOLAIS, N. PANIN, H.K. WONG & L. DROZ, 2001, Late Quaternary channel avulsion on the Danube deep-sea fan, Black Sea: Marine Geology 179, p. 25-37.

POPESCU, I., G. LERICOLAIS, N. PANIN, A. NORMAND, C. DINU & E. Le DREZEN, 2004, The Danube submarine canyon (Black Sea): morphology and sedimentary processes: Marine Geology 206, p. 249-265.

POPOV, G.I., 1973, New data on the stratigraphy of Quaternary marine sediments of the Kerch Strait: Dokl. Akad. Nauk SSSR 213, p. 84-86.

POPOV, G.I., 1975, New data on the stratigraphy of Quaternary marine sediments of the Kerch Strait: Transactions (Doklady) of the U.S.S.R, v. Academy of Sciences: Earth Science Sections. 213(1973), no. 1-6, p. 84-86.

POPOV, G.I., 1983, Pleistocene of the Black Sea-Caspian straits: Nauka, Moscow.

POPP, N., 1969, The Quaternary deposits in the Danube valley in Romania and the paleo-Danube river bed: Roum. Geol. Geophys. Geogr.-Ser. Geogr. 12, p. 67-72.

POSEA, G., 1964, Defileul Dunării: Natura, seria Geogr.-Geol., XVI, 1, Bucureşti, p. 45-49.

ROBINSON, A., G. SPADINI, S. CLOETINGH & J. RUDAT, 1995, Stratigraphic evolution of the Black Sea: inferences from basin modelling: Mar. and Petr. Geology, v. 12, no. 8, p. 821-835.

ROBINSON, A.G., J.H. RUDAT, C.J. BANKS & R.L.F. WILES, 1996, Petroleum geology of the Black Sea: Marine and Petroleum Geology No. 2, vol. 13, p.195-223.

ROMANESCU, G., 1996, L'évolution hydrogéomorphologique du delta du Danube Étape Pleistocène-Holocène inférieur: Z. Geomorph., 106 (Suppl.), p. 267-295.

ROSS, D.A., P. STOFFERS & E.S. TRIMONIS, 1978, Black Sea sedimentary framework: Initial reports of the Deep Sea Drilling Project, 42 (2), U.S. Govt. Printing Office, Washington, D.C., p. 359-372.

ROSS, D.A. & E.T. DEGENS, 1974, Recent sediments of Black Sea. In: E.T. DEGENS & D.A. ROSS (Eds.), The Black Sea-Geology, Chemistry, and Biology, vol. 20: AAPG Mem., p. 183-199.

RUBEY, W.W. & M.K. HUBBERT, 1960, Role of fluid pressure in mechanics of overthrust faulting, II, Overthrust belt in geosynclinal area of western Wyoming in light of fluid-pressure hypothesis: Bull. geol. Soc. Am., vol. 60, p. 167-205.

RYAN, W. B. F., 2004, The Black Sea Flood; a seed for a Myth?. In: 32nd IGC Florence 2004, Florence, p. Session T17.05 - Myth and geology.

RYAN, W.B.F., C. MAJOR, G. LERICOLAIS & S. GOLDSTEIN, 2003, Catastrophic flooding of the Black Sea: Annu. Rev. Earth Planet. Sci. 31, p. 525-554.

RYAN, W.B.F., W.C. PITMAN III, C.O. MAJOR, K. SHIMKUS, V. MASKALENKO, G.A. JONES, P. DIMITROV, N. GÖRÜR, M. SAKINC & H. YÜCE, 1997, An abrupt drowning of the Black Sea shelf: Mar. Geol. 138, p. 119-126.

RYAN, W.B.F. & W.C. PITMAN III, 1999, Noah's Flood: the New Scientific Discoveries about Events that Changed History: Touchstone Book, Simion and Schuster, New York, 319 pp.

SAKINC, M., C. YALTIRAK & F.Y. OKTAY, 1999, Paleogeographical evolution of the Thrace Neogene Basin and the Tethys - Para-Tethys relations at northwestern Turkey (Thrace): Palaeogeogr. Paleoclimatol. Paleoecol. 153, p. 17-40.

SĂNDULESCU, M., 1978, The Moesic Platform and the North Dobrogea orogen. In: M. LEMOINE (Ed.), Geological atlas of Alpine Europe and adjoining areas: Elsevier, Amsterdam, p. 427-460.

SCHRADER, H.J., 1978, Quaternary through Neogene history of the Black Sea deduced from the palaeocology of diatoms, silicoflagellates, ebridians and chrysomonads: Init. Rep. DSDP XLII, p. 789-902.

SEGHEDI, A., G. OAIE, D. IOANE & R. DIMITRIU, 2004, East European Craton - Scythian Platform - Dobrogea - Balkanides - Rhodope Massif - Hellenides - East Mediterranean - Cyrenaica; Eastern European Craton, Scythian Platform, N. Dobrogea Orogen and Moesian Platform: TRANSMED Transect VII. In: CAVAZZA, W., et al. (eds). The TRANSMED Atlas - The Mediterranean region from crust to mantle: Springer Verlag, Berlin Heidelberg, 141pp.

SHCHERBAKOV, F. A. & Y. V. BABAK, 1979, Stratigraphic subdivision of the Neoeuxinian deposits in the Black Sea: Oceanology, v. 19, no. 3, p. 298-300.

SHIMKUS, K.M. & E.S. TRIMONIS, 1974, Modern sedimentation in Black Sea. In: E.T. DEGENS & D.A. ROSS (Eds.), The Black Sea-Geology, Chemistry, and Biology, vol. 20. AAPG Mem., p. 249-279.

SHIMKUS, K.M., A.V. KOMAROV & I.V. GRAKOVA, 1978, Stratigraphy of the upper Quaternary deep sea sediments in the Black Sea: Oceanology 17, p. 443-446.

SHNYUKOV, Y. F. & N. N. TRASHCHUK, 1976, A new region of occurence of Karangatian deposits on the southern slope of the Kerch Peninsula: Ukrainian Academy of Sciences, Doklady, v. B, no. 12, p. 1078-1080.

SHOPOV, V.L., S. CHOCHOV & V. GEORGIEV, 1986, Lithostratigraphy of Upper Quaternary sediments from the northwestern Black Sea shelf between the parallels of the Cape Emine and Danube River mouth: Geol. Balc. 16, p. 99-112.

SHOPOV, V., E. BOZILOVA & J. ATANASSOVA, 1992, Biostratigraphy and radiocarbon data of Upper Quaternary sediments from western part of the Black Sea (In Bulgarian with English summary): Geol. Balcanica, v. 22, p. 59-69.

SKIBA, S.I., F.A. SCHERBAKOV & P.N. KUPRIN, 1976, Paleogeography of the Kerch-Taman region during the late Pleistocene and Holocene: Oceanology 15, p. 575-578.

SPÂNOCHE, S. & N. PANIN, 1997, Contribution to knowing the Danube Delta: Delta deposits structure through high resolution seismic: Bucharest, Geo-Eco-Marina, v. 2, p. 41-45.

SPERLING, M., G. SCHMIEDL, C. HEMLEBEN, K.C. EMEIS, H. ERLENKEUSER & P.M. GROOTES, 2003, Black Sea impact on the formation of eastern Mediterranean sapropel S1? Evidence from the Marmara Sea: Palaeogeogr. Palaeoclimatol. Palaeoecol. 190, p. 9-21.

STECKLER, M.S. & A.B. WATTS, 1978, Subsidence of the Atlantic-type continental margin off New York: Earth and Planetary Science Letters 41, p. 1-13.

STEPHENSON, R., Y. MART, A. OKAY, H.F. ROBERTSON, A. SAINTOT, S. STOVBA & O. KHRIACHTCHEVSKAIA, 2004, Eastern European Craton - Crimea - Black Sea - Anatolia - Cyprus - Levant Sea - Sinai - Red Sea: TRANSMED Transect VIII. In: CAVAZZA, W., et al.

(eds). The TRANSMED Atlas - The Mediterranean region from crust to mantle: Springer Verlag, Berlin Heidelberg, 141pp.

SUNAL, G. & O. TÜYSÜZ, 2002, Palaeostress analysis of tertiary post-collisional structures in the Western Pontides, northern Turkey: Geological Magazine, vol. 139, p. 343-359.

TERNEK, Z., 1964, The Geological Map of Turkey, Istanbul Map Sheet (1:500 000): Institute of Mineral Research and Exploration (MTA), Ankara.

TODOROVA, H., 1989, Durankulak 1: Sofia, Bulgarian Academy of Sciences.

TOKAY, M., 1964, The Geological Map of Turkey, Zonguldak Map Sheet (1:500 000): Institute of Mineral Research and Exploration (MTA), Ankara.

TRASHCHUK, N. N. & V. A. BOLIVETS, 1978, A new area of occurrence of Karangatian deposits on the NW coast of the Black Sea: Ukrainian Academy of Sciences, Doklady, v. B, no. 8.

TÜYSÜZ, O., 1999, Geology of the Cretaceous sedimentary basins of the Western Pontides: Geological Journal, vol. 34, p. 75-93.

UCHUPI, E. & D.A. ROSS, 2000, Early Holocene marine flooding of the Black Sea: Quat. Res. 54, p. 68-71.

UNESCO, 1969, Discharge of Selected Rivers of the World, Vol. 1: General and Regime Characteristics of Stations Selected: Studies and Reports in Hydrology, 70 pp.

UNESCO, 1993, Discharge of Selected Rivers of the World, Vol. 2: Monthly and Annual Discharges Recorded at Various Selected Station: Studies and Reports in Hydrology, 600 pp.

USTAÖMER, T. & A.H.F. ROBERTSON, 1994, Late Palaeozoic marginal basin and subduction-accretion, the Paleotethyan Küre Complex, Central Pontides, northern Turkey: Journal of Geol. Soc. London, vol. 151, p. 291-305.

USTAÖMER, P.A. & G. ROGERS, 1999, The Bolu Massif: remnant of a pre-Early Ordovician active margin in the west Pontides, northern Turkey: Geological Magazine, vol. 126, p. 579-592.

VAIL, P.R., R.M. MITCHUM & S. THOMPSON III, 1977, Seismic stratigraphy and global changes of sea level, part 3: relative changes of sea level from coastal onlap. In: C.W. PAYTON (Ed.), Seismic stratigraphy applications to hydrocarbon exploration: AAPG Memoir 26, p. 63-97.

VAIL, P.R., F. AUDEMARD, S.A. BOWMAN, P.N. EISNER & C. PEREZ-CRUZ, 1991, The stratigraphic signatures of tectonics, eustasy and sedimentology - an overview. In: G. EINSELE, W. RICKEN & A. SEILACHER (Eds.), Cycles and events in stratigraphy: Springer-Verlag, New York, p. 611-659.

VAN HINTE, J.E., 1978, Geohistory analysis-application of micropalaeontology in exploration geology: Bull. Am. Assoc. Petrol. Geol., 62, p. 201-222.

VAN WAGONER, J.C., H.W. POSAMENTIER, R.M. MITCHUM, P.R. VAIL, J.F. SARG, T.S. LOUTIT & J. HARDENBOL, 1988, An overview of sequence stratigraphy and key definitions. In: C.W. WILGUS et al. (Eds.), Sea level changes: an integrated approach: Society of Economic Paleontologists and Mineralogists Special Publication No. 42, p. 39-45.

VAN WAGONER, J.C., R.M. MITCHUM, K.M. CAMPION & V.D. RAHMANIAN, 1990, Siliciclastic sequence stratigraphy in well logs, cores, and outcrops: concepts for high-resolution correlation of time and facies: AAPG Methods in Exploration Series, No. 7.

VISARION, M., M. SĂNDULESCU, V. ROŞCA, D. STĂNICA & L. ATANASIU, 1990, La Dobrogea dans le cadre de l'avantpays Carpatique: Rev. Roum. Géophys. 34, p. 55-65.

WALL, D. & B. DALE, 1974. Dinoflagellates in the late Quaternary deep-water sediments of the Black Sea. In: DEGENS, E.T., ROSS, D.A. (Eds.), The Black Sea – Geology, Chemistry and Biology: AAPG Memoir 20, Tulsa, OK, p. 364–380.

WATTS, A.B., G.D. KARNER & M.S. STECKLER, 1982, Lithospheric flexure and the evolution of sedimentary basins: Philosophical Transactions of the Royal Society, London, 305, p. 249-281.

WEIMER, P., 1990, Sequence stratigraphy, facies geometries, and depositional history of the Mississippi fan, Gulf of Mexico: AAPG Bull., 74, p. 425-453.

WINGUTH, C., 1998, Pleistozäne Meeresspiegelschwankungen und Sedimentation im nordwestlichen Schwarzen Meer: Zentrum für Meeres- und Klimaforschung der Universität Hamburg, Institut für Biogeochemie und Meereschemie.

WINGUTH, C., H.K. WONG, N. PANIN, C. DINU, P. GEORGESCU, G. UNGUREANU, V.V. KRUGLIAKOV & V. PODSHUVEIT, 2000, Upper Quaternary water level history and sedimentation in the northwestern Black Sea: Marine Geology 167, p. 127-146.

WONG, H.K., N. PANIN, C.DINU, P. GEORGESCU & C. RAHN, 1994, Morphology and post-Chaudian (Late Pleistocene) evolution of the submarine Danube fan complex: Terra Nova 6, p. 502-511.

YALTIRAK, C., M. SAKINÇ, A.E. AKSU, R.N. HISCOTT, B. GALLEB, U.B. ULGEN, 2002. Late Pleistocene uplift history along the southwestern Marmara Sea determined from raised coastal deposits and global sea-level variations: Marine Geology 190, p. 283-305.

YANKO-HOMBACH, V., 2004. The Black Sea flood controversy in light of the geological and foraminiferal evidence. In: YANKO-HOMBACH, V., GO¨RMUS-, M., ERTUNCC- , A., MCGANN, M., MARTIN, R., JACOB, J., ISHMAN, S. (Eds.), Program and Extended Abstracts of the Fourth International Congress on Environmental Micropalaeontology, Microbiology, and Meiobenthology: 13–18 September, Isparta, Turkey, p. 224–227.

YANKO-HOMBACH, V.V., 2006. Controversy over Noah's Flood in the Black Sea: geological and foraminiferal evidence from the shelf. In: YANKO-HOMBACH, V., GILBERT, A.S., PANIN, N., DOLUKHANOV, P.M. (Eds.), The Black Sea Flood Question: Changes in Coastline, Climate, and Human Settlement: Springer, Dordrecht, p. 149–203.

YILMAZ, Y., O. TÜYSÜZ, E. YIGITBAS, S. CAN GENC & A.M.C. SENGÖR, 1997, Geology and Tectonic evolution of the Pontides. In: A.G. ROBINSON (Ed.), Regional and Petroleum

Geology of the Black Sea and Surrounding Regions: AAPG Memoir 68, Tulsa, OK, p. 183-226.

ZENKOVITCH, V.P., 1960, Evolution of the Soviet Union Coasts of the Black Sea, Part II, Akad. Nauk. USSR, Moscow, 215 pp (in Russian).

ZONENSHAIN, L. P. & X. Le PICHON, 1986, Deep basins of the Black Sea and Caspian Sea as remnants of Mesozoic back-arc basins: Tectonophysics, 123, p. 181-211.